Lecture Notes

Physics of Neutron Stars

Galileo Galilei Institute for Theoretical Physics

March 3 to 7, 2014

Fridolin Weber

Department of Physics
San Diego State University
5500 Campanile Drive
San Diego, California, USA

March 5, 2014

Chapter 4

Physics of neutron star matter

4.1 Low-density regime

For neutron stars the density of matter spans an enormous range, from about ten times the density of normal nuclear matter in the star's core down to the density of iron, 7.9 g/cm^3, at the star's surface. Most of the mass of the star is contributed by highly compressed matter at nuclear and supernuclear densities, as can be seen in figure 4.1. It shows the energy density profiles of several neutron star models constructed for different equations of state, which will be introduced later in chapter 12 (cf. table 12.4 for the labeling and the characteristic features of these equations of state). Gravity compresses the matter in the cores of these neutron stars to densities between 9 to 13 the density of ordinary nuclear matter. Each stellar model is constructed for the largest possible central density beyond which these stars become unstable against radial oscillations. The corresponding stellar masses, which therefore are maximal in each case, are listed in table 14.3. The pressure profiles of these neutron stars are shown in figure 4.2.

Depending on density, the structure of neutron stars, schematically illustrated in figure 2.1, is presently understood to be as follows [56, 58, 70, 71, 297]:

- *Surface:* Matter at mass densities in the range of 10^4 g/cm^3 $< \epsilon <$ 10^6 g/cm^3 is composed of normal nuclei and non-relativistic electrons. The outermost layer, with an optical depth of $\tau \sim 1$, is called photosphere. The thermal radiation, observed in X-ray telescopes, is emitted from this region. This radiation dominates the cooling of neutron stars older than $\sim 10^6$ years. During the first $\sim 10^6$ years cooling is dominated by emission of neutrinos for the core region (see below). Depending on the neutrino reactions there, one distinguishes

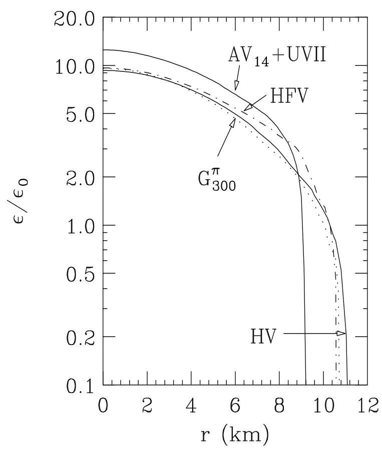

Figure 4.1. Energy density ϵ (in units of normal nuclear matter density, ϵ_0) versus radial distance in non-rotating maximum-mass neutron star models.

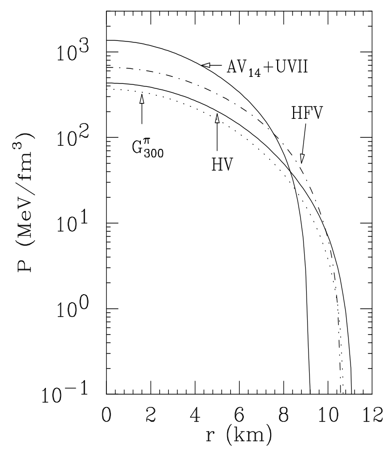

Figure 4.2. Pressure P versus radial distance in non-rotating maximum-mass neutron star models.

between standard and enhanced cooling (cf. chapter 19). Both the outer and inner crust act as thermal insulators between the cooling core and the surface.

- *Outer crust:* At densities of 7×10^6 g/cm^3 $< \epsilon <$ 4.3×10^{11} g/cm^3 the electrons become relativistic and form a relativistic electron gas. The atomic nuclei (lighter metals), while becoming more and more neutron rich, form a solid Coulomb lattice.
- *Inner crust:* It ranges from densities of about 4.3×10^{11} g/cm^3 to 2×10^{14} g/cm^3. At 4.3×10^{11} g/cm^3 neutrons begin to drip out of the neutron-saturated nuclei and populate free states outside of them. This density value is therefore referred to as neutron drip density. For increasing density matter clusters into extremely neutron rich nuclei (heavy metals) that are arranged on a lattice and immersed in a gas of neutrons and relativistic electrons.
- *Core region:* For densities beyond 2×10^{14} g/cm^3 the clusters begin to dissolve and neutrons, protons, and electrons form a relativistic Fermi fluid. Model calculations show that hyperon production sets in at about twice nuclear matter density, 5×10^{14} g/cm^3. As we shall see later, the population of Δ's appears to favored by many-body approximations that go beyond the relativistic mean-

field approximation (relativistic Hartree–Fock, relativistic Brueckner–Hartree–Fock). Other unresolved issues concern the formation of meson condensates in the cores of neutron stars and the possible transition of confined hadronic matter into quark matter. Finally, the possible absolute stability of 3-flavor strange quark matter, as described in section 2.3, would make 'conventional' neutron star matter, made up of either only hadrons or hadrons in equilibrium with quarks, metastable with respect to the lower energy state occupied by strange quark matter. In this case probably all 'neutron' stars would be made up entirely of pure 3-flavor strange quark matter, except a thin nuclear crust that may envelope the strange matter core. More than that, new and distinct classes of compact stars that are entirely different from neutron stars and white dwarfs should exist.

The surface and crust regions of neutron stars, whose equations of state are rather reliably known as opposed to the equation of state of the core region, are so thin that these contribute only little to the bulk properties like masses, radii, moments of inertia, and limiting rotational periods of the more massive members (that is, $M \gtrsim 1\,M_\odot$) of a neutron star sequence [61]. The equations of state of these density regimes therefore is only of minor importance for our studies. We shall use two models for the equation of state of the surface and crust region published in the literature. The first has been computed by Harrison-Wheeler [69] and Negele-Vautherin [72], the second by Baym–Pethick–Sutherland [70] and Baym–Bethe–Pethick [71]. Details about these models are listed in table 4.1. Hereafter we shall refer to these two models as HW–NV and BPS–BBP, respectively. In the stellar structure calculations that will be performed in the second part of this volume, these equations of state are joined with the models for the equation of state of the superdense core matter at densities between $10^{-2}\epsilon_0$ and $10^{-1}\epsilon_0$.[1]

4.2 High-density regime

At densities greater than the density of nuclear matter, ϵ_0, the Fermi momenta of the nucleons, N, in neutron star matter are so high that particle reactions such as

$$N + N \longrightarrow N + H + M \tag{4.1}$$

[1] The intense magnetic fields ($B \sim 10^{12}$ G) that are believed to exist on the surfaces of neutron stars will plausibly modify the structure of bulk matter. Abrahams and Shapiro improved on previous statistical calculations of the equation of state of matter subject to such strong magnetic fields. Moreover, finite temperature corrections were taken into account too [298].

Table 4.1. Two models for the EOS of neutron star matter at subnuclear densities.

Equation of state	Density range † (g/cm^3)	Composition
Harrison, Wheeler (HW) ‡	$7.9 \leq \epsilon \leq 10^{11}$	Crystalline; light metals, electron gas
Negele, Vautherin (NV)	$10^{11} \leq \epsilon \leq 10^{13}$	Crystalline; heavy metals, relativistic electron gas
Baym, Pethick, Sutherland (BPS) ‡	$7.9 \leq \epsilon \leq 4.3 \times 10^{11}$	Similar to HW but with Coulomb lattice correction
Baym, Bethe, Pethick (BBP)	$4.3 \times 10^{11} \leq \epsilon \leq 10^{14}$	Electrons, neutrons, and equilibrium nuclei

† For the conversion from g/cm^3 to MeV/fm^3, see table 1.4.

‡ The low-density part, from 7.9 g/cm^3 to 10^4 g/cm^3, has been computed by Feynman, Metropolis, and Teller [68].

become possible, where H denotes a hyperon and M a meson. A sample reaction for (4.1) is, for instance,

$$N + N \longrightarrow N + \Lambda + K\,. \tag{4.2}$$

As described by Glendenning [61], strangeness is conserved by the strong interaction but not by the weak force, which enables the corresponding mesons, such as the K, for instance, to transform as

$$K^0 \longrightarrow 2\,\gamma\,, \qquad K^- \longrightarrow \mu^- + \nu\,, \tag{4.3}$$

$$\mu^- + K^+ \longrightarrow \mu^- + \mu^+ + \nu \longrightarrow 2\,\gamma + \nu\,. \tag{4.4}$$

The situation is different if the meson is driven by a phase transition, as will be discussed below in this section. Aside from the very early stages of a newly formed neutron star, the star's energy is lowered through the leakage of the photons and neutrinos, γ and ν respectively. Consequently, the hyperon, of which we choose without loss of generality the Λ, becomes Pauli blocked, and a net strangeness can evolve for sufficiently dense neutron stars. Other particle states, ranging from the more massive hyperons $\Sigma^{\pm}$, Σ^0, Ξ^0, Ξ^- and the Δ-resonance states (cf. table 5.1) to the up, down and strange quarks, will become populated as the density of nucleons increases further. More than that, this may be accompanied by the formation of meson condensates, of which the K^- condensate has attracted a great deal of interest lately (see below). The governing principle that determines the complex particle population is known as *chemical equilibrium*, which is also referred to as β-equilibrium. Fortunately solving the problem of chemical equilibrium does not require that all kinds of these individual reactions be studied, as pointed out by Glendenning [61]. What is only required instead is the recognition which charges are conserved by the system. For neutron star matter these charges are baryon number, q_B, and electric charge, $q_B^{\rm el}$. Associated with these two conserved charges are two independent chemical potentials, μ^n and μ^e respectively. All other particle chemical potentials can be expressed as a linear combination of these two. This considerably eases the problem of determining the composition of superdense neutron star matter in the ground state. For an arbitrary particle, chemical equilibrium in a star can then be expressed as

$$\mu^\chi = q_\chi \, \mu^n \, - \, q_\chi^{\rm el} \, \mu^e \, , \tag{4.5}$$

where χ stands for the various hadronic and quark fields, that is, $\chi = B, Q, L, M$ with baryons like $B = p, n, \Sigma^{\pm,0}, \Lambda, \Xi^{0,-}, \Delta^-$, quarks $Q = u, d, s$, leptons $L = e^-, \mu^-$, and mesons $M = \pi^-, K^-$. A particle state χ will be populated when its chemical potential μ^χ exceeds the particle's lowest energy eigenstate in the medium, that is, only if

$$\mu^\chi \geq \omega^\chi(\boldsymbol{p} = 0) \, . \tag{4.6}$$

The situation is schematically illustrated in figure 4.3.

As long as the neutrinos and photons do not accumulate inside the star, as will be the case for the stars studied here, their respective chemical potentials μ^ν and μ^γ are equal to zero. This implies for the weak and electromagnetic decays (4.3) and (4.4)

$$\mu^\gamma = 0 \quad \Longrightarrow \quad \mu^{K^0} = 0 \tag{4.7}$$

for the first reaction of (4.3), and

$$\mu^\nu = 0 \quad \Longrightarrow \quad \mu^{K^-} = \mu^{\mu^-} \tag{4.8}$$

for the second reaction of (4.3). Reaction (4.4) tells us that

$$\mu^{K^+} = - \, \mu^{\mu^-} \, . \tag{4.9}$$

To enlighten the above principles in more detail, let us consider, as a first example, chemically equilibrated matter at such densities where it is

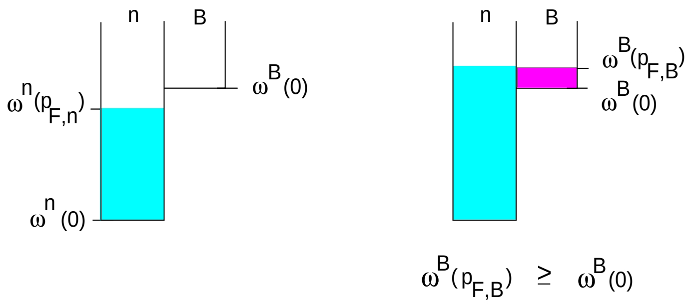

Figure 4.3. Condition for the onset of hyperon population in chemically equilibrated matter. Left: the single-particle energy is not high enough for the neutrons to transform to baryons of type B. Right: high-energy neutrons overcome the baryon threshold, that is, $\mu^B \equiv \omega^B(p_{F_B}) \geq \omega^B(0)$, and therefore transform to particle state B.

made up of only protons and neutrons, which is the case around nuclear matter density. The protons and neutrons then obey $n \leftrightarrow p + e^- + \bar{\nu}_e$, which, for vanishing antineutrino population (that is, $\mu^{\bar{\nu}_e} = 0$) leads to $\mu^n = \mu^p + \mu^e$. As the neutron density increases, so does that of protons and electrons. Eventually μ^e reaches a value equal to the muon mass. If so the muon then too will be populated. Equilibrium with respect to $e^- \leftrightarrow \mu^- + \nu_e + \bar{\nu}_\mu$ is assured when

$$\mu^{\mu^-} = \mu^e \,. \tag{4.10}$$

Note that because of (4.8), this leads for the chemical potential of the K^- meson to

$$\mu^{K^-} = \mu^e \,. \tag{4.11}$$

If this condition is fulfilled at a certain density, then the K^- mesons begin to form a condensate, according to the reaction $e^- \rightarrow K^- + \nu$. Similarly, the condition for π^- condensation is obtained by replacing μ^{K^-} with μ^{π^-} in equation (4.11), that is,

$$\mu^{\pi^-} = \mu^e \,. \tag{4.12}$$

The particle reaction underlying to π^- condensation is $n \rightarrow p + \pi^-$.

As a second example, let us proceed to densities where hyperon population is expected to set in. According to what has been said above in connection with equation (4.6), hyperons are energetically favored at densities for which the threshold condition $\omega^B(p_{F_B}) \equiv \mu^B \geq \omega^B(0)$ has a real solution. In case of the Λ hyperon, for instance, this condition reads $\omega^\Lambda(p_{F_\Lambda}) \equiv \mu^\Lambda \geq \omega^\Lambda(0)$. Since Λ is electrically neutral, equation (4.5) reduces to $\mu^\Lambda = \mu^n$. So the threshold condition for a gas of free, relativistic Λ's is given by $m_n^2 + p_{F_n}^2 \geq m_\Lambda^2$, from which it follows that for neutron Fermi momenta $p_{F_n} \geq \sqrt{m_\Lambda^2 - m_n^2}$ neutrons begin to leak into the Λ potential pot.

Equations (4.11) and (4.12) specifying the onset of meson condensation in neutron star matter are special cases of the general relation (4.5) applied to the possible formation of meson condensates in neutron stars. For mesons $q_B = 0$ and so one obtains from (4.5) as threshold condition for the onset of meson condensation

$$\mu^M = -\, q_M^{\rm el}\, \mu^e, \quad \text{where } M = \pi,\, K\,, \tag{4.13}$$

with $q_M^{\rm el} = -1$ for the negatively charged mesons π^- and K^-. The condensation of mesons other than π^- and K^- is strongly unfavored because of electric charge reasons. A brief description of the microphysical processes associated with the condensation of mesons can be found in section 7.9.

We recall that *electric charge neutrality* of neutron star matter is an absolute constraint on the composition of such matter, since it is imposed by a long-range force. If the net charge on a star is Ze and an additional charged particle is added, stability requires that the particle's gravitational attraction to the star dominates over the Coulomb repulsion [61], that is,

$$\frac{G\,(Am)\,m}{R} \geq \frac{Z\,e^2}{R}\,. \tag{4.14}$$

Here m denotes the mass of a nucleon, A is the star's baryon number, Am the star's mass, and R its radius. For net positive (proton) or negative (electron) charge, this means that

$$\frac{Z}{A} = \begin{cases} 10^{-36} & \text{(positive charge)}, \\ 10^{-39} & \text{(negative charge)}. \end{cases} \tag{4.15}$$

Therefore the electric charge density must be effectively zero. Otherwise the Coulomb repulsion would always win over gravity and the extra particle would not be bound to the star.

Accordingly, the particle populations must arrange themselves in such a way as to minimize the energy density in accord with electric charge neutrality and chemical equilibrium. As we shall see later, at normal nuclear matter density, neutron star matter consists primarily of neutrons and a small admixture of protons. The positive charge carried by the protons is neutralized at each density by a corresponding number of electrons.

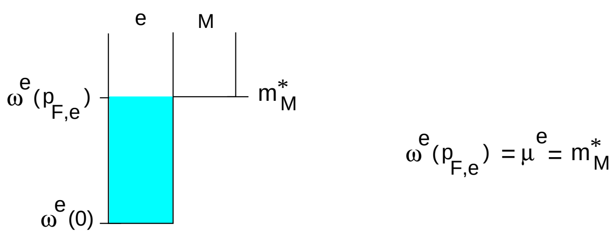

Figure 4.4. Condition for the onset of meson condensation in chemically equilibrated matter. For $\mu^e \equiv \omega^e(p_{F_e}) \geq m^*_M$ high-energy electrons can be replaced with negatively charged mesons ($M = \pi^-, K^-$), which, being bosons, can condense collectively into the ground state.

Since the number of protons increases with density, so does the number of electrons and thus μ^e. This trend is followed until μ^e is equal to the effective meson mass in matter, $\mu^e = m^*_M$. As illustrated in figure 4.4, at this density it may become energetically more favorable to fulfill the constraint of electric charge neutrality by means of populating negatively charged meson states rather than keep increasing the number of electrons. Being bosons, any number of mesons can go into the same quantum state, in contrast to the electrons whose Fermi energy were to built up monotonically with density, which is energetically less favorable of course. Of course there may be other sources like the Σ^- or deconfined d and s quarks that deliver negative electric charge to the system before the meson threshold is reached. If so the chemical electron potential will saturate (rather than increase monotonically) before the threshold for meson condensation is reached and then drop with increasing density, possibly ruling out a condensate.

Whether or not mesons actually condense depends decisively on the density dependence of the effective meson mass m^*_M in neutron star matter, since, as outlined just above, to trigger meson condensation the meson energy must cross the electron chemical potential. In case of K^- mesons, for instance, only then highly degenerated electrons can change through the reaction

$$e^- \longrightarrow K^- + \nu\,. \tag{4.16}$$

Once this reaction becomes possible in a neutron star, the star can lower its energy by replacing electrons with K^- mesons. How does the mass of the K^- in dense matter behave? It is known that the K^- has a mass of $m_{K^-} = 495$ MeV in the middle of the ^{56}Ni nucleus. On the other hand, the study of kaonic atoms indicates that the kaon appears to be bound by -200 ± 20 MeV [299]. That is, the attraction from nuclear matter at a density ρ_0 seems to be sufficient to greatly lower the mass of the kaon. The initial value of -200 MeV however turned out to be too large in magnitude, as has become clear from an analysis of the high quality K^- kinetic energy spectra extracted from Ni+Ni collisions at SIS (Schwerionen Synchrotron) energies, measured by the KaoS collaboration [300] at the Gesellschaft für Schwerionenforschung (GSI). An analysis of the Kaos data shows that the attraction at nuclear matter density is somewhat less, around -100 MeV [301, 255, 256], but nonetheless sufficient to bring the in-medium K^- mass down to $m^*_{K^-} \sim 200$ MeV at $\rho \sim 3\,\rho_0$, according to the relation [254]

$$m^*_{K^-} \sim m_{K^-} \left(1 - 0.2\,\frac{\rho}{\rho_0}\right) \tag{4.17}$$

for neutron rich matter. A value of $m^*_{K^-} \sim 200$ MeV lies in the vicinity of the value of the electron chemical potential in neutron star matter, for which competing theories predict values in the range from $\mu^e \sim 120$ to 220 MeV [61, 62, 79]. Whether or not the conditions for the transformation of electrons to K^- mesons are fulfilled in the dense pressure environment inside neutron stars remains to bee seen. The extension of the K^-–nucleus interaction from ^{56}Ni to matter at densities $\rho \sim 3\,\rho_0$ surely is quite an extrapolation, which upcoming relativistic heavy-ion experiments may or may not confirm [254]. Concerning the present theoretical status of dense matter calculations, we have repeatedly mentioned that there exists a number of unresolved open issues that enter in such calculations. This makes it very hard to come up with stringent quantitative predictions [302].

Finally we mention the possibility of the transition of confined hadronic matter into quark matter in the high-pressure environment of neutron stars. Quarks have baryon number $q_Q = \frac{1}{3}$. Equation (4.5) thus leads for the quark chemical potentials to

$$\begin{aligned} \mu^Q &= \frac{1}{3}\,\mu^n - \frac{2}{3}\,\mu^e\,, \quad \text{if } Q = u, c, \\ \mu^Q &= \frac{1}{3}\,\mu^n + \frac{1}{3}\,\mu^e\,, \quad \text{if } Q = d, s. \end{aligned} \tag{4.18}$$

Modelling the transition of confined hadronic matter to quark matter in a neutron star as a first order one, then, according to Gibbs criteria, phase equilibrium will exist if the pressure of both phases is equal, that is,

$$P_H(\{\chi\}, \mu^n, \mu^e) = P_Q(\mu^n, \mu^e)\,. \tag{4.19}$$

Note that because of relation (4.18) no additional unknowns enter other than the two independent chemical potentials μ^e and μ^n and the unknown matter fields, $\{\chi\}$, when solving equation (4.19) for the region of phase equilibrium between hadronic matter and quark matter. To find this region, one has to solve (4.19) in the three-space spanned by these two chemical potentials and the pressure. This has been done for the first time only a few years ago by Glendenning [88]. We shall come back to this issue in greater detail in chapter 8.

Chapter 5

Relativistic field-theoretical description of neutron star matter

5.1 Choice of Lagrangian

According to what has been outlined in chapter 4, neutron star matter at supernuclear densities constitutes a very complex many-body system whose fundamental constituents will be protons, neutrons, hyperons, eventually even more massive baryons like the Δ, possibly an admixture of u, d, s quarks (other quark flavors are too massive to become populated in stable neutron stars), and eventually condensed mesons. The dynamics of the baryonic degrees of freedom, summarized in table 5.1, is described by a Lagrangian of the following type [79]:

$$\begin{aligned}\mathcal{L}(x) \;=\; & \sum_{B=p,n,\Sigma^{\pm,0},\Lambda,\Xi^{0,-},\Delta^{++,+,0,-}} \mathcal{L}_B^0(x) \\ & + \sum_{M=\sigma,\omega,\pi,\rho,\eta,\delta,\phi} \Big\{ \mathcal{L}_M^0(x) \;+ \sum_{B=p,n,\dots,\Delta^{++,+,0,-}} \mathcal{L}_{BM}(x) \Big\} \\ & + \mathcal{L}^{(\sigma^4)}(x) \;+ \sum_{L=e^-,\mu^-} \mathcal{L}_L(x)\,. \end{aligned} \tag{5.1}$$

Summed are all baryon states B whose thresholds will be reached in the dense interiors of neutron stars. The summation also includes the Δ resonance whose appearance is favored by many-body theories that go beyond the relativistic mean-field approximation, as we shall see later in section 7. One may wonder to which extent hyperons and the Δ resonance may each be treated as a *separate* species. Such a treatment, however, seems to be well vindicated not only in finite nuclei, but also in nuclear matter at as high a density as encountered in neutron stars [303, 304].

Table 5.1. Masses (m_B) and quantum numbers (spin, J_B; isospin, I_B; strangeness, S_B; hypercharge, Y_B; third component of isospin, I_{3B}; electric charge, $q_B^{\rm el}$) of those baryons that have been found to become populated in the cores of neutron stars.

Baryon (B)	m_B (MeV)	J_B	I_B	S_B	Y_B	I_{3B}	$q_B^{\rm el}$
n	939.6	1/2	1/2	0	1	$-1/2$	0
p	938.3	1/2	1/2	0	1	1/2	1
Σ^+	1189	1/2	1	-1	0	1	1
Σ^0	1193	1/2	1	-1	0	0	0
Σ^-	1197	1/2	1	-1	0	-1	-1
Λ	1116	1/2	0	-1	0	0	0
Ξ^0	1315	1/2	1/2	-2	-1	1/2	0
Ξ^-	1321	1/2	1/2	-2	-1	$-1/2$	-1
Δ^{++}	1232	3/2	3/2	0	1	3/2	2
Δ^+	1232	3/2	3/2	0	1	1/2	1
Δ^0	1232	3/2	3/2	0	1	$-1/2$	0
Δ^-	1232	3/2	3/2	0	1	$-3/2$	-1

Constraints, if any, due to anti-symmetrization between nucleons and the possible nucleon content of the resonances were found to be negligibly small. Besides that, the number density of a given nucleon resonance in a large assembly of nucleons and pions was found to obey the usual equation of thermal equilibrium $\mu^B = \mu^\pi + \mu^N$ in therm of chemical potentials. (The equilibrium concept and, thus, chemical potentials will be introduced in chapter 4.) Finally, we mention, that the largeness of resonance widths would not affect their elementarity. Its effects may be interpreted as part of the interaction between the resonance species and the nucleon or meson species [304].

The interaction between the baryons is described by the exchange of mesons with masses up to about 1 GeV, depending on the many-body approximation. At the level of the simplest approximation – the relativistic mean-field (or Hartree) approximation – these are the σ, ω and ρ meson only [78, 79, 84, 92]. Because of their spin and parity quantum numbers, which are listed in table 5.2, this approximation is also referred to as scalar-vector-isovector theory. The relativistic Hartree–Fock (RHF) approximation differs from the mean-field theory because of the exchange (Fock) term, which, by definition, is absent in the mean-field theory. For that reason the π meson, which contributes only to the exchange term of the self-energy, does not contribute to the self-energy computed at the relativistic

Table 5.2. Mesons and their quantum numbers [305]. The entries are: spin J_M, parity π, isospin I_M, and mass m_M of meson M.

Meson (M)	J_M^π	I_M	Coupling	Mass (MeV)	Dominant decay mode
σ	0^+	0	scalar	550	–
ω	1^-	0	vector	783	3π
$\pi^\pm$	0^-	1	pseudovector	140	$\mu^\pm\nu$
π^0	0^-	1	pseudovector	135	$\gamma\gamma$
ρ	1^-	1	vector	769	2π
η	0^-	0	pseudovector	549	$\gamma\gamma$, $3\pi^0$
δ	0^+	1	scalar	983	$\eta\pi$, $K\bar{K}$
ϕ	1^-	0	vector	1020	K^+K^-
K^+	0^-	1/2	pseudovector	494	$\mu^+\nu$, $\pi^+\pi^0$
K^-	0^-	1/2	pseudovector	494	$\mu^-\nu$, $\pi^-\pi^0$

mean-field level. The whole set of mesons summed in (5.1) is generally employed in the construction of relativistic meson-exchange models for the nucleon–nucleon interaction, of which the Bonn meson exchange model [119, 306] is a particularly sophisticated representative. Among other features, it not only accounts for single-meson exchange processes among the nucleons but also for explicit 2π-exchange contributions, involving the Δ isobar in intermediate states, and $\pi\rho$-exchange diagrams, which replace to a large extent the fictitious σ exchange used in former one-boson-exchange interactions OBEP [104, 119, 120, 307]. Such potentials can only be used in many-body methods that account for dynamical two-nucleon correlations calculated from the nucleon–nucleon scattering matrix in matter ($\mathbf{T}$-matrix), like it is the case for the relativistic Brueckner–Hartree–Fock (RBHF) approximation. In contrast to RBHF, the Hartree and Hartree–Fock approximations account only for what is called statistical correlations.

Models for the equation of state derived in the framework of the linear mean-field model are extremely stiff and cannot be reconciled with the empirical value for the incompressibility [92]. This can be cured by either introducing derivative couplings in the Lagrangian, which shall be done in section 7.3, or by means of adding non-linear terms to it. Here we shall follow the suggestion of Boguta and Bodmer [308] and Boguta and Rafelski [309] and add cubic and quartic self-interactions of the σ field to the Lagrangian.

The equations of motion of the baryon and meson fields, which shall be derived below, are to be solved subject to the two constraints imposed on neutron star matter, outlined in section 4.2. These are electric charge neutrality and β-equilibrium. Both constraints imply the presence of leptons in neutron star matter. Mathematically we account for them by adding the Lagrangian of free relativistic leptons, $\mathcal{L}_L$, to the system's total Lagrangian, given in equation (5.1).

The individual terms in equation (5.1) will be given next. We begin with the Lagrangians of free baryon and meson fields which are given by

$$\mathcal{L}^0_B(x) = \bar{\psi}_B(x)\ \left(i\,\gamma^\mu \partial_\mu\ -\ m_B\right)\ \psi_B\,, \tag{5.2}$$

$$\mathcal{L}^0_\sigma(x) = \frac{1}{2}\left(\partial^\mu \sigma(x)\,\partial_\mu \sigma(x) - m_\sigma^2\ \sigma^2(x)\right)\,, \tag{5.3}$$

$$\mathcal{L}^0_\omega(x) = -\ \frac{1}{4} F^{\mu\nu}(x)\,F_{\mu\nu}(x) + \frac{1}{2}\ m_\omega^2\ \omega^\nu(x)\,\omega_\nu(x)\,, \tag{5.4}$$

$$\mathcal{L}^0_\pi(x) = \frac{1}{2}\left(\partial^\mu \boldsymbol{\pi}(x)\cdot\partial_\mu \boldsymbol{\pi}(x)\ -\ m_\pi^2\ \boldsymbol{\pi}(x)\cdot\boldsymbol{\pi}(x)\right)\,, \tag{5.5}$$

$$\mathcal{L}^0_\rho(x) = -\ \frac{1}{4}\boldsymbol{G}^{\mu\nu}(x)\cdot\boldsymbol{G}_{\mu\nu}(x)\ +\ \frac{1}{2}\ m_\rho^2\ \boldsymbol{\rho}^\mu(x)\cdot\boldsymbol{\rho}_\mu(x)\,. \tag{5.6}$$

The interaction Lagrangians read as follows,

$$\mathcal{L}_{B\sigma}(x) = -\sum_B (\mathbf{1}\ g_{\sigma B})\ \bar{\psi}_B(x)\ \sigma(x)\ \psi_B(x)\,, \tag{5.7}$$

$$\begin{aligned}\mathcal{L}_{B\omega}(x) = &-\sum_B g_{\omega B}\ \bar{\psi}_B(x)\ \gamma^\mu \omega_\mu(x)\ \psi_B(x)\\ &-\sum_B \frac{f_{\omega B}}{4\,m_B}\ \bar{\psi}_B(x)\ \sigma^{\mu\nu}\ F_{\mu\nu}(x)\ \psi_B(x)\,,\end{aligned} \tag{5.8}$$

$$\mathcal{L}_{B\pi}(x) = -\sum_B \frac{f_{\pi B}}{m_\pi}\ \bar{\psi}_B(x)\ \gamma^5\gamma^\mu\ \left(\partial_\mu \boldsymbol{\tau}\cdot\boldsymbol{\pi}(x)\right)\ \psi_B(x)\,, \tag{5.9}$$

$$\begin{aligned}\mathcal{L}_{B\rho}(x) = &-\sum_B g_{\rho B}\ \bar{\psi}_B(x)\ \gamma^\mu \boldsymbol{\tau}\cdot\boldsymbol{\rho}_\mu(x)\ \psi_B(x)\\ &-\sum_B \frac{f_{\rho B}}{4\,m_B}\ \bar{\psi}_B(x)\ \sigma^{\mu\nu}\ \boldsymbol{\tau}\cdot\boldsymbol{G}_{\mu\nu}(x)\ \psi_B(x)\,.\end{aligned} \tag{5.10}$$

The quantity $\mathbf{1}$ in (5.7) denotes the unity matrix in Dirac space [cf. (5.132)]. The second terms in (5.8) and (5.10) describes so-called tensor couplings, all other couplings are of standard Yukawa-type. For the π meson we choose the pseudovector coupling scheme, since pseudoscalar coupling is known to lead to several inconsistencies when applied to nuclear matter calculations [92]. These originate from the circumstance that pseudoscalar coupling gives so much repulsion that the Hartree–Fock approximation becomes inadequate for the description of the properties of nuclear matter. As an example, the nucleon self-energy in nuclear matter calculated for the pseudoscalar coupling is about 40 times larger than for the pseudovector case. This leads to a ground state configuration at saturation density which is a Fermi-shell state rather than a Fermi-sphere. The pseudovector coupling, on the other hand, is much weaker. The lowest energy configuration calculated for it is again a Fermi-sphere. Finally we note that the pseudoscalar coupling is equivalent to pseudovector coupling for on-shell nucleons if one uses a pseudovector coupling constant, $f_{\pi N}$, which satisfies the so-called equivalence principle $g_{\pi N}/(2m_N) = f_{\pi N}/m_\pi$ in free space, that is, $f^2_{\pi N}/(4\pi) \approx 0.08$ [92]. It should be kept in mind, however, that the equivalence principle applied to dense nuclear matter can only be regarded as a guideline, since it may not be correct in dense matter.

As a final point on the coupling 'constants', we note that they may plausibly change with increasing density and/or temperature of the matter. The pion constant $f_{\pi N}$, for instance, is expected to decrease in the nuclear medium [310], according to the Brown-Rho scaling. The incorporation of density and/or temperature effects into fully self-consistent dense matter calculations constitutes an extremely cumbersome problem that has not been solved yet, though significant progress has been made in recent years toward accomplishing this problem [302, 311, 312]. This is different for the influence of such effects on the meson and baryon masses in dense matter [302, 311, 312], the latter of which will be discussed in great detail immediately below.

After these remarks, let us turn back to the field-theoretical description of dense matter. The still undefined field tensors $F^{\mu\nu}$ and $\boldsymbol{G}^{\mu\nu}$ are given by

$$F^{\mu\nu}(x) = \partial^\mu \omega^\nu(x) - \partial^\nu \omega^\mu(x) , \tag{5.11}$$

$$\boldsymbol{G}^{\mu\nu}(x) = \partial^\mu \boldsymbol{\rho}^\nu(x) - \partial^\nu \boldsymbol{\rho}^\mu(x) . \tag{5.12}$$

The latter tensor is of vectorial nature because the ρ meson is a vector in isospin space (cf. table 5.2). The quantity $\sigma^{\mu\nu}$ is an abbreviation for the commutator made up of a pair of γ matrices,

$$\sigma^{\mu\nu} = \frac{\mathrm{i}}{2} \, [\, \gamma^\mu, \gamma^\nu \,] \, , \tag{5.13}$$

from which one reads off that $\sigma^{\nu\mu} = -\sigma^{\mu\nu}$. The γ matrices are defined in appendix A, where an overview of some of their properties can be found too. The above mentioned cubic and quartic self-interactions of the σ field are described by a Lagrangian of the form

$$\mathcal{L}^{(\sigma^4)}(x) = -\frac{1}{3}\, m_N\, b_N\, \{g_{\sigma N}\, \sigma(x)\}^3 - \frac{1}{4}\, c_N\, \{g_{\sigma N}\, \sigma(x)\}^4\,. \tag{5.14}$$

Finally the Lagrangian of free leptons reads

$$\mathcal{L}_L(x) = \bar{\psi}_L(x)\ (\mathrm{i}\,\gamma^\mu \partial_\mu\ -\ m_L)\ \psi_L(x)\,. \tag{5.15}$$

Above we have restricted ourselves to listing the Lagrangians of σ, ω, π, and ρ mesons only. The Lagrangians of δ, ϕ, and η mesons, which enter in one-boson-exchange interactions in addition, will not be given explicitly. Their form can be easily inferred however by looking at the quantum numbers of these mesons given in table 5.2. This reveals, for instance, that the δ meson has the same spin and parity as the σ meson, namely 0^+. Apart from isopin, which requires multiplication of the δ field with the Pauli matrix $\boldsymbol{\tau}$ $[= (\tau^1, \tau^2, \tau^3)]$ in the interaction Lagrangian, the Lagrangians of the δ are then obtained from equations (5.3) and (5.7) by replacing σ with δ in (5.3), and σ with $\boldsymbol{\tau}\delta$ in (5.7). Similarly, the Lagrangians of ϕ and η mesons are obtainable from those of ω and π mesons by replacing ω with ϕ, and π with η, respectively.

The baryon fields obey the anti-commutation relations

$$\begin{aligned} \{\bar{\psi}_\zeta(x^0, \boldsymbol{x}), \psi_\zeta(x^0, \boldsymbol{x}')\} &= \gamma^0_{\zeta\zeta'}\, \delta^3(\boldsymbol{x} - \boldsymbol{x}')\,, \\ \{\bar{\psi}_\zeta(x^0, \boldsymbol{x}), \bar{\psi}_\zeta(x^0, \boldsymbol{x}')\} &= \{\psi_\zeta(x^0, \boldsymbol{x}), \psi_\zeta(x^0, \boldsymbol{x}')\} = 0\,. \end{aligned} \tag{5.16}$$

The commutator relations of the scalar meson field, $\sigma(x)$, read

$$\begin{aligned} [\Pi_\sigma(x^0, \boldsymbol{x}), \sigma(x^0, \boldsymbol{x}')] &=\ -\ \mathrm{i}\, \delta^3(\boldsymbol{x} - \boldsymbol{x}')\,, \\ [\Pi_\sigma(x^0, \boldsymbol{x}), \Pi_\sigma(x^0, \boldsymbol{x}')] &= [\sigma(x^0, \boldsymbol{x}), \sigma(x^0, \boldsymbol{x}')] = 0\,, \end{aligned} \tag{5.17}$$

where $\Pi_\sigma(x)$ denotes the conjugate momentum of the σ field,

$$\Pi_\sigma(x) \equiv \frac{\partial \mathcal{L}}{\partial \dot{\sigma}(x)} = \dot{\sigma}(x)\,. \tag{5.18}$$

The fields Π_σ and σ commutate with the baryon field operators,

$$\begin{aligned} [\sigma(x^0, \boldsymbol{x}), \psi(x^0, \boldsymbol{x}')] &= [\Pi_\sigma(x^0, \boldsymbol{x}), \psi(x^0, \boldsymbol{x}')] = 0\,, \\ [\sigma(x^0, \boldsymbol{x}), \bar{\psi}(x^0, \boldsymbol{x}')] &= [\Pi_\sigma(x^0, \boldsymbol{x}), \bar{\psi}(x^0, \boldsymbol{x}')] = 0\,. \end{aligned} \tag{5.19}$$

Since the interaction Lagrangians of the π, ω and ρ mesons contain derivatives of these fields, as can be seen in equations (5.8) to (5.10), the corresponding conjugate momenta possess a somewhat more complicated structure than (5.18), derived for the σ field. One obtains ($j = 1, 2, 3$):

$$\boldsymbol{\Pi}_\pi(x) = \dot{\boldsymbol{\pi}}(x) - \sum_B \frac{f_{\pi B}}{m_\pi} \bar{\psi}_B(x)\, \gamma^0\, \gamma^5\, \boldsymbol{\tau}\, \psi_B(x)\,, \tag{5.20}$$

$$\Pi_{\omega_j}(x) = F^{j0}(x) + \sum_B \frac{f_{\omega B}}{2\, m_B} \bar{\psi}_B(x)\, \sigma^{j0}\, \psi_B(x)\,, \tag{5.21}$$

$$\boldsymbol{\Pi}_{\rho_j}(x) = \boldsymbol{G}^{j0}(x) + \sum_B \frac{f_{\rho B}}{2\, m_B} \bar{\psi}_B(x)\, \boldsymbol{\tau}\, \sigma^{j0}\, \psi_B(x)\,, \tag{5.22}$$

with

$$\Pi_{\omega_j}(x) \equiv \frac{\partial \mathcal{L}}{\partial(\partial_0\, \omega_j)}\,. \tag{5.23}$$

Because of the γ matrices in equations (5.20) through (5.22), the quantities $\dot{\boldsymbol{\pi}}$, G^{j0} and $\boldsymbol{G}^{j0}$ do not commute with the nucleon field operators anymore, as it was the case in (5.19) for $\dot{\sigma}$. One gets instead

$$[\dot{\boldsymbol{\pi}}(x^0, \boldsymbol{x}), \psi_{B'\zeta'}(x^0, \boldsymbol{x}')] = -\frac{f_{\pi B'}}{m_\pi} \delta^3(\boldsymbol{x} - \boldsymbol{x}')\, (\gamma_5 \otimes \boldsymbol{\tau})_{\zeta'\zeta}\, \psi_{B\zeta}(x)\,, \tag{5.24}$$

and for the ω meson

$$[F^{j0}(x^0, \boldsymbol{x}), \psi_{B'\zeta'}(x^0, \boldsymbol{x}')] = -\mathrm{i}\, \frac{f_{\omega B'}}{2\, m_{B'}} \delta^3(\boldsymbol{x} - \boldsymbol{x}')\, (\gamma^j)_{\zeta'\zeta}\, \psi_{B'\zeta}(x)\,, \tag{5.25}$$

$$[F^{j0}(x^0, \boldsymbol{x}), \bar{\psi}_{B'\zeta'}(x^0, \boldsymbol{x}')] = -\mathrm{i}\, \frac{f_{\omega B'}}{2\, m_{B'}} \delta^3(\boldsymbol{x} - \boldsymbol{x}')\, \bar{\psi}_{B'\zeta}(x)\, (\gamma^j)_{\zeta\zeta'}\,. \tag{5.26}$$

The corresponding expressions for the ρ meson follow from (5.25) and (5.26) by replacing F^{j0} with $\boldsymbol{G}^{j0}$, and σ^{j0} with $\sigma^{j0} \otimes \boldsymbol{\tau}$ etc.

5.2 Field equations

In this section we shall derive the equations of motion for the numerous particle fields from the Euler–Lagrange equation, which is a condition on the Lagrangian which guarantees that the action I, defined as

$$I \equiv \int \mathrm{d}^4x\ \mathcal{L}(\chi(x), \partial_\mu \chi(x)) \tag{5.27}$$

is an extremum, that is, $\delta I = 0$. We only consider the case where $\mathcal{L}$ depends explicitly on the matter fields and their derivatives, χ and $\partial_\mu \chi$

respectively, but not on the coordinates x^μ itself. Writing out the variation of (5.27) explicitly gives

$$\int \mathrm{d}^4x \ \{\mathcal{L}(\chi + \delta\chi, \partial_\mu\chi + \delta\,\partial_\mu\chi) - \mathcal{L}(\chi, \partial_\mu\chi)\} = 0\,, \tag{5.28}$$

where the replacements

$$\begin{aligned} \chi(x) &\to \chi'(x) = \chi(x) + \delta\chi(x)\,, \\ \partial_\mu\chi(x) &\to \partial_\mu\chi'(x) = \partial_\mu\chi(x) + \partial_\mu\delta\chi(x)\,, \end{aligned} \tag{5.29}$$

denote variations of the fields. Taylor expansion of the first integrand in (5.28) leads to

$$\mathcal{L}(\chi + \delta\chi, \partial_\mu\chi + \delta\,\partial_\mu\chi) = \mathcal{L}(\chi, \partial_\mu\chi) + \frac{\partial\mathcal{L}}{\partial\chi}\,\delta\chi + \frac{\partial\mathcal{L}}{\partial(\partial_\mu\chi)}\,\delta(\partial_\mu\chi)\,. \tag{5.30}$$

Substituting (5.30) into (5.28) and making use of

$$\delta(\partial_\mu\chi) = \partial_\mu(\chi + \delta\chi) - \partial_\mu\chi = \partial_\mu\,(\delta\chi) \tag{5.31}$$

gives

$$\int \mathrm{d}^4x \left\{ \frac{\partial\mathcal{L}}{\partial\chi}\,\delta\chi + \frac{\partial\mathcal{L}}{\partial(\partial_\mu\chi)}\,\partial_\mu(\delta\chi) \right\} = 0\,. \tag{5.32}$$

Upon integrating the second term by parts, one obtains

$$\int \mathrm{d}^4x \left\{ \left[\frac{\partial\mathcal{L}}{\partial\chi} - \partial_\mu \left(\frac{\partial\mathcal{L}}{\partial(\partial_\mu\chi)} \right) \right] \delta\chi \right\} = 0\,, \tag{5.33}$$

provided the contribution from the surface of spacetime may be dropped. Thus, for arbitrary variations of the fields $\delta\chi$, the condition for the action to be stationary ($\delta I = 0$) reads

$$\partial_\mu \left(\frac{\partial\mathcal{L}}{\partial(\partial_\mu\chi)} \right) - \frac{\partial\mathcal{L}}{\partial\chi} = 0\,. \tag{5.34}$$

This is the Euler–Lagrange equation for given fields χ, which, in our case, are the fermion and boson fields ψ_B, ψ_L and $\sigma, \omega, \pi, \rho, \eta, \delta, \phi$.

We begin with deriving the equation of motion for the baryon fields ψ_B from (5.34). Since (5.34) does not contain derivatives of $\bar\psi_B$, the first term of the Euler–Lagrange equation give no contribution. The second term leads to

$$\frac{\partial\mathcal{L}}{\partial\bar\psi_B} = (\mathrm{i}\gamma^\mu\partial_\mu - m_B)\ \psi_B(x)\ +\ g_{\sigma B}\,\sigma(x)\,\psi_B(x)$$

$$
\begin{aligned}
&- \left\{ g_{\omega B} \gamma^\mu \omega_\mu(x) + \frac{f_{\omega B}}{4 m_B} \sigma^{\mu\nu} F_{\mu\nu}(x) \right\} \psi_B(x) \\
&- \left\{ g_{\rho B}\, \gamma^\mu\, \boldsymbol{\tau} \cdot \boldsymbol{\rho}_\mu(x) + \frac{f_{\rho B}}{4\, m_B}\, \sigma^{\mu\nu}\, \boldsymbol{\tau} \cdot \boldsymbol{G}_{\mu\nu}(x) \right\} \psi_B(x) \\
&- \frac{f_{\pi B}}{m_\pi}\, \gamma^\mu \gamma^5 \left(\partial_\mu\, \boldsymbol{\tau} \cdot \boldsymbol{\pi}(x) \right) \psi_B(x) \,. \qquad (5.35)
\end{aligned}
$$

From $\partial \mathcal{L} / \partial \bar{\psi}_B = 0$ one gets as the final result for the inhomogeneous Dirac equation

$$
\begin{aligned}
(\mathrm{i}\gamma^\mu \partial_\mu - m_B)\; \psi_B(x) = {} & g_{\sigma B}\, \sigma(x)\, \psi_B(x) \\
&+ \left\{ g_{\omega B} \gamma^\mu \omega_\mu(x) + \frac{f_{\omega B}}{4 m_B} \sigma^{\mu\nu} F_{\mu\nu}(x) \right\} \psi_B(x) \\
&+ \left\{ g_{\rho B}\, \gamma^\mu\, \boldsymbol{\tau} \cdot \boldsymbol{\rho}_\mu(x) + \frac{f_{\rho B}}{4\, m_B}\, \sigma^{\mu\nu}\, \boldsymbol{\tau} \cdot \boldsymbol{G}_{\mu\nu}(x) \right\} \psi_B(x) \\
&+ \frac{f_{\pi B}}{m_\pi}\, \gamma^\mu \gamma^5 \left(\partial_\mu\, \boldsymbol{\tau} \cdot \boldsymbol{\pi}(x) \right) \psi_B(x) \,. \qquad (5.36)
\end{aligned}
$$

To find the equation of motion for the scalar σ field, we differentiate (5.1) with respect to σ, which leads to

$$
\frac{\partial \mathcal{L}}{\partial \sigma} = -\, m_\sigma^2 \sigma - \sum_B g_{\sigma B}\, \bar{\psi}_B \psi_B - m_N\, b_N\, g_{\sigma N}\, (g_{\sigma N} \sigma)^2 - c_N\, g_{\sigma N}\, (g_{\sigma N} \sigma)^3 \,. \tag{5.37}
$$

The last two terms, which originate from $\mathcal{L}^{(\sigma^4)}$, shall be kept only when solving the equations of motion at the mean-field level. The differentiation of $\mathcal{L}$ with respect to $\partial_\mu \sigma$ is slightly more complicated since the partial derivative carries a covariant four-index. So when differentiating (5.1) with respect to $\partial_\mu \sigma$ we have to make sure that all the relevant partial derivatives are written in covariant form. This is accomplished via the metric tensor of flat spacetime (see appendix A) which allows us to write for a contravariant derivative $\partial^\kappa = g^{\kappa\nu} \partial_\nu$. Bearing this in mind, one readily verifies that

$$
\begin{aligned}
\frac{\partial \mathcal{L}}{\partial(\partial_\mu \sigma)} &= \frac{1}{2}\, \frac{\partial}{\partial(\partial_\mu \sigma))} \left\{ (g^{\kappa\nu} \partial_\nu \sigma)\, (\partial_\kappa \sigma) \right\} && (5.38) \\
&= \frac{1}{2} \left\{ g^{\kappa\nu} \frac{\partial(\partial_\nu \sigma)}{\partial(\partial_\mu \sigma)}\, (\partial_\kappa \sigma) + (g^{\kappa\nu} \partial_\nu \sigma)\, \frac{\partial(\partial_\kappa \sigma)}{\partial(\partial_\mu \sigma)} \right\} && (5.39) \\
&= \frac{1}{2}\, \left\{ g^{\kappa\nu}\, \delta_{\mu\nu}\, \partial_\kappa \sigma + g^{\kappa\nu}\, \delta_{\kappa\mu}\, \partial \sigma \right\} && (5.40) \\
&= \frac{1}{2}\, \left\{ g^{\kappa\mu}\, \partial_\kappa \sigma + g^{\kappa\nu}\, \partial_\nu \sigma \right\} = \partial^\mu \sigma \,. && (5.41)
\end{aligned}
$$

From (5.39) to (5.40) we have used that $\partial(\partial_\nu \sigma)/\partial(\partial_\mu \sigma)$ only contributes if the subscripts obey $\nu = \mu$. Letting ∂_μ act on (5.41) leads to

$$\partial_\mu \frac{\partial \mathcal{L}}{\partial(\partial_\mu \sigma)} = \partial_\mu \partial^\mu \sigma \,. \tag{5.42}$$

Subtracting (5.37) from (5.42) leads to the equation of motion for the σ field,

$$\begin{aligned}(\partial^\mu \partial_\mu + m_\sigma^2)\,\sigma(x) = & -\sum_B g_{\sigma B}\,\bar{\psi}_B(x)\psi_B(x) - m_N\, b_N\, g_{\sigma N}\,(g_{\sigma N}\sigma(x))^2 \\ & - c_N\, g_{\sigma N}\,(g_{\sigma N}\sigma(x))^3 \,,\end{aligned} \tag{5.43}$$

which constitutes an inhomogeneous Klein-Gordon equation.

To derive the equation of motion for the ω field, we proceed in a similar fashion as just above. The main difference with respect to the σ field arises from the vectorial nature of the ω field. Via the metric tensor, the fields and derivatives are transformed to their covariant or contravariant representations, as the case may be, and as before derivatives like $\partial\omega_{\mu'}/\partial\omega_\mu$ lead to factors of $\delta_{\mu\mu'}$. One then obtains

$$\frac{\partial \mathcal{L}}{\partial \omega_\mu} = -\sum_B g_{\omega B}\;\bar{\psi}_B \gamma^\mu \psi_B + m_\omega^2\,\omega^\mu \,, \tag{5.44}$$

where use of

$$\frac{\partial}{\partial \omega_\mu}\,(\omega^\nu \omega_\nu) = \left(\frac{\partial}{\partial \omega_\mu} g^{\nu\lambda}\omega_\lambda\right)\omega_\nu + \omega^\nu \frac{\partial \omega_\nu}{\partial \omega_\mu} = 2\,\omega^\mu \tag{5.45}$$

has been made. The other term of the Euler–Lagrange equation gives

$$\begin{aligned}\frac{\partial \mathcal{L}}{\partial(\partial_\lambda \omega_\mu)} &= -\,\frac{1}{4}\,\frac{\partial(F^{\kappa\nu}F_{\kappa\nu})}{\partial(\partial_\lambda \omega_\mu)} - \sum_B \frac{f_{\omega B}}{4m_B}\,\bar{\psi}_B\,\sigma^{\kappa\nu}\,\frac{\partial\,(F_{\kappa\nu}\,\psi_B)}{\partial(\partial_\lambda \omega_\mu)} \\ &= -\,\frac{1}{4}\,\frac{\partial}{\partial(\partial_\lambda \omega_\mu)}\,\{(\partial^\kappa \omega^\nu - \partial^\nu \omega^\kappa)\,(\partial_\kappa \omega_\nu - \partial_\nu \omega_\kappa)\} \\ &\quad - \sum_B \frac{f_\omega B}{4m_B}\bar{\psi}_B \sigma^{\kappa\nu}\left\{\frac{\partial}{\partial(\partial_\lambda \omega_\mu)}\,(\partial_\kappa \omega_\nu - \partial_\nu \omega_\kappa)\right\}\psi_B \,.\end{aligned} \tag{5.46}$$

Since the partial derivatives in (5.46) lead to

$$\frac{\partial(\partial^\kappa \omega^\nu)}{\partial(\partial_\lambda \omega_\mu)} = \frac{\partial}{\partial(\partial_\lambda \omega_\mu)}\; g^{\kappa\epsilon}\partial_\epsilon g^{\nu\tau}\omega_\tau = g^{\kappa\lambda}\, g^{\nu\mu} \,, \tag{5.47}$$

equation (5.46) can be rewritten as

$$
\begin{aligned}
\frac{\partial \mathcal{L}}{\partial(\partial_\lambda \omega_\mu)} = & -\frac{1}{4}\left\{\left(g^{\kappa\lambda} g^{\nu\lambda} - g^{\nu\lambda} g^{\kappa\mu}\right)\left(\partial_\kappa \omega_\nu - \partial_\nu \omega_\kappa\right)\right. \\
& \left. + \left(\partial^\kappa \omega^\nu - \partial^\nu \omega^\kappa\right)\left(\delta_{\kappa\lambda}\delta_{\nu\mu} - \delta_{\nu\lambda}\delta_{\kappa\mu}\right)\right\} \\
& - \sum_B \frac{f_{\omega B}}{4 m_B}\, \bar{\psi}_B\, \sigma^{\kappa\nu}\left(\delta_{\kappa\lambda}\delta_{\nu\mu} - \delta_{\nu\lambda}\delta_{\kappa\mu}\right)\psi_B \qquad (5.48) \\
= & \, \partial^\mu \omega^\lambda - \partial^\lambda \omega_\mu - \sum_B \frac{f_{\omega B}}{4 m_B}\, \bar{\psi}_B \left(\sigma^{\lambda\mu} - \sigma^{\mu\lambda}\right)\psi_B \,. \qquad (5.49)
\end{aligned}
$$

The quantity $\sigma^{\lambda\mu}$ in (5.49) is antisymmetric with respect to interchanging λ and μ, which follows readily from (5.13) as

$$
\sigma^{\lambda\mu} = \frac{\mathrm{i}}{2}\left[\gamma^\lambda, \gamma^\mu\right] = \frac{\mathrm{i}}{2}\left(\gamma^\lambda\gamma^\mu - \gamma^\mu\gamma^\lambda\right) = -\frac{\mathrm{i}}{2}\left[\gamma^\mu, \gamma^\lambda\right] = -\sigma^{\mu\lambda} \,. \qquad (5.50)
$$

This enables us to write equation (5.49) as

$$
\frac{\partial \mathcal{L}}{\partial(\partial_\lambda \omega_\mu)} = \partial^\mu \omega^\lambda - \partial^\lambda \omega_\mu - 2\sum_B \frac{f_{\omega B}}{4 m_B} \bar{\psi}_B \sigma^{\lambda\mu} \psi_B \,. \qquad (5.51)
$$

Combining (5.44) and (5.51) gives for the equation of motion of the ω field

$$
\begin{aligned}
\partial^\mu F_{\mu\nu}(x) + m_\omega^2\, \omega_\nu(x) = \sum_B \Big\{ & g_{\omega B}\, \bar{\psi}_B(x)\gamma_\nu \psi_B(x) \\
& - \frac{f_{\omega B}}{2 m_B}\, \partial^\mu \left(\bar{\psi}_B(x)\sigma_{\mu\nu}\psi_B(x)\right)\Big\} \,, \qquad (5.52)
\end{aligned}
$$

which constitutes an inhomogeneous Proca equation.

The equation of motion of ρ mesons is similar to (5.52). The only differences originate from the isovectorial nature of the ρ, which has $I_\rho = 1$ (table 5.2), as opposed to the ω meson which is an isoscalar. This manifests itself in the occurrence of the Pauli isopin-matrix $\boldsymbol{\tau}$ in the equation of motion for the ρ meson,

$$
\begin{aligned}
\partial^\mu \boldsymbol{G}_{\mu\nu}(x) + m_\rho^2\, \boldsymbol{\rho}_\nu(x) = \sum_B \Big\{ & g_{\rho B}\, \bar{\psi}_B(x)\boldsymbol{\tau}\gamma_\nu \psi_B(x) \\
& - \frac{f_{\rho B}}{2 m_B}\, \partial^\lambda \left(\bar{\psi}_B(x)\boldsymbol{\tau}\sigma_{\mu\nu}\psi_B(x)\right)\Big\} \,. \qquad (5.53)
\end{aligned}
$$

The still missing meson, whose equation of motion will be derived next, is the pion. Differentiating $\mathcal{L}$ with respect to π leads to

$$
\frac{\partial \mathcal{L}}{\partial \boldsymbol{\pi}} = -\, m_\pi^2\, \boldsymbol{\pi} \,, \qquad (5.54)
$$

where use of the derivative of the scalar product $\boldsymbol{\pi}\cdot\boldsymbol{\pi} = \sum_i \pi^i \pi^i$ was made, from which one calculates

$$\frac{\partial}{\partial \pi^j}\left(\pi^i \pi^i\right) = 2\,\delta_{ij}\,\pi^i = 2\,\pi^j\,. \tag{5.55}$$

With the aid of the metric tensor, which, as before, is being used to shuffle indices up or down, one finds

$$\begin{aligned}\frac{\partial \mathcal{L}}{\partial(\partial_\mu \boldsymbol{\pi})} &= \frac{1}{2}\,\frac{\partial}{\partial(\partial_\mu \boldsymbol{\pi})}\left(g^{\nu\lambda}\partial_\lambda \boldsymbol{\pi}\cdot\partial_\nu \boldsymbol{\pi}\right) - \sum_B \frac{f_{\pi B}}{m_\pi}\,\bar{\psi}_B \gamma^5 \gamma^\mu \boldsymbol{\tau}\psi_B \\ &= \partial^\mu \boldsymbol{\pi} - \sum_B \frac{f_{\pi B}}{m_\pi}\,\bar{\psi}_B \gamma^5 \gamma^\mu \boldsymbol{\tau}\psi_B\,.\end{aligned} \tag{5.56}$$

Letting ∂_μ act on (5.56) gives

$$\partial_\mu \frac{\partial \mathcal{L}}{\partial(\partial_\mu \boldsymbol{\pi})} = \partial_\mu \partial^\mu \boldsymbol{\pi} \;-\; \sum_B \frac{f_{\pi B}}{m_\pi}\,\partial_\mu\left(\bar{\psi}_B \gamma^5 \gamma^\mu \boldsymbol{\tau}\psi_B\right)\,, \tag{5.57}$$

which, combined with (5.54), leads to the equation of motion for the pion field. It is of the form

$$\left(\partial^\mu \partial_\mu + m_\pi^2\right)\,\boldsymbol{\pi}(x) = \sum_B \frac{f_{\pi B}}{m_\pi}\,\partial^\mu\left(\bar{\psi}_B(x)\,\gamma_5\,\gamma_\mu\,\boldsymbol{\tau}\;\psi_B(x)\right)\,. \tag{5.58}$$

The equations of motion of all meson fields other than those already discussed above posses a mathematical structure that, depending on the meson's quantum nature which can be inferred from table 5.2, coincide with one of the above equations of motion. The equation of motion of the δ meson, for instance, coincides with the one of the σ meson except for the non-linear self-interactions and the isopin. Subject to these modifications one obtains

$$\left(\partial^\mu \partial_\mu + m_\delta^2\right)\boldsymbol{\delta}(x) = \sum_B g_{\delta B}\;\bar{\psi}_B(x)\,\boldsymbol{\tau}\,\psi_B(x)\,. \tag{5.59}$$

The equations of motion of ϕ and η meson fields are given by

$$\partial^\mu F_{\mu\nu} + m_\phi^2\,\phi_\nu = \sum_B \Big\{ g_{\phi B}\;\bar{\psi}_B \gamma_\nu \psi_B - \frac{f_{\phi B}}{2m_B}\,\partial^\mu\left(\bar{\psi}_B \sigma_{\mu\nu}\psi_B\right)\Big\}\,, \tag{5.60}$$

and

$$\left(\partial^\mu \partial_\mu + m_\eta^2\right)\,\eta(x) = \sum_B \frac{f_{\eta B}}{m_\eta}\,\partial^\mu\left(\bar{\psi}_B(x)\,\gamma_5\,\gamma_\mu\;\psi_B(x)\right)\,. \tag{5.61}$$

Solving the coupled equations of motion derived above for the numerous matter fields $(\psi_B, \sigma, \omega, \pi, \rho, \ldots)$ constitutes an extremely complicated problem. An exact numerical solution is probably out of reach for the foreseeable future. So, to carry the problem beyond the formal equations for the fields, it is unavoidable at this stage to introduce suitable approximation schemes. This can accomplished by means of introducing the so-called Green function technique [79, 84, 85, 125, 313]. Green functions are made up of time-ordered products of baryon or meson field operators. Instead of studying the equations of motion for the baryon fields themselves, one then deals with the equation of motion for the Green functions. On a first glance this may leave one with the impression that this renders the problem even more cumbersome than attempting to solve the field equations directly. This however is not true. As we shall see in the next section, the Green function technique will allows us to introduce physically motivated many-body approximations, which, combined with additional mathematical techniques (e.g. a spectral representation of the two-point Green function) will finally render the equations of motion numerically tractable. The mentioned many-body approximations are the (1) relativistic Hartree, (2) relativistic Hartree–Fock, and (3) relativistic latter approximation to the scattering T-matrix. The latter will be solved for the so-called $\boldsymbol{\Lambda}^{00}$ propagator as well as the more physical Brueckner–Hartree–Fock propagator. The level of sophistication and complexity of these three approximations increase considerably from (1) through (3).

5.3 Relativistic Green functions

The general definition of the $2n$-point Green function is given as the ground state expectation value of the time-ordered product of n baryon field operators, ψ_B, and n' operators $\bar{\psi}_B$ $(\equiv \psi_B^\dagger \gamma^0)$ in the form [117, 118, 125, 313, 314]

$$\begin{aligned} & \boldsymbol{g}_n^{B_1,\ldots,B_{n'}}(1,\ldots,n;1',\ldots,n') \\ & \quad = \mathrm{i}^n \; < \boldsymbol{\Phi}_0|\hat{T}\left(\psi_{B_1}(1)\ldots\psi_{B_n}(n)\,\bar{\psi}_{B_{n'}}(n')\ldots\bar{\psi}_{B_{1'}}(1')\right)|\boldsymbol{\Phi}_0 > . \end{aligned} \tag{5.62}$$

The quantity $|\boldsymbol{\Phi}_0>$ denotes the ground state of infinite nuclear matter, the integers $1 \equiv (x_1;\zeta_1)$ to $n \equiv (x_n;\zeta_n)$ stand for the spacetime coordinates $x_1 = (x_1^0, \boldsymbol{x}_1)$,...,$x_n = (x_n^0, \boldsymbol{x}_n)$ and spin and isospin quantum numbers ζ_1,...,ζ_n. Physically, the $2n$-point Green function describes the propagation of n baryons relative to a many-particle background, which, in our case, is the nuclear matter ground-state $|\boldsymbol{\Phi}_0>$. Its graphical representation, shown in figure 5.1, is characterized by n' ingoing and n outgoing baryon lines. The quantity $\hat{T}$ is the time-ordering operator. It orders the field operators

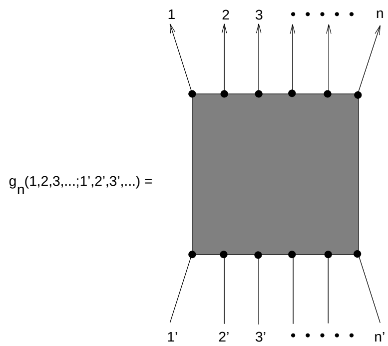

Figure 5.1. Graphical representation of the $2n$-point Green function defined in equation (5.62). The vertical lines denote the propagation of baryons in and out of the many-body vertex (shaded area).

according to their value of x^0, with the smallest at the right. $\hat{T}$ also includes the signature factor $(-1)^P$, where P is the number of permutations of fermion field operators needed to restore the original ordering. Of particular interest is the two-point Green function obtained from (5.62) by setting $n = 1$, i.e.

$$\boldsymbol{g}_1^{BB'}(x,\zeta;x',\zeta') \equiv \boldsymbol{g}_{\zeta\zeta'}^{BB'}(x,x') = \mathrm{i}\, < \boldsymbol{\Phi}_0|\hat{T}\big(\psi_B(x,\zeta)\,\bar{\psi}_{B'}(x',\zeta')\big)|\boldsymbol{\Phi}_0 > \, . \tag{5.63}$$

The physical interpretation of $\boldsymbol{g}_1^{BB'}$ is illustrated in figure 5.2. It is this Green function that attains particular attention in the field-theoretical treatment of the many-body system, for all the relevant observables of the system can be calculated from it. Writing out the time-ordering operator in (5.63) leads to

$$\boldsymbol{g}_{\zeta\zeta'}^{BB'}(x;x') = \Theta(x_0 - x_0')\,\boldsymbol{g}_{>}^{BB'}(x,\zeta;x',\zeta') + \Theta(x_0' - x_0)\,\boldsymbol{g}_{<}^{BB'}(x,\zeta;x',\zeta')\,, \tag{5.64}$$

with the definitions

$$\boldsymbol{g}_{>}^{BB'}(x,\zeta;x',\zeta') \equiv \mathrm{i}\, < \boldsymbol{\Phi}_0|\psi_B(x,\zeta)\,\bar{\psi}_{B'}(x',\zeta')|\boldsymbol{\Phi}_0 >\,, \tag{5.65}$$

$$\boldsymbol{g}_{<}^{BB'}(x,\zeta;x',\zeta') \equiv \, -\mathrm{i}\, < \boldsymbol{\Phi}_0|\bar{\psi}_{B'}(x',\zeta')\,\psi_B(x,\zeta)|\boldsymbol{\Phi}_0 > \, . \tag{5.66}$$

To find the equation of motion of $\boldsymbol{g}_1^{BB'}$ we apply the operator $(\mathrm{i}\gamma^\mu\partial_{\mu,1} - m_B)$ to the two-point Green function (5.64), which gives

$$(\mathrm{i}\,\gamma^\mu\partial_{\mu,1} - m_B)\,\boldsymbol{g}^{BB'}(x_1,x_1') = (\mathrm{i}\gamma^\mu\partial_{\mu,1} - m_B)$$

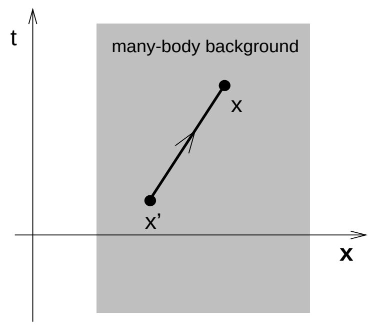

Figure 5.2. Physical interpretation of two-point Green function $\boldsymbol{g}_{>}(x, x')$ defined in equation (5.65): A baryon is created relative to the many-body background (shaded area) at spacetime point x', propagates to x, where it is removed again.

$$\times\, \mathrm{i}\, \Big\{ \Theta(t_1 - t_1') < \psi_B(x_1) \bar{\psi}_{B'}(x_1') > \, - \Theta(t_1' - t_1) < \bar{\psi}_{B'}(x_1') \psi_B(x_1) > \Big\} \; . \tag{5.67}$$

The subscript '1' attached to the partial derivative in (5.67) indicates that the derivative, explicitly given by

$$\gamma^\mu \partial_{\mu,1} \equiv \gamma^\mu \frac{\partial}{\partial x_1^\mu} = \gamma^0 \frac{\partial}{\partial t_1} + \boldsymbol{\gamma} \cdot \boldsymbol{\nabla}_1 \,, \tag{5.68}$$

is to be performed with respect to the spacetime coordinate x_1. Equation (5.67) thus reads

$$\begin{aligned}
(\mathrm{i}\, \gamma^\mu \partial_{\mu,1} - m_B)\, \boldsymbol{g}^{BB'}(x_1, x_1') = & - \gamma^0 \frac{\partial}{\partial t_1} \big\{ \Theta(t_1 - t_1') < \psi_B(x_1) \bar{\psi}_{B'}(x_1') > \big\} \\
& + \gamma^0 \frac{\partial}{\partial t_1} \big\{ \Theta(t_1' - t_1) < \bar{\psi}_{B'}(x_1') \psi_B(x_1) > \big\} \\
& + \mathrm{i}\, (\mathrm{i}\, \boldsymbol{\gamma} \cdot \boldsymbol{\nabla}_1 - m_B)\, \Theta(t_1 - t_1') < \psi_B(x_1) \bar{\psi}_{B'}(x_1') > \\
& - \mathrm{i}\, (\mathrm{i}\, \boldsymbol{\gamma} \cdot \boldsymbol{\nabla}_1 - m_B)\, \Theta(t_1' - t_1) < \bar{\psi}_{B'}(x_1') \psi_B(x_1) > \; .
\end{aligned} \tag{5.69}$$

Performing the time derivatives in (5.69) gives

$$\begin{aligned}
& \frac{\partial}{\partial t_1} \big\{ \Theta(t_1 - t_1') < \psi(x_1) \bar{\psi}(x_1') > \big\} = \\
& \delta(t_1 - t_1') < \psi(x_1) \bar{\psi}(x_1') > + \Theta(t_1 - t_1') < \frac{\partial \psi(x_1)}{\partial t_1} \bar{\psi}(x_1') > \,,
\end{aligned} \tag{5.70}$$

and

$$\frac{\partial}{\partial t_1}\left\{\Theta(t_1'-t_1) < \bar{\psi}(x_1')\psi(x_1) >\right\} =$$
$$-\,\delta(t_1'-t_1) < \bar{\psi}(x_1')\psi(x_1) > +\Theta(t_1'-t_1) < \bar{\psi}(x_1')\frac{\partial\psi(x_1)}{\partial t_1} > \, . \qquad (5.71)$$

For the sake of brevity, we have dropped the subscripts and superscripts B, B' in the side-calculations (5.70) and (5.71). Hereafter, use of this simplification will be made occasionally without further notice. With the aid of (5.70) and (5.71), equation (5.69) can now be written as

$$(\mathrm{i}\,\gamma^\mu\partial_{\mu,1} - m_B)\,\boldsymbol{g}^{BB'}(x_1,x_1') = -\gamma^0\delta(t_1-t_1') < \left\{\psi_B(x_1),\bar{\psi}_{B'}(x_1')\right\} >$$
$$-\,\gamma^0\Theta(t_1-t_1') < \frac{\partial\psi_B(x_1)}{\partial t_1}\bar{\psi}_{B'}(x_1') > +\gamma^0\Theta(t_1'-t_1) < \bar{\psi}_{B'}(x_1')\frac{\partial\psi_B(x_1)}{\partial t_1} >$$
$$+\,\mathrm{i}\,\Theta(t_1-t_1') < (\mathrm{i}\,\boldsymbol{\gamma}\cdot\boldsymbol{\nabla}_1 - m_B)\,\psi_B(x_1)\bar{\psi}_{B'}(x_1') >$$
$$-\,\mathrm{i}\,\Theta(t_1'-t_1) < \bar{\psi}_{B'}(x_1')\,(\mathrm{i}\,\boldsymbol{\gamma}\cdot\boldsymbol{\nabla}_1 - m_B)\,\psi_B(x_1) > \, . \qquad (5.72)$$

In the next step we employ the equation of motion for the baryon fields, derived in (5.36), to get rid of the two time derivatives in (5.72). For this purpose, we write (5.36) in the form

$$\Big(\mathrm{i}\,\gamma^0\frac{\partial}{\partial t_1} + \mathrm{i}\,\boldsymbol{\gamma}\cdot\boldsymbol{\nabla}_1 - m_B\Big)\psi_B(x_1)$$
$$= g_{\sigma B}\sigma(x_1)\psi_B(x_1) + g_{\omega B}\gamma^\mu\omega_\mu(x_1)\psi_B(x_1) \pm \,\dots\, , \qquad (5.73)$$

which, upon multiplying through with $-\mathrm{i}$ and rearranging terms, leads to

$$\gamma^0\frac{\partial}{\partial t_1}\psi_B(x_1) - \mathrm{i}\,(\mathrm{i}\,\boldsymbol{\gamma}\cdot\boldsymbol{\nabla}_1 - m_B)\,\psi_B(x_1)$$
$$= -\,\mathrm{i}\,g_{\sigma B}\,\sigma(x_1)\,\psi_B(x_1) - \mathrm{i}\,g_{\omega B}\,\gamma^\mu\omega_\mu(x_1)\,\psi_B(x_1) \pm \dots \qquad (5.74)$$

By means of substituting equation (5.74) into (5.72) and noticing that $\{\bar{\psi}(x),\psi(x')\} = \gamma^0\delta^3(\boldsymbol{x}-\boldsymbol{x}')$, according to (5.16), we then obtain

$$(\mathrm{i}\,\gamma^\mu\partial_{\mu,1} - m_B)\,\boldsymbol{g}^{BB'}(x_1,x_1') = -\,\delta^4(x_1-x_1')\,\delta_{BB'}$$
$$+\,\mathrm{i}\,g_{\sigma B}\big\{\Theta(t_1-t_1') < \psi_B(x_1)\sigma(x_1)\bar{\psi}_{B'}(x_1') >$$
$$-\,\Theta(t_1'-t_1) < \bar{\psi}_{B'}(x_1')\sigma(x_1)\psi_B(x_1) >\big\}$$
$$+\,\mathrm{i}\,g_{\omega B}\big\{\Theta(t_1-t_1') < \gamma^\mu\omega_\mu(x_1)\psi_B(x_1)\bar{\psi}_{B'}(x_1') >$$
$$-\,\Theta(t_1'-t_1) < \bar{\psi}_{B'}(x_1')\gamma^\mu\omega_\mu(x_1)\psi_B(x_1) >\big\}\, , \qquad (5.75)$$

which, upon introducing the time-ordering operator [cf. equations (5.63) and (5.64)] into this equation, leads to

$$
\begin{aligned}
&(\mathrm{i}\,\gamma^\mu \partial_{\mu,1} - m_B)\, \boldsymbol{g}^{BB'}(x_1, x_1') = -\,\delta^4(x_1 - x_1')\,\delta_{BB'} \\
&+ \mathrm{i}\, g_{\sigma B} < \hat{T}\left[\psi_B(x_1)\sigma(x_1)\bar{\psi}_{B'}(x_1')\right] > \\
&+ \mathrm{i}\, g_{\omega B} < \hat{T}\left[\gamma^\mu \omega_\mu(x_1)\psi_B(x_1)\bar{\psi}_{B'}(x_1')\right] > +\, \mathrm{i}\, g_{\rho B} \\
&< \hat{T}\Big[\Big(\gamma^\mu \psi_B(x_1)\boldsymbol{\tau}\cdot\boldsymbol{\rho}_\mu(x_1) + \frac{f_{\rho B}}{4 m_B}\sigma^{\mu\nu}\psi_B(x_1)\boldsymbol{\tau}\cdot\boldsymbol{G}_{\mu\nu}(x_1)\Big)\bar{\psi}_{B'}(x_1')\Big] > \\
&+ \mathrm{i}\,\frac{f_{\pi B}}{m_\pi} < \hat{T}\left[\gamma^5\gamma^\mu \psi_B(x_1)\left(\partial_\mu \boldsymbol{\tau}\cdot\boldsymbol{\pi}(x_1)\right)\bar{\psi}_{B'}(x_1')\right] > \,. \qquad (5.76)
\end{aligned}
$$

Equation (5.76) constitutes the Green-function analog to the inhomogeneous Dirac equation derived in (5.36). It still depends on the numerous unknown meson field operators, which we shall eliminate next. For this purpose we invert the meson field equations, derived in section 5.2, for the fields which are then substituted into (5.76). This will lead to the occurrence of higher-order Green functions in (5.76), which however can be approximated by lower-order ones.

To accomplish the inversion of the meson field equations, note that all meson field equations constitute partial differential equations for the fields,

$$D^{(M)}(x)\, M(x) = R^{(M)}(x)\,, \qquad (5.77)$$

where $D^{(M)}$ is a linear differential operator whose mathematical structure varies from meson to meson (M). The operator acts on a meson field $M(x)$. $R^{(M)}$ stands for the inhomogeneous part of each differential equation. Partial differential equations of this type can immediately be inverted if the free Green function Δ^{0M} associated with (5.77) is known. Δ^{0M} is defined as the solution of

$$D^{(M)}(x)\, \Delta^{0M}(x, x') = \delta(x - x')\,, \qquad (5.78)$$

from which it then follows that $M(x)$ of equation (5.77) is given by

$$M(x) = \int \mathrm{d}^4 y\, \Delta^{0M}(x, y)\, R^{(M)}(y)\,. \qquad (5.79)$$

To make this trick applicable to our problem the equations of motion for the meson Green functions need to be derived first.

We begin with defining the two-point Green function associated with the scalar σ mesons, which, in analogy to the two-point baryon Green function of equation (5.63), is defined as

$$\Delta^\sigma(x, x') = \mathrm{i}\, < \boldsymbol{\Phi}_0 | \hat{T}\left(\sigma(x)\sigma(x')\right) | \boldsymbol{\Phi}_0 > \,. \qquad (5.80)$$

A comparison of (5.77) with the σ-meson field equation (5.43) shows that the differential operator $D^{(M)}$ is given by

$$D^{(\sigma)} \equiv \partial^\mu \partial_\mu + m_\sigma^2 = \frac{\partial^2}{\partial t^2} - \boldsymbol{\nabla}^2 + m_\sigma^2 \,. \tag{5.81}$$

To find the result of $D^{(\sigma)} \Delta^\sigma$ let us consider first the action of the time derivative operator on the propagator Δ^σ, that is,

$$\frac{\partial^2}{\partial t^2} \left\{ \Theta(t-t') < \sigma(x)\sigma(x') > + \Theta(t'-t) < \sigma(x')\sigma(x) > \right\} . \tag{5.82}$$

The chain rule then leads for (5.82) to

$$\begin{aligned} &\frac{\partial}{\partial t} \left\{ \Theta(t-t') < \dot\sigma(x)\sigma(x') > + \Theta(t'-t) < \sigma(x')\dot\sigma(x) > \right\} \\ &\quad = \delta(t-t') < \dot\sigma(x)\sigma(x') > + \Theta(t-t') < \ddot\sigma(x)\sigma(x') > \\ &\quad - \delta(t'-t) < \sigma(x')\dot\sigma(x) > + \Theta(t'-t) < \sigma(x')\ddot\sigma(x) > \qquad (5.83) \\ &\quad = \delta(t-t') < [\dot\sigma(x), \sigma(x')] > + < \hat T \left(\ddot\sigma(x)\sigma(x') \right) > . \qquad (5.84) \end{aligned}$$

To get from equation (5.83) to (5.84), use of the commutator relation

$$[\dot\sigma(x), \sigma(x')] = \dot\sigma(x)\sigma(x') - \sigma(x')\dot\sigma(x) \tag{5.85}$$

and the definition of $\hat T$ has been made. To calculate the commutator in (5.84), let us replace $\dot\sigma$ with its associated conjugate field Π_σ,

$$\Pi_\sigma(t, \boldsymbol{x}) = \frac{\partial \mathcal{L}}{\partial \partial_0 \sigma(t, \boldsymbol{x})} = \dot\sigma(t, \boldsymbol{x}) \,, \tag{5.86}$$

which leads for the commutator to [see equation (5.17)]

$$[\dot\sigma(x), \sigma(x')] = [\Pi_\sigma(x), \sigma(x')] = -\,\mathrm{i}\, \delta^3(\boldsymbol{x} - \boldsymbol{x}') \,. \tag{5.87}$$

With the aid of (5.87), we arrive for (5.82) at the final result,

$$\frac{\partial^2}{\partial t^2} < \hat T \left(\sigma(x)\sigma(x') \right) > = -\,\mathrm{i}\, \delta^4(x - x') + < \hat T \left(\ddot\sigma(x)\sigma(x') \right) > . \tag{5.88}$$

Now we have all ingredients at hand that are required to calculate $D^{(\sigma)}\Delta^\sigma$. With the help of (5.88), one then gets for the Δ^σ propagator,

$$\begin{aligned} \left(\partial^\mu \partial_\mu + m_\sigma^2 \right) \Delta^\sigma(x, x') &= \delta^4(x - x') + \mathrm{i}\, < \hat T \left(\ddot\sigma(x)\sigma(x') \right) > \\ &\quad + \left(-\Delta_x + m_\sigma^2 \right) \Delta^\sigma(x, x') \,. \end{aligned} \tag{5.89}$$

Substituting equation (5.80) for Δ^σ then leads for the right-hand side of this equation to

$$\delta^4(x-x') + \mathrm{i} < \hat{T}\left\{\left[\left(\partial^\mu \partial_\mu + m_\sigma^2\right)\sigma(x)\right]\sigma(x')\right\} > . \tag{5.90}$$

The expression in square brackets can be replaced with its source term, equation (5.43), which leads to the desired result for the equation of motion of the full σ-meson propagator, given by

$$\begin{aligned}\left(\partial^\mu \partial_\mu + m_\sigma^2\right)\Delta^\sigma(x,x') &= \delta^4(x-x') \\ &\quad - \mathrm{i}\sum_B g_{\sigma B} < \hat{T}\big(\bar{\psi}_B(x^+)\psi_B(x)\sigma(x')\big) > . \end{aligned}\tag{5.91}$$

By definition, the free meson Green function associated with (5.91), denoted by $\Delta^{0\sigma}$, is given as the solution of

$$\left(\partial^\mu \partial_\mu + m_\sigma^2\right)\Delta^{0\sigma}(x,x') = \delta^4(x-x') . \tag{5.92}$$

Four-dimensional Fourier transformation of (5.92) into energy–momentum space, as outlined in section B.2 of appendix B, leads for the meson propagator to

$$\Delta^{0\sigma}(p) = -\frac{1}{p_0^2 - \boldsymbol{p}^2 - m_\sigma^2 + \mathrm{i}\,\eta} . \tag{5.93}$$

Now we have all ingredients at hand to invert the equation of motion of the σ field. Proceeding as described in equations (5.77) through (5.79), we get for the σ-meson field

$$\sigma(x) = -\sum_{B'} g_{\sigma B'} \int \mathrm{d}^4x'\ \Delta^{0\sigma}(x,x')\ \bar{\psi}_{B'}(x')\psi_{B'}(x') . \tag{5.94}$$

In the next step we invert the field equations of the vector mesons ω^μ and ρ^μ. Their associated two-point Green functions are given by

$$\left(\mathcal{D}^\omega\right)^{\mu\nu}(x,x') = \mathrm{i} < \mathbf{\Phi}_0|\hat{T}\left(\omega^\mu(x)\omega^\nu(x')\right)|\mathbf{\Phi}_0 > \tag{5.95}$$

and

$$\left(\mathcal{D}^\rho\right)^{\mu\nu}(x,x';r,r') = \mathrm{i} < \mathbf{\Phi}_0|\hat{T}\left(\rho^{r\mu}(x)\rho^{r'\nu}(x')\right)|\mathbf{\Phi}_0 > , \tag{5.96}$$

respectively. The equations of motion of these two propagators are obtained in complete analogy to the σ field. What complicates matter is the vectorial nature of these mesons. Moreover the ρ field additionally is a three-vector in isospin space. We begin with writing the left hand side of (5.52) as

$$\partial^\lambda F_{\lambda\nu} + m_\omega^2\omega_\nu = \left(\partial^\lambda\partial_\lambda \delta_\nu{}^\mu - \partial^\mu\partial_\nu + m_\omega^2\delta_\nu{}^\mu\right)\omega_\mu , \tag{5.97}$$

which leads for the field equation of the ω meson to

$$\left(\partial^\lambda\partial_\lambda\delta_\nu{}^\mu - \partial^\mu\partial_\nu + m_\omega^2\delta_\nu{}^\mu\right)\omega_\mu = \sum_B\Big\{g_{\omega B}\bar{\psi}_B\gamma_\nu\psi_B - \frac{f_{\omega B}}{2m_B}\,\partial^\lambda\left(\bar{\psi}_B\sigma_{\lambda\nu}\psi_B\right)\Big\}. \tag{5.98}$$

Next let us define

$$\mathcal{D}^{0\omega}_{\mu\kappa}(x,x') = \left(g_{\mu\kappa} + \frac{\partial_\mu\partial_\kappa}{m_\omega^2}\right)\Delta^{0\omega}(x,x')\,, \tag{5.99}$$

whose Fourier transform reads (cf. appendix B.2)

$$\mathcal{D}^{0\omega}_{\mu\kappa}(p) = \left(g_{\mu\kappa} - \frac{p_\mu p_\kappa}{m_\omega^2}\right)\Delta^{0\omega}(p)\,, \tag{5.100}$$

with $\Delta^{0\omega}(p)$ as in (5.93). It is readily shown that the propagator (5.99) obeys

$$\left(\partial^\lambda\partial_\lambda\delta_\nu{}^\mu - \partial^\mu\partial_\nu + m_\omega^2\delta_\nu{}^\mu\right)\mathcal{D}^{0\omega}_{\mu\kappa}(x,x') = g_{\nu\kappa}\;\delta^4(x-x')\,. \tag{5.101}$$

The field equation (5.52) can now be inverted following the procedure outlined just above. One obtains

$$\omega_\mu(x) = \int \mathrm{d}^4x'\;\mathcal{D}^{0\omega}_{\mu\kappa}(x,x')\times \sum_B\Big\{g_{\omega B}\bar{\psi}_B(x')\gamma^\kappa\psi_B(x') - \frac{f_{\omega B}}{2m_B}\,\partial^\lambda\left(\bar{\psi}_B(x')\sigma_\lambda{}^\kappa\psi_B(x')\right)\Big\}\,. \tag{5.102}$$

The corresponding expressions for the ρ-meson field are very similar to those of the ω-meson field derived in equations (5.97) to (5.102). The only differences arise from the isovectorial nature of the ρ-meson field. It therefore carries an extra index r (=1,2,3) which discriminates between the meson's three isospin components. Bearing this in mind, one can proceed in complete analogy to above. The individual equations are then given by

$$\left(\partial^\lambda\partial_\lambda\delta_\nu{}^\mu - \partial^\mu\partial_\nu + m_\rho^2\delta_\nu{}^\mu\right)\rho^r_\mu = \sum_B\Big\{g_{\rho B}\;\bar{\psi}_B\tau^r\gamma_\nu\psi_B - \frac{f_{\rho B}}{2m_B}\,\partial^\lambda\left(\bar{\psi}_B\tau^r\sigma_{\lambda\nu}\psi_B\right)\Big\}\,, \tag{5.103}$$

which defines the free ρ-meson Green function via the equation

$$\left(\partial^\lambda\partial_\lambda\delta_\nu{}^\mu - \partial^\mu\partial_\nu + m_\rho^2\delta_\nu{}^\mu\right)\mathcal{D}^{0\rho}_{\mu\kappa}(x,x';r,r') = g_{\nu\kappa}\;\delta^4(x-x')\,\delta_{rr'}\,, \tag{5.104}$$

with

$$\mathcal{D}^{0\rho}_{\mu\kappa}(x,x';r,r') = \left(g_{\mu\kappa} + \frac{\partial_\mu\partial_\kappa}{m_{\rho,r}^2}\right)\Delta^{0\rho}(x,x';r,r')\,, \tag{5.105}$$

and [$\Delta^{0\rho}(p)$ as in equation (5.93)]

$$\mathcal{D}^{0\rho}_{\mu\kappa}(p) = \left(g_{\mu\kappa} - \frac{p_\mu p_\kappa}{m^2_{\rho,r}} \right) \Delta^{0\rho}(p) \, . \tag{5.106}$$

The ρ-meson field is therefore given by

$$\rho^r_\mu(x) = \sum_{r'} \int \mathrm{d}^4x' \; \mathcal{D}^{0\rho}_{\mu\kappa}(x, x'; r, r') \\ \times \sum_B \Big\{ g_{\rho B} \bar\psi_B(x') \tau^r \gamma^\kappa \psi_B(x') - \frac{f_{\rho B}}{2m_B} \, \partial^\lambda \left(\bar\psi_B(x') \tau^{r'} \sigma_\lambda{}^\kappa \psi_B(x') \right) \Big\} \, . \tag{5.107}$$

The π mesons, being an isovector particle too, also carries an index r. Its two-point function is given by

$$\Delta^{0\pi}(x, x'; r, r') = \mathrm{i} \, < \mathbf{\Phi}_0 | \hat T \left(\pi^r(x) \pi^{r'}(x') \right) | \mathbf{\Phi}_0 > , \tag{5.108}$$

which obeys

$$\left(\partial^\mu \partial_\mu + m^2_\pi \right) \Delta^{0\pi}(x, x'; r, r') = \delta^4(x - x') \, \delta_{rr'} \, . \tag{5.109}$$

The momentum-space representation of $\Delta^{0\pi}(x, x'; r, r')$ is given by

$$\Delta^{0\pi}(p) = - \frac{1}{p_0^2 - \boldsymbol{p}^2 - m^2_{\pi,r} + \mathrm{i}\, \eta} \, . \tag{5.110}$$

The equation for the pion field then follows as

$$\pi^r(x) = \sum_{B,r'} \frac{f_{\pi B}}{m_\pi} \int \mathrm{d}^4x' \; \Delta^{0\pi}(x, x'; r, r') \; \partial_{\mu, x'} \left(\bar\psi_B(x') \gamma^5 \gamma^\mu \tau^{r'} \psi_B(x') \right) \, . \tag{5.111}$$

With the aid of the explicit expressions for the meson fields derived in equations (5.94), (5.102), (5.107) and (5.111), the meson fields in (5.76) can now be replaced with meson Green functions. Dropping the tensor part of the ρ meson (term $\propto f_{\rho B}$) for the moment, which can be easily restored again, as we shall see later, this yields for (5.76) to ($\partial\!\!\!/ \equiv \gamma^\mu \partial_\mu$)

$$\left(\mathrm{i} \, \partial\!\!\!/_{x_1} - m_B \right) \boldsymbol{g}^{BB'}_1(x_1, x'_1) = - \, \delta^4(x_1 - x'_1) \, \delta_{BB'} + F^{BB'}(x_1, x'_1) \, , \tag{5.112}$$

where $F^{BB'}$ is given by [$\boldsymbol{\tau} \Delta^{0\pi}(x, x') \boldsymbol{\tau} \equiv \sum_{r,r'} \tau^r \Delta^{0\pi}(x, x'; r, r') \tau^{r'}$]

$$F^{BB'}(x_1, x'_1) = \mathrm{i} \sum_{B''} \int \mathrm{d}^4x' \; \big\{ - \, g_{\sigma B} \, g_{\sigma B''} \; \Delta^{0\sigma}(x_1, x')$$

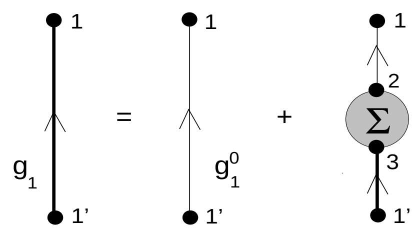

Figure 5.3. Graphical representation of Dyson's equation for the self-consistent two-point baryon Green function $\boldsymbol{g}_1$. The quantity $\boldsymbol{g}_1^0$ denotes the propagator of free baryons, which do not feel the nuclear medium (i.e. $\boldsymbol{\Sigma} \equiv 0$). The momentum-space representation of Dyson's equation is given in (5.126).

$$
\begin{aligned}
&\times < \hat{T}\left(\psi_B(x_1)\bar{\psi}_{B''}(x'^{+})\psi_{B''}(x')\bar{\psi}_{B'}(x'_1)\right) > \\
&+ g_{\omega B}\, g_{\omega B''}\; \gamma^\mu \mathcal{D}^{0\omega}_{\mu\kappa}(x_1, x') < \hat{T}\left(\psi_B(x_1)\bar{\psi}_{B''}(x'^{+})\gamma^\kappa \psi_{B''}(x')\bar{\psi}_{B'}(x'_1)\right) > \\
&+ g_{\rho B}\, g_{\rho B''}\; \gamma^\mu \boldsymbol{\tau} \mathcal{D}^{0\rho}_{\mu\kappa}(x_1, x') < \hat{T}\left(\psi_B(x_1)\bar{\psi}_{B''}(x'^{+})\boldsymbol{\tau}\, \gamma^\kappa \psi_{B''}(x')\bar{\psi}_{B'}(x'_1)\right) > \\
&+ \frac{f_{\pi B}}{m_\pi}\,\frac{f_{\pi B''}}{m_\pi}\; \gamma^5 \gamma^\mu \left(\partial_{\mu, x_1} \boldsymbol{\tau} \Delta^{0\pi}(x_1, x')\right) \\
&\quad \times < \hat{T}\left(\psi_B(x_1)\partial_{\kappa, x'}\left[\bar{\psi}_{B''}(x'^{+})\gamma^5\, \gamma^\kappa\, \boldsymbol{\tau} \psi_{B''}(x')\right]\bar{\psi}_{B'}(x'_1)\right) > \big\}\,.
\end{aligned}
\tag{5.113}
$$

The major mathematical advantage of (5.112) over (5.76) is that instead of the meson fields themselves, we are now dealing with the expectation values of time-ordered products of baryon-field operators which, upon closer inspection [cf. equation (5.62)] turn out to constitute noting else but four-point Green functions, $\boldsymbol{g}_2$. These have the advantage over the meson fields that physically motivated many-body approximations can be introduced that allow one to solve equation (5.112) in a physically transparent manner, as will be discussed subsequently.

Before, however, we shall introduce two more field-theoretical concepts, namely the Dyson equation and the self-energy $\boldsymbol{\Sigma}^B$ of a baryon, which is also known as mass operator, or effective single-particle potential). Both, the Dyson equation as well as $\boldsymbol{\Sigma}^B$ play an equally important role in field theory than the baryon propagators, $\boldsymbol{g}_1$. Let us begin with decomposing $F^{BB'}$ of (5.113) in the following manner,

$$
F^{BB'}(x_1, x'_1) \equiv \sum_{B''} \int \mathrm{d}^4x'\; \boldsymbol{\Sigma}^{BB''}(x_1, x')\; \boldsymbol{g}_1^{B''B'}(x', x'_1)\,. \tag{5.114}
$$

The equation of motion for $\boldsymbol{g}_1^{BB'}$ derived in (5.112) can then be written as

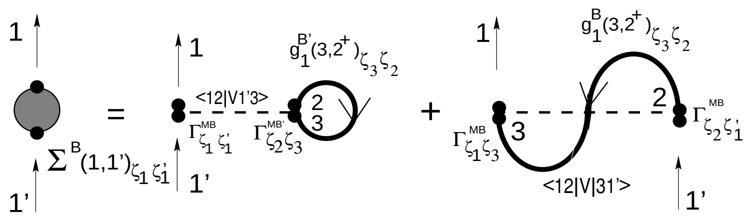

Figure 5.4. Diagrammatic equation of baryon self-energy, $\mathbf{\Sigma}^B$, in Hartree–Fock approximation. The matrix elements $< 12|\mathbf{V}^{BB'}|1'3 >$ and $< 12|\mathbf{V}^{BB'}|31' >$, defined in equation (5.151), describe the meson-exchange interaction in the direct (Hartree) and exchange (Fock) term of $\mathbf{\Sigma}^B$, respectively. Γ^{MB} and $\Gamma^{MB'}$ denote baryon–meson vertices ($M = \sigma, \omega, \ldots$; $B = p, n, \Sigma^{\pm}, \ldots$). The analytic expression of $\mathbf{\Sigma}^B(1, 1')$ can be inferred from (5.115) in reference to (5.120), or, alternatively, from equations (7.2) and (7.3).

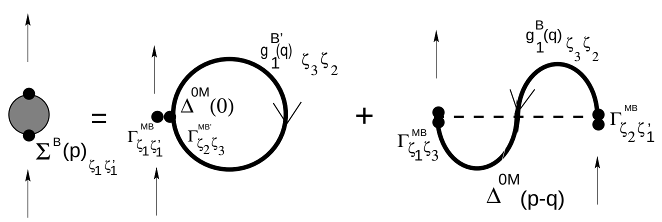

Figure 5.5. Diagrammatic representation of Hartree–Fock baryon self-energy $\mathbf{\Sigma}^B$ in momentum space. $\Delta^{0M}(0)$ and $\Delta^{0M}(p - q)$ denote meson propagators, derived, for instance, in equations (5.93) and (5.100). All other quantities are explained in figure 5.4. For the analytic form of $\mathbf{\Sigma}^B(p)$, see, for example, equations (5.134) through (5.142).

$$
\begin{aligned}
\left(\mathrm{i}\,\partial\!\!\!/_{x_1} - m_B\right) \boldsymbol{g}_1^{BB'}(x_1, x_1') = &-\delta^4(x_1 - x_1')\,\delta_{BB'} \\
&+ \sum_{B''} \int \mathrm{d}^4x'\ \mathbf{\Sigma}^{BB''}(x_1, x')\ \boldsymbol{g}_1^{B''B'}(x', x_1')\,. \quad (5.115)
\end{aligned}
$$

Employing the method outlined in connection with (5.77), equation (5.115) can be readily transformed into the alternative form

$$
\boldsymbol{g}_1^{BB'}(x_1, x_1') = \boldsymbol{g}_1^{0BB'}(x_1, x_1') - \sum_{B_2, B_3} \int \mathrm{d}^4x_2 \int \mathrm{d}^4x_3\ \boldsymbol{g}_1^{0BB_2}(x_1, x_2)
$$

$$\times\, \boldsymbol{\Sigma}^{B_2 B_3}(x_2, x_3)\, \boldsymbol{g}_1^{B_3 B'}(x_3, x_1')\,, \quad (5.116)$$

Since we shall be dealing with scenarios where a given baryon does not transform into another baryon along its path $x_1' \to x_1$ (see figure 5.2), we may write $\boldsymbol{g}^{BB'} = \delta_{BB'}\, \boldsymbol{g}^B$. Incorporating this feature into (5.116) leads for the Dyson equation to

$$\boldsymbol{g}_1^B(x_1, x_1') = \boldsymbol{g}_1^{0B}(x_1, x_1') - \int \mathrm{d}^4 x_2 \int \mathrm{d}^4 x_3\; \boldsymbol{g}_1^{0B}(x_1, x_2)\, \boldsymbol{\Sigma}^B(x_2, x_3)\, \boldsymbol{g}_1^B(x_3, x_1'). \quad (5.117)$$

Its graphical representation is illustrated in figure 5.3, with the corresponding diagrammatic representation of the self-energy shown in figure 5.4. The representation of the latter diagrams in momentum space is given in figure 5.5.

5.4 Relativistic Hartree and Hartree–Fock approximation

The two simplest many-body approximations that will be introduced in this volume are the relativistic Hartree and the relativistic Hartree–Fock (HF) approximations. The mathematical structure of the latter is already considerably more complicated than the former whose self-energies, as we shall see later, depend only on density but neither on energy nor momentum. Besides that there are quantitative differences between both approximations which originate from the Fock terms contained in the HF approximation and the different coupling constants of both theories. This is specifically the case for the coupling constant of the ρ meson, which plays a crucial role for the composition of neutron star matter.

The relativistic HF approximation is obtained by factorizing the four-point baryon Green functions in (5.113), given by

$$\begin{aligned} &< \hat{T}\left(\psi_B(x_1)\bar{\psi}_{B''}(x'^{+})\psi_{B''}(x')\bar{\psi}_{B'}(x_1')\right) > \\ &\qquad = - < \hat{T}\left(\psi_B(x_1)\psi_{B''}(x')\bar{\psi}_{B''}(x'^{+})\bar{\psi}_{B'}(x_1')\right) > \\ &\qquad = \boldsymbol{g}_2(x_1 B, x' B''; x'^{+} B'', x_1' B')\,, \end{aligned} \quad (5.118)$$

into products of two-point baryon Green functions,

$$\begin{aligned} &\boldsymbol{g}_2(x_1 B, x' B''; x'^{+} B'', x_1' B) \\ &\approx \boldsymbol{g}_1(x_1 B, x_1' B')\, \boldsymbol{g}_1(x' B'', x'^{+} B'') - \boldsymbol{g}_1(x_1 B, x'^{+} B'')\, \boldsymbol{g}_1(x' B'', x_1' B')\, \delta_{BB''} \\ &\equiv \boldsymbol{g}_1^{BB'}(x_1, x_1')\, \boldsymbol{g}_1^{B''B''}(x', x'^{+}) - \boldsymbol{g}_1^{BB''}(x_1, x'^{+})\, \boldsymbol{g}_1^{B''B'}(x', x_1')\, \delta_{BB''}\,. \end{aligned} \quad (5.119)$$

A graphical illustration of the factorization scheme is displayed in figure 5.6. The first term on the right-hand side of (5.119), referred to as Hartree (or

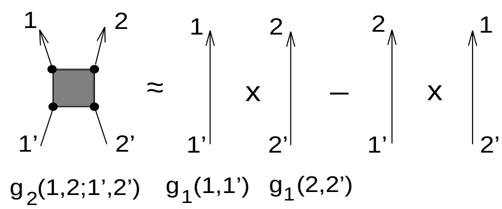

Figure 5.6. Factorization scheme of four-point baryon Green function, $\boldsymbol{g}_2$, into antisymmetrized products of two-point baryon Green functions, $\boldsymbol{g}_1 \times \boldsymbol{g}_1$ [cf. (5.119)]. Direct (Hartree) and exchange (Fock) contribution are shown. This factorization scheme truncates the many-body equations at the Hartree–Fock level.

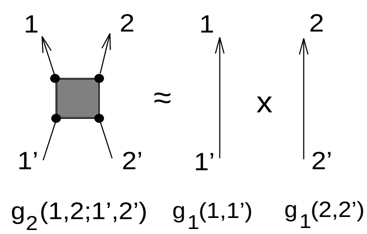

Figure 5.7. Factorization scheme of four-point baryon Green function, $\boldsymbol{g}_2$, into a product of two-point baryon Green functions, $\boldsymbol{g}_1 \times \boldsymbol{g}_1$. Keeping only the first term of (5.119), this truncates the many-body equations at the Hartree level.

direct) term, truncates the many-body equations at the relativistic Hartree level. The second term, referred to as Fock (or exchange) contribution, whose final states are interchanged, leads to the HF approximation. Neglecting the Fock term in (5.119) leads to the frequently used Hartree approximation (figure 5.7). A characteristic feature of these approximations is that both baryons propagate independent from each other in the medium, aside from effects stemming from the Pauli exclusion principle. Any *dynamical* correlations between the baryons are completely lost for these approximations, in sharp contrast to the relativistic ladder (Brueckner–Hartree–Fock type) approximation where an effective **T**-matrix in matter is calculated form one-boson-exchange interactions. We shall follow up this approximation in section 5.5 and chapters 9 and 10.

Substituting the HF approximated $\boldsymbol{g}_2$ function of (5.119) into equation (5.113) leads to an equation of motion for the two-point baryon

Green function given by

$$\begin{aligned}
&\big(\mathrm{i}\,\partial\!\!\!/_{x_1} - m_B\big)\, \boldsymbol{g}_1^{BB'}(x_1, x_1') = -\,\delta^4(x_1 - x_1')\,\delta_{BB'} \\
&+ \mathrm{i}\sum_{B''}\int \mathrm{d}^4x' \,\big\{-g_{\sigma B}\, g_{\sigma B''}\ \Delta^{0\sigma}(x_1, x') + \mathrm{i}\, g_{\omega B}\, g_{\omega B''}\ \gamma^\mu\, \gamma^\kappa\, \mathcal{D}^{0\omega}_{\mu\kappa}(x_1, x') \\
&\qquad + g_{\rho B}\, g_{\rho B''}\ \big(\gamma^\mu \boldsymbol{\tau}\big)\,\big(\gamma^\kappa \boldsymbol{\tau}\big)\,\mathcal{D}^{0\rho}_{\mu\kappa}(x_1, x') \qquad\qquad (5.120)\\
&\qquad + \frac{f_{\pi B}}{m_\pi}\,\frac{f_{\pi B''}}{m_\pi}\,\big(\gamma^5\gamma^\mu\boldsymbol{\tau}\partial_{\mu,x_1}\big)\,\big(\gamma^5\gamma^\kappa\boldsymbol{\tau}\partial_{\kappa,x'}\big)\,\Delta^{0\pi}(x_1, x')\big\} \\
&\times \big\{\boldsymbol{g}_1^{BB'}(x_1, x_1')\,\boldsymbol{g}_1^{B''B''}(x', x'^+) - \boldsymbol{g}_1^{BB''}(x_1, x'^+)\,\boldsymbol{g}_1^{B''B'}(x', x_1')\ \delta_{BB''}\big\}\,.
\end{aligned}$$

In the next step we transform (5.120) into four-momentum space. There the equations become much simpler, since we are dealing with a spatially uniform system that is invariant under translations. All functions in (5.120) therefore depend only on the coordinate differences, as already indicated for the argument of the δ-function in (5.120). The four-dimensional Fourier transforms in these coordinates are given for the Hartree term by expressions like (cf. appendix B.2)

$$\begin{aligned}
&\int \mathrm{d}^4x'\ \Delta^{0\sigma}(x_1 - x')\ \boldsymbol{g}_1^{BB'}(x_1 - x_1')\ \boldsymbol{g}_1^{B''B''}(x' - x'^+) \\
&= \int \frac{\mathrm{d}^4q}{(2\pi)^4}\int \frac{\mathrm{d}^4p}{(2\pi)^4}\, \mathrm{e}^{\mathrm{i}\eta q^0}\ \mathrm{e}^{-\mathrm{i}p(x_1 - x_1')}\ \Delta^{0\sigma}(0)\ \boldsymbol{g}_1^{BB'}(p)\ \boldsymbol{g}_1^{B''B''}(q)\,, \qquad (5.121)
\end{aligned}$$

depending on the meson propagator, and for the respective Fock terms by

$$\begin{aligned}
&\int \mathrm{d}^4x'\,\Delta^{0\sigma}(x_1 - x')\,\boldsymbol{g}_1^{BB''}(x_1 - x'^+)\,\boldsymbol{g}_1^{B''B'}(x' - x_1') \\
&= \int \frac{\mathrm{d}^4q}{(2\pi)^4}\int \frac{\mathrm{d}^4p}{(2\pi)^4}\, \mathrm{e}^{\mathrm{i}\eta q^0}\ \mathrm{e}^{-\mathrm{i}p(x_1 - x_1')}\ \Delta^{0\sigma}(p - q)\,\boldsymbol{g}_1^{BB''}(p)\,\boldsymbol{g}_1^{B''B'}(q)\,. \qquad (5.122)
\end{aligned}$$

Equation (5.120) can then be written very neatly as

$$(p\!\!\!/ - m_B)\,\boldsymbol{g}_1^B(p) = -\,1\, +\, \boldsymbol{\Sigma}^B(p)\ \boldsymbol{g}_1^B(p)\,, \qquad (5.123)$$

which constitutes Dyson's equation (5.115) in momentum space, with the baryon self-energy in the Hartree–Fock approximation given by (see also the results derived in equations (5.135) through (5.142) as well as in chapter D)

$$\begin{aligned}
\boldsymbol{\Sigma}^B(p) \equiv\ -\,\mathrm{i}\sum_{B'} g_{\sigma B}\, g_{\sigma B'}\int \frac{\mathrm{d}^4q}{(2\pi)^4}\, \mathrm{e}^{\mathrm{i}\eta q^0}\big\{&\Delta^{0\sigma}(0)\ \boldsymbol{g}_1^{B'}(q) \\
&- \delta_{BB'}\Delta^{0\sigma}(p - q)\ \boldsymbol{g}_1^{B}(q)\big\}
\end{aligned}$$

$$
\begin{aligned}
&+\mathrm{i}\sum_{B'} g_{\omega B}\, g_{\omega B'} \int \frac{\mathrm{d}^4 q}{(2\pi)^4}\, \mathrm{e}^{\mathrm{i}\eta q^0} \big\{ \gamma^\mu\, \gamma^\nu\, \mathcal{D}^{0\omega}_{\mu\nu}(0)\, \boldsymbol{g}_1^{B'}(q) \\
&\qquad\qquad - \delta_{BB'} \gamma^\mu\, \gamma^\nu\, \mathcal{D}^{0\omega}_{\mu\nu}(p-q)\, \boldsymbol{g}_1^{B}(q) \big\} \\
&+\mathrm{i}\sum_{B'} g_{\rho B}\, g_{\rho B'} \int \frac{\mathrm{d}^4 q}{(2\pi)^4}\, \mathrm{e}^{\mathrm{i}\eta q^0} \big\{ \big(\gamma^\mu \boldsymbol{\tau}\big)\, \big(\gamma^\nu \boldsymbol{\tau}\big)\, \mathcal{D}^{0\rho}_{\mu\nu}(0)\, \boldsymbol{g}_1^{B'}(q) \\
&\qquad\qquad - \delta_{BB'} \big(\gamma^\mu \boldsymbol{\tau}\big)\, \big(\gamma^\nu \boldsymbol{\tau}\big)\, \mathcal{D}^{0\rho}_{\mu\nu}(p-q)\, \boldsymbol{g}_1^{B}(q) \big\} \\
&+\mathrm{i}\Big(\frac{f_{\pi B}}{m_B}\Big)^2 \int \frac{\mathrm{d}^4 q}{(2\pi)^4}\, \mathrm{e}^{\mathrm{i}\eta q^0} \big\{ \big(\gamma^5 \gamma^\lambda \boldsymbol{\tau}\big) \big(\gamma^5 \gamma^\mu \boldsymbol{\tau}\big) (p-q)_\lambda \\
&\qquad\qquad \times (p-q)_\mu\, \Delta^{0\pi}(p-q)\, \boldsymbol{g}_1^{B}(q) \big\} \,. \qquad (5.124)
\end{aligned}
$$

The two-point baryon function associated with a non-interacting many-body system, characterized by $\boldsymbol{\Sigma}^B \equiv 0$, follows from (5.123) in the form

$$
\boldsymbol{g}_1^{0B}(p) = -\left(\not{p} - m_B\right)^{-1} \,. \qquad (5.125)
$$

Substituting (5.125) into (5.123) and multiplying both sides with $\boldsymbol{g}_1^{0B}$ gives the momentum-space analog of Dyson's equation in coordinate space, derived in (5.117), in the form

$$
\boldsymbol{g}^B_{1\,\zeta_1\zeta_2}(p) = \boldsymbol{g}^{0B}_{1\,\zeta_1\zeta_2}(p) - \boldsymbol{g}^{0B}_{1\,\zeta_1\zeta_1'}(p)\, \boldsymbol{\Sigma}^B_{\zeta_1'\zeta_2'}(p)\, \boldsymbol{g}^B_{1\,\zeta_2'\zeta_2}(p) \,. \qquad (5.126)
$$

Equations (5.123) and (5.126) constitute matrix equations in Dirac (spin) and isospin space. The corresponding indices are denoted by α and i, respectively, which we combine frequently to the single symbol ζ $[\equiv (\alpha, i)]$. Assigning the spin and isospin indices to $\boldsymbol{g}_1^B$ and $\boldsymbol{\Sigma}^B$ leads for (5.123) to

$$
(\not{p} - m_B)_{\zeta_1\zeta_1'}\ \boldsymbol{g}^B_{\zeta_1'\zeta_2}(p) \ = \ -\,\delta_{\zeta_1\zeta_2} \ + \ \boldsymbol{\Sigma}^B_{\zeta_1\zeta_1'}(p)\, \boldsymbol{g}^B_{\zeta_1'\zeta_2}(p) \,, \qquad (5.127)
$$

with the σ-mesons self-energy matrix $\boldsymbol{\Sigma}^B_{\zeta_1\zeta_1'}(p)$ given by

$$
\begin{aligned}
\boldsymbol{\Sigma}^B_{\zeta_1\zeta_1'}(p)\Big|_\sigma &= -\mathrm{i}\ (g_{\sigma B}\,\mathbf{1})_{\zeta_1\zeta_1'} \sum_{B'} (g_{\sigma B'}\,\mathbf{1})_{\zeta_3\zeta_4} \int \frac{\mathrm{d}^4 q}{(2\pi)^4}\, \mathrm{e}^{\mathrm{i}\eta q^0}\, \Delta^{0\sigma}(0)\, \boldsymbol{g}^{B'}_{\zeta_4\zeta_3}(q) \\
&+\mathrm{i}\ (g_{\sigma B}\,\mathbf{1})_{\zeta_1\zeta_3} \int \frac{\mathrm{d}^4 q}{(2\pi)^4}\, \mathrm{e}^{\mathrm{i}\eta q^0}\, \Delta^{0\sigma}(p-q)\, \boldsymbol{g}^{B'}_{\zeta_3\zeta_2}(q)\ (g_{\sigma B}\,\mathbf{1})_{\zeta_2\zeta_1'} \,. \qquad (5.128)
\end{aligned}
$$

The other mesons of our collection lead to the same matrix structure for $\boldsymbol{\Sigma}$ as in (5.128), aside from deviations that originate from the different baryon–meson couplings. As known from (5.7) through (5.10), these are simplest for the scalar σ and most complicated for the vector mesons ω and ρ. Before we shall turn our interest to the latter mesons, however, let us point out a few notational simplifications concerning the summations over the spin and isospin indices in (5.128). For instance, the coupling constant $(g_{\sigma B'}\mathbf{1})_{\zeta_3\zeta_4}$ in the Hartree term of (5.128) can be combined with the two-point Green function $\boldsymbol{g}^{B'}_{\zeta_4\zeta_3}(q)$ there according to

$$(g_{\sigma B'}\,\mathbf{1})_{\zeta_3\zeta_4}\;\boldsymbol{g}^{B'}_{\zeta_4\zeta_3}(q) \equiv g_{\sigma B'}\;\mathrm{Tr}\left(\mathbf{1}\,\boldsymbol{g}^{B'}(q)\right) \equiv g_{\sigma B'}\;\mathrm{Tr}\;\boldsymbol{g}^{B'}(q)\,. \qquad (5.129)$$

The trace in (5.129), denoted Tr, sums the diagonal elements of the matrix $\mathbf{1}\,\boldsymbol{g}^B(q) = \boldsymbol{g}^B(q)$. One of its interesting properties, which we shall encounter in chapter 6, is that the trace of a product of two matrices $\mathbf{A}$ and $\mathbf{B}$ is independent of the order of multiplication (cyclic behavior of trace),

$$\mathrm{Tr}\;(\mathbf{A}\,\mathbf{B}) \equiv \sum_i (\mathbf{A}\,\mathbf{B})_{ii} = \sum_{ij} a_{ij}\,b_{ji} = \sum_{ji} b_{ji}\,a_{ij} = \sum_j (\mathbf{B}\,\mathbf{A})_{jj} = \mathrm{Tr}\;(\mathbf{B}\,\mathbf{A})\;. \qquad (5.130)$$

The symbol $\mathbf{1}$ in (5.128) stands either for the unity matrix in Dirac (spin) space or both Dirac-spin and isospin space combined. In the latter case it reads

$$\mathbf{1} \equiv \mathbf{1}^{\mathrm{Dirac}} \otimes \mathbf{1}^{\mathrm{iso}}\,, \qquad (5.131)$$

where $\otimes$ denotes the direct tensor (Kronecker) product of the 4×4 Dirac matrix $\mathbf{1}^{\mathrm{Dirac}}$ with the 2×2 isospin matrix $\mathbf{1}^{\mathrm{iso}}$. Thus $\mathbf{1}$ is a 8×8 matrix with matrix elements

$$(\mathbf{1})_{\zeta\zeta'} = \left(\mathbf{1}^{\mathrm{Dirac}}\right)_{\alpha\alpha'}\;\left(\mathbf{1}^{\mathrm{iso}}\right)_{ii'}\;, \qquad (5.132)$$

which is equivalent to

$$\delta_{\zeta\zeta'} = \delta_{\alpha\alpha'}\;\delta_{ii'}\;. \qquad (5.133)$$

The factor $(g_{\sigma B}\mathbf{1})_{\zeta_1\zeta_1'}$ in the Hartree term of (5.128) can therefore be replaced with $g_{\sigma B}\,\delta_{\zeta_1\zeta_1'}$. This is a particular feature that holds only for the scalar coupling case. For the more complicated couplings involving Dirac matrices one gets instead factors like $(\gamma^\mu)_{\zeta_1\zeta_1'}$, or combinations thereof. Finally we add that mesons like the ρ particle, which is a vector in isospin space, require for the additional occurrence of Pauli matrices $\boldsymbol{\tau}$ in the respective coupling constants [cf. equation (5.124)].

Taking these considerations into account, equation (5.128) can then be brought into the alternative, somewhat more compact form

$$\begin{aligned}\boldsymbol{\Sigma}^B_{\zeta_1\zeta_1'}(p)\Big|_\sigma &= -\mathrm{i}\,\delta_{\zeta_1\zeta_1'}\,\Delta^{0\sigma}(0)\,g_{\sigma B}\sum_{B'} g_{\sigma B'}\int\frac{\mathrm{d}^4q}{(2\pi)^4}\,\mathrm{e}^{\mathrm{i}\eta q^0}\;\mathrm{Tr}\;\boldsymbol{g}^{B'}(q)\\ &+\mathrm{i}\,g^2_{\sigma B}\int\frac{\mathrm{d}^4q}{(2\pi)^4}\,\mathrm{e}^{\mathrm{i}\eta q^0}\,\Delta^{0\sigma}(p-q)\;\Big(\mathbf{1}\otimes\boldsymbol{g}^{B'}(q)\otimes\mathbf{1}\Big)_{\zeta_1\zeta_1'}\;. \end{aligned} \qquad (5.134)$$

Hence, the contribution of the σ meson to the baryon self-energy can be written in the following manner:

$$\mathbf{\Sigma}^{\mathrm{H},B}_{\zeta_1\zeta_1'}(p)\Big|_{\sigma} = -\mathrm{i}\,\delta_{\zeta_1\zeta_1'}\,\Delta^{0\sigma}(0)\,g_{\sigma B}\sum_{B'} g_{\sigma B'}\int\frac{\mathrm{d}^4q}{(2\pi)^4}\,\mathrm{e}^{\mathrm{i}\eta q^0}\;\mathrm{Tr}\;\boldsymbol{g}^{B'}(q)\,, \tag{5.135}$$

and

$$\mathbf{\Sigma}^{\mathrm{F},B}_{\zeta_1\zeta_1'}(p)\Big|_{\sigma} = \mathrm{i}\,g^2_{\sigma B}\int\frac{\mathrm{d}^4q}{(2\pi)^4}\,\mathrm{e}^{\mathrm{i}\eta q^0}\;\Delta^{0\sigma}(p-q)\,\big(\mathbf{1}\otimes\boldsymbol{g}^{B}(q)\otimes\mathbf{1}\big)_{\zeta_1\zeta_1'}\,, \tag{5.136}$$

where $\mathbf{\Sigma}^{\mathrm{H},B}$ and $\mathbf{\Sigma}^{\mathrm{F},B}$ denote the Hartree and the Fock contributions to $\mathbf{\Sigma}^{\mathrm{B}}$, respectively. From equation (5.124) one finds that the other mesons, inclusive of the tensor coupling term of the ρ meson, contribute to $\mathbf{\Sigma}^{\mathrm{B}}$ as follows:

$$\mathbf{\Sigma}^{\mathrm{H},B}_{\zeta_1\zeta_1'}(p)\Big|_{\omega} = \mathrm{i}\,\gamma^{\mu}_{\zeta_1\zeta_1'}\,\mathcal{D}^{0\omega}_{\mu\nu}(0)\,g_{\omega B}\sum_{B'} g_{\omega B'}\int\frac{\mathrm{d}^4q}{(2\pi)^4}\,\mathrm{e}^{\mathrm{i}\eta q^0}\;\mathrm{Tr}\,\big(\gamma^{\nu}\boldsymbol{g}^{B'}(q)\big)\,, \tag{5.137}$$

$$\mathbf{\Sigma}^{\mathrm{F},B}_{\zeta_1\zeta_1'}(p)\Big|_{\omega} = -\,\mathrm{i}\,g^2_{\omega B}\int\frac{\mathrm{d}^4q}{(2\pi)^4}\,\mathrm{e}^{\mathrm{i}\eta q^0}\;\gamma^{\mu}_{\zeta_1\zeta_3}\,\gamma^{\nu}_{\zeta_2\zeta_1'}\,\mathcal{D}^{0\omega}(p-q)_{\mu\nu}\,\boldsymbol{g}^{B}_{\zeta_3\zeta_2}(q)\,, \tag{5.138}$$

$$\mathbf{\Sigma}^{\mathrm{H},B}_{\zeta_1\zeta_1'}(p)\Big|_{\pi} = 0\,, \tag{5.139}$$

$$\begin{aligned}\mathbf{\Sigma}^{\mathrm{F},B}_{\zeta_1\zeta_1'}(p)\Big|_{\pi} = \mathrm{i}\left(\frac{f_{\pi B}}{m_\pi}\right)^2\int\frac{\mathrm{d}^4q}{(2\pi)^4}\,\mathrm{e}^{\mathrm{i}\eta q^0}\;&\big(\gamma_5\gamma_\mu\otimes\boldsymbol{\tau}\big)_{\zeta_1\zeta_3}\big(\gamma_5\gamma_\nu\otimes\boldsymbol{\tau}\big)_{\zeta_2\zeta_1'}\\ &\times(p-q)^{\mu}\,(p-q)^{\nu}\,\Delta^{0\pi}(p-q)\,\boldsymbol{g}^{B}_{\zeta_3\zeta_2}(q)\,,\end{aligned} \tag{5.140}$$

$$\begin{aligned}\mathbf{\Sigma}^{\mathrm{H},B}_{\zeta_1\zeta_1'}(p)\Big|_{\rho} &= \mathrm{i}\sum_{B'}\int\frac{\mathrm{d}^4q}{(2\pi)^4}\,\mathrm{e}^{\mathrm{i}\eta q^0}\Big[\Big(g_{\rho B}\gamma_\mu - \mathrm{i}\,\frac{f_{\rho B}}{2m_B}\,(p-q)^{\lambda}\,\sigma_{\lambda\mu}\Big)\otimes\boldsymbol{\tau}\Big]_{\zeta_1\zeta_1'}\\ &\times\mathcal{D}^{0\rho}(0)^{\mu\nu}\;\mathrm{Tr}\Big\{\Big[\Big(g_{\rho B'}\gamma_\nu + \mathrm{i}\,\frac{f_{\rho B'}}{2m_{B'}}\,(p-q)^{\kappa}\,\sigma_{\kappa\nu}\Big)\otimes\boldsymbol{\tau}\Big]\,\boldsymbol{g}^{B'}(q)\Big\}\,,\end{aligned} \tag{5.141}$$

and

$$\begin{aligned}\mathbf{\Sigma}^{\mathrm{F},B}_{\zeta_1\zeta_1'}(p)\Big|_{\rho} &= -\,\mathrm{i}\int\frac{\mathrm{d}^4q}{(2\pi)^4}\,\mathrm{e}^{\mathrm{i}\eta q^0}\Big[\Big(g_{\rho B}\gamma_\mu - \mathrm{i}\,\frac{f_{\rho B}}{2m_B}\,(p-q)^{\lambda}\,\sigma_{\lambda\mu}\Big)\otimes\boldsymbol{\tau}\Big]_{\zeta_1\zeta_3}\\ &\times\Big[\Big(g_{\rho B}\gamma_\nu + \mathrm{i}\,\frac{f_{\rho B}}{2m_B}\,(p-q)^{\kappa}\,\sigma_{\kappa\nu}\Big)\otimes\boldsymbol{\tau}\Big]_{\zeta_2\zeta_1'}\mathcal{D}^{0\rho}(p-q)^{\mu\nu}\,\boldsymbol{g}^{B}_{\zeta_3\zeta_2}(q)\,.\end{aligned} \tag{5.142}$$

Chapter 6

Spectral representation of two-point Green function

6.1 Finite-temperature two-point function

For technical purposes, it is extremely useful to introduce a spectral representation for the two-point baryon Green function $\boldsymbol{g}_1^B$, for it will enables us to perform the energy integrations in the numerous baryon self-energy expressions, derived in equations (5.135) to (5.142), analytically. Instead of having to deal with $\boldsymbol{g}_1^B$, we are then left with the determination of the baryon spectral function associated with $\boldsymbol{g}_1^B$. This technique is particularly useful for systems whose self-energies are pure real functions, since then a *single-particle* description for the baryons in matter holds. Mathematically, this reflects itself in a spectral function which separates a δ-function which contributes only for energies equal to the single-particle energy of a baryon in matter. This feature renders the integrations over the energy variable mentioned just above nearly trivial. The single-particle behavior, which is exact for pure real self-energies, breaks down if the self-energy becomes complex. In this case the δ-function spreads out over a certain finite energy range, which is the broader the larger the imaginary part of the baryon self-energy. Nevertheless for not too large imaginary parts the single-particle picture appears to be well applicable [336].

In the following discussion we shall be somewhat more general than in section 5.3, where we have introduced the two-point baryon Green function at zero temperature only, by extending its definition to finite temperatures. It is given by

$$\boldsymbol{g}^{BB'}(x,\zeta;x',\zeta') = \mathrm{i}\, \frac{\mathrm{Tr}\left(\mathrm{e}^{-\beta\mathcal{H}}\, \hat{T}\big(\psi_B(x,\zeta)\; \bar{\psi}_{B'}(x',\zeta')\big)\right)}{\mathrm{Tr}\ \mathrm{e}^{-\beta\mathcal{H}}}\,, \tag{6.1}$$

which denotes the quantum mechanical average of time-ordered baryon field operators over a canonical ensemble [337, 338, 339]. The auxiliary functions $\boldsymbol{g}_<$ and $\boldsymbol{g}_>$, defined in equations (5.65) and (5.66), are now given by

$$\begin{aligned} \boldsymbol{g}_>^{BB'}(x,\zeta;x',\zeta') &\equiv \mathrm{i} \, < \psi_B(x,\zeta)\, \bar{\psi}_{B'}(x',\zeta') >_\beta \\ &= \mathrm{i}\, \frac{\mathrm{Tr}\left(\mathrm{e}^{-\beta\mathcal{H}}\; \psi_B(x,\zeta)\; \bar{\psi}_{B'}(x',\zeta')\right)}{\mathrm{Tr}\; \mathrm{e}^{-\beta\mathcal{H}}} , \end{aligned} \tag{6.2}$$

$$\begin{aligned} \boldsymbol{g}_<^{BB'}(x,\zeta;x',\zeta') &\equiv -\mathrm{i} \, < \bar{\psi}_{B'}(x',\zeta')\, \psi_B(x,\zeta) >_\beta \\ &= -\mathrm{i}\, \frac{\mathrm{Tr}\left(\mathrm{e}^{-\beta\mathcal{H}}\; \bar{\psi}_{B'}(x',\zeta')\; \psi_B(x,\zeta)\right)}{\mathrm{Tr}\; \mathrm{e}^{-\beta\mathcal{H}}} , \end{aligned} \tag{6.3}$$

where $< \ldots >_\beta$ refers to the definition at finite-temperatures. The quantity $\mathcal{H}$ denotes the system's Hamiltonian. The time-development operator $\mathrm{e}^{-\mathrm{i}\mathcal{H}x_0}$ contained in the fields ψ_B and $\bar{\psi}_B$,

$$\psi_B(x_0,\boldsymbol{x}) = \mathrm{e}^{\mathrm{i}\mathcal{H}x_0}\; \psi_B(0,\boldsymbol{x})\; \mathrm{e}^{-\mathrm{i}\mathcal{H}x_0} , \tag{6.4}$$

bears a strong formal similarity to the weighting factor $\mathrm{e}^{-\beta\mathcal{H}}$ that occurs in the canonical average of (6.1) to (6.3). By means of considering the time variables x_0, x_0' of $\boldsymbol{g}^B(x,x')$ to being restricted to $0 \le \mathrm{i}x_0,\, \mathrm{i}x_0' \le \beta$ and, secondly, extending the definition of the time-ordering operator to mean $\mathrm{i}x_0$ and $\mathrm{i}x_0'$ ordering when times are imaginary, then the Green functions are again well defined in the interval $\mathrm{i}x_0,\, \mathrm{i}x_0' \in (0,\beta)$ [337, 338].

By making use of the cyclic property of the trace, shown in (5.130), one then readily verifies the following relations for imaginary times in the interval $(0, -\mathrm{i}\beta)$:

$$\boldsymbol{g}^B(x,\zeta;x',\zeta')\big|_{x_0=0} = \boldsymbol{g}_<^B(x,\zeta;x',\zeta')\big|_{x_0=0} , \tag{6.5}$$

$$\boldsymbol{g}^B(x,\zeta;x',\zeta')\big|_{x_0=-\mathrm{i}\beta} = \boldsymbol{g}_>^B(x,\zeta;x',\zeta')\big|_{x_0=-\mathrm{i}\beta} . \tag{6.6}$$

This remarkable periodicity of the finite-temperature baryon Green function in the limited imaginary-time domain will be fundamental to all of the subsequent work. For definiteness, let us consider the case that $\mathrm{i}x_0'$ is fixed $(0 < \mathrm{i}x_0' < \beta)$. It is then verified that (as before, we drop the B's carried by $\boldsymbol{g}$ and the baryon field operators in side-calculations):

$$\begin{aligned} \left(\mathrm{Tr}\; \mathrm{e}^{-\beta\mathcal{H}}\right)\; \boldsymbol{g}_<(x,x')|_{x_0=0} &= -\,\mathrm{i}\;\mathrm{Tr}\; \left[\mathrm{e}^{-\beta\mathcal{H}}\, \bar{\psi}(x')\, \psi(x)\right]_{x_0=0} \\ &= -\,\mathrm{i}\;\mathrm{Tr}\; \left[\mathrm{e}^{-\beta\mathcal{H}}\, \bar{\psi}(x')\, \mathrm{e}^{-\mathrm{i}\mathcal{H}x_0}\, \psi(0,\boldsymbol{x})\, \mathrm{e}^{\mathrm{i}\mathcal{H}x_0}\right] \\ &= -\,\mathrm{i}\;\mathrm{Tr}\; \left[\mathrm{e}^{\mathrm{i}\mathcal{H}x_0}\, \mathrm{e}^{-\beta\mathcal{H}}\, \bar{\psi}(x')\, \mathrm{e}^{-\mathrm{i}\mathcal{H}x_0}\, \psi(x)\right]_{x_0=-\mathrm{i}\beta} \\ &= -\,\mathrm{i}\;\mathrm{Tr}\; \left[\mathrm{e}^{-\beta\mathcal{H}}\, \psi(x)\, \bar{\psi}(x')\right]_{x_0=-\mathrm{i}\beta} \\ &= -\left(\mathrm{Tr}\; \mathrm{e}^{-\beta\mathcal{H}}\right)\; \boldsymbol{g}_>(x,x')|_{x_0=-\mathrm{i}\beta} , \end{aligned} \tag{6.7}$$

from which it follows that

$$\boldsymbol{g}^B_<(x,\zeta;x',\zeta')\big|_{x_0=0} = -\,\boldsymbol{g}^B_>(x,\zeta;x',\zeta')\big|_{x_0=-\mathrm{i}\beta}\,, \tag{6.8}$$

and

$$\boldsymbol{g}^B(x,\zeta;x',\zeta')\big|_{x_0=0} = -\,\boldsymbol{g}^B(x,\zeta;x',\zeta')\big|_{x_0=-\mathrm{i}\beta}\,. \tag{6.9}$$

The latter relation follows via substituting (6.8) into equations (6.5) and (6.6). The minus signs in (6.8) and (6.9) is a consequence of the Fermi statistic obeyed by the baryons.

In the next step we incorporate the anti-periodic behavior of (6.9) into $\boldsymbol{g}^B(x,x')$, which is accomplished by introducing Fourier series and integrals as follows. For discrete frequencies of $\omega_n \equiv \frac{2n+1}{-\mathrm{i}\beta}\,\pi$ with $n = 0, \pm 1, \ldots$, the Fourier representation of the two-point baryon function reads [337, 340, 341, 342]

$$\begin{aligned}\boldsymbol{g}^B(x,\zeta;x',\zeta') &= \frac{1}{(-\mathrm{i}\beta)^2}\sum_{n,n'} \mathrm{e}^{-\mathrm{i}\omega_n x_0 + \mathrm{i}\omega_{n'} x'_0} \\ &\times \int \frac{\mathrm{d}^3\boldsymbol{k}}{(2\pi)^3}\int \frac{\mathrm{d}^3\boldsymbol{k}'}{(2\pi)^3}\, \mathrm{e}^{\mathrm{i}k\cdot x - \mathrm{i}k'\cdot x'}\, \boldsymbol{g}^B(\omega_n,\boldsymbol{k},\zeta;\omega_{n'},\boldsymbol{k}',\zeta')\,,\end{aligned} \tag{6.10}$$

with its inverse given by

$$\begin{aligned}\boldsymbol{g}^B(\omega_n,\boldsymbol{k},\zeta;\omega_{n'},\boldsymbol{k}',\zeta') &= \int_0^{-\mathrm{i}\beta}\mathrm{d}x_0 \int_0^{-\mathrm{i}\beta}\mathrm{d}x'_0\, \mathrm{e}^{\mathrm{i}\omega_n x_0 - \mathrm{i}\omega_{n'} x'_0} \\ &\times \int \mathrm{d}^3\boldsymbol{x} \int \mathrm{d}^3\boldsymbol{x}'\, \mathrm{e}^{-\mathrm{i}k\cdot x + \mathrm{i}k'\cdot x'}\, \boldsymbol{g}^B_{\zeta\zeta'}(x-x')\,.\end{aligned} \tag{6.11}$$

The δ-function for discrete energies has the form

$$\delta(x_0) = \frac{1}{-\mathrm{i}\beta}\sum_n \mathrm{e}^{-\mathrm{i}\omega_n x_0}\,, \quad \delta_{nn'} = \frac{1}{-\mathrm{i}\beta}\int_0^{-\mathrm{i}\beta}\mathrm{d}x_0\, \mathrm{e}^{\mathrm{i}x_0(\omega_n-\omega_{n'})}\,. \tag{6.12}$$

Because of translational invariance of space and time, the arguments of the two-point function obey the relation $\boldsymbol{g}^B(x,x') = \boldsymbol{g}^B(x-x')$, which implies for $\boldsymbol{g}^B(\omega_n,\omega_{n'})$ of equation (6.10),

$$\boldsymbol{g}^B(\omega_n,\boldsymbol{k},\zeta;\omega_{n'},\boldsymbol{k}',\zeta') = (-\mathrm{i}\beta)\,(2\pi)^3\,\delta_{nn'}\,\delta^3(\boldsymbol{k}-\boldsymbol{k}')\,\boldsymbol{g}^B_{\zeta\zeta'}(\omega_n,\boldsymbol{k})\,. \tag{6.13}$$

The momentum-space representation of the free baryon propagator, $\boldsymbol{g}^{0B}$, is given by

$$\big(\gamma^\mu k_\mu - m_B\big)_{\zeta\zeta''}\,\boldsymbol{g}^{0B}_{\zeta''\zeta'}(k) = -\,\delta_{\zeta\zeta'}\,. \tag{6.14}$$

This expression is formally identical with the Fourier transformed of (5.144). Here, however, the four-momenta are given by $k = (k^0, \boldsymbol{k}) = (\omega_n, \boldsymbol{k})$. So there is no ambiguity in the division process when solving (6.14) for $\boldsymbol{g}^{0B}(k)$, that is $(\gamma^\mu k_\mu - m_B) \neq 0$ [337].

In the next step we combine the anti-periodicity properties derived for $\boldsymbol{g}^B$ above with the real-time formalism to represent $\boldsymbol{g}^B(x - x')$ by Fourier integrals. With the definitions for Fourier integrals given in appendix B.2, one obtains

$$\boldsymbol{g}_<(k_0, \boldsymbol{k}) = \int \mathrm{d}^4x \; \mathrm{e}^{\mathrm{i}kx} \; \boldsymbol{g}_<(x^0, \boldsymbol{x}) \tag{6.15}$$

$$= -\int \mathrm{d}x_0 \int \mathrm{d}^3\boldsymbol{x} \; \mathrm{e}^{\mathrm{i}(k_0 x_0 - \boldsymbol{k}\cdot x)} \; \boldsymbol{g}_>(x_0 - \mathrm{i}\beta, \boldsymbol{x})\,. \tag{6.16}$$

To get from (6.15) to (6.16) use of the anti-periodicity condition (6.8) was made. The Fourier transform of the integrand $\boldsymbol{g}_>(x_0 - \mathrm{i}\beta, \boldsymbol{x})$ is given by

$$\boldsymbol{g}_>(x_0 - \mathrm{i}\beta, \boldsymbol{x}) = \int \frac{\mathrm{d}^4k'}{(2\pi)^4} \, \mathrm{e}^{-\mathrm{i}(k'_0(x_0 - \mathrm{i}\beta) - k'\cdot x)} \; \boldsymbol{g}_>(k'_0, \boldsymbol{k}') \tag{6.17}$$

$$= \int \frac{\mathrm{d}^4k'}{(2\pi)^4} \, \mathrm{e}^{-\mathrm{i}(k'_0 x_0 - k'\cdot x)} \; \mathrm{e}^{-\beta k'_0} \; \boldsymbol{g}_>(k'_0, \boldsymbol{k}')\,. \tag{6.18}$$

Substituting (6.18) into (6.16) then leads to

$$\begin{aligned}\boldsymbol{g}_<(k_0, \boldsymbol{k}) = -\int \mathrm{d}x_0 \int \mathrm{d}^3\boldsymbol{x} \int \frac{\mathrm{d}k'_0}{2\pi} \int \frac{\mathrm{d}^3\boldsymbol{k}'}{(2\pi)^3} \, \mathrm{e}^{\mathrm{i}(k_0 x_0 - \boldsymbol{k}\cdot x)} \\ \times \; \mathrm{e}^{-\mathrm{i}(k'_0 x_0 - k'\cdot x)} \, \mathrm{e}^{-\beta k'_0} \; \boldsymbol{g}_>(k'_0, \boldsymbol{k}')\,,\end{aligned} \tag{6.19}$$

which, upon integrating over the two δ-functions $\delta(k_0 - k'_0)$ and $\delta^3(\boldsymbol{k} - \boldsymbol{k}')$ inherently contained in (6.19), can be written in the following manner,

$$\boldsymbol{g}^B_<(k_0, \boldsymbol{k})_{\zeta\zeta'} = -\,\mathrm{e}^{-\beta k_0} \; \boldsymbol{g}^B_>(k_0, \boldsymbol{k})_{\zeta\zeta'}\,. \tag{6.20}$$

Denoting the difference between $\boldsymbol{g}^B_<$ and $\boldsymbol{g}^B_>$ as

$$\boldsymbol{\Xi}^B(k) \equiv \frac{1}{2\mathrm{i}\pi} \left(\boldsymbol{g}^B_>(k) \; - \; \boldsymbol{g}^B_<(k) \right), \tag{6.21}$$

and replacing $\boldsymbol{g}^B_<$ by $\boldsymbol{g}^B_>$ with the aid of equation (6.20) leads for (6.21) to

$$2\mathrm{i}\pi \, \boldsymbol{\Xi}^B(k) = \left(1 \; + \; \mathrm{e}^{-\beta k_0}\right) \, \boldsymbol{g}^B_>(k)\,. \tag{6.22}$$

With the aid of the Fermi–Dirac function, given by

$$f(k_0) = \frac{1}{\mathrm{e}^{\beta k_0} + 1}\,, \tag{6.23}$$

equation (6.22) can be written as

$$\boldsymbol{g}^B_>(k)_{\zeta\zeta'} = 2\mathrm{i}\pi\ \boldsymbol{\Xi}^B_{\zeta\zeta'}(k)\ \left(1 - f(k_0)\right)\ . \tag{6.24}$$

Substituting (6.24) into (6.20) gives

$$\boldsymbol{g}^B_<(k)_{\zeta\zeta'} = -\,2\mathrm{i}\pi\ \boldsymbol{\Xi}^B_{\zeta\zeta'}(k)\ f(k_0)\,. \tag{6.25}$$

The Fourier representation of $\boldsymbol{g}^B(\omega_n, \boldsymbol{k})$ reads

$$\boldsymbol{g}(\omega_n, \boldsymbol{k}) = \int_0^{-\mathrm{i}\beta} \mathrm{d}x_0\ \mathrm{e}^{-\frac{(2n+1)\pi}{\beta}x_0} \int \mathrm{d}^3\boldsymbol{x}\ \mathrm{e}^{-\mathrm{i}\boldsymbol{k}\cdot\boldsymbol{x}} \boldsymbol{g}(x_0, \boldsymbol{x})\,, \tag{6.26}$$

with

$$\boldsymbol{g}(x_0, \boldsymbol{x}) = \Theta(\mathrm{i}x_0)\,\boldsymbol{g}_>(x_0, \boldsymbol{x}) + \Theta(-\mathrm{i}x_0)\,\boldsymbol{g}_<(x_0, \boldsymbol{x})\,. \tag{6.27}$$

Because $x_0 \in (0, -\mathrm{i}\beta)$ in (6.26), equation (6.27) simplifies to $\boldsymbol{g}(x_0, \boldsymbol{x}) = \boldsymbol{g}_>(x_0, \boldsymbol{x})$, and therefore from (6.26),

$$\boldsymbol{g}(\omega_n, \boldsymbol{k}) = \int_0^{-\mathrm{i}\beta} \mathrm{d}x_0\ \mathrm{e}^{-\frac{(2n+1)\pi}{\beta}x_0} \int \mathrm{d}^3\boldsymbol{x}\ \mathrm{e}^{-\mathrm{i}\boldsymbol{k}\cdot\boldsymbol{x}}\ \boldsymbol{g}_>(x_0, \boldsymbol{x})\,. \tag{6.28}$$

Inspection of the second integral in (6.28) shows that this expression is nothing but the Fourier transform of $\boldsymbol{g}_>(x_0, \boldsymbol{k})$. Replacing $\boldsymbol{g}_>(x_0, \boldsymbol{k})$ with its Fourier transform $\boldsymbol{g}_>(k_0, \boldsymbol{k})$ in (6.28) leads to

$$\boldsymbol{g}(\omega_n, \boldsymbol{k}) = \int_0^{-\mathrm{i}\beta} \mathrm{d}x_0\ \mathrm{e}^{-\frac{(2n+1)\pi}{\beta}x_0} \int_{-\infty}^{+\infty} \frac{\mathrm{d}k_0}{2\pi}\ \mathrm{e}^{-\mathrm{i}k_0 x_0}\ g > (k_0, \boldsymbol{k})\,. \tag{6.29}$$

Rearranging terms and substituting (6.24) for $\boldsymbol{g}^B_>(k_0, \boldsymbol{k})$ then gives

$$\boldsymbol{g}(\omega_n, \boldsymbol{k}) = \int_{-\infty}^{+\infty} \frac{\mathrm{d}k_0}{2\pi} \left\{ \int_0^{-\mathrm{i}\beta} \mathrm{d}x_0\, \mathrm{e}^{-\frac{(2n+1)\pi}{\beta}x_0 - \mathrm{i}k_0 x_0} \right\} \left\{ 2\mathrm{i}\pi\, \boldsymbol{\Xi}(k)\, [1 - f(k_0)] \right\}. \tag{6.30}$$

The first term in curly brackets can be integrated which results in

$$\int_0^{-\mathrm{i}\beta} \mathrm{d}x_0\ \mathrm{e}^{-(\frac{(2n+1)\pi}{\beta} + \mathrm{i}k_0)\,x_0} = \frac{\mathrm{i}}{\omega_n - k_0}\ \left(\mathrm{e}^{-\beta k_0} + 1\right)\ . \tag{6.31}$$

Equation (6.30) can thus be brought to the form

$$\boldsymbol{g}^B_{\zeta\zeta'}(\omega_n, \boldsymbol{k}) = -\int_{-\infty}^{+\infty} \mathrm{d}k_0\ \frac{\boldsymbol{\Xi}^B_{\zeta\zeta'}(k)}{\omega_n - k_0}\,. \tag{6.32}$$

Replacing ω_n with the continuous, complex variable z leads to the analytically continued spectral representation of $\boldsymbol{g}^B$, given by[1]

$$\tilde{\boldsymbol{g}}^B_{\zeta\zeta'}(z, \boldsymbol{k}) = \int\limits_{-\infty}^{+\infty} \mathrm{d}\omega \; \frac{\boldsymbol{\Xi}^B_{\zeta\zeta'}(\omega, \boldsymbol{k})}{\omega - z} \,. \tag{6.33}$$

The quantity $\boldsymbol{\Xi}^B$ is referred to as spectral function. It will be calculated for dense nuclear matter in section 6.2. With help of the relation

$$\frac{1}{x \pm \mathrm{i}\,\eta} = \mathsf{P}\;\frac{1}{x} \mp \mathrm{i}\,\pi\,\delta(x)\,, \tag{6.34}$$

with P denoting the principal value, one readily verifies that the spectral function is given in terms of $\tilde{\boldsymbol{g}}^B$ as

$$\boldsymbol{\Xi}^B_{\zeta\zeta'}(\omega, \boldsymbol{k}) = \frac{\tilde{\boldsymbol{g}}^B_{\zeta\zeta'}(\omega + \mathrm{i}\eta, \boldsymbol{k}) \;-\; \tilde{\boldsymbol{g}}^B_{\zeta\zeta'}(\omega - \mathrm{i}\eta, \boldsymbol{k})}{2\mathrm{i}\pi} \,. \tag{6.35}$$

Expressions (6.33) and (6.35) are formally identical with their non-relativistic counterparts [316, 318, 338, 343]. Here however we are dealing with spectral functions that possess a Dirac–Lorentz structure, that is, $\boldsymbol{\Xi}^B$ consists of a number of individual functions which altogether form $\boldsymbol{\Xi}^B$. This is in sharp contrast to the non-relativistic case where $\boldsymbol{\Xi}^B$ is a single scalar function.

The Fourier transform of $\boldsymbol{g}(x) = \Theta(x_0)\boldsymbol{g}_>(x) + \Theta(-x_0)\boldsymbol{g}_<(x)$ is given by

$$\boldsymbol{g}(k) = \int \mathrm{d}^4x\;\mathrm{e}^{\mathrm{i}kx}\;\left[\Theta(x_0)\,\boldsymbol{g}_>(x) + \Theta(-x_0)\,\boldsymbol{g}_<(x)\right] \,. \tag{6.36}$$

Expressing the Heaviside step function as

$$\Theta(\pm\, x_0) = \frac{\mathrm{i}}{2\pi} \int\limits_{-\infty}^{+\infty} \mathrm{d}\omega \; \frac{\mathrm{e}^{\mp \mathrm{i}\omega x_0}}{\omega + \mathrm{i}\eta} \,, \tag{6.37}$$

and replacing $\boldsymbol{g}_>(x)$ and $\boldsymbol{g}_<(x)$ with their Fourier transforms leads to

$$\begin{aligned} \boldsymbol{g}(k) = \frac{\mathrm{i}}{2\pi} \int \mathrm{d}x_0 \int \mathrm{d}^3\boldsymbol{x} \int \mathrm{d}\omega \int \frac{\mathrm{d}k'_0}{2\pi} \int \frac{\mathrm{d}^3\boldsymbol{k}'}{(2\pi)^3}\;\mathrm{e}^{-\mathrm{i}(k-k')\cdot x} \\ \times \left\{ \mathrm{e}^{\mathrm{i}(k_0 - k'_0 - \omega)x_0}\,\frac{\boldsymbol{g}_>(k'_0, \boldsymbol{k}')}{\omega + \mathrm{i}\eta} + \mathrm{e}^{\mathrm{i}(k_0 - k'_0 + \omega)x_0}\,\frac{\boldsymbol{g}_<(k'_0, \boldsymbol{k}')}{\omega + \mathrm{i}\eta} \right\} . \end{aligned} \tag{6.38}$$

[1] Throughout this text, analytically continued functions carry a tilde.

The integrals over x_0 and $\boldsymbol{x}'$ constitute δ-functions of the form $\delta^3(\boldsymbol{k}-\boldsymbol{k}')$ and $\delta(k_0 - k_0' - \omega)$, respectively. Introducing them in (6.38) leads to

$$\boldsymbol{g}(k) = \frac{\mathrm{i}}{2\pi}\int \mathrm{d}\omega \int \frac{\mathrm{d}k_0'}{2\pi}\int \frac{\mathrm{d}^3\boldsymbol{k}'}{(2\pi)^3}\,(2\pi)^4\,\delta^3(\boldsymbol{k}-\boldsymbol{k}')$$
$$\times \left\{ \delta(k_0 - k_0' - \omega)\frac{\boldsymbol{g}_>(k_0', \boldsymbol{k}')}{\omega + \mathrm{i}\eta} + \delta(k_0 - k_0' + \omega)\frac{\boldsymbol{g}_<(k_0', \boldsymbol{k}')}{\omega + \mathrm{i}\eta} \right\}, \quad (6.39)$$

which, upon carrying out the integrals containing δ-functions, leads to

$$\boldsymbol{g}^B_{\zeta\zeta'}(k) = \frac{\mathrm{i}}{2\pi}\int_{-\infty}^{+\infty} \mathrm{d}k_0' \left\{ \frac{\boldsymbol{g}^B_>(k_0', \boldsymbol{k}')_{\zeta\zeta'}}{k_0 - k_0' + \mathrm{i}\eta} - \frac{\boldsymbol{g}^B_<(k_0', \boldsymbol{k}')_{\zeta\zeta'}}{k_0 - k_0' - \mathrm{i}\eta} \right\}. \quad (6.40)$$

In the last step we replace the functions $\boldsymbol{g}^B_>$ and $\boldsymbol{g}^B_<$ in (6.40) by the expressions derived for them in equations (6.24) and (6.25), respectively. This results in

$$\boldsymbol{g}^B_{\zeta\zeta'}(k) = -\int_{-\infty}^{+\infty} \mathrm{d}k_0' \left\{ \frac{1 - f(k_0')}{k_0 - k_0' + \mathrm{i}\eta} + \frac{f(k_0')}{k_0 - k_0' - \mathrm{i}\eta} \right\} \boldsymbol{\Xi}^B_{\zeta\zeta'}(k_0', \boldsymbol{k})\,. \quad (6.41)$$

By means of the well-known mathematical relation

$$\frac{1}{k_0 - k_0' + i\eta} - \frac{1}{k_0 - k_0' - i\eta} = -2\mathrm{i}\pi\,\delta(k_0 - k_0')\,, \quad (6.42)$$

which is a consequence of equation (6.34), equation (6.41) can be brought into the form

$$\boldsymbol{g}^B_{\zeta\zeta'}(k_0, \boldsymbol{k}) = \int_{-\infty}^{+\infty} \mathrm{d}\omega\,\frac{\boldsymbol{\Xi}^B_{\zeta\zeta'}(\omega, \boldsymbol{k})}{\omega - k_0 - \mathrm{i}\eta} - 2\mathrm{i}\pi\,\boldsymbol{\Xi}^B_{\zeta\zeta'}(k_0, \boldsymbol{k})\,f(k_0)\,. \quad (6.43)$$

The numerator in (6.43) can be written in a somewhat different fashion. For this purpose we formally add

$$0 \equiv -\int_{-\infty}^{0} \mathrm{d}\omega\,\frac{\boldsymbol{\Xi}(\omega, \boldsymbol{k})}{k_0 - \omega - \mathrm{i}\eta} + \int_{-\infty}^{0} \mathrm{d}\omega\,\frac{\boldsymbol{\Xi}(\omega, \boldsymbol{k})}{k_0 - \omega - \mathrm{i}\eta} \quad (6.44)$$

to (6.43), which leads to

$$\boldsymbol{g}(k) = -\left\{ \int_{-\infty}^{0} \mathrm{d}\omega\,\frac{\boldsymbol{\Xi}(\omega, \boldsymbol{k})}{k_0 - \omega + \mathrm{i}\eta} + \int_{0}^{+\infty} \mathrm{d}\omega\,\frac{\boldsymbol{\Xi}(\omega, \boldsymbol{k})}{k_0 - \omega + \mathrm{i}\eta}\right.$$

$$- \int_{-\infty}^{0} \mathrm{d}\omega \, \frac{\boldsymbol{\Xi}(\omega, \boldsymbol{k})}{k_0 - \omega - \mathrm{i}\eta} + \int_{-\infty}^{0} \mathrm{d}\omega \, \frac{\boldsymbol{\Xi}(\omega, \boldsymbol{k})}{k_0 - \omega - \mathrm{i}\eta} \Bigg\} - 2\mathrm{i}\pi \, f(k_0) \, \boldsymbol{\Xi}(k_0, \boldsymbol{k}) \, . \tag{6.45}$$

Introducing the signum function $\Theta(-\omega)$ in the first and third integral of (6.45), the interval of integration can be extended from $(-\infty, 0)$ to $(-\infty, +\infty)$. The second and fourth integral can be combined to one integral. This is not immediately clear from equation (6.45). To see this, note that the integrand of the second integral has a pole only if $k_0 > 0$. Therefore, without loss of generality, we can multiply $\mathrm{i}\eta$ of the denominator of this integrand with k_0. Similarly, the pole of the integrand of the fourth integral occurs only if $k_0 < 0$, and correspondingly we may multiply $i\eta$ of this integrand with $-k_0$. Hence we are left with

$$\begin{aligned} \boldsymbol{g}(k) = & - \Bigg\{ \int_{-\infty}^{+\infty} \mathrm{d}\omega \; \boldsymbol{\Xi}(\omega, \boldsymbol{k}) \left[\frac{1}{k_0 - \omega + \mathrm{i}\eta} - \frac{1}{k_0 - \omega - \mathrm{i}\eta} \right] \Theta(-\omega) \\ & - \Bigg[\int_{-\infty}^{0} \mathrm{d}\omega \, \frac{\boldsymbol{\Xi}(\omega, \boldsymbol{k})}{\omega - k_0 + \mathrm{i}\eta \cdot (-k_0)} + \int_{0}^{+\infty} \mathrm{d}\omega \, \frac{\boldsymbol{\Xi}(\omega, \boldsymbol{k})}{\omega - k_0 - \mathrm{i}\eta \cdot (k_0)} \Bigg] \Bigg\} \\ & - \, 2 \, \mathrm{i}, \pi \, f(k_0) \, \boldsymbol{\Xi}(k_0, \boldsymbol{k}) \, . \end{aligned} \tag{6.46}$$

The integrand of the first integral in (6.46) can be replaced with $-2\mathrm{i}\pi\delta(k_0 - \omega)$. So the integral over ω simply gives $2\mathrm{i}\pi\Theta(k_0)\boldsymbol{\Xi}(k_0, \boldsymbol{k})$, which we combine with the last term in (6.46). One gets $-2\mathrm{i}\pi\mathrm{sign}(k_0) f(|k_0|)\boldsymbol{\Xi}(k)$, where use of the relation

$$f(x) - \Theta(-x) = \mathrm{sign}(x) \; f(|x|) \tag{6.47}$$

was made. Equation (6.47) is readily verified by means of making use of $f(-|x|) - 1 = -f(|x|)$ and the definition of the signum function, $\mathrm{sign}(x) = \Theta(x) - \Theta(-x)$. The remaining two integrals in (6.46) can be combined, which leads to the final result for the spectral representation of $\boldsymbol{g}^B$ in the form

$$\boldsymbol{g}^B_{\zeta\zeta'}(k) = \int_{-\infty}^{+\infty} \mathrm{d}\omega \, \frac{\boldsymbol{\Xi}^B_{\zeta\zeta'}(\omega, \boldsymbol{k})}{\omega - k_0 \, (1 + \mathrm{i}\eta)} \; - \; 2\mathrm{i}\pi \; \mathrm{sign}(k_0) \; f(|k_0|) \; \boldsymbol{\Xi}^B_{\zeta\zeta'}(k) \, . \tag{6.48}$$

As an easy illustration, let us apply the technique developed just above to the derivation of the finite-density, finite-temperature expression of the free baryon propagator. The free baryon propagator is know from equation (5.125). It reads

$$\boldsymbol{g}^{0B}(k) = -\frac{1}{\not{k} - m_B}\,, \tag{6.49}$$

where $\not{k}$ is given by $\not{k} \equiv \gamma^\mu k_\mu = \gamma^0 k_0 - \boldsymbol{\gamma}\cdot\boldsymbol{k}$. Multiplying both numerator and denominator of (6.49) with $\not{k} + m$ and making use of $\not{k}^2 = k^2$, which follows from the relation (see also appendix A.2)

$$\not{k}^2 = (\gamma^\mu k_\mu)^2 = \gamma^\mu k_\mu\, \gamma^\nu k_\nu = k_\mu k_\nu \{2g^{\mu\nu} - \gamma^\nu\gamma^\mu\} = 2k^\nu k_\nu - \not{k}^2\,, \tag{6.50}$$

one gets

$$\boldsymbol{g}^{0B}(k_0, \boldsymbol{k}) = -\frac{\gamma^0 k_0 - \boldsymbol{\gamma}\cdot\boldsymbol{k} + m_B}{k_0^2 - \boldsymbol{k}^2 - m_B^2}\,, \tag{6.51}$$

and for the analytically continued propagator,

$$\tilde{\boldsymbol{g}}^{0B}(z, \boldsymbol{k}) = -\frac{\gamma^0 z - \boldsymbol{\gamma}\cdot\boldsymbol{k} + m_B}{z^2 - \boldsymbol{k}^2 - m_B^2}\,. \tag{6.52}$$

Evaluating equation (6.52) for energies $z = k_0 \pm \mathrm{i}\eta$ leads to

$$\tilde{\boldsymbol{g}}^{0B}(k_0, \boldsymbol{k}) = -\frac{\gamma^0(k_0 \pm \mathrm{i}\eta) - \boldsymbol{\gamma}\cdot\boldsymbol{k} + m_B}{(k_0 \pm \mathrm{i}\eta)^2 - \boldsymbol{k}^2 - m_B^2}\,, \tag{6.53}$$

which can be rewritten as

$$\tilde{\boldsymbol{g}}^{0B}(k_0, \boldsymbol{k}) = -\frac{\not{k} + m_B}{k^2 - m_B^2 \pm \mathrm{i}\,\eta\,\mathrm{sign}(k_0)}\,. \tag{6.54}$$

Here we have made use of the fact that the term whose denominator is proportional to $\pm\mathrm{i}\eta$ does not give a contribution, as is the case for the term in the numerator proportional to η^2. A straightforward evaluation of $\tilde{\boldsymbol{g}}^{0B}$ at the cut along the k_0 axis gives

$$\begin{aligned}
\tilde{\boldsymbol{g}}^{0B}(k_0 + \mathrm{i}\eta, \boldsymbol{k}) - \tilde{\boldsymbol{g}}^{0B}(k_0 - \mathrm{i}\eta, \boldsymbol{k}) &= -\,(\not{k} + m_B) \\
&\times \left[\frac{1}{k^2 - m_B^2 + \mathrm{i}\,\eta\,\mathrm{sign}(k_0)} - \frac{1}{k^2 - m_B^2 - \mathrm{i}\,\eta\,\mathrm{sign}(k_0)}\right] \\
&= 2\,\mathrm{i}\,\pi\,(\not{k} + m_B)\,\delta(k^2 - m_B^2)\,\mathrm{sign}(k_0)\,,
\end{aligned} \tag{6.55}$$

from which we find for the spectral function associated with the free baryon Green functions,

$$\begin{aligned}
\boldsymbol{\Xi}^{0B}_{\zeta\zeta'}(k) &= \frac{\tilde{\boldsymbol{g}}^{0B}_{\zeta\zeta'}(k_0 + \mathrm{i}\eta, \boldsymbol{k}) - \tilde{\boldsymbol{g}}^{0B}_{\zeta\zeta'}(k_0 - \mathrm{i}\eta, \boldsymbol{k})}{2\,\mathrm{i}\,\pi} \\
&= (\not{k} + m_B)_{\zeta\zeta'}\,\delta(k^2 - m_B^2)\,\mathrm{sign}(k_0)\,.
\end{aligned} \tag{6.56}$$

The representation of the free baryon Green functions is found by means of substituting $\boldsymbol{\Xi}^{0B}$ of (6.56) into equation (6.48). This leads to (as usual, to keep the notation at a minimum, the superscript B is dropped)

$$\begin{aligned}\boldsymbol{g}^0(k) = &\int_{-\infty}^{+\infty} \mathrm{d}\omega \, \frac{(\gamma^0\omega - \boldsymbol{\gamma}\cdot\boldsymbol{k} + m)\,[\delta(\omega-\omega^0(\boldsymbol{k})) + \delta(\omega+\omega^0(\boldsymbol{k}))]\,\mathrm{sign}(\omega)}{2\,\omega(\boldsymbol{k})\,[\omega - k_0(1+\mathrm{i}\,\eta)]} \\ &- \frac{\mathrm{i}\pi}{\omega^0(\boldsymbol{k})}\, f(|k_0|)\,(\not{k} + m)\,[\delta(k_0 - \omega^0(\boldsymbol{k})) + \delta(k_0 + \omega^0(\boldsymbol{k}))]\,, \end{aligned} \tag{6.57}$$

with the free single-particle energy given by $\omega^0(\boldsymbol{k}) = \sqrt{m^2 + \boldsymbol{k}^2}$. To arrive at equation (6.57), use of

$$\begin{aligned}\delta(k^2 - m^2) &= \delta\big(k_0^2 - \big(\omega^0(\boldsymbol{k})\big)^2\big) \\ &= \frac{1}{2\,\omega^0(\boldsymbol{k})}\,[\delta(k_0 - \omega^0(\boldsymbol{k})) + \delta(k_0 + \omega^0(\boldsymbol{k}))]\end{aligned} \tag{6.58}$$

and $\delta(ax) = \frac{1}{|a|}\delta(x)$ has been made. The expression $[\delta(\omega - \omega(\boldsymbol{k})) + \delta(\omega + \omega(\boldsymbol{k}))]\,\mathrm{sign}(\omega)$ in the numerator of (6.57) can be rewritten as

$$\begin{aligned}&[\delta(\omega - \omega^0(\boldsymbol{k})) + \delta(\omega + \omega^0(\boldsymbol{k}))]\,[\Theta(\omega) - \Theta(-\omega)] \\ &\qquad = [\delta(\omega - \omega^0(\boldsymbol{k})) - \delta(\omega + \omega^0(\boldsymbol{k}))]\,.\end{aligned} \tag{6.59}$$

Substituting (6.59) into (6.57) and integrating over ω gives for the integrand

$$\frac{\gamma^0\omega^0(\boldsymbol{k}) - \boldsymbol{\gamma}\cdot\boldsymbol{k} + m}{\omega^0(\boldsymbol{k}) - (k_0 + \mathrm{i}\,\eta\,k_0)} + \frac{-\gamma^0\omega^0(\boldsymbol{k}) - \boldsymbol{\gamma}\cdot\boldsymbol{k} + m}{\omega^0(\boldsymbol{k}) + (k_0 + \mathrm{i}\,\eta\,k_0)} = \frac{2\,\omega^0(\boldsymbol{k})\;(\not{k} + m)}{-k^2 + m^2 - \mathrm{i}\,\eta}\,, \tag{6.60}$$

and thus for $\boldsymbol{g}^{0B}$,

$$\begin{aligned}\boldsymbol{g}^{0B}_{\zeta\zeta'}(k) = \frac{(\gamma^\mu k_\mu + m_B)_{\zeta\zeta'}}{k^2 - m_B^2 + \mathrm{i}\eta} &+ \mathrm{i}\pi\, f(|k_0|)\,\frac{(\gamma^\mu k_\mu + m_B)_{\zeta\zeta'}}{\omega^{0B}(\boldsymbol{k})} \\ &\times \big[\,\delta(k_0 - \omega^{0B}(\boldsymbol{k})) \;+\; \delta(k_0 + \bar{\omega}^{0B}(\boldsymbol{k}))\,\big]\,.\end{aligned} \tag{6.61}$$

The poles of $\boldsymbol{g}^{0B}(k)$ in the absence of a medium are graphically illustrated in figure 6.1. The presence of a medium doubles the number of poles, from two to four. To see this it is illustrative to rewrite (6.61) as follows. First, expand the first term of (6.61) as

$$\frac{(\not{k} + m_B)_{\zeta\zeta'}}{k^2 - m_B^2 + \mathrm{i}\eta} = \frac{\not{k} + m_{B\,\zeta\zeta'}}{2\,\omega^{0B}(\boldsymbol{k})}\,\frac{2\,\omega^{0B}(\boldsymbol{k})}{k^2 - m_B^2 + \mathrm{i}\eta}\,, \tag{6.62}$$

and then write for the second term of this expansion

$$\frac{2\,\omega^0(\boldsymbol{k})}{k^2 - m^2 + \mathrm{i}\,\eta} = \frac{1}{k_0 - \omega^0(\boldsymbol{k}) + \mathrm{i}\,\eta} - \frac{1}{k_0 + \omega^0(\boldsymbol{k}) - \mathrm{i}\,\eta}\,. \tag{6.63}$$

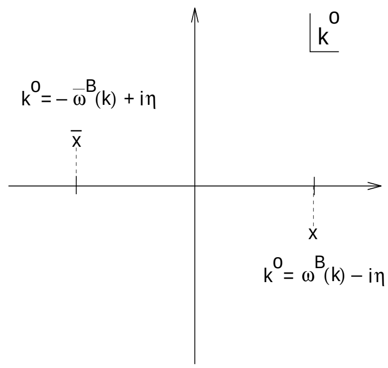

Figure 6.1. Poles of baryon propagator in free space. The symbols 'x' and 'x̄' refer to the locations of particle and antiparticle poles, respectively.

Substituting (6.62) and (6.63) into equation (6.61) leads to

$$\begin{aligned} \boldsymbol{g}^{0B}_{\zeta\zeta'}(k) = \frac{(\gamma^\mu k_\mu + m_B)_{\zeta\zeta'}}{2\,\omega^{0B}(\boldsymbol{k})} \Bigg\{ & \frac{1 - f^B(\boldsymbol{k})}{k_0 - \omega^{0B}(\boldsymbol{k}) + \mathrm{i}\,\eta} + \frac{f^B(\boldsymbol{k})}{k_0 - \omega^{0B}(\boldsymbol{k}) - \mathrm{i}\eta} \\ & - \frac{1 - \bar{f}^B(\boldsymbol{k})}{k_0 + \omega^{0B}(\boldsymbol{k}) - \mathrm{i}\eta} - \frac{\bar{f}^B(\boldsymbol{k})}{k_0 + \omega^{0B}(\boldsymbol{k}) + \mathrm{i}\eta} \Bigg\}. \end{aligned} \tag{6.64}$$

In the above equations, the single-particle energy of free baryons is given by

$$\omega^{0B}(\boldsymbol{k}) = + \sqrt{m_B^2 + \boldsymbol{k}^2} = -\,\bar{\omega}^{0B}(\boldsymbol{k})\,, \tag{6.65}$$

and for the Fermi–Dirac functions,

$$f^B(\boldsymbol{k}) \equiv f(\omega^{0B}(\boldsymbol{k})) = \frac{1}{\mathrm{e}^{\beta\omega^{0B}(k)+1}}\,, \quad \bar{f}^B(\boldsymbol{k}) \equiv \bar{f}(\bar{\omega}^{0B}(\boldsymbol{k})) = \frac{1}{\mathrm{e}^{\beta|\bar{\omega}^{0B}(k)|+1}}\,, \tag{6.66}$$

Introducing the chemical potential of baryons, μ^B, and antibaryons, $\bar{\mu}^B$, in to the the Fermi–Dirac functions of baryons and antibaryons leads to

$$f^B(\boldsymbol{k}) = \frac{1}{\mathrm{e}^{\beta(\omega^B(k)-\mu^B)}+1}\,, \quad \bar{f}^B(\boldsymbol{k}) = \frac{1}{\mathrm{e}^{\beta|\bar{\omega}^B(k)+\bar{\mu}^B|}+1}\,. \tag{6.67}$$

The physical interpretation of $\boldsymbol{g}^{0B}(k)$ is as follows [344]. Both particle and antiparticle states occur as in the usual (causal) Feynman propagator. But due to the nuclear (stellar) medium two new states corresponding to holes in the particle Fermi sea (unfilled states in the Fermi sea of particles) and antiholes in the antiparticle Fermi sea (unfilled states in the Fermi sea of

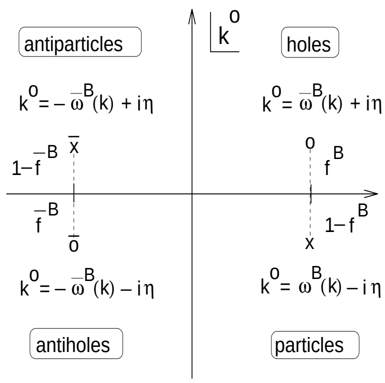

Figure 6.2. Poles of baryon propagator in case of a medium. The crosses 'x' and 'x̄' refer to the locations of particle and antiparticle poles, respectively. The circles 'o' and 'ō' denote hole and antihole poles, respectively.

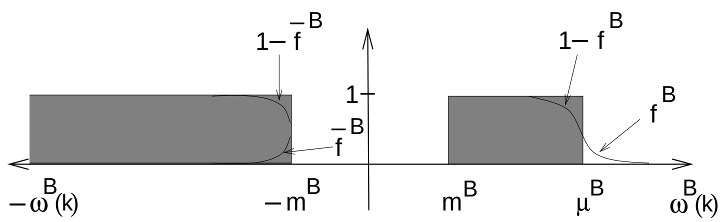

Figure 6.3. Depletion of single-particle states at finite temperature.

antiparticles) result, as illustrated in figures6.2 and 6.3. Thus, the principle effect of finite temperatures on baryon propagation results in states with momenta $|\boldsymbol{k}| > k_F$ and $|\boldsymbol{k}| > \bar{k}_F$ (that is, states outside the Fermi seas of particles and antiparticles become populated), as do hole (antihole) states in the corresponding Fermi seas of particles (antiparticles).

The zero-temperature limit of (6.64) is obtained by noticing that $\bar{f} \to 0$ and

$$f(\omega(\boldsymbol{k}) - \mu) \longrightarrow \Theta(k_F - |\boldsymbol{k}|)\,. \tag{6.68}$$

Equation (6.64) then reduces to

$$\boldsymbol{g}^{0B}_{\zeta\zeta'}(k) = \frac{(\gamma^\mu k_\mu + m_B)_{\zeta\zeta'}}{2\,\omega^{0B}(\boldsymbol{k})}$$

$$\times \left\{ \frac{1-\Theta(k_F-|\boldsymbol{k}|)}{\omega^{0B}(\boldsymbol{k})-k_0-\mathrm{i}\,\eta} + \frac{\Theta(k_F-|\boldsymbol{k}|)}{\omega^{0B}(\boldsymbol{k})-k_0-\mathrm{i}\eta} \right\}. \qquad (6.69)$$

With the help of (6.42) it is seen that the two terms proportional to $\Theta(k_F-|\boldsymbol{k}|)$ can be combined to a δ-function. So in the zero-temperature limit

$$\boldsymbol{g}^{0B}_{\zeta\zeta'}(k) = \frac{(\not{k}+m_B)_{\zeta\zeta'}}{2\,\omega^B(\boldsymbol{k})} \left\{ \frac{1}{\omega^B(\boldsymbol{k})-k_0-i\,\eta} - 2\,\mathrm{i}\,\pi\,\delta(\omega^B(\boldsymbol{k})-k_0)\,\Theta(k_{F_B}-|\boldsymbol{k}|) \right\}. \qquad (6.70)$$

The first term is the usual Dirac propagator of free fermions, which is corrected for the medium by the second term. This follows from the zero-density of (6.69), in which case the Fermi momentum becomes zero and therefore $\Theta(k_F-|\boldsymbol{k}|)\to\Theta(-|\boldsymbol{k}|)=0$. Hence only the first term of (6.70) survives for particles in free space.

In the interacting particle case the spectral function $\boldsymbol{\Xi}^B$ has a more complicated structure than in (6.56). The corresponding baryon Green function however is similar in structure to (6.64). This is specifically the case for the relativistic Hartree (mean-field) approximation, as will be shown in section 6.2.2. The modifications of (6.64) can formally be taken into account by making the following replacements: $k_0\to k_0-\boldsymbol{\Sigma}^{\mathrm{H,B}}_0$, $m_B\to m_B+\boldsymbol{\Sigma}^{\mathrm{H,B}}_S$, and $\omega^{0B}\to\omega^{\mathrm{H,B}}$ [cf. equation (6.170)]. That is, the coupling of the motion of a baryon to the nuclear background, which implies non-vanishing self-energy components, modifies the baryon masses and single-particle energy spectra. The single-particle description carries over as long as the many-particle system is treated for approximation schemes for which the self-energy does not become complex, as is the case for the relativistic Hartree, Hartree–Fock, and some versions of the $\mathbf{T}$-matrix approximation [336].

6.2 Determination of baryon spectral function

In many-body treatments it is customary and useful to measure energies relative to the chemical potential, μ. The concept of chemical potentials has already been discussed in great detail in chapter 4 in connection with the particle composition of neutron star matter at equilibrium. In the previous section we have seen how the single particle distribution changes with temperature relative to the zero-temperature distribution, whereby the chemical potential plays a most intuitive role. To introduce μ^B into the spectral representation of $\boldsymbol{g}^B(k)$ we rescale the energy argument in (6.48) according to the replacement $k_0 \to k_0 - \mu^B$, which gives

$$\boldsymbol{g}^B_{\zeta\zeta'}(k_0, \boldsymbol{k}) = \int_{-\infty}^{+\infty} \mathrm{d}\omega \, \frac{\boldsymbol{\Xi}^B_{\zeta\zeta'}(\omega, \boldsymbol{k})}{\omega - (k_0 - \mu^B)\,(1 + \mathrm{i}\,\eta)} - 2\,\mathrm{i}\,\pi \,\mathrm{sign}(k_0 - \mu^B)\; f(|k_0 - \mu^B|)\; \boldsymbol{\Xi}^B_{\zeta\zeta'}(k_0 - \mu^B, \boldsymbol{k}) \,. \tag{6.71}$$

To ensure compatibility between (6.71) and its analytically continued representation, derived in equation (6.33), we must ensure that

$$\boldsymbol{g}^B(k_0 + \mu^B, \boldsymbol{k}) = \int_{-\infty}^{+\infty} \mathrm{d}\omega \, \frac{\boldsymbol{\Xi}^B(\omega, \boldsymbol{k})}{\omega - k_0(1 + \mathrm{i}\,\eta)} = \tilde{\boldsymbol{g}}^B(k_0(1 + \mathrm{i}\eta), \boldsymbol{k}) \,, \tag{6.72}$$

with the identification $z = k_0(1 + \mathrm{i}\eta)$. We know that $\boldsymbol{g}^B(k_0, \boldsymbol{k})$ is obtained from Dyson's equation, given in (5.123). So $\boldsymbol{g}^B(k_0 + \mu^B, \boldsymbol{k})$ of (6.72) must be made compatible with

$$\big(\gamma^0 k_0 - \boldsymbol{\gamma} \cdot \boldsymbol{k} - m_B \, \mathbf{1} - \boldsymbol{\Sigma}^B(k_0, \boldsymbol{k})\big) \; \boldsymbol{g}^B(k_0, \boldsymbol{k}) = -\,\mathbf{1} \,, \tag{6.73}$$

which is accomplished by the replacement $k_0 \to k_0 + \mu^B$ in (6.73),

$$\big\{\gamma^0(k_0{+}\mu^B) {-} \boldsymbol{\gamma}{\cdot}\boldsymbol{k} {-} m_B \, \mathbf{1} {-} \boldsymbol{\Sigma}^B(k_0{+}\mu^B, \boldsymbol{k})\big\} \, \boldsymbol{g}^B(k_0{+}\mu^B, \boldsymbol{k}) = -\,\mathbf{1} \,. \tag{6.74}$$

Because of (6.72) we have

$$\boldsymbol{\Sigma}^B(k_0 + \mu^B, \boldsymbol{k}) = \tilde{\boldsymbol{\Sigma}}^B(k_0(1 + \mathrm{i}\eta), \boldsymbol{k}) \,, \tag{6.75}$$

$$\boldsymbol{g}^B(k_0 + \mu^B, \boldsymbol{k}) = \tilde{\boldsymbol{g}}^B(k_0(1 + \mathrm{i}\eta), \boldsymbol{k}) \,, \tag{6.76}$$

and thus for Dyson's equation

$$\big\{\gamma^0(k_0 + \mu^B) - \boldsymbol{\gamma} \cdot \boldsymbol{k} - m_B \, \mathbf{1} - \tilde{\boldsymbol{\Sigma}}^B(k_0(1 + \mathrm{i}\eta), \boldsymbol{k})\big\} \tilde{\boldsymbol{g}}^B(k_0(1 + \mathrm{i}\eta), \boldsymbol{k}) = -\mathbf{1} \,,$$

which, upon replacing $k_0(1 + \mathrm{i}\eta)$ with z, leads to the desired analytically continued representation of Dyson's equation,

$$\big\{\gamma^0(z + \mu^B) - \boldsymbol{\gamma} \cdot \boldsymbol{k} - m_B \, \mathbf{1} - \tilde{\boldsymbol{\Sigma}}^B(z, \boldsymbol{k})\big\} \, \tilde{\boldsymbol{g}}^B(z, \boldsymbol{k}) = -\,\mathbf{1} \,. \tag{6.77}$$

Finally we note that from equation (6.76), the *physical* two-point baryon Green function and self-energy, $\boldsymbol{g}^B$ and $\boldsymbol{\Sigma}^B$, are obtained from their analytically continued counterparts as

$$\boldsymbol{g}^B(k_0, \boldsymbol{k}) = \tilde{\boldsymbol{g}}^B((k_0 - \mu^B)(1 + \mathrm{i}\eta), \boldsymbol{k}) \,, \tag{6.78}$$

and

$$\boldsymbol{\Sigma}^B(k_0, \boldsymbol{k}) = \tilde{\boldsymbol{\Sigma}}^B((k_0 - \mu^B)(1 + \mathrm{i}\eta), \boldsymbol{k})\,. \tag{6.79}$$

As outlined in reference [92], because of the translational and rotational invariance in the rest frame of infinite nuclear matter and the assumed invariance under parity and time reversal, the self-energy may be written quite generally as

$$\begin{aligned}\boldsymbol{\Sigma}^B(k) &= \Sigma^B_S(k) + \gamma^\mu\, \Sigma^B_\mu(k) \\ &\equiv \Sigma^B_S(k^0, |\boldsymbol{k}|) + \gamma^0\, \Sigma^B_0(k^0, |\boldsymbol{k}|) + \boldsymbol{\gamma}\cdot\hat{\boldsymbol{k}}\, \Sigma^B_V(k^0, |\boldsymbol{k}|)\,, \end{aligned} \tag{6.80}$$

The functions Σ^B_S, Σ^B_V and Σ^B_0 are referred to as scalar, vector, and timelike components of the baryon self-energy. The proof of this decomposition is as follows [92]. At finite density, the self-energy may depend on two four-vectors, k^μ and B^μ, and three Lorentz scalars, k^2, B^2, and kB. In the rest frame of nuclear matter ($B^\mu = \delta^{\mu 0}\rho$), the latter may be replaced with $\boldsymbol{k}^2$, ρ, and k^0, which leads to the arguments of the Lorentz-scalar functions in (6.80). The matrix structure of $\boldsymbol{\Sigma}^B$ is determined by combining k^μ and B^μ with gamma matrices, which leads to the four independent, parity-conserving choices

$$1, \quad \gamma_\mu\, k^\mu, \quad \gamma_\mu\, B^\mu, \quad \sigma_{\mu\nu}\, k^\mu\, B^\nu\,, \tag{6.81}$$

or

$$1, \quad \gamma_\mu\, k^\mu, \quad \gamma^0\, \rho, \quad \sigma_{0i}\, k^i\, \rho^\nu\,. \tag{6.82}$$

The tensor piece proportional to σ_{0i} does not contribute if one assumes time-reversal invariance and the hermiticity of $\boldsymbol{\Sigma}^B$. Linear combination of the other three forms then results in the three terms in (6.80).

Attaching the spin and isospin indices to (6.80), i.e.

$$\boldsymbol{\Sigma}^B_{\zeta\zeta'} \;\equiv\; (\mathbf{1})_{\zeta\zeta'}\, \Sigma^B_S + (\boldsymbol{\gamma}\cdot\hat{\boldsymbol{k}})_{\zeta\zeta'}\, \Sigma^B_V + (\gamma^0)_{\zeta\zeta'}\, \Sigma^B_0\,, \tag{6.83}$$

and substituting this result into Dyson's equation (6.73) leads to

$$\begin{aligned}\big\{\mathbf{1}\, [m_B + \Sigma^B_S(k_0, \boldsymbol{k})] \;+\; \boldsymbol{\gamma}\cdot\hat{\boldsymbol{k}}\, [|\boldsymbol{k}| + \Sigma^B_V(k_0, \boldsymbol{k})] \\ +\; \gamma^0\, [\Sigma^B_0(k_0, \boldsymbol{k}) - k_0]\big\}\, \boldsymbol{g}^B(k_0, \boldsymbol{k}) \;=\; 1\,, \end{aligned} \tag{6.84}$$

and for the analytically continued Dyson equation

$$\begin{aligned}\big\{\mathbf{1}\, [m_B + \tilde{\Sigma}^B_S(z, \boldsymbol{k})] \;+\; \boldsymbol{\gamma}\cdot\hat{\boldsymbol{k}}\, [|\boldsymbol{k}| + \tilde{\Sigma}^B_V(z, \boldsymbol{k})] \\ +\; \gamma^0\, [\tilde{\Sigma}^B_0(z, \boldsymbol{k}) + (z + \mu^B)]\big\}\, \tilde{\boldsymbol{g}}^B(z, \boldsymbol{k}) \;=\; 1\,. \end{aligned} \tag{6.85}$$

To derive the explicit form of the baryon spectral function, which follows from equation (6.35), we need to know the analytic properties of Dyson's equation, that is, of the functions $\tilde{\boldsymbol{\Sigma}}^B$ and $\tilde{\boldsymbol{g}}^B$. For this purpose we express $\tilde{\boldsymbol{\Sigma}}^B$ via a spectral representation of the form

$$\tilde{\boldsymbol{\Sigma}}^B_{\zeta\zeta'}(z, \boldsymbol{k}) \;=\; \boldsymbol{\Sigma}^{(\infty)\,B}_{\zeta\zeta'} \;+\; \int\limits_{-\infty}^{+\infty} \mathrm{d}\omega \, \frac{\boldsymbol{\mathcal{S}}^B_{\zeta\zeta'}(\omega, \boldsymbol{k})}{\omega - z} \,, \tag{6.86}$$

with

$$\boldsymbol{\Sigma}^{(\infty)\,B}_{\zeta\zeta'} \;\equiv\; (\gamma_\mu \, k^\mu \;-\; m_B)_{\zeta\zeta'} \,. \tag{6.87}$$

The associated spectral function, $\boldsymbol{\mathcal{S}}^B$, is then obtained as

$$\tilde{\boldsymbol{\Sigma}}(\omega + \mathrm{i}\eta, \boldsymbol{k}) - \tilde{\boldsymbol{\Sigma}}(\omega - \mathrm{i}\eta, \boldsymbol{k}) \;=\; 2\,\mathrm{i}\,\pi \, \boldsymbol{\mathcal{S}}(\omega, \boldsymbol{k}) \,. \tag{6.88}$$

Since $\boldsymbol{\Sigma}^{(\infty)B}$ and $\boldsymbol{\mathcal{S}}$ are real functions, one readily finds from (6.86) that the self-energy obeys the relation

$$\tilde{\boldsymbol{\Sigma}}(z^*, \boldsymbol{k}) = \tilde{\boldsymbol{\Sigma}}^*(z, \boldsymbol{k}) \,, \tag{6.89}$$

and, similarly, for the analytically continued two-point baryon Green function,

$$\tilde{\boldsymbol{g}}(z^*, \boldsymbol{k}) = \tilde{\boldsymbol{g}}^*(z, \boldsymbol{k}) \,. \tag{6.90}$$

Moreover one has

$$\mathrm{Re}\ \tilde{\boldsymbol{\Sigma}}(\omega + \mathrm{i}\eta, \boldsymbol{k}) = \mathrm{Re}\ \tilde{\boldsymbol{\Sigma}}(\omega - \mathrm{i}\eta, \boldsymbol{k}) \,, \tag{6.91}$$

and

$$\mathrm{Im}\ \boldsymbol{\Sigma}(\omega + \mathrm{i}\eta, \boldsymbol{k}) = -\mathrm{Im}\ \boldsymbol{\Sigma}(\omega - \mathrm{i}\eta, \boldsymbol{k}) = -\,\pi \, \mathcal{S}(\omega, \boldsymbol{k}) \,. \tag{6.92}$$

Because of equations (6.79) and (6.91), we can write for the real part of the physical self-energy

$$\boldsymbol{\Lambda}(\omega, \boldsymbol{k}) \equiv \mathrm{Re}\ \tilde{\boldsymbol{\Sigma}}(\omega - \mu - \mathrm{i}\eta, \boldsymbol{k}) = \mathrm{Re}\ \tilde{\boldsymbol{\Sigma}}(\omega - \mu + \mathrm{i}\eta, \boldsymbol{k}) \,, \tag{6.93}$$

which, upon rescaling the energy argument according to $\omega \to \omega + \mu$, reads

$$\boldsymbol{\Lambda}(\omega + \mu, \boldsymbol{k}) = \mathrm{Re}\ \tilde{\boldsymbol{\Sigma}}(\omega - \mathrm{i}\eta, \boldsymbol{k}) = \mathrm{Re}\ \tilde{\boldsymbol{\Sigma}}(\omega + \mathrm{i}\eta, \boldsymbol{k}) \,. \tag{6.94}$$

The mathematical structure of the imaginary part of the physical self-energy demands for somewhat more consideration. Turning back to (6.79), one finds

$$\begin{aligned} \mathrm{Im}\ \boldsymbol{\Sigma}(\omega, \boldsymbol{k}) &= \mathrm{Im}\ \tilde{\boldsymbol{\Sigma}}((\omega - \mu)(1 + \mathrm{i}\eta), \boldsymbol{k}) \\ &= \mathrm{Im}\ \tilde{\boldsymbol{\Sigma}}(\omega - \mu + \mathrm{i}\eta \, \mathrm{sign}(\omega - \mu), \boldsymbol{k}) \,. \end{aligned} \tag{6.95}$$

Since $\tilde{\boldsymbol{\Sigma}}(\omega - \mu + \mathrm{i}\eta, \boldsymbol{k})$ and $\tilde{\boldsymbol{\Sigma}}(\omega - \mu - \mathrm{i}\eta, \boldsymbol{k})$ differ only by a sign, as can be seen from (6.92), equation (6.95) may be written as

$$\mathrm{Im}\ \boldsymbol{\Sigma}(\omega, \boldsymbol{k}) = \mathrm{sign}(\mu - \omega)\ \mathrm{Im}\ \tilde{\boldsymbol{\Sigma}}(\omega - \mu - \mathrm{i}\eta, \boldsymbol{k}) \equiv \boldsymbol{\Gamma}(\omega, \boldsymbol{k})\,. \tag{6.96}$$

Multiplying both sides of (6.96) with $\mathrm{sign}(\mu - \omega)$ leads for $\mathrm{Im}\ \tilde{\boldsymbol{\Sigma}}$ to

$$\mathrm{Im}\ \tilde{\boldsymbol{\Sigma}}(\omega - \mu \mp \mathrm{i}\eta, \boldsymbol{k})\ =\ \pm\,\mathrm{sign}(\mu - \omega)\ \boldsymbol{\Gamma}(\omega, \boldsymbol{k})\,, \tag{6.97}$$

which, upon rescaling the energy argument as just above, $\omega \to \omega + \mu$, reads

$$\mathrm{Im}\ \tilde{\boldsymbol{\Sigma}}(\omega \mp \mathrm{i}\eta, \boldsymbol{k}) = \pm\,\mathrm{sign}(-\omega)\ \boldsymbol{\Gamma}(\omega + \mu, \boldsymbol{k})\,. \tag{6.98}$$

To keep the notation in the subsequent analysis to a minimum, let us introduce an auxiliary functions F_S for the scalar part of the baryon self-energy, defined as

$$\begin{aligned} F_S^{\pm} &\equiv F_S(\omega \pm \mathrm{i}\eta, \boldsymbol{k}) \equiv m + \tilde{\Sigma}_S(\omega \pm \mathrm{i}\eta, \boldsymbol{k}) \\ &= m + \mathrm{Re}\ \tilde{\Sigma}_S(\omega \pm \mathrm{i}\eta, \boldsymbol{k}) + \mathrm{i}\ \mathrm{Im}\ \tilde{\Sigma}_S(\omega \pm \mathrm{i}\eta, \boldsymbol{k}) \\ &= m + \Lambda_S(\omega + \mu, \boldsymbol{k}) \pm \mathrm{i}\ \mathrm{sign}(+\omega)\Gamma_S(\omega + \mu, \boldsymbol{k}) \\ &\equiv m + \Lambda_S^+ \pm \mathrm{i}\,\sigma^+\Gamma_S^+\,, \end{aligned} \tag{6.99}$$

where use of (6.94) and (6.98), and of the relation $\mathrm{sign}(\omega) = -\mathrm{sign}(-\omega)$ was made. The plus signs attached as superscripts to Λ and Γ in (6.99) refer to the plus signs that occur in their arguments, i.e. $\omega + \mu$. Similarly we introduced the abbreviation $\sigma^{\pm} \equiv \mathrm{sign}(\pm\omega)$. In close analogy to $F_S^{\pm}$, we introduce for the vector component of the baryon self-energy

$$\begin{aligned} F_V^{\pm} &\equiv F_V(\omega \pm \mathrm{i}\eta, \boldsymbol{k}) \equiv |\boldsymbol{k}| + \tilde{\Sigma}_V(\omega \pm \mathrm{i}\eta, \boldsymbol{k}) \\ &= |\boldsymbol{k}| + \mathrm{Re}\ \tilde{\Sigma}_V(\omega \pm \mathrm{i}\eta, \boldsymbol{k}) + \mathrm{i}\ \mathrm{Im}\ \tilde{\Sigma}_V(\omega \pm \mathrm{i}\eta, \boldsymbol{k}) \\ &= |\boldsymbol{k}| + \Lambda_V(\omega + \mu, \boldsymbol{k}) \pm \mathrm{i}\ \mathrm{sign}(+\omega)\Gamma_V(\omega + \mu, \boldsymbol{k}) \\ &\equiv |\boldsymbol{k}| + \Lambda_V^+ \pm \mathrm{i}\,\sigma^+\Gamma_V^+\,, \end{aligned} \tag{6.100}$$

and for the timelike component of the self-energy,

$$\begin{aligned} F_0^{\pm} &\equiv F_0(\omega \pm \mathrm{i}\eta, \boldsymbol{k}) \equiv \tilde{\Sigma}_0(\omega \pm \mathrm{i}\eta, \boldsymbol{k}) - \mu \\ &= \mathrm{Re}\ \tilde{\Sigma}_0(\omega \pm \mathrm{i}\eta, \boldsymbol{k}) + \mathrm{i}\ \mathrm{Im}\ \tilde{\Sigma}_0(\omega \pm \mathrm{i}\eta, \boldsymbol{k}) - \mu \\ &= \Lambda_0(\omega + \mu, \boldsymbol{k}) \pm \mathrm{i}\ \mathrm{sign}(+\omega)\Gamma_0(\omega + \mu, \boldsymbol{k}) - \mu \\ &\equiv \Lambda_0^+ - \mu \pm \mathrm{i}\,\sigma^+\Gamma_0^+\,. \end{aligned} \tag{6.101}$$

From equations (6.99) through (6.101) one calculates that

$$\begin{aligned} &\left(F_S^{\pm}\right)^2 + \left(F_V^{\pm}\right)^2 - \left(F_0^{\pm} - (\omega \pm \mathrm{i}\eta)\right)^2 \\ &\qquad = \left[m + \Lambda_S^+ \pm \mathrm{i}\,\sigma^+\Gamma_S^+\right]^2 + \left[|\boldsymbol{k}| + \Lambda_V^+ \pm \mathrm{i}\,\sigma^+\Gamma_V^+\right]^2 \\ &\qquad\quad - \left[\Lambda_0^+ - \mu - \omega \pm \mathrm{i}(\sigma^+\Gamma_0^+ - \eta)\right]^2\,, \end{aligned} \tag{6.102}$$

which can be written as

$$
\begin{aligned}
&\left(F_S^{\pm}\right)^2 + \left(F_V^{\pm}\right)^2 - \left(F_0^{\pm} - (\omega \pm \mathrm{i}\eta)\right)^2 \\
&\qquad = \big[(m + \Lambda_S^+)^2 - {\Gamma_S^+}^2 + (\boldsymbol{k} + \Lambda_V^+)^2 - {\Gamma_V^+}^2 \\
&\qquad\quad - (\Lambda_0^+ - \mu - \omega)^2 + {\Gamma_0^+}^2 - 2\,\sigma^+ \Gamma_0^+ \eta + \eta^2\big] \\
&\qquad\quad \pm \mathrm{i}\,\sigma^+ \big[2(m + \Lambda_S^+)\Gamma_S^+ + 2(|\boldsymbol{k}| + \Lambda_V^+)\Gamma_V^+ \\
&\qquad\quad - 2(\Lambda_0^+ - \mu - \omega)(\Gamma_0^+ - \sigma^+ \eta)\big]\,. \qquad (6.103)
\end{aligned}
$$

With the above definitions at our disposal, we now solve Dyson's equation (6.85) for the analytically continued two-point Green function, which gives

$$
\tilde{\boldsymbol{g}}(z) = \frac{1}{\mathbf{1}\, F_S(z) \;+\; \boldsymbol{\gamma}\boldsymbol{\cdot}\hat{\boldsymbol{k}}\; F_V(z) \;+\; \gamma^0\,(F_0(z) - z)}\,. \qquad (6.104)
$$

By means of multiplying both numerator and denominator of (6.104) with $\mathbf{1}F_S(z) + \boldsymbol{\gamma}\boldsymbol{\cdot}\hat{\boldsymbol{k}}F_V(z) + \gamma^0(F_0(z) - z)$ we can get rid of the Dirac matrices, as outlined in appendix A.2. One then obtains

$$
\tilde{\boldsymbol{g}}(z) = \frac{\mathbf{1}\, F_S(z) \;-\; \boldsymbol{\gamma}\boldsymbol{\cdot}\hat{\boldsymbol{k}}\; F_V(z) \;-\; \gamma^0\,(F_0(z) - z)}{F_S^2(z) \;+\; F_V^2(z) \;-\; (F_0(z) - z)^2}\,. \qquad (6.105)
$$

In order to derive the expression for the spectral function $\boldsymbol{\Xi}$, we need to calculate the discontinuity of $\tilde{\boldsymbol{g}}(z)$ across the real energy axis. With the aid of (6.105), one arrives for $\boldsymbol{\Xi}$ at

$$
\begin{aligned}
\boldsymbol{\Xi}(\omega, \boldsymbol{k}) &= \frac{1}{2\,\mathrm{i}\,\pi}\left\{\tilde{\boldsymbol{g}}(\omega + \mathrm{i}\eta, \boldsymbol{k}) \;-\; \tilde{\boldsymbol{g}}(\omega - \mathrm{i}\eta, \boldsymbol{k})\right\} \\
&= \frac{1}{2\,\mathrm{i}\,\pi}\left\{\frac{\mathbf{1}\,F_S^+ - \boldsymbol{\gamma}\boldsymbol{\cdot}\hat{\boldsymbol{k}}\,F_V^+ - \gamma^0\,(F_0^+ - \omega + \mathrm{i}\eta)}{\left(F_S^+\right)^2 + \left(F_V^+\right)^2 - \left(F_0^+ - \omega + \mathrm{i}\eta\right)^2}\right. \\
&\qquad\quad \left. - \frac{\mathbf{1}\,F_S^- - \boldsymbol{\gamma}\boldsymbol{\cdot}\hat{\boldsymbol{k}}\,F_V^- - \gamma^0\,(F_0^- - \omega - \mathrm{i}\eta)}{\left(F_S^-\right)^2 + \left(F_V^-\right)^2 - \left(F_0^- - \omega - \mathrm{i}\eta\right)^2}\right\} \qquad (6.106) \\
&\equiv \frac{1}{2\,\mathrm{i}\,\pi}\left\{a^+ \;-\; a^-\right\}\,. \qquad (6.107)
\end{aligned}
$$

The calculation of the difference between a^+ and a^- in (6.107) is somewhat lengthy and cumbersome. To keep it as easy to survey as possible, let us define the following additional auxiliary functions:

$$
\begin{aligned}
N &\equiv \big[(m + \Lambda_S)^2 + (|\boldsymbol{k}| + \Lambda_V)^2 - (\Lambda_0 - (\omega + \mu))^2 \\
&\quad - \Gamma_S^2 - \Gamma_V^2 + \Gamma_0^2\big]^2 + 4\big[\Gamma_S(m + \Lambda_S) + \Gamma_V(|\boldsymbol{k}| + \Lambda_V) \\
&\quad - (\Gamma_0 - \sigma(\omega)\eta)(\Lambda_0 - (\omega + \mu))\big]^2 \\
&\equiv \big[F - \Gamma_S^2 - \Gamma_V^2 + \Gamma_0^2\big]^2 + \hat{\Gamma}^2\,, \qquad (6.108)
\end{aligned}
$$

where,

$$F \equiv F(\omega+\mu) = (m+\Lambda_S)^2 + (|\boldsymbol{k}|+\Lambda_V)^2 - (\Lambda_0 - (\omega+\mu))^2\,, \tag{6.109}$$

$$\begin{aligned}\hat\Gamma &\equiv \hat\Gamma(\omega+\mu)\\ &= 2\big[\Gamma_S(m+\Lambda_S) + \Gamma_V(|\boldsymbol{k}|+\Lambda_V) - (\Gamma_0 - \sigma(\omega)\eta)(\Lambda_0 - (\omega+\mu))\big]\,,\end{aligned} \tag{6.110}$$

$$F_1 \equiv \frac{1}{2}\,\sigma(-\omega)\,\hat\Gamma(\omega+\mu)\,, \tag{6.111}$$

and

$$F_2 \equiv F(\omega+\mu) - \Gamma_S^2 - \Gamma_V^2 + \Gamma_0^2 - 2\sigma(\omega)\Gamma_0^+\eta + \eta^2\,. \tag{6.112}$$

With the definitions (6.108) through (6.112) the functions $a^\pm$ in (6.107) are given by

$$a^\pm = \frac{\big[\mathbf{1}\,F_S^\pm - \boldsymbol{\gamma}\cdot\hat{\boldsymbol{k}}\,F_V^\pm - \gamma^0\left(F_0^\pm - (\omega\pm\mathrm{i}\eta)\right)\big]\big[F_2\,\pm\,\mathrm{i}\,\sigma^-\,\hat\Gamma\big]}{N}\,. \tag{6.113}$$

Substituting (6.99) to (6.101) for $F_S^\pm$, $F_V^\pm$ and $F_0^\pm$ into (6.113) leads to

$$\begin{aligned}N\,a^\pm = \big[\mathbf{1}\,&\big((m+\Lambda_S)\mp\mathrm{i}\sigma^-\Gamma_S\big) - \boldsymbol{\gamma}\cdot\hat{\boldsymbol{k}}\,\big((|\boldsymbol{k}|+\Lambda_V)\mp\mathrm{i}\sigma^-\Gamma_V\big)\\ &-\gamma^0\left((\Lambda_0-(\omega+\mu\pm\mathrm{i}\eta))\mp\mathrm{i}\sigma^-\Gamma_0\right)\big]\left[F_2\,\pm\,\mathrm{i}\sigma^-\,\hat\Gamma\right].\end{aligned} \tag{6.114}$$

Collecting terms according to their matrix structure then gives

$$\begin{aligned}N\,a^\pm = \mathbf{1}\,&\big\{F_2\left[m+\Lambda_S\mp\mathrm{i}\sigma^-\Gamma_S\right]\pm\mathrm{i}\sigma^-\hat\Gamma\left[m+\Lambda_S\mp\mathrm{i}\sigma^-\Gamma_S\right]\big\}\\ &-\boldsymbol{\gamma}\cdot\hat{\boldsymbol{k}}\,\big\{F_2\left[|\boldsymbol{k}|+\Lambda_V\mp\mathrm{i}\sigma^-\Gamma_V\right]\pm\mathrm{i}\sigma^-\hat\Gamma\left[|\boldsymbol{k}|+\Lambda_V\mp\mathrm{i}\sigma^-\Gamma_V\right]\big\}\\ &-\gamma^0\,\big\{F_2\left[\Lambda_0-(\omega+\mu\pm\mathrm{i}\eta)\mp\mathrm{i}\sigma^-\Gamma_0\right]\\ &\qquad\qquad\pm\mathrm{i}\sigma^-\hat\Gamma\left[\Lambda_0-(\omega+\mu\pm\mathrm{i}\eta)\mp\mathrm{i}\sigma^-\Gamma_0\right]\big\}\,.\end{aligned} \tag{6.115}$$

Putting this expression back into (6.107) results in

$$\begin{aligned}\frac{a^+-a^-}{2\,\mathrm{i}\,\pi} = \mathbf{1}\,&\frac{1}{\pi\,N}\left\{\sigma^-\hat\Gamma(m+\Lambda_S) - F_2\sigma^-\Gamma_S\right\}\\ &-\boldsymbol{\gamma}\cdot\hat{\boldsymbol{k}}\,\frac{1}{\pi\,N}\left\{\sigma^-\hat\Gamma(|\boldsymbol{k}|+\Lambda_V) - F_2\sigma^-\Gamma_V\right\}\\ &-\gamma^0\,\frac{1}{\pi\,N}\left\{\sigma^-\hat\Gamma(\Lambda_0-(\omega+\mu)) - F_2\sigma^-\Gamma_0\right\}.\end{aligned} \tag{6.116}$$

From equation (6.116) one sees that the spectral function splits up into the same three different Dirac–Lorentz components as the self-energy (6.83). We therefore introduce the decomposition

$$\boldsymbol{\Xi}(\omega,\boldsymbol{k}) = \mathbf{1}\;\Xi_S(\omega,\boldsymbol{k}) + \boldsymbol{\gamma}\cdot\hat{\boldsymbol{k}}\;\Xi_V(\omega,\boldsymbol{k}) + \gamma^0\;\Xi_0(\omega,\boldsymbol{k})\,. \tag{6.117}$$

The expressions for the individual terms in (6.117) can then be identified by comparing (6.117) with (6.116). This leads to

$$\Xi_S(\omega,\boldsymbol{k}) = \frac{\sigma^-}{\pi}\,\frac{\hat\Gamma(m+\Lambda_S) - \big[F-\Gamma_S^2-\Gamma_V^2+\Gamma_0^2\big]\Gamma_S}{\big[F-\Gamma_S^2-\Gamma_V^2+\Gamma_0^2\big]+\hat\Gamma^2}\,, \tag{6.118}$$

$$\Xi_V(\omega,\boldsymbol{k}) = -\,\frac{\sigma^-}{\pi}\,\frac{\hat\Gamma(|\boldsymbol{k}|+\Lambda_V) - \big[F-\Gamma_S^2-\Gamma_V^2+\Gamma_0^2\big]\Gamma_V}{\big[F-\Gamma_S^2-\Gamma_V^2+\Gamma_0^2\big]+\hat\Gamma^2}\,, \tag{6.119}$$

$$\Xi_S(\omega,\boldsymbol{k}) = -\,\frac{\sigma^-}{\pi}\,\frac{\hat\Gamma(\Lambda_0-(\omega+\mu)) - \big[F-\Gamma_S^2-\Gamma_V^2+\Gamma_0^2\big]\Gamma_0}{\big[F-\Gamma_S^2-\Gamma_V^2+\Gamma_0^2\big]+\hat\Gamma^2}\,. \tag{6.120}$$

The spectral functions derived in equations (6.118) to (6.120) look considerably simpler for systems whose baryon self-energies are real functions, as will be demonstrated next. The real-self-energy limit is obtained by taking $\Gamma_i \to 0$, with $i = S, V, 0$. So the second terms in (6.118) to (6.120) vanish trivially. Care, however, is to be taken with respect to the terms proportional to $\sigma^-\hat\Gamma \equiv \mathrm{sign}(-\omega)\hat\Gamma$. By making use of the general relation

$$|x|\,\mathrm{sign}(x\,y) = x\,\mathrm{sign}(y) \tag{6.121}$$

and setting $x = \hat\Gamma$ and $y = -\omega$, these products can be written as

$$|\hat\Gamma(\omega+\mu)|\,\mathrm{sign}\big(-\omega\,\hat\Gamma(\omega+\mu)\big) = \hat\Gamma(\omega+\mu)\,\mathrm{sign}(-\omega)\,. \tag{6.122}$$

Substituting (6.122) into (6.118) to (6.120) then gives for the spectral functions

$$\begin{aligned}\Xi_S(\omega,\boldsymbol{k}) &= \frac{1}{\pi}\,\frac{|\hat\Gamma(\omega+\mu)|}{\big[F-\Gamma_S^2-\Gamma_V^2+\Gamma_0^2\big]^2+\hat\Gamma^2}\,\mathrm{sign}(-\omega\hat\Gamma)(m+\Lambda_S)\\ &\quad -\frac{1}{\pi}\,\frac{|\hat\Gamma_S|}{\big[F-\Gamma_S^2-\Gamma_V^2+\Gamma_0^2\big]^2+\hat\Gamma^2}\\ &\quad \times \mathrm{sign}(-\omega\hat\Gamma_S)\big[F-\Gamma_S^2-\Gamma_V^2+\Gamma_0^2\big] &(6.123)\\ &\quad \longrightarrow \delta[F(\omega+\mu,\boldsymbol{k})]\,\mathrm{sign}[-\omega\,\hat\Gamma(\omega+\mu,\boldsymbol{k})]\\ &\qquad \times [m+\Lambda_S(\omega+\mu,\boldsymbol{k})] \qquad \text{for} \quad \hat\Gamma\to 0\,, &(6.124)\end{aligned}$$

$$\begin{aligned}\Xi_V(\omega,\boldsymbol{k}) = &-\frac{1}{\pi}\,\frac{|\hat\Gamma(\omega+\mu)|}{\big[F-\Gamma_S^2-\Gamma_V^2+\Gamma_0^2\big]^2+\hat\Gamma^2}\,\mathrm{sign}(-\omega\hat\Gamma)(|\boldsymbol{k}|+\Lambda_V)\\ &+\frac{1}{\pi}\,\frac{|\hat\Gamma_V|}{\big[F-\Gamma_S^2-\Gamma_V^2+\Gamma_0^2\big]^2+\hat\Gamma^2}\end{aligned}$$

$$
\begin{aligned}
&\times \operatorname{sign}(-\omega\hat{\Gamma}_V)\big[F - \Gamma_S^2 - \Gamma_V^2 + \Gamma_0^2\big] && (6.125)\\
&\longrightarrow -\delta[F(\omega+\mu,\boldsymbol{k})]\ \operatorname{sign}[-\omega\,\hat{\Gamma}(\omega+\mu,\boldsymbol{k})]\\
&\qquad \times [|\boldsymbol{k}| + \Lambda_V(\omega+\mu,\boldsymbol{k})] \qquad \text{for} \quad \hat{\Gamma}\to 0\,, && (6.126)
\end{aligned}
$$

and

$$
\begin{aligned}
\Xi_0(\omega,\boldsymbol{k}) = &-\frac{1}{\pi}\frac{|\hat{\Gamma}(\omega+\mu)|}{\big[F - \Gamma_S^2 - \Gamma_V^2 + \Gamma_0^2\big]^2 + \hat{\Gamma}^2}\operatorname{sign}(-\omega\hat{\Gamma})(\Lambda_0 - (\omega+\mu))\\
&+\frac{1}{\pi}\frac{|\hat{\Gamma}_S|}{\big[F - \Gamma_S^2 - \Gamma_V^2 + \Gamma_0^2\big]^2 + \hat{\Gamma}^2}\\
&\times \operatorname{sign}(-\omega\hat{\Gamma}_0)\big[F - \Gamma_S^2 - \Gamma_V^2 + \Gamma_0^2\big] && (6.127)\\
&\longrightarrow -\delta[F(\omega+\mu,\boldsymbol{k})]\ \operatorname{sign}[-\omega\,\hat{\Gamma}(\omega+\mu,\boldsymbol{k})]\\
&\qquad \times [\Lambda_0(\omega+\mu,\boldsymbol{k}) - (\omega+\mu)] \qquad \text{for} \quad \hat{\Gamma}\to 0\,. && (6.128)
\end{aligned}
$$

The quantity $\hat{\Gamma}$ reduces for $\Gamma_i \to 0$ to

$$\hat{\Gamma}(\omega+\mu,\boldsymbol{k}) \longrightarrow 2\eta\,\operatorname{sign}(\omega)\ \ [\Lambda_0(\omega+\mu,\boldsymbol{k}) - (\omega+\mu)]\ , \tag{6.129}$$

where ω is to be set equal to the respective single-particle energy, that is, $\omega_1 \equiv \omega(\boldsymbol{k}) - \mu$ for particles and $\omega_2 \equiv \bar{\omega}(\boldsymbol{k}) - \mu$ for antiparticles. Thus

$$\hat{\Gamma}(\omega+\mu,\boldsymbol{k})\big|_{\omega=\omega_1-\mu} \longrightarrow 2\eta\ \operatorname{sign}(\omega_1-\mu)\ \ [\Lambda_0(\omega_1,\boldsymbol{k}) - \omega_1]\ , \tag{6.130}$$

and

$$\hat{\Gamma}(\omega+\mu,\boldsymbol{k})\big|_{\omega=\omega_2-\mu} \longrightarrow 2\eta\ \operatorname{sign}(\omega_2-\mu)\ \ [\Lambda_0(\omega_2,\boldsymbol{k}) - \omega_2]\ . \tag{6.131}$$

Inspection of the signs in (6.130) and (6.131) leads to

$$\operatorname{sign}\big[\hat{\Gamma}(\omega+\mu,\boldsymbol{k})\big|_{\omega=\omega_{1/2}-\mu}\big]_{\Gamma_i=0} = \pm\,1\,, \tag{6.132}$$

where the plus (minus) sign refers to particles (antiparticles). Via equations (6.130) and (6.131) we find for the sign of the expression $\operatorname{sign}(-\omega\hat{\Gamma})$ the result

$$
\begin{aligned}
&\operatorname{sign}\left[\Big(-\omega\,\hat{\Gamma}(\omega+\mu,\boldsymbol{k})\Big)\Big|_{\omega=\omega_{1/2}-\mu}\right]_{\Gamma_i=0}\\
&\qquad\qquad = \operatorname{sign}\big[\mp(\omega_{1/2}-\mu)]\,\Gamma(\omega_{1/2},\boldsymbol{k})\big]_{\Gamma_i=0}\\
&\qquad\qquad = \operatorname{sign}(\pm\,|\omega_{1/2}-\mu|) = \pm\,1\,. && (6.133)
\end{aligned}
$$

Finally, we are left with evaluating the function $\delta[F(\omega+\mu,\boldsymbol{k})]$ in equations (6.124), (6.126), and (6.128). To find the zeroes of the argument of this δ-function,

$$F(\omega+\mu,\boldsymbol{k}) = [m_B + \Lambda_S(\omega+\mu,\boldsymbol{k})]^2 + [|\boldsymbol{k}| + \Lambda_V(\omega+\mu,\boldsymbol{k})]^2 - [\Lambda_0(\omega+\mu,\boldsymbol{k}) - (\omega+\mu)]^2\,, \tag{6.134}$$

we make use of the general mathematical relation

$$\delta[F(\omega+\mu,\boldsymbol{k})] = \sum_{l=1}^{2} \left| \left(\frac{\partial F}{\partial \omega}\right)_{\omega_l(k)} \right| \delta(\omega+\mu-\omega_l(k))\,, \tag{6.135}$$

where ω_l denotes the two solutions for which $F(\omega_l) = 0$. This is the case for

$$\omega_{1/2} = \Lambda_0(\omega_{1/2}) \pm \sqrt{[m + \Lambda_S(\omega_{1/2})]^2 + [|\boldsymbol{k}| + \Lambda_V(\omega_{1/2})]^2}\,, \tag{6.136}$$

as can be inferred from (6.134). The partial derivative in (6.135) is readily found to read

$$\frac{\partial F(\omega,|\boldsymbol{k}|)}{\partial \omega} = 2\Big\{[m + \Lambda_S(\omega,\boldsymbol{k})]\,\frac{\partial \Lambda_S}{\partial \omega} + [|\boldsymbol{k}| + \Lambda_V(\omega,\boldsymbol{k})]\,\frac{\partial \Lambda_V}{\partial \omega} + [\Lambda_0(\omega,\boldsymbol{k}) - \omega]\Big[1 - \frac{\partial \Lambda_0}{\partial \omega}\Big]\Big\}\,. \tag{6.137}$$

In the case of the relativistic Hartree approximation the self-energies are energy independent and so the partial derivatives $\partial \Lambda_i/\partial \omega$ vanish. Equation (6.137) therefore simplifies for this approximation to

$$\left| \left(\frac{\partial F(\omega,\boldsymbol{k})}{\partial \omega}\right)_{\omega_1} \right| = 2\sqrt{[m + \Lambda_S]^2 + [|\boldsymbol{k}| + \Lambda_V]^2} = \left| \left(\frac{\partial F(\omega,\boldsymbol{k})}{\partial \omega}\right)_{\omega_2} \right|. \tag{6.138}$$

Substituting equations (6.135) and (6.138) into equations (6.124), (6.126) and (6.128) leads for the components of the spectral function to

$$\Xi_S(\omega,\boldsymbol{k}) = \ [m + \Lambda_S(\omega_1(\boldsymbol{k}),\boldsymbol{k})]\ \frac{\partial F(\omega,\boldsymbol{k})}{\partial \omega}\Big|_{\omega_1(k)} \delta[\omega + \mu - \omega_1(\boldsymbol{k})] - \ [m + \Lambda_S(\omega_2(\boldsymbol{k}),\boldsymbol{k})]\ \frac{\partial F(\omega,\boldsymbol{k})}{\partial \omega}\Big|_{\omega_2(k)} \delta[\omega + \mu - \omega_2(\boldsymbol{k})]\,, \tag{6.139}$$

$$\Xi_V(\omega,\boldsymbol{k}) = \ -[|\boldsymbol{k}| + \Lambda_V(\omega_1(\boldsymbol{k}),\boldsymbol{k})]\ \frac{\partial F(\omega,\boldsymbol{k})}{\partial \omega}\Big|_{\omega_1(k)} \delta[\omega + \mu - \omega_1(\boldsymbol{k})] + \ [|\boldsymbol{k}| + \Lambda_V(\omega_2(\boldsymbol{k}),\boldsymbol{k})]\ \frac{\partial F(\omega,\boldsymbol{k})}{\partial \omega}\Big|_{\omega_2(k)} \delta[\omega + \mu - \omega_2(\boldsymbol{k})]\,, \tag{6.140}$$

and

$$\Xi_0(\omega,\boldsymbol{k}) = -\left[\Lambda_0(\omega_1(\boldsymbol{k}),\boldsymbol{k}) - \omega_1\right] \frac{\partial F(\omega,\boldsymbol{k})}{\partial\omega}\Big|_{\omega_1(k)} \delta[\omega+\mu-\omega_1(\boldsymbol{k})]$$
$$+ \left[\Lambda_0(\omega_2(\boldsymbol{k}),\boldsymbol{k}) - \omega_2\right] \frac{\partial F(\omega,\boldsymbol{k})}{\partial\omega}\Big|_{\omega_2(k)} \delta[\omega+\mu-\omega_2(\boldsymbol{k})]\,. \quad (6.141)$$

The mathematical structure of equations (6.139) to (6.141) suggests a decomposition of the spectral function according to

$$\big(\boldsymbol{\Xi}_i^B\big)_{\zeta\zeta'}(\omega,\boldsymbol{k}) \equiv \delta\big(\omega+\mu^B-\omega^B(\boldsymbol{k})\big)\,\big(\boldsymbol{\Xi}_i^B\big)_{\zeta\zeta'}(\boldsymbol{k})$$
$$+\,\delta\big(\omega+\bar{\mu}^B-\bar{\omega}^B(\boldsymbol{k})\big)\,\big(\bar{\boldsymbol{\Xi}}_i^B\big)_{\zeta\zeta'}(\boldsymbol{k})\,, \quad (6.142)$$

with the individual, energy independent spectral functions $\Xi_i^B(\boldsymbol{k})$ ($i = S, V, 0$) given by

$$\Xi_S^B(\boldsymbol{k}) \equiv \frac{m_B + \Sigma_S^B(\omega^B(\boldsymbol{k}),\boldsymbol{k})}{2\sqrt{(m_B+\Sigma_S^B(\omega^B(\boldsymbol{k}),\boldsymbol{k}))^2 + (|\boldsymbol{k}+\Sigma_V^B(\omega^B(\boldsymbol{k}),\boldsymbol{k}))^2}}\,, \quad (6.143)$$

$$\Xi_V^B(\boldsymbol{k}) \equiv -\frac{|\boldsymbol{k}| + \Sigma_V^B(\omega^B(\boldsymbol{k}),\boldsymbol{k})}{2\sqrt{(m_B+\Sigma_S^B(\omega^B(\boldsymbol{k}),\boldsymbol{k}))^2 + (|\boldsymbol{k}+\Sigma_V^B(\omega^B(\boldsymbol{k}),\boldsymbol{k}))^2}}\,, \quad (6.144)$$

$$\Xi_0^B(\boldsymbol{k}) \equiv \frac{1}{2}\,. \quad (6.145)$$

The corresponding expressions for the antibaryons are given by

$$\bar{\Xi}_S^B(\boldsymbol{k}) \equiv -\frac{m_B + \Sigma_S^B(\bar{\omega}^B(\boldsymbol{k}),\boldsymbol{k})}{2\sqrt{(m_B+\Sigma_S^B(\bar{\omega}^B(\boldsymbol{k}),\boldsymbol{k}))^2 + (|\boldsymbol{k}+\Sigma_V^B(\bar{\omega}^B(\boldsymbol{k}),\boldsymbol{k}))^2}}\,, \quad (6.146)$$

$$\bar{\Xi}_V^B(\boldsymbol{k}) \equiv \frac{|\boldsymbol{k}| + \Sigma_V^B(\bar{\omega}^B(\boldsymbol{k}),\boldsymbol{k})}{2\sqrt{(m_B+\Sigma_S^B(\bar{\omega}^B(\boldsymbol{k}),\boldsymbol{k}))^2 + (|\boldsymbol{k}+\Sigma_V^B(\bar{\omega}^B(\boldsymbol{k}),\boldsymbol{k}))^2}}\,, \quad (6.147)$$

$$\bar{\Xi}_0^B(\boldsymbol{k}) \equiv \frac{1}{2}\,. \quad (6.148)$$

The single-particle energies in (6.143) through (6.145) read

$$\omega^B(\boldsymbol{k}) = \Sigma_0^B(\omega^B(\boldsymbol{k}),\boldsymbol{k})$$
$$+\left\{\big(m_B+\Sigma_S^B(\omega^B(\boldsymbol{k}),\boldsymbol{k})\big)^2 + (|\boldsymbol{k}|+\Sigma_V^B(\omega^B(\boldsymbol{k}),\boldsymbol{k}))^2\right\}^{1/2} \quad (6.149)$$
$$\equiv \Sigma_0^B(\boldsymbol{k})\left\{(m_B^*)^2 + (\boldsymbol{k}^*)^2\right\}^{1/2}, \quad (6.150)$$

and for the antibaryons

$$\bar{\omega}^B(\boldsymbol{k}) = \Sigma_0^B(\bar{\omega}^B(\boldsymbol{k}),\boldsymbol{k})$$
$$-\left\{\big(m_B+\Sigma_S^B(\bar{\omega}^B(\boldsymbol{k}),\boldsymbol{k})\big)^2 + (|\boldsymbol{k}|+\Sigma_V^B(\bar{\omega}^B(\boldsymbol{k}),\boldsymbol{k}))^2\right\}^{1/2}. \quad (6.151)$$

Table 6.1. Masses m_L, spin quantum numbers J_L, and electric charges $q_L^{\rm el}$ of those leptons which contribute to the EOS of neutron star matter.

Lepton (L)	m_L (MeV)	J_L	$q_L^{\rm el}$
e^-	0.511	1/2	−1
μ^-	106	1/2	−1

Finally the chemical potentials of baryons and antibaryons propagating in the medium with Fermi momenta k_{F_B} and $\bar{k}_{F_B}$ are given by

$$\mu^B = \omega^B(k_{F_B})\,, \qquad \text{and} \qquad \bar{\mu}^B = \bar{\omega}^B(\bar{k}_{F_B})\,, \tag{6.152}$$

respectively.

6.2.1 Application to free lepton propagators

The mathematical content of the spectral formalism developed in the previous section 6.2 can be nicely demonstrated for the simple case of a gas of free, relativistic fermions, for which we chose the leptons. We recall that leptons, whose masses and quantum numbers are listed in table 6.1, are present in neutron star matter because of chemical equilibrium, the guiding principle by means of which neutron star matter settles down into the lowest possible energy state. The stating point is the spectral representation for the fermion propagator derived in equation (6.40). Replacing the label B with L, where $L = e^-, \mu^-$ gives for equation (6.40)

$$\boldsymbol{g}^L_{\zeta\zeta'}(k) = \frac{\mathrm{i}}{2\pi} \int_{-\infty}^{+\infty} \mathrm{d}\omega \left\{ \frac{\boldsymbol{g}^L_{>}(\omega, \boldsymbol{k})_{\zeta\zeta'}}{k_0 - \omega - \mu^L + \mathrm{i}\eta} - \frac{\boldsymbol{g}^L_{<}(\omega, \boldsymbol{k})_{\zeta\zeta'}}{k_0 - \omega - \mu^L - \mathrm{i}\eta} \right\}. \tag{6.153}$$

For simplicity, we shall restrict ourselves to zero temperature, in which case the Fermi–Dirac functions reduce to

$$f^L(\omega - \mu^L) \longrightarrow \Theta(\mu^L - \omega)\,. \tag{6.154}$$

Equation (6.41) then reads

$$\boldsymbol{g}^L_{\zeta\zeta'}(k) = -\int_{-\infty}^{+\infty} \mathrm{d}\omega \left\{ \frac{1 - \Theta(\mu^L - k_0)}{k_0 - \omega - \mu^L + \mathrm{i}\eta} + \frac{\Theta(\mu^L - k_0)}{k_0 - \omega - \mu^L - \mathrm{i}\eta} \right\} \boldsymbol{\Xi}^L_{\zeta\zeta'}(\omega, \boldsymbol{k})\,, \tag{6.155}$$

which can be brought to the shorter form

$$\boldsymbol{g}^L_{\zeta\zeta'}(k) = \int_{-\infty}^{+\infty} \mathrm{d}\omega \frac{\boldsymbol{\Xi}^L_{\zeta\zeta'}(\omega, \boldsymbol{k})}{\omega - (k_0 - \mu^L)\,(1 + \mathrm{i}\eta)}\,. \tag{6.156}$$

Equation (6.156) is the analog to (6.48), except that the energy argument has been shifted by the chemical potential of the leptons, μ^L, in analogy to the rescaling procedure for the baryon chemical potential outlined at the beginning of section 6.2.

The mathematical form of the lepton spectral function, $\boldsymbol{\Xi}^L$, is obtained from the cutline of the analytically continued two-point lepton function,

$$\tilde{\boldsymbol{g}}^L_{\zeta\zeta'}(z, \boldsymbol{k}) \;=\; \int_{-\infty}^{+\infty} \mathrm{d}\omega \;\frac{\boldsymbol{\Xi}^L_{\zeta\zeta'}(\omega, \boldsymbol{k})}{\omega - z}\,, \tag{6.157}$$

along the real energy axis, that is,

$$\boldsymbol{\Xi}^L_{\zeta\zeta'}(\omega, \boldsymbol{k}) = \frac{\tilde{\boldsymbol{g}}^L_{\zeta\zeta'}(\omega + \mathrm{i}\eta, \boldsymbol{k}) - \tilde{\boldsymbol{g}}^L_{\zeta\zeta'}(\omega - \mathrm{i}\eta, \boldsymbol{k})}{2\,\mathrm{i}\,\pi}\,. \tag{6.158}$$

Leptons do not carry isospin. So for them the unity matrix introduced in (5.131) consists only of the Dirac part, and therefore the labels ζ, ζ' reduce to α, α'. Hence one has for the matrix elements of the unity matrix

$$\big(\mathbf{1}\big)_{\alpha\alpha'} \equiv \big(\mathbf{1}^{\mathrm{Dirac}}\big)_{\alpha\alpha'} \;=\; \delta_{\alpha\alpha'}\,. \tag{6.159}$$

Inversion of the lepton Dyson equation,

$$\big\{\mathbf{1}\, m_B \;+\; \boldsymbol{\gamma}\cdot\hat{\boldsymbol{k}}\,|\boldsymbol{k}| \;-\; \gamma^0\; k_0\big\}\; \boldsymbol{g}^L(k_0, \boldsymbol{k}) \;=\; 1\,, \tag{6.160}$$

gives for the lepton two-point function [cf. equation (6.105)]

$$\tilde{\boldsymbol{g}}^L(z, \boldsymbol{k}) \;=\; \frac{m_L\,\mathbf{1} - |\boldsymbol{k}|\,\boldsymbol{\gamma}\cdot\hat{\boldsymbol{k}} + (z + \mu^L)\,\gamma^0}{m_L^2 + \boldsymbol{k}^2 - (z + \mu^L)^2}\,. \tag{6.161}$$

The *physical* lepton propagator, $\boldsymbol{g}^L$, is obtained from the analytically continued expression (6.157) as

$$\boldsymbol{g}^L_{\alpha\alpha'}(k) = \tilde{\boldsymbol{g}}^L_{\alpha\alpha'}((k_0 - \mu^L)(1 + \mathrm{i}\eta), \boldsymbol{k})\,. \tag{6.162}$$

Substituting (6.161) into (6.158) then leads for $\boldsymbol{\Xi}^L$ to

$$\boldsymbol{\Xi}^L_{\alpha\alpha'}(\omega, \boldsymbol{k}) = \delta\big(\omega + \mu^L - \omega^L(\boldsymbol{k})\big)\; \boldsymbol{\Xi}^L_{\alpha\alpha'}(\boldsymbol{k}) + \delta\big(\omega + \bar{\mu}^L - \bar{\omega}^L(\boldsymbol{k})\big)\; \bar{\boldsymbol{\Xi}}^L_{\alpha\alpha'}(\boldsymbol{k})\,, \tag{6.163}$$

where the first term on the right-hand side corresponds to particles and the second to antiparticles. The energy-independent spectral functions in (6.163) are given by

$$\boldsymbol{\Xi}^L_{\alpha\alpha'}(\boldsymbol{k}) = +\frac{m_L\,(\mathbf{1})_{\alpha\alpha'} - |\boldsymbol{k}|\,(\boldsymbol{\gamma}\cdot\hat{\boldsymbol{k}})_{\alpha\alpha'} + \omega^L(\boldsymbol{k})\,(\gamma^0)_{\alpha\alpha'}}{2\sqrt{m_L^2+\boldsymbol{k}^2}} \tag{6.164}$$

$$\equiv \Xi^L_S\,(\mathbf{1})_{\alpha\alpha'} + \Xi^L_V\,(\boldsymbol{\gamma}\cdot\hat{\boldsymbol{k}})_{\alpha\alpha'} + \Xi^L_0\,(\gamma)^0_{\alpha\alpha'} \tag{6.165}$$

for particles, and by

$$\bar{\boldsymbol{\Xi}}^L_{\alpha\alpha'}(\boldsymbol{k}) = -\frac{m_L\,(\mathbf{1})_{\alpha\alpha'} - |\boldsymbol{k}|\,(\boldsymbol{\gamma}\cdot\hat{\boldsymbol{k}})_{\alpha\alpha'} + \bar{\omega}^L(\boldsymbol{k})\,(\gamma^0)_{\alpha\alpha'}}{2\sqrt{m_L^2+\boldsymbol{k}^2}} \tag{6.166}$$

$$\equiv \bar{\Xi}^L_S\,(\mathbf{1})_{\alpha\alpha'} + \bar{\Xi}^L_V\,(\boldsymbol{\gamma}\cdot\hat{\boldsymbol{k}})_{\alpha\alpha'} + \bar{\Xi}^L_0\,(\gamma)^0_{\alpha\alpha'} \tag{6.167}$$

for the antiparticles. Finally, the energy–momentum relation of free leptons and antileptons read

$$\omega^L(\boldsymbol{k}) = +\sqrt{m_L^2+\boldsymbol{k}^2} = -\bar{\omega}^L(\boldsymbol{k})\,, \tag{6.168}$$

so that the lepton (antilepton) chemical potentials are given by

$$\mu^L = \omega^L(k_{F_L}) \qquad \text{and} \qquad \bar{\mu}^L = \bar{\omega}^L(\bar{k}_{F_L})\,, \tag{6.169}$$

where k_{F_L} and $\bar{k}_{F_L}$ denote the respective lepton Fermi momenta.

6.2.2 Baryon propagator in relativistic Hartree approximation

As a second example, we consider the explicit mathematical structure of the baryon two-point function in the interacting particle case. The relativistic Hartree approximation is chosen as the underlying many-body approach [313, 345]. The spectral function for this approximation has already been derived in equations (6.142) through (6.145). Repeating the steps outlined at the end of section 6.1, which have led us to the two-point baryon function in the non-interacting particle case [equation (6.64)], one arrives at

$$\begin{aligned}
-\,\boldsymbol{g}^{\mathrm{H},B}_{\zeta\zeta'}(k^\mu) \;=\; & \frac{\gamma^0_{\zeta\zeta'}\,(k_0-\Sigma^{\mathrm{H},B}_0(\boldsymbol{k})) \,-\, (\boldsymbol{\gamma}\cdot\boldsymbol{k})_{\zeta\zeta'} \,+\, (\mathbf{1})_{\zeta\zeta'}\,(m_B+\Sigma^{\mathrm{H},B}_S(\boldsymbol{k}))}{2\,\epsilon^{\mathrm{H},B}(\boldsymbol{k})} \\
&\times\,\left\{\frac{1-f^B(\boldsymbol{k})}{k_0-\Sigma^{\mathrm{H},B}_0(\boldsymbol{k})-\epsilon^{\mathrm{H},B}(\boldsymbol{k})+\mathrm{i}\eta} + \frac{f^B(\boldsymbol{k})}{k_0-\boldsymbol{\Sigma}^{\mathrm{H},B}_0(\boldsymbol{k})-\epsilon^{\mathrm{H},B}(\boldsymbol{k})-\mathrm{i}\eta}\right. \\
&-\left.\frac{1-\bar{f}^B(\boldsymbol{k})}{k_0-\Sigma^{\mathrm{H},B}_0(\boldsymbol{k})+\epsilon^{\mathrm{H},B}(\boldsymbol{k})-\mathrm{i}\eta} - \frac{\bar{f}^B(\boldsymbol{k})}{k_0-\Sigma^{\mathrm{H},B}_0(\boldsymbol{k})+\epsilon^{\mathrm{H},B}(\boldsymbol{k})+\mathrm{i}\eta}\right\},
\end{aligned} \tag{6.170}$$

with the single-particle energy $\epsilon^{\mathrm{H},B}$ given by

$$\epsilon^{\mathrm{H},B}(\boldsymbol{k}) = \sqrt{(m+\Sigma_S^{\mathrm{H},B})^2+\boldsymbol{k}^2} = \frac{1}{2}\left|\frac{\partial F^B}{\partial\omega}\right|_{\omega^B(|k|)} . \qquad (6.171)$$

The physical interpretation of the individual terms in (6.170) is given too at the end of section 6.1. The free-particle limit is obtained from equations (6.170) and (6.171) if the interactions among the baryons are switched off, which implies that $\boldsymbol{\Sigma}^B \to 0$.

6.3 Baryon number density

In the next step we outline how the number density of baryons is obtained from the baryon two-point Green function [79, 118, 125, 313, 346]. Let us begin with defining the total baryon number operator,

$$A \equiv \int d^3\boldsymbol{x}\, [\psi_B^\dagger(x,\zeta), \psi_B(x,\zeta)]\,, \qquad (6.172)$$

from which the definition of the density of baryons follows as

$$\rho^B \equiv \frac{1}{\Omega} < \boldsymbol{\Phi}_0|A|\boldsymbol{\Phi}_0 >\,, \qquad (6.173)$$

with Ω a volume element. Substituting (6.172) into (6.173) gives

$$\rho^B = \frac{1}{\Omega}\int_\Omega d^3\boldsymbol{x}\left\{< \boldsymbol{\Phi}_0|\psi_B^\dagger(x,\zeta)\psi_B(x,\zeta) - \psi_B(x,\zeta)\psi_B^\dagger(x,\zeta)|\boldsymbol{\Phi}_0 >\right\} . \qquad (6.174)$$

Inspection of the defining relation for the two-point function, equation (5.63), shows that the field-operator products in (6.174) can be expressed as

$$\begin{aligned}\boldsymbol{g}^B(x,\zeta;x'=x^+,\zeta') &= -\,\mathrm{i} < \bar\psi_B(x^+,\zeta')\psi_B(x,\zeta) > \\ &= -\,\mathrm{i}\,\gamma^0 < \psi_B^\dagger(x^+,\zeta')\psi_B(x,\zeta) >\,, \end{aligned} \qquad (6.175)$$

and

$$\begin{aligned}\boldsymbol{g}^B(x,\zeta;x'=x^-,\zeta') &= \mathrm{i} < \bar\psi_B(x,\zeta)\psi_B(x^-,\zeta') > \\ &= \mathrm{i}\,\gamma^0 < \psi_B(x,\zeta)\psi_B^\dagger(x^-,\zeta') > . \end{aligned} \qquad (6.176)$$

With the aid of these relations, equation (6.174) can be written as

$$\rho^B = \mathrm{i}\,\gamma^0\frac{1}{\Omega}\int_\Omega d^3\boldsymbol{x}\left\{\boldsymbol{g}^B(x,\zeta;x^+,\zeta') + \boldsymbol{g}^B(x,\zeta;x^-,\zeta')\right\}, \qquad (6.177)$$

for which we introduce the more compact notation

$$\rho^B \equiv \mathrm{i}\left(\gamma^0\right)_{\zeta\zeta'} \frac{1}{\Omega} \sum_{y=x^+,x^-} \lim_{x'\to y} \int_\Omega \mathrm{d}^3\boldsymbol{x}\ \boldsymbol{g}^B_{\zeta'\zeta}(x;y)\,. \tag{6.178}$$

The Fourier transform of (6.178) reads

$$\lim_{x'\to x^\pm} \frac{1}{\Omega} \int_\Omega \mathrm{d}^3\boldsymbol{x}\ \boldsymbol{g}(x;x') = \int \frac{\mathrm{d}^4 q}{(2\pi)^4}\, \mathrm{e}^{\pm\,\mathrm{i}\eta q^0}\ \boldsymbol{g}(q)\,, \tag{6.179}$$

and therefore

$$\rho^B = \mathrm{i}\ \left(\gamma^0\right)_{\zeta\zeta'} \sum_{s=+,-} \int \frac{\mathrm{d}^4 q}{(2\pi)^4}\, \mathrm{e}^{\mathrm{i}s\eta q^0}\ \boldsymbol{g}^B_{\zeta'\zeta}(q)\,. \tag{6.180}$$

After contour integration and rearranging terms one gets (cf. appendix B.1)

$$\begin{aligned}\rho^B =\ & \left(\gamma^0\right)_{\zeta\zeta'} \int \frac{\mathrm{d}^3\boldsymbol{q}}{(2\pi)^3}\ \boldsymbol{\Xi}^B_{\zeta\zeta'}(\boldsymbol{q})\ f(\omega^B(\boldsymbol{q})-\mu^B) \\ & -\left(\gamma^0\right)_{\zeta\zeta'} \int \frac{\mathrm{d}^3\boldsymbol{q}}{(2\pi)^3}\ \bar{\boldsymbol{\Xi}}^B_{\zeta\zeta'}(\boldsymbol{q})\ f(-(\bar{\omega}^B(\boldsymbol{q})-\mu^B))\,.\end{aligned} \tag{6.181}$$

The traces in (6.181) are evaluated as follows:

$$\begin{aligned}\left(\gamma^0\right)_{\zeta\zeta'}\ \boldsymbol{\Xi}^B_{\zeta'\zeta} =\ & \mathrm{Tr}\ \left(\gamma^0\,\boldsymbol{\Xi}^B\right) \\ =\ & \mathrm{Tr}\left\{\gamma^0\,(\mathbf{1}\ \Xi^B_S + \boldsymbol{\gamma}\cdot\hat{\boldsymbol{q}}\ \Xi^B_V + \gamma^0\ \Xi^B_0)\otimes\mathbf{1}^{\mathrm{iso}}\right\} \\ =\ & \mathrm{Tr}\left\{\left(\gamma^0\right)^2\ \Xi^B_0\right\}\ \mathrm{Tr}\left\{\mathbf{1}^{\mathrm{iso}}\right\} \\ =\ & 2\,(2I_B+1)\,(2J_B+1)\ \Xi^B_0 \equiv 2\,\nu_B\,\Xi^B_0\,,\end{aligned} \tag{6.182}$$

where the quantity ν_B, defined as

$$\nu_B \equiv 2\,(2I_B+1)\,(2J_B+1)\,, \tag{6.183}$$

accounts for the spin and isospin degeneracy of the baryon in question (cf. table 5.1). Expression (6.183) applies to the nuclear matter case. In the case of neutron star matter one has $I_B = 0$ and therefore (6.183) reduces to

$$\nu_B \equiv 2\,(2J_{B'}+1)\,. \tag{6.184}$$

Substituting (6.182) into (6.181) gives for the baryon number density

$$\rho^B = 2\,\nu_B \int \frac{\mathrm{d}^3\boldsymbol{q}}{(2\pi)^3}\left\{\Xi^B_0(\boldsymbol{q})\ f^B(\boldsymbol{q}) - \bar{\Xi}^B_0(\boldsymbol{q})\ \bar{f}^B(\boldsymbol{q})\right\}, \tag{6.185}$$

with f^B and $\bar{f}^B$ defined in (6.67). Equation (6.185) simplifies at zero temperature to the expression

$$\rho^B = 2\,(2J_B+1)(2I_B+1)\int \frac{\mathrm{d}^3\boldsymbol{q}}{(2\pi)^3}\,\Xi_0^B(\boldsymbol{q})\,\Theta^B(\boldsymbol{q})\,. \tag{6.186}$$

For theories with $\Xi_0^B = \frac{1}{2}$, one readily verifies from (6.186) the expression

$$\rho^B = \frac{\nu_B}{2}\,\frac{k_{F_B}^3}{3\pi^2}\,, \tag{6.187}$$

which leads to the well-known relations

$$\rho = \frac{2k_F^3}{3\pi^2}\,, \quad \text{nuclear matter case}\,, \tag{6.188}$$

$$\rho = \frac{k_F^3}{3\pi^2}\,, \quad \text{neutron matter case}\,. \tag{6.189}$$

Finally, the total baryon number density, ρ, is obtained by summing the partial number densities,

$$\rho \equiv \sum_B \rho^B\,. \tag{6.190}$$

Another frequently encountered quantity, besides the baryon number density, is the scalar baryon density, $\bar{\rho}^B$. It is defined, somewhat similarly to the baryon density, by

$$\bar{A} \equiv \int \mathrm{d}^3\boldsymbol{x}\,[\bar{\psi}_B(x,\zeta), \psi_B(x,\zeta)]\,, \tag{6.191}$$

with the decisive difference, however, that $\psi_B^\dagger$ is replaced with $\bar{\psi}_B$. $\bar{\rho}^B$ is then obtained from (6.191) as

$$\bar{\rho}^B \equiv \frac{1}{\Omega}\, < \boldsymbol{\Phi}_0|\bar{A}|\boldsymbol{\Phi}_0 > \,. \tag{6.192}$$

Repeating the steps as for ρ^B just obove, one gets

$$\bar{\rho}^B = \frac{1}{\Omega}\int_\Omega \mathrm{d}^3\boldsymbol{x}\,\left\{< \boldsymbol{\Phi}_0|\bar{\psi}_B(x,\zeta)\psi_B(x,\zeta) - \psi_B(x,\zeta)\bar{\psi}_B(x,\zeta)\boldsymbol{\Phi}_0 >\right\}. \tag{6.193}$$

Substituting the baryon fields by the associated baryon two-point function gives for (6.193)

$$\bar{\rho}^B = \mathrm{i}\,\frac{1}{\Omega}\int_\Omega \mathrm{d}^3\boldsymbol{x}\,\left\{\boldsymbol{g}^B(x,\zeta;x^+,\zeta) + \boldsymbol{g}^B(x,\zeta;x^-,\zeta)\right\} \tag{6.194}$$

$$\equiv \mathrm{i}\,\frac{1}{\Omega}\sum_{y=x^+,x^-}\lim_{x'\to y}\int_\Omega \mathrm{d}^3\boldsymbol{x}\;\boldsymbol{g}^B_{\zeta\zeta}(x;y)\,. \tag{6.195}$$

Fourier transformation of (6.195) gives

$$\bar{\rho}^B = \mathrm{i} \sum_{s=+,-} \int \frac{\mathrm{d}^4 q}{(2\pi)^4}\, \mathrm{e}^{\mathrm{i}s\eta q^0}\; \boldsymbol{g}^B_{\zeta\zeta}(q)\,. \tag{6.196}$$

In accordance with the standard procedure, the next step consists in replacing the two-point function with its spectral representation. Contour integration then leaves us with [cf. equations (B.8) and (B.10)]

$$\bar{\rho}^B = \int \frac{\mathrm{d}^3 \boldsymbol{q}}{(2\pi)^3} \left\{ \boldsymbol{\Xi}^B_{\zeta\zeta}(\boldsymbol{q})\; f^B(\boldsymbol{q}) - \bar{\boldsymbol{\Xi}}^B_{\zeta\zeta}(\boldsymbol{q})\; \bar{f}^B(\boldsymbol{q}) \right\}, \tag{6.197}$$

with the trace given by

$$\begin{aligned} \boldsymbol{\Xi}^B_{\zeta\zeta} &= \mathrm{Tr}\left(\boldsymbol{\Xi}^B\right) \equiv \mathrm{Tr}\left\{ \mathbf{1}\; \Xi^B_S + \boldsymbol{\gamma}\cdot\hat{\boldsymbol{q}}\; \Xi^B_V + \gamma^0\; \Xi^B_0] \otimes \mathbf{1}^{\mathrm{iso}} \right\} \\ &= \mathrm{Tr}\left\{ \mathbf{1}\; \Xi^B_S \right\}\; \mathrm{Tr}\left\{ \mathbf{1}^{\mathrm{iso}} \right\} = 2\,\nu_B\; \Xi^B_S\,. \end{aligned} \tag{6.198}$$

Substituting (6.198) into (6.197) leads to

$$\bar{\rho}^B = 2\,\nu_B \int \frac{\mathrm{d}^3 \boldsymbol{q}}{(2\pi)^3} \left\{ \Xi^B_S(\boldsymbol{q})\; f^B(\boldsymbol{q}) - \bar{\Xi}^B_S(\boldsymbol{q})\; \bar{f}^B(\boldsymbol{q}) \right\}. \tag{6.199}$$

Replacing the spectral functions $\boldsymbol{\Xi}^B$ and $\bar{\boldsymbol{\Xi}}^B$ in (6.199) with their explicit representations (6.143) and (6.146) finally gives for the scalar density

$$\begin{aligned} \bar{\rho}^B = 2\,\nu_B \int \frac{\mathrm{d}^3 \boldsymbol{q}}{(2\pi)^3}\, & \frac{m^*_B}{2\sqrt{(m^*_B)^2 + (\boldsymbol{q}^*)^2}} \\ & \times \left\{ f(\omega^B(\boldsymbol{q}) - \mu^B) + f(-(\bar{\omega}^B(\boldsymbol{q}) - \mu^B)) \right\}. \end{aligned} \tag{6.200}$$

The zero-temperature limit of (6.200) can be handled analytically for the relativistic Hartree approximation, since the masses and self-energies are independent of momentum for this approximation. With the aid of the momentum integrals given in appendix B.3, one readily calculates from

$$\bar{\rho}^B = 2\,(2J_B + 1)(2I_B + 1) \int \frac{\mathrm{d}^3 \boldsymbol{q}}{(2\pi)^3}\; \Xi^B_S(\boldsymbol{q})\; \Theta^B(\boldsymbol{q}) \tag{6.201}$$

the relation

$$\begin{aligned} \bar{\rho}^B \;\xrightarrow{T\to 0}\; \frac{\nu_B}{6\pi^2}\, m^*_B \Bigg\{ & \frac{k_{F_B}}{2} \sqrt{(m^*_B)^2 + k^2_{F_B}} \\ & - \frac{(m^*_B)^2}{2}\, \ln\left| \frac{k_{F_B} + \sqrt{(m^*_B)^2 + k^2_{F_B}}}{m^*_B} \right| \Bigg\}. \end{aligned} \tag{6.202}$$

We close this section by noting that the total scalar density, $\bar{\rho}$, is obtained from (6.200) as

$$\bar{\rho} \equiv \sum_{B} \bar{\rho}^{B} \,. \tag{6.203}$$

Chapter 7

Dense matter in relativistic Hartree and Hartree–Fock

7.1 Self-energies in Hartree–Fock approximation

We recall that the HF approximation to the many-body system is obtained by keeping only the Born term of the T-matrix equation (5.179), that is by replacing $\mathsf{T} \to \mathsf{T}^{\rm HF} \equiv \mathsf{V} - \mathsf{V}^{\rm ex}$, with the matrix elements of V explicitly given in equations (5.151) through (5.155). The antisymmetrized HF T-matrix has the form

$$< 1\,2|\mathsf{T}^{{\rm HF},BB'}|3\,4> \equiv < 1\,2|\mathsf{V}^{BB'}|3\,4> - < 1\,2|\mathsf{V}^{BB'}|4\,3>\,, \quad (7.1)$$

where the first respectively second term on the right-hand side constitute the direct (Hartree) and exchange (Fock) contribution to $\mathsf{T}^{\rm HF}$. The graphical illustration of $\mathsf{T}^{\rm HF}$ is displayed in figure 7.1. A comparison with the structure of the full scattering matrix, displayed in figure 5.10, shows that the repeated two-baryon scattering processes in matter summed in the full T-matrix approximation are absent for the HF approach. Substituting (7.1) into (5.186), which defines $\mathbf{\Sigma}$, leads to

$$\mathbf{\Sigma}^{{\rm H},B}(1,1') = {\rm i} \sum_{B'} \; < 1\,2|\mathsf{V}^{BB'}|1'\,3> \; \boldsymbol{g}_1^{B'}(3,2^+)\,, \quad (7.2)$$

$$\mathbf{\Sigma}^{{\rm F},B}(1,1') = -\,{\rm i} \sum_{B'} \; < 1\,2|\mathsf{V}^{BB'}|3\,1'> \; \boldsymbol{g}_1^{B'}(3,2^+)\,, \quad (7.3)$$

where (7.2) is the Hartree self-energy and (7.3) the Fock contribution to the self-energy. Both expressions added together give the total HF self-energy in the form

$$\mathbf{\Sigma}^{{\rm HF},B}(1,1') \equiv \mathbf{\Sigma}^{{\rm H},B}(1,1') + \mathbf{\Sigma}^{{\rm F},B}(1,1')\,. \quad (7.4)$$

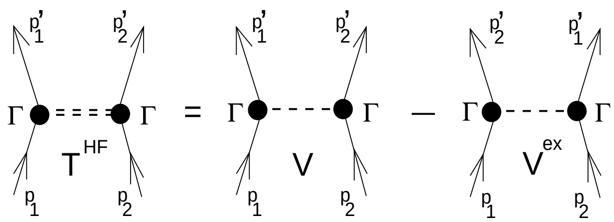

Figure 7.1. Graphical representation of the Hartree–Fock **T**-matrix, $\mathbf{T}^{\rm HF}$, obtained by restriction to the Born term of the **T**-matrix equation (5.203). Γ denote baryon–meson vertices listed in (5.156) through (5.158). The analytic form of $\mathbf{T}^{\rm HF}$ is given in equation (7.1).

The explicit expressions of $\boldsymbol{\Sigma}^{{\rm H},B}$ and $\boldsymbol{\Sigma}^{{\rm F},B}$ in momentum space [79, 125, 313] are derived in equations (5.135) through (5.142). For the σ meson, for instance, we obtained for the Hartree term

$$\boldsymbol{\Sigma}^{{\rm H},B}_{\zeta_2\zeta_1}\Big|_\sigma = -\,{\rm i}\,\delta_{\zeta_2\zeta_1}\,\Delta^{0\sigma}(0)\,g_{\sigma B}\sum_{B'} g_{\sigma B'}\int\frac{{\rm d}^4q}{(2\pi)^4}\,{\rm e}^{{\rm i}\eta q^0}\ {\rm Tr}\ \boldsymbol{g}^{B'}(q)\,. \tag{7.5}$$

Upon replacing $\boldsymbol{g}^{B'}(q)$ with its spectral representation, derived in equation (6.71), and performing the contour integrations (cf. figure D.1) over the energy variable q^0, as described in appendix B, we find for (7.5)

$$\boldsymbol{\Sigma}^{{\rm H},B}_{\zeta_2\zeta_1}\Big|_\sigma = -\ \delta_{\zeta_2\zeta_1}\left(\frac{g_{\sigma B}}{m_\sigma}\right)^2\sum_{B'}\left(\frac{g_{\sigma B'}}{g_{\sigma B}}\right)\int\frac{{\rm d}^3\boldsymbol{q}}{(2\pi)^3}\ {\rm Tr}\ \boldsymbol{\Xi}^{B'}(\boldsymbol{q})\,\Theta(q_{F_{B'}}-|\boldsymbol{q}|)\,. \tag{7.6}$$

The σ-meson propagator in (7.5) at zero energy and momentum has been replaced with $\Delta^{0\sigma}(0) = 1/m_\sigma^2$, which follows from (5.93). Moreover, to get from (7.5) to (7.6) we have restricted ourselves to the zero-temperature limit, in which case the thermal distribution function can be replaced with the step function, $f(\omega^B(\boldsymbol{k}) - \mu^B) \longrightarrow \Theta(k_{F_B} - |\boldsymbol{k}|)$, and no thermally excited antibaryons contribute (that is, $\bar{f}^B \to 0$), as discussed in connection with the physical interpretation of the zero-temperature two-point Green function (6.69). The baryon self-energies at finite temperatures are summarized in appendix D. The trace in (7.6) is to be calculated with respect to the Dirac (spin) and isospin indices carried by $\boldsymbol{\Xi}^B$. Since the Dirac matrices γ^0 and γ^i are traceless (cf. appendix A.2), that is,

$$ {\rm Tr}\ \gamma^0 = {\rm Tr}\ \gamma^i = 0\,, \tag{7.7}$$

we arrive for the trace of $\boldsymbol{\Xi}^B$ of (6.117) at

$$\begin{aligned}\mathrm{Tr}\ \boldsymbol{\Xi}^{B'}(\boldsymbol{q}) &\equiv \mathrm{Tr}\left\{\left(\mathbf{1}\,\Xi_S^{B'}(\boldsymbol{q}) + \gamma\cdot\hat{\boldsymbol{q}}\,\Xi_V^{B'}(\boldsymbol{q}) + \gamma^0\,\Xi_0^{B'}(\boldsymbol{q})\right)\otimes\mathbf{1}^{\mathrm{iso}}\right\} \\ &= \mathrm{Tr}\ \left(\mathbf{1}\otimes\mathbf{1}^{\mathrm{iso}}\right)\,\Xi_S^{B'}(\boldsymbol{q})\,. \end{aligned} \tag{7.8}$$

As already known from the discussion of the baryon self-energy in section 5.4, the expression $\mathrm{Tr}(\mathbf{1}\otimes\mathbf{1}^{\mathrm{iso}})$ denotes the direct product of the two matrices $\mathbf{1}$ and $\mathbf{1}^{\mathrm{iso}}$, which can be written as (cf. appendix A.3) $\mathrm{Tr}(\mathbf{1}\otimes\mathbf{1}^{\mathrm{iso}}) = \mathrm{Tr}(\mathbf{1})\ \mathrm{Tr}(\mathbf{1}^{\mathrm{iso}})$. Equation (7.8) therefore can be brought into the form

$$\mathrm{Tr}\ \boldsymbol{\Xi}^{B'}(\boldsymbol{q}) = \mathrm{Tr}\,(\mathbf{1})\ \ \mathrm{Tr}\,(\mathbf{1}^{\mathrm{iso}})\ \Xi_S^{B'}(\boldsymbol{q})\,. \tag{7.9}$$

Upon evaluating the traces of the two individual matrices in the Dirac (spin) and isospin space in the form

$$\mathrm{Tr}\ (\mathbf{1})\ \ \mathrm{Tr}\ \left(\mathbf{1}^{\mathrm{iso}}\right) = 2\,(2I_{B'}+1)\,(2J_{B'}+1)\,, \tag{7.10}$$

equation (7.9) can be written as

$$\mathrm{Tr}\ \boldsymbol{\Xi}^{B'}(\boldsymbol{q}) = 2\,(2I_{B'}+1)\,(2J_{B'}+1)\ \Xi_S^{B'}(\boldsymbol{q}) \equiv 2\,\nu_{B'}\ \Xi_S^{B'}(\boldsymbol{q})\,. \tag{7.11}$$

Substituting the result (7.11) into (7.6) gives for the baryon self-energy

$$\begin{aligned}\boldsymbol{\Sigma}^{\mathrm{H},B}_{\zeta_2\zeta_1}(\{p_{F_B}\})\Big|_\sigma = &-2\,\delta_{\zeta_2\zeta_1}\left(\frac{g_{\sigma B}}{m_\sigma}\right)^2\sum_{B'}\frac{g_{\sigma B'}}{g_{\sigma B}}\,\nu_{B'} \\ &\times\int\frac{\mathrm{d}^3\boldsymbol{q}}{(2\pi)^3}\,\Xi_S^{B'}(\boldsymbol{q})\,\Theta(p_{F_{B'}}-|\boldsymbol{q}|)\,. \end{aligned} \tag{7.12}$$

One sees from (7.12) that in order to determine $\boldsymbol{\Sigma}^{\mathrm{H},B}|_\sigma$, knowledge of the Fermi momenta $p_{F_{B'}}$ (and thus the densities) of all other the baryons, predicted to be present in the system at a given total baryon density, is necessary. This functional dependence is indicated by $\{p_{F_{B'}}\}$ as the argument of $\boldsymbol{\Sigma}^{\mathrm{H},B}|_\sigma$. Alternatively to equation (7.12), the self-energy contribution can be expressed as

$$\begin{aligned}\Sigma^{\mathrm{H},B}_S(\{p_{F_B}\})\Big|_\sigma = &-2\left(\frac{g_{\sigma B}}{m_\sigma}\right)^2\sum_{B'}\frac{g_{\sigma B'}}{g_{\sigma B}}\,\nu_{B'} \\ &\times\int\frac{\mathrm{d}^3\boldsymbol{q}}{(2\pi)^3}\,\Xi_S^{B'}(\boldsymbol{q})\,\Theta(p_{F_{B'}}-|\boldsymbol{q}|)\,, \end{aligned} \tag{7.13}$$

which follows immediately by comparing (7.12) with the general decomposition for $\boldsymbol{\Sigma}^B$ given in (6.83). This leaves us with a simple scalar function for $\Sigma^{\mathrm{H},B}_S|_\sigma$, in contrast to $\boldsymbol{\Sigma}^{\mathrm{H},B}_{\zeta_2\zeta_1}|_\sigma$ of (7.12) which is a matrix equation in spin-isospin space. Besides that we note the general feature that after contour integration an explicit determination of the baryon two-point function is not necessary anymore, neither here nor for the determination of the equation of state of the many-body system, as we shall see in chapter 12.

Having calculated the Hartree expression of the baryon self-energy which originates from σ-meson exchange among the baryons, we proceed now to the calculation of the self-energy that originates from ω-meson exchange. (Contributions arising from the exchange of π and ρ mesons are listed in appendices C and D for matter at zero and finite temperatures, respectively.) In close analogy to above, we go back to the momentum-space representation of $\boldsymbol{\Sigma}^{\mathrm{H},B}(1,1')$, now, however, derived for the case of ω-meson exchange. This expression is given in (5.137). Replacing $\boldsymbol{g}^{B'}(q)$ with its associated spectral representation (6.71) and performing the contour integrations over q^0, exactly as in (7.5), leaves us with

$$\boldsymbol{\Sigma}^{\mathrm{H},B}_{\zeta_2\zeta_1}(\{p_{F_B}\})\Big|_{\omega} = \gamma^{\mu}_{\zeta_2\zeta_1}\,\frac{g_{\mu\nu}}{m_\omega^2}\,g_{\omega B}\sum_{B'} g_{\omega B'} \times \int \frac{\mathrm{d}^3\boldsymbol{q}}{(2\pi)^3}\ \mathrm{Tr}\left(\gamma^{\nu}\,\boldsymbol{\Xi}^{B'}(\boldsymbol{q})\right)\Theta(p_{F_{B'}} - |\boldsymbol{q}|)\,. \tag{7.14}$$

The calculation of the trace in (7.14),

$$\mathrm{Tr}\left(\gamma^{\nu}\boldsymbol{\Xi}^{B'}\right) = \mathrm{Tr}\left\{\left[\gamma^{\nu}\left(\mathbf{1}\,\Xi_S^{B'} + \gamma\cdot\hat{\boldsymbol{q}}\,\Xi_V^{B'} + \gamma^0\,\Xi_0^{B'}\right)\right]\otimes\mathbf{1}^{\mathrm{iso}}\right\}, \tag{7.15}$$

is somewhat more complicated than for the scalar σ meson in (7.6). We begin with the trace of the first term in (7.15), which is trivially found to given

$$\mathrm{Tr}\ (\mathbf{1}\,\gamma^{\nu}) = \mathrm{Tr}\ \gamma^{\nu} = 0\,, \tag{7.16}$$

since the traces of the γ matrices vanish. When calculating the contribution of the trace of the second term in (7.15), we note that (see appendices A.2 and A.3):

$$\begin{aligned}\mathrm{Tr}\ (\gamma^{\nu}\,\boldsymbol{\gamma}\cdot\hat{\boldsymbol{q}}) &= \mathrm{Tr}\ \left(\gamma^{\nu}\,\gamma^{i}\,\hat{q}^{i}\right)\\ &= \hat{q}^{i}\ \mathrm{Tr}\ \left(\gamma^{\nu}\,\gamma^{i}\right)\\ &= \hat{q}^{i}\ \mathrm{Tr}\ \left(2\,g^{\nu i}\,\mathbf{1} - \gamma^{i}\,\gamma^{\nu}\right)\\ &= \hat{q}^{i}\ \mathrm{Tr}\ \left(8\,g^{\nu i} - \mathrm{Tr}\ \left(\gamma^{i}\,\gamma^{\nu}\right)\right)\\ &= 8\,\hat{q}^{i}\,g^{\nu i} - \mathrm{Tr}\ (\gamma^{\nu}\,\boldsymbol{\gamma}\cdot\hat{\boldsymbol{q}})\ ,\end{aligned} \tag{7.17}$$

and therefore, by moving the second term on the right-hand side of (7.17) to the left-hand side of this equation,

$$\mathrm{Tr}\ (\gamma^{\nu}\,\boldsymbol{\gamma}\cdot\hat{\boldsymbol{q}}) = 4\,\hat{q}^{i}\,g^{\nu i}\,. \tag{7.18}$$

Multiplying both sides of (7.18) with $g_{\mu\nu}$ and summing over ν leads to

$$\sum_\nu g_{\mu\nu}\ \mathrm{Tr}\ (\gamma^\nu\, \boldsymbol{\gamma}\cdot\hat{\boldsymbol{q}}) = 4\sum_\nu \hat{q}^i\, g_{\mu\nu}\, g^{\nu i} = 4\sum_{i=1}^{3} \hat{q}^i\, \delta_\mu^{\ i}\,. \tag{7.19}$$

To pick up the last Dirac matrix, γ^μ, of equation (7.14), we multiply (7.19) with γ^μ and sum over the doubly occurring index μ. This leads to the final result

$$\sum_\mu \gamma^\mu \Big\{ \sum_\nu g_{\mu\nu}\ \mathrm{Tr}\ (\gamma^\nu\, \boldsymbol{\gamma}\cdot\hat{\boldsymbol{q}}) \Big\} = 4\sum_\mu \sum_{i=1}^{3} \gamma^\mu\, \hat{q}^i\, \delta_\mu^{\ i} = 4\, \boldsymbol{\gamma}\cdot\hat{\boldsymbol{q}} \tag{7.20}$$

The Dirac algebra thus gives a non-vanishing contribution for the $\boldsymbol{\gamma}\cdot\hat{\boldsymbol{q}}$ term in (7.14). Nevertheless, we can forget about this term because of the vanishing integrals over the solid angle,

$$\begin{aligned} &\int_{(4\pi)} \mathrm{d}\Omega_{\boldsymbol{q}}\ \boldsymbol{\gamma}\cdot\hat{\boldsymbol{q}} \\ &= \boldsymbol{\gamma}\cdot \int_0^{2\pi} \mathrm{d}\phi \int_0^{\pi} \mathrm{d}\theta\, \sin\theta \times (\sin\theta\, \cos\phi, \sin\theta\, \sin\phi, \cos\theta) = 0\,, \end{aligned} \tag{7.21}$$

with $\hat{\boldsymbol{q}} = \boldsymbol{q}/|\boldsymbol{q}| = (\sin\theta\, \cos\phi, \sin\theta\, \sin\phi, \cos\theta)$. Each integral of (7.21) vanishes because of symmetry reasons.

Finally, the contribution of the trace of the third term of (7.15) is readily found by noticing that

$$\begin{aligned} \mathrm{Tr}\ (\gamma^\nu\, \gamma_0) &= \mathrm{Tr}\ (g^{\nu\mu}\, \gamma_\mu\, \gamma_0) \\ &= \mathrm{Tr}\ (g^{\nu\mu}\, (2\, g_{\mu\nu}\, \mathbf{1} - \gamma_0\, \gamma_\mu)) \\ &= 2\, g^{\nu\mu}\, g_{\mu 0}\ \mathrm{Tr}\ \mathbf{1} - \mathrm{Tr}\ (\gamma_0\, \gamma^\nu)\ . \end{aligned} \tag{7.22}$$

Since $\mathrm{Tr}\ \mathbf{1} = 4$ and $g^{\nu\mu}\, g_{\mu 0} = \delta^\nu_{\ 0}$, we find from (7.22) for the desired trace

$$\mathrm{Tr}\ (\gamma^\nu\, \gamma_0) = 4\, \delta^\nu_{\ 0}\,. \tag{7.23}$$

Having the results of all relevant traces at our disposal, now we proceed with the calculation of $\boldsymbol{\Sigma}^{\mathrm{H},B}_{\zeta_2\zeta_1}|_\omega$. Upon substituting the results derived in (7.16), (7.21), and (7.23) into (7.14), we arrive for $\boldsymbol{\Sigma}^{\mathrm{H},B}_{\zeta_2\zeta_1}|_\omega$ at the expression

$$\begin{aligned} \boldsymbol{\Sigma}^{\mathrm{H},B}_{\zeta_2\zeta_1}(\{p_{F_B}\})\Big|_\omega &= 2\, \gamma^0_{\zeta_2\zeta_1} \Big(\frac{g_{\omega B}}{m_\omega^2}\Big)^2 \sum_{B'} \nu_{B'}\, \frac{g_{\omega B'}}{g_{\omega B}} \\ &\quad \times \int \frac{\mathrm{d}^3\boldsymbol{q}}{(2\pi)^3}\, \Xi_0^{B'}(\boldsymbol{q})\, \Theta(p_{F_{B'}} - |\boldsymbol{q}|)\,. \end{aligned} \tag{7.24}$$

A comparison with the general decomposition of $\boldsymbol{\Sigma}^B$ of (6.83) shows that

$$\Sigma_0^{\mathrm{H},B}(\{p_{F_B}\})\Big|_\omega = 2\left(\frac{g_{\omega B}}{m_\omega^2}\right)^2 \sum_{B'} \nu_{B'}\, \frac{g_{\omega B'}}{g_{\omega B}} \times \int \frac{\mathrm{d}^3\boldsymbol{q}}{(2\pi)^3}\, \Xi_0^{B'}(\boldsymbol{q})\, \Theta(p_{F_{B'}} - |\boldsymbol{q}|)\,. \tag{7.25}$$

Note that at the level of the relativistic Hartree approximation, there is neither a scalar nor a vector-component contribution to $\boldsymbol{\Sigma}^B$.

We conclude this section with giving the expressions for the Fock contributions $\boldsymbol{\Sigma}^{\mathrm{F},B}(1,1')$ of (7.3) which arise from the exchange of σ and ω mesons. In analogy to the Hartree case, we turn back to the momentum-space representations of $\boldsymbol{\Sigma}^{\mathrm{F},B}(1,1')|_\sigma$ and $\boldsymbol{\Sigma}^{\mathrm{F},B}(1,1')|_\omega$ given in (5.136) and (5.138), respectively. Replacing $\boldsymbol{g}^{B'}(q)$ in these equations with its associated spectral representation, derived in (6.71), and subsequently performing the contour integrations leads to

$$\boldsymbol{\Sigma}^{\mathrm{F},B}_{\zeta_1\zeta_1'}(k)\Big|_\sigma = g_{\sigma B}^2 \int \frac{\mathrm{d}^3\boldsymbol{q}}{(2\pi)^3} \big\{\delta_{\zeta_1\zeta_1'}\, \Xi_S^B(\omega^B(\boldsymbol{q}),\boldsymbol{q}) + (\boldsymbol{\gamma}\cdot\hat{\boldsymbol{k}})_{\zeta_1\zeta_1'}\, \hat{\boldsymbol{k}}\cdot\hat{\boldsymbol{q}}\, \times \Xi_V^B(\omega^B(\boldsymbol{q}),\boldsymbol{q}) + \gamma^0_{\zeta_1\zeta_1'}\, \Xi_0^B(\omega^B(\boldsymbol{q}),\boldsymbol{q})\big\}\, \Delta^{0\sigma}(k_0 - \omega^B(\boldsymbol{q}), \boldsymbol{k}-\boldsymbol{q})\, \Theta^B(\boldsymbol{q})\,. \tag{7.26}$$

In the case of ω mesons one arrives as

$$\begin{aligned}
\boldsymbol{\Sigma}^{\mathrm{F},B}_{\zeta_1\zeta_1'}(k)\Big|_\omega = {} & g_{\omega B}^2 \int \frac{\mathrm{d}^3\boldsymbol{q}}{(2\pi)^3} \Big\{ -\delta_{\zeta_1\zeta_1'} \left[4 - \frac{(k^0-\omega^B(\boldsymbol{q}))^2 - (\boldsymbol{k}-\boldsymbol{q})^2}{m_\omega^2}\right] \\
& \times \Xi_S^B(\omega^B(\boldsymbol{q}),\boldsymbol{q}) + (\boldsymbol{\gamma}\cdot\hat{\boldsymbol{k}})_{\zeta_1\zeta_1'} \left[\left(\hat{\boldsymbol{k}}\cdot\hat{\boldsymbol{q}}\left(2 - \frac{\boldsymbol{k}^2 + \boldsymbol{q}^2 + (k^0-\omega^B(\boldsymbol{q}))^2}{m_\omega^2}\right)\right.\right. \\
& \left. + \frac{2\,|\boldsymbol{k}|\,|\boldsymbol{q}|}{m_\omega^2}\right) \Xi_V^B(\omega^B(\boldsymbol{q}),\boldsymbol{q}) \;-\; \left.\frac{2}{m_\omega^2}\, \hat{\boldsymbol{k}}\cdot(\boldsymbol{k}-\boldsymbol{q})\,(k^0-\omega^B(\boldsymbol{q}))\, \Xi_0^B(\omega^B(\boldsymbol{q}),\boldsymbol{q})\right] \\
& + \gamma^0_{\zeta_1\zeta_1'} \left[\frac{2}{m_\omega^2}\, \hat{\boldsymbol{q}}\cdot(\boldsymbol{k}-\boldsymbol{q})\,(k^0-\omega^B(\boldsymbol{q}))\, \Xi_V^B(\omega^B(\boldsymbol{q}),\boldsymbol{q})\right. \\
& \left. + \left(2 + \frac{(k^0-\omega^B(\boldsymbol{q}))^2 + (\boldsymbol{k}-\boldsymbol{q})^2}{m_\omega^2}\right) \Xi_0^B(\omega^B(\boldsymbol{q}),\boldsymbol{q})\right]\Big\} \\
& \times\, \Delta^{0\omega}(k^0 - \omega^B(\boldsymbol{q}), \boldsymbol{k}-\boldsymbol{q})\, \Theta(q_{F_B} - |\boldsymbol{q}|)\,.
\end{aligned} \tag{7.27}$$

The Hartree and Fock contributions to $\boldsymbol{\Sigma}^B$ which originate from π and ρ mesons exchange among the baryons are listed in appendix C. The extension of $\boldsymbol{\Sigma}^B$ to finite-temperatures is performed in appendix D. In closing this section, we note that the effective baryon mass, m_B^*, is defined as

$$m_B^* \equiv m_B^*(\omega^B(\boldsymbol{k}),\boldsymbol{k}) \equiv m_B^* + \Sigma_S^{\mathrm{HF},B}(\omega^B(\boldsymbol{k}),\boldsymbol{k})\,. \tag{7.28}$$

7.2 Self-energies in Hartree approximation (Walecka model)

At the level of the relativistic Hartree approximation, the mathematical structure of the baryon self-energies becomes extremely simple. This originates primarily from the very simple form of the baryon spectral functions $\mathbf{\Xi}^B$ for this approximation, which, as demonstrated at the end of section (6.2), simplify to

$$\Xi_S^{\mathrm{H},B}(\boldsymbol{q}) = \frac{m_B^*}{2\,\epsilon^{\mathrm{H},B}(\boldsymbol{q})}\,, \quad \Xi_V^{\mathrm{H},B}(\boldsymbol{q}) = \frac{-\,|\boldsymbol{q}|}{2\,\epsilon^{\mathrm{H},B}(\boldsymbol{q})}\,, \quad \Xi_0^{\mathrm{H},B}(\boldsymbol{q}) = \frac{1}{2}\,. \tag{7.29}$$

The quantity m_B^* denotes the effective, medium-modified mass of a baryon in dense matter, defined, in accordance with (7.28), as

$$m_B^* \equiv m_B + \Sigma_S^{\mathrm{H},B}\,. \tag{7.30}$$

Moreover we have introduced the auxiliary quantity $\epsilon^{\mathrm{H},B}$ given by [cf. equation (6.171)]

$$\epsilon^{\mathrm{H},B}(\boldsymbol{q}) = \sqrt{(m_B^*)^2 + \boldsymbol{q}^2}\,, \tag{7.31}$$

by means of which the single-baryon energy (6.150) can be expressed as

$$\omega^{\mathrm{H},B}(\boldsymbol{q}) = \Sigma_0^{\mathrm{H},B}(\boldsymbol{q}) + \epsilon^{\mathrm{H},B}(\boldsymbol{q})\,. \tag{7.32}$$

The above equations follow immediately from (6.143) through (6.145) by noticing that the baryon self-energies (and thus m^*) at the Hartree level are independent of both energy and momentum, as we know from the expressions for $\mathbf{\Sigma}^B$ derived in equations (7.13) and (7.25). Only the density dependence survives because of the proportionality $\mathbf{\Sigma}^B \propto k_{F_B}^3$. This simplification is lost for the HF approximation, where the exchange term depends on both energy and momentum.

Upon substituting (7.29) into equation (7.13), one obtains for the scalar component of the *nucleon* self-energy in dense nuclear matter at

$$\begin{aligned}\Sigma_S^{\mathrm{H},N} = \frac{1}{4\pi^2}\left(\frac{g_{\sigma N}}{m_\sigma}\right)^2 \sum_B \frac{g_{\sigma B}}{g_{\sigma N}}\,\nu_B \Bigg\{ & k_{F_B}\sqrt{(m_B^*)^2 + k_{F_B}^2} \\ & - (m_B^*)^2\,\ln\left|\frac{k_{F_B} + \sqrt{(m_B^*)^2 + k_{F_B}^2}}{m_B^*}\right|\Bigg\} \\ + \left(\frac{g_{\sigma N}}{m_\sigma}\right)^2 & \left\{ b_N\, m_N\,\left(\mathbf{\Sigma}_S^N\right)^2 - c_N\,\left(\mathbf{\Sigma}_S^N\right)^3\right\}.\end{aligned} \tag{7.33}$$

The timelike component, $\Sigma_0^{\mathrm{H},N}$, follows from (7.25) as

$$\Sigma_0^{\mathrm{H},N} = \frac{1}{6\,\pi^2}\Big(\frac{g_{\omega N}}{m_\omega}\Big)^2 \sum_B \Big(\frac{g_{\omega B}}{g_{\omega N}}\Big)\, \nu_B\; k_{F_B}^3\,. \tag{7.34}$$

Equations (7.33) and (7.34) are special cases of the more general expressions

$$\Sigma_0^{\mathrm{H},B} = \Big(\frac{g_{\omega B}}{m_\omega}\Big)^2 \sum_{B'} \frac{g_{\omega B'}}{g_{\omega B}}\; \rho^{H,B'}\,, \tag{7.35}$$

and

$$\Sigma_S^{\mathrm{H},B} = -\Big(\frac{g_{\sigma B}}{m_\sigma}\Big)^2 \Big\{ \sum_{B'} \frac{g_{\sigma B'}}{g_{\sigma B}}\; \bar\rho^{\mathrm{H},B'} - b_B\, m_N\, \big(\Sigma_S^{\mathrm{H},B}\big)^2 + c_B\, \big(\boldsymbol{\Sigma}_S^{\mathrm{H},B}\big)^3 \Big\}\,, \tag{7.36}$$

with the definitions

$$b_B \equiv \Big(\frac{g_{\sigma N}}{g_{\sigma B}}\Big)^4\, b_N\,, \qquad c_B = \Big(\frac{g_{\sigma N}}{g_{\sigma B}}\Big)^5\, c_N\,. \tag{7.37}$$

These follow from equations (7.13) and (7.25) by making use of the baryon number densities ρ^B and $\bar\rho^B$, derived in equations 6.185 and 6.199, for the relativistic Hartree approximation.

Note that there is no contribution to the vector component Σ_V^B at the level of the relativistic Hartree approximation. The results (7.33) and (7.34) are noting but Walecka's σ–ω mean-field equations in their non-linear form [92, 347, 348, 349] for uniform static matter, in which space and time derivatives of the fields can be dropped. This can be readily verified by setting [79, 125, 313]

$$\Sigma_S^B = -g_{\sigma B}\; <\sigma_0> \qquad \text{and} \qquad \Sigma_0^B = g_{\omega B}\; <\omega_0>\,, \tag{7.38}$$

where $<\sigma_0>$ and $<\omega_0>$ denote the static amplitudes of the meson-field equations (5.43) and (5.44), with space and time derivatives ignored. The baryon source currents in these meson-field equations are replaced with their ground-state expectation values, with the ground state defined as having the single-particle momentum eigenstates of the Dirac equations filled to the top of the Fermi sea of each baryon species, in accord with the condition of chemical equilibrium and electric charge neutrality.

The last term in equation (7.33) contributes only if cubic and quartic self-interactions of the σ field are included in the Lagrangian (5.1). This leads to a self-energy contribution, denoted by $\boldsymbol{\Sigma}^{(\sigma^4)}$, which has the form [79, 125, 313]

$$\boldsymbol{\Sigma}^{(\sigma^4)}_{\zeta_2\zeta_1} = \delta_{\zeta_2\zeta_1}\, \Big(\frac{g_{\sigma N}}{m_\sigma}\Big)^2 \Big\{ m_N\; b_N\, \big(\Sigma_S^{\mathrm{H},N}\big)^2 -\; c_N\, \big(\Sigma_S^{\mathrm{H},N}\big)^3 \Big\}\,. \tag{7.39}$$

Such cubic and quartic terms are known to be important since the linear σ–ω theory fails to account for an effective nucleon mass in matter, m_N^*, and a incompressibility, K, which are compatible with experimental values [100, 124, 308, 309]. Alternatively to supplementing the Lagrangian with non-linear terms, it has recently been pointed out by Zimanyi and Moszkowski [350] and Glendenning, Weber, and Moszkowsi [86] that if the scalar field is coupled to the derivative of the nucleon field, these two nuclear properties are automatically in fairly reasonable accord with present knowledge of their values. We introduce this model in the following section.

7.3 Derivative coupling model

The linear σ–ω nuclear field theory has been broadly studied in both spherical and deformed nuclei. However, in the linear version [347, 348, 349] it has too small a nucleon effective mass ($\sim 0.55\, m_N$) at saturation density of nuclear matter and too large an incompressibility ($\sim$ 560 MeV). As discussed in section 5.1, these properties can be brought under control at the cost of two additional parameters by the addition of scalar cubic and quartic self-interactions in the so-called non-linear model [308]. Alternatively it has been recently noticed by Zimanyi and Moszkowski [350] that, if the scalar field is coupled to the derivative of the nucleon field, these two nuclear properties are automatically in reasonable accord with our present knowledge of their values, the two coupling constants of the theory being fixed by the empirical saturation density and binding as in the linear σ–ω theory. The agreement with bulk nuclear properties can be further improved by a slight modification of the model of Zimanyi and Moszkowski, which we shall call the hybrid derivative coupling model, and which we shall discuss below. Renormalization is irrevocably lost in derivative coupling models, but since (strong interacting) nuclear field theory is usually regarded as an effective one, this does not seem to be a weighty objection.

In place of the purely derivative coupling of the scalar field to the baryons and vector meson of the Zimanyi-Moszkowski model, we couple it here by both Yukawa point and derivative coupling to baryons and both vector fields. This improves the agreement with the incompressibility and effective nucleon mass at saturation density. The nuclear matter properties obtained for the hybrid derivative coupling model will be listed below. To account for the symmetry force, we include the coupling of the ρ meson to the isospin current. The ρ-meson contribution to this current vanishes in the mean-field approximation and so we do not write its formal contribution in the Lagrangian [351]:

$$
\begin{aligned}
\mathcal{L} = & \sum_B \Big\{ \Big(1 + \frac{g_{\sigma B}\sigma}{2m_B}\Big) \Big[\bar{\psi}_B (\mathrm{i}\gamma_\mu \partial^\mu - g_{\omega B}\gamma_\mu \omega^\mu - \frac{1}{2} g_{\rho B}\, \gamma_\mu \boldsymbol{\tau} \cdot \boldsymbol{\rho}^\mu) \psi_B \Big] \\
& - \Big(1 - \frac{g_{\sigma B}\sigma}{2m_B}\Big) m_B \bar{\psi}_B \psi_B \Big\} + \frac{1}{2} \left(\partial_\mu \sigma \partial^\mu \sigma - m_\sigma^2 \sigma^2 \right) - \frac{1}{4} F_{\mu\nu} F^{\mu\nu} \\
& + \frac{1}{2} m_\omega^2\, \omega_\mu \omega^\mu - \frac{1}{4} \boldsymbol{G}_{\mu\nu} \boldsymbol{G}^{\mu\nu} + \frac{1}{2} m_\rho^2\, \boldsymbol{\rho}_\mu \cdot \boldsymbol{\rho}^\mu + \sum_{L=e^-,\mu^-} \mathcal{L}_L \, .
\end{aligned}
\tag{7.40}
$$

In the first term one sees the coupling of the scalar field to the derivatives of the baryon fields and to the vector mesons. The Yukawa point coupling to the baryon fields is contained in the second term. In the last line one recognizes the free scalar, vector, and vector-isovector mesons, and the lepton Lagrangian of (5.15). As we know from section 4.2, leptons must be present because of electric charge neutrality and chemical equilibrium of neutron star matter. (The notation in (7.40) is the same as at the beginning of section 5.1 where we introduced the standard Lagrangian of neutron star matter.) The baryon Lagrangian is in the first line together with the interaction terms with the above-mentioned mesons. The sum over B in (7.40) is extended over all higher-mass baryons listed in table 5.1 for which the baryon chemical potential exceeds their rest mass in dense matter, i.e. corrected for interactions and electric charge. The solution is most easily obtained by means of transforming all baryon fields as

$$
\psi_B = \Big(1 + \frac{g_{\sigma B}\sigma}{2m_B}\Big)^{-1/2} \, \Psi_B \, .
\tag{7.41}
$$

The equivalent Lagrangian is then given by

$$
\begin{aligned}
\mathcal{L} = & \sum_B \bar{\Psi}_B \Big(\mathrm{i}\gamma_\mu \partial^\mu - m_B^* - g_{\omega B}\, , \gamma_\mu \omega^\mu - \frac{1}{2} g_{\rho B}\, \gamma_\mu \boldsymbol{\tau} \cdot \boldsymbol{\rho}^\mu \Big) \Psi_B \\
& + \frac{1}{2} \left(\partial_\mu \sigma \partial^\mu \sigma - m_\sigma^2 \sigma^2 \right) - \frac{1}{4} F_{\mu\nu} F^{\mu\nu} + \frac{1}{2} m_\omega^2\, \omega_\mu \omega^\mu \\
& - \frac{1}{4} \boldsymbol{G}_{\mu\nu} \cdot \boldsymbol{G}^{\mu\nu} + \frac{1}{2} m_\rho^2\, \boldsymbol{\rho}_\mu \cdot \boldsymbol{\rho}^\mu + \sum_L \bar{\psi}_L \left(i\gamma_\mu \partial^\mu - m_L \right) \psi_L \, .
\end{aligned}
\tag{7.42}
$$

It is evident that the baryons now have effective masses

$$
m_B^* = \Big(1 - \frac{g_{\sigma B}\sigma}{2m_B}\Big) \Big(1 + \frac{g_{\sigma B}\sigma}{2m_B}\Big)^{-1} m_B \, .
\tag{7.43}
$$

In the next step we solve the field equations in the mean-field (Hartree) approximation, introduced in section 7.2. The meson-field equations in uniform static matter, in which space and time derivatives can be dropped, are then given by

$$< \omega_0 > \; = \sum_B \frac{g_{\omega B}}{m_\omega^2} \; \rho^B \,, \tag{7.44}$$

$$< \boldsymbol{\rho}_{03} > \; = \sum_B \frac{g_{\rho B}}{m_\rho^2} \; I_{3B} \; \rho^B \,, \tag{7.45}$$

$$\begin{aligned} m_\sigma^2 \; \sigma &= \sum_B g_{\sigma B} \Big(1 + \frac{g_{\sigma B} \sigma}{2 m_B} \Big)^{-2} \; < \boldsymbol{\Phi}_0 | \bar{\Psi}_B \Psi_B | \boldsymbol{\Phi}_0 > \\ &= \sum_B g_{\sigma B} \Big(1 + \frac{g_{\sigma B} \sigma}{2 m_B} \Big)^{-2} \; \frac{2J_B + 1}{2\pi^2} \int_0^{k_{F_B}} \mathrm{d}k \; k^2 \; \frac{m_B^*}{\sqrt{k^2 + (m_B^*)^2}} \,. \end{aligned} \tag{7.46}$$

As we know from section 7.2, the spacelike components of both vector fields vanish, for the physical reason that the ground state is isotropic and has definite charge [61]. The baryon density ρ^B is given by

$$\rho^B \equiv < \boldsymbol{\Phi}_0 | \Psi_B^\dagger \Psi_B | \boldsymbol{\Phi}_0 > = \frac{1}{6\pi^2} \; (2J_B + 1) \; k_{F_B}^3 \,. \tag{7.47}$$

The condition of electric charge neutrality is expressed by

$$\frac{1}{6\pi^2} \sum_B \; (2J_B + 1) \; q_B^{\mathrm{el}} \; k_{F_B}^3 - \frac{1}{3\pi^2} \sum_L \; k_{F_L}^3 = 0 \,, \tag{7.48}$$

where the first sum is over the baryons whose electric charges are listed in table 5.1, and the second sum is over the leptons e^- and μ^-. Chemical equilibrium is imposed through the two independent chemical potentials μ^n and μ^e, which lead for the baryon chemical potential to $\mu^B = \mu^n - q_B^{\mathrm{el}} \mu^e$.

7.4 Coupling constants and masses

At the level of the relativistic Hartree and relativistic HF approximation, the parameters (i.e. coupling constants and particle masses) of the Lagrangian (5.1) are not determined by the nucleon–nucleon interaction in free space combined with the data of the deuteron [92, 118], as for the **T**-matrix approximation, but are to be adjusted to the bulk properties of infinite nuclear matter at saturation density, ρ_0 [92, 100, 123, 124]. These properties are the binding energy E/A, effective nucleon mass m_N^*/m_N, incompressibility K, and the symmetry energy $a_{\rm sym}$ whose respective values are given by,

$$\rho_0 = 0.16 \text{ fm}^{-3}\,, \quad E/A = -16.0 \text{ MeV}\,, \quad a_{\rm sym} = 32.5 \text{ MeV}\,,$$
$$K = 265 \text{ MeV}\,, \quad m_N^*/m_N = 0.796\,. \tag{7.49}$$

Of the five, the value for the incompressibility of nuclear matter carries some uncertainty. Its value is currently believed to lie in the range between about 200 and 300 MeV.

At first sight it seems as if $\mathcal{L}$ of (5.1) would contain an enormous number of unknowns, which is in fact not the case. If one imposes the principal of universal coupling, which consists in setting the baryon couplings to the meson fields, g_{MB}, equal to the nucleon couplings to the respective meson field, g_{MN}, then there remain only a few unknown parameters. These are the four mesons masses

$$m_\sigma\,, \quad m_\omega\,, \quad m_\pi\,, \quad m_\rho\,, \tag{7.50}$$

and the seven baryon–meson coupling constants

$$g_{\sigma N}\,, \quad g_{\omega N}\,, \quad f_{\pi N}\,, \quad g_{\rho N}\,, \quad f_{\rho N}\,, \quad b_N\,, \quad c_N\,. \tag{7.51}$$

As for the baryons, the meson masses usually are taken to be equal to their physical values [352], except for the hypothetical σ meson, which is introduced to simulate the correlated 2π exchange. For it one generally takes a tentative value of about 550 MeV. The ρ-meson vector coupling constant, $g_{\rho N}$, can be deduced from the description of the nucleon–nucleon interaction, and the ratio of the tensor to the vector coupling strength, that is $f_{\rho N}/g_{\rho N}$, can be obtained from the vector dominance model [353] which leads to $f_{\rho N}/g_{\rho N} \approx 3.7$. Hence, there remain four undetermined coupling strengths in the theory,

$$g_{\sigma N}\,, \quad g_{\omega N}\,, \quad b_N\,, \quad c_N\,. \tag{7.52}$$

This set reduces to only the first two if σ^4 self-interactions are taken into account, in which case $b_N = c_N = 0$. It are these four respectively two coupling constants that are to be adjusted to the ground-state properties of nuclear matter quoted in equation (7.49), in so far as they are left undetermined by the nucleon–nucleon interaction data, of course. Recall that the latter can be used to determine the ρ-meson vector coupling constant which, in turn, fixes $a_{\rm sym}$. A parameter set adjusted along these lines, which allows for HF calculations based of the scalar-vector-isovector Lagrangian, but without the σ^4 terms, has been given by Bouyssy *et al*

Table 7.1. Coupling constants and masses of several different parameter sets applicable to relativistic Hartree and HF calculations (see table 12.4).† The corresponding nuclear matter properties are listed in table 12.7.

Quantity	HV	HFV	$G_{\rm B180}^{\rm K240}$	G_{300}	$G_{\rm B180}^{\rm K300}$	$G_{265}^{\rm DCM2}$
m_N (MeV)	939	939	938	939	938	939
m_σ (MeV)	550	550	550	600	550	550
m_ω (MeV)	783	783	783	783	783	783
m_π (MeV)	–	138	–	–	–	–
m_ρ (MeV)	770	770	770	770	770	770
$g_{\sigma N}^2/4\pi$	6.16	7.10	6.14	6.644	7.29	5.34
$g_{\omega N}^2/4\pi$	6.71	6.80	6.04	5.930	8.96	5.15
$f_{\pi N}^2/4\pi$	–	0.08	–	–	–	–
$g_{\rho N}^2/4\pi$	7.51	0.55	5.81	5.846	5.34	5.50
$f_{\rho N}/g_{\rho N}$	–	6.6	–	–	–	–
$10^3\ b_N$	4.14	–	8.65	3.305	2.95	–
$10^3\ c_N$	7.16	–	−2.42	15.29	−1.07	–
References	[61]	[98]	[66]	[354]	[66]	[86]

† HFV is a relativistic Hartree–Fock parametrization, all others are relativistic Hartree parameter sets.

[98]. We shall adopt this parameter set, which is denoted by HFV [84]. Its parameter values are given in table 7.1.

In the framework of the non-linear Hartree approximation the nuclear forces are described via the exchange of σ, ω, π mesons among the baryons. There are no π-meson contributions because of parity reasons. This leaves one with a one-to-one correspondence between the number of coupling constants, $g_{\sigma N}$, $g_{\omega N}$, g_{ρ_N}, b_N, c_N, and the nuclear matter properties of (7.49). To determine these couplings for nuclear matter near saturation, one simply needs to fix the Fermi momenta $k_{F_n} = k_{F_p} \equiv k_F$. The scalar and vector coupling constants are then fixed by the known saturation density, ρ_0, and the binding energy per nucleon, $E/A = (\epsilon/\rho)_0 - m_N$. The ρ-meson vector-coupling constant is adjusted to give the empirical symmetry coefficient which is given by the expression [86]

$$a_{\rm sym} = \frac{1}{2}\left(\frac{\partial^2(\epsilon/\rho)}{\partial\delta^2}\right)_{t=0} = \left(\frac{g_\rho}{m_\rho}\right)^2 \frac{k_{F_0}^3}{12\,\pi^2} + \frac{k_{F_0}^2}{6\sqrt{k_{F_0}^2 + (m_N^*)^2}}\,, \quad (7.53)$$

where $\delta \equiv (\rho^n - \rho^p)/\rho$, and k_{F_0} the Fermi momentum of symmetric nuclear matter at saturation density, ρ_0. Finally, the non-linear σ-meson self-

Table 7.2. Model parameter sets applicable to relativistic Hartree and Hartree–Fock calculations based on the *standard* (i.e. restriction to only σ and ω meson exchange) scalar-vector Lagrangian . The coupling constants are obtained by fitting the binding energy and density of equilibrium nuclear matter in the relativistic Hartree (HI, HII, HIII, HIV) and relativistic Hartree–Fock (HFI, HFII) approximation (cf. table 7.3).

	HI	HII	HIII	HIV	HFI	HFII
m_N (MeV)	939	939	938	939	939	939
m_σ (MeV)	570	550	492.36	550	550	550
m_ω (MeV)	782.8	783	795.36	783	783	783
$g^2_{\sigma N}/4\pi$	7.826	6.718	8.180	5.958	6.614	8.658
$g^2_{\omega N}/4\pi$	10.824	8.650	14.049	5.678	8.598	11.889
$10^4\ \left(\frac{g_{\sigma N}}{m_\sigma}\right)^2$	3.0267	2.7906	4.2424	2.4749	2.7474	3.5967
$10^4\ \left(\frac{g_{\omega N}}{m_\omega}\right)^2$	2.2197	1.7730	2.7908	1.1638	1.7624	2.4368
$10^3\ b_N$	–	1.8	2.46	8.95	–	–
$10^4\ c_N$	–	2.87	−34.3	36.89	–	–
References	[92, 355]	[356, 357, 358]	[359]	[360]	[92]	[92]

interactions, proportional to b_N and c_N, are chosen such that a consistent value for the incompressibility of nuclear matter is obtained. Parameter sets adjusted in this way by Glendenning are listed in table 7.1. (The nuclear matter data associated with these parametrizations, which individually varies about the properties quoted in (7.49), will be surveyed in table 12.7.) The parameter sets of table 7.1, which will be applied to stellar structure calculations in the second part of the book, are complemented several extra Hartree and HF parameter sets, listed in table 7.2, which have been widely used in the literature for the calculation of the properties of finite nuclei as well as nuclear and neutron matter. Listed are the nucleon mass m_N, σ-meson mass m_σ, ω-meson mass m_ω, the respective baryon–meson coupling constants $g_{\sigma N}$, $g_{\omega N}$, and the parameters (if any) of cubic and quartic σ-meson self-interactions. In should be noted that none of these parameter sets accounts for ρ-meson exchange, for which reason the value of the symmetry energy coefficient remain practically uncontrolled, aside from the contribution to $a_{\rm sym}$ that originates from the Fermi momentum [second term in equation (7.53)]. This becomes very obvious from table 7.3. These parameter sets should therefore not be applied to neutron star matter calculations, whose properties depend rather crucially on $a_{\rm sym}$.

Table 7.3. Energy per nucleon E/A, Fermi momentum k_{F_0}, incompressibility K, effective nucleon mass m_N^*/m_N, and symmetry energy $a_{\rm sym}$ (MeV) of equilibrium nuclear matter obtained for the different Hartree (labels 'H') and Hartree–Fock (labels 'HF') parameter sets listed in table 7.2.

	E/A (MeV)	k_{F_0} (fm^{-1})	K (MeV)	m_N^*/m_N	$a_{\rm sym}$ (MeV)
HI	−15.74	1.42	540	0.56	22.1
HII	−15.75	1.34	360	0.693	16.6
HIII	−16.34	1.31	195	0.582	18.4
HIV	−15.95	1.29	237	0.798	13.6
HFI	−15.75	1.42	540	0.529	36.5
HFII	−15.75	1.30	580	0.515	33.6

The ratio of hyperon to nucleon couplings to the meson fields,

$$x_\sigma = g_{\sigma H}/g_{\sigma N}\,, \quad x_\omega = g_{\omega H}/g_{\omega N}\,, \quad x_\rho = g_{\rho H}/g_{\rho N}\,, \tag{7.54}$$

are not defined by the ground-state properties of normal nuclear matter and so must be chosen according to other considerations [86, 361]. In studies of hypernuclear levels [362, 363, 364], these ratios are typically taken to be equal. In that case, small values between 0.33 and 0.4 are required. These are too small as regards neutron star masses, as shown in table 7.4. We recall that the most accurately determined mass, which is not necessarily the maximal possible mass, is that of PSR 1913+16 with $M = (1.442 \pm 0.003) M_\odot$ [232] (see also figure 3.2). There is another relevant measurement, that of Vela X-1 (4U 0900–40) with $M = 1.79^{+0.19}_{-0.24}\, M_\odot$ [31, 236]. However, the error is so large that many authors take the other measurement as the limit. The actual number of known masses at the present time is about 20 and we cannot exclude that a more massive neutron star will be found, as indicated by the observation of QPOs for neutron star 4U 1636–536 (cf. section 3.1). However, to the imperfect extent to which the type–II supernova mechanism is understood, it appears that neutron stars are created in a fairly narrow range of masses, around $M \sim 1.4\, M_\odot$, so that independent of whether or not the true equation of state would support more massive neutron stars, none may be made in type–II supernovae explosions.

As noted just above, when hypernuclear levels are analyzed with the constraint $x_\sigma = x_\omega$, the result is a small hyperon coupling leading to a neutron star family with much too small a limiting mass. However, one is

Table 7.4. Values of the hyperon to nucleon scalar and vector coupling that are compatible with the binding of -28 MeV for the lambda hyperon in nuclear matter and the corresponding maximum neutron star mass, as determined by Glendenning *et al* [86, 361]. Agreement with the lower bound on the observed maximum neutron star masses is achieved for hyperon-to-nucleon scalar couplings $x_\sigma > 0.65$, which implies for the vector coupling $x_\omega > 0.75$.

x_σ	x_ω	$M/M_\odot$
0.3	0.262	1.08
0.4	0.415	1.13
0.5	0.566	1.23
0.6	0.714	1.36
0.7	0.859	1.51
0.8	1.00	1.66
0.9	1.14	1.79
1.0	1.27	1.88

not compelled to take the ratios in equation (7.54) to be equal, but there are large correlation errors in $x_\sigma = 0.464 \pm 0.255$ and $x_\omega = 0.481 \pm 0.315$, in the published analysis of hypernuclear levels that leave them uncorrelated [364]. These correlation errors are probably due to the degeneracy with respect to the Λ binding in nuclear matter which we derive next. As noted elsewhere [361], this binding energy serves to strictly correlate the values of x_σ and x_ω but leaves a continuous pairwise ambiguity which hypernuclear levels may be able to resolve. The published analysis so far does not take account of this [364]. Millener, Dover and Gall inferred in [365] the binding of the Λ hyperon in nuclear matter to be -28 MeV. To impose this constraint on the values of x_σ and x_ω, we need to derive the expression for this binding in the derivative coupling model. From the Weisskopf relation [366] between the Fermi energy and the energy per nucleon of a self-bound system at saturation density, $\omega(k_F) = (\epsilon/\rho)_0$, which is a special case of the Hugenholtz-Van Hove theorem [367], we obtain for the binding energy of the lowest Λ level in nuclear matter, for which $k_{F_\Lambda} = 0$, the relation [361]

$$\begin{aligned} \frac{E}{A}\bigg|_\Lambda &= x_\omega\, \Sigma_0^N \;+\; m_\Lambda^* \;-\; m_\Lambda \\ &= x_\omega\, \Sigma_0^N \;-\; \frac{x_\sigma\, \Sigma_S^N}{1 \;+\; x_\sigma\, \Sigma_S^N/(2\, m_\Lambda)}\,, \end{aligned} \tag{7.55}$$

where we have made use of

$$\Sigma_S^N \equiv -g_{\sigma N} \ < \sigma_0 > , \qquad \Sigma_0^N \equiv g_{\omega N} \ < \omega_0 > , \tag{7.56}$$

which are special cases of equation (7.38), and of equations (6.149) and (7.43). The first line in (7.55) holds for both the linear and non-linear σ–ω theory as well as for this one. The second line specializes to this theory. Thus, as far as the Λ binding in nuclear matter is concerned, the scalar and vector ratios x_σ and x_ω need not be equal, but when so, they must be small, about 0.37. We show a few typical values in table 7.4. Since the neutron star mass limit must exceed a value of about 1.44 to $1.5\,M_\odot$, and as it depends on the hyperon coupling, we infer that $x_\sigma > 0.65$ and a corresponding value of x_ω, as given by equation (7.55).

There are additional constraints on the values of the hyperon constants that can be invoked. There is good reason to believe [82] that these ratios are less than unity. Moreover, according to the analysis of hypernuclear levels in finite nuclei, it is found that when the ratios are taken unequal, the maximum likely values is $x_\sigma < 0.719$ [364]. It is not clear how strong this last constraint is because it applies to the non-linear field theory [308] whose results would carry over only approximately to the present one. For such relatively simple theories of matter, perhaps one should not insist that when the interest is focused on bulk matter, the level spacings of finite nuclei are compelling constraints. In any case, for x_σ and x_ω chosen to be compatible with the Λ binding in nuclear matter, neutron star masses place a *lower* bound on the coupling, and hypernuclear levels appear to place an *upper* bound, but so far less well determined. Within this range hyperons have a large population in neutron stars and neutrons have a bare majority.[1]

We have assumed that other hyperons in the lowest SU(6) octet have the same coupling as the Λ, and also we have arbitrarily taken $x_\rho = x_\sigma$. This choice produces results that are very close to another possible choice, namely $x_\rho = x_\omega$ [361].

We add here a parenthetical note on the analysis of hypernuclei, involving both the Λ hyperon or any other hyperon. We quoted above the $\sim 50\%$ correlation error found in the least-square fit of x_σ and x_ω to the hypernuclear levels when these parameters are treated independently [364]. But these are not independent parameters as derived just above. They are correlated in a specific way to the binding of the Λ in saturated nuclear matter, a binding that can be inferred quite accurately by an extrapolation from hypernuclear levels in finite-A nuclei [365]. The correlation found in the least-square fit is simply a reflection of the fact that, as a function of A,

[1] This in the case for universal coupling of the hyperons too.

the finite nuclei are 'pointing' to this binding in $A \to \infty$ matter. It is clear, therefore, that it would be advantageous in the analysis of hypernuclei to take into account the relation that x_σ and x_ω must obey, if the Λ binding in nuclear matter is to come out right [361]. In the linear [347, 348, 349] and non-linear scalar version [308] of nuclear field theory, the difference in masses entering the first line of equation (7.55) is $m^*_H - m_H = x_\sigma \Sigma^N_S$, whereas in the present hybrid derivative coupling model it is given by the second line of equation (7.55).

7.5 Summary of the many-body equations

In the following we summarize those many-body equations that determine the properties of dense nuclear matter as well as dense neutron star matter treated in the framework of either the relativistic Hartree approximation or the relativistic HF approximation [61, 79]. The sets of equations are to be solved self-consistently for a given density until numerical convergency is achieved. The individual equations are:

1) Equations (6.143) through (6.145) which determine the baryon spectral functions $\mathbf{\Xi}^B$, and (6.149) which expresses the medium-modified energy–momentum relation ω^B of a baryon B propagating in dense matter. B stands for

$$B = p\,,\ n\,,\ \Sigma^{\pm,0}\,,\ \Lambda\,,\ \Xi^{0,-}\,,\ \Delta^{++,+,0,-}\,. \tag{7.57}$$

Calculating the energy–momentum relation at the Fermi momentum of each respective baryon listed in (7.57), that is, at

$$k_{F_p}\,,\ k_{F_n}\,,\ k_{F_{\Sigma^{\pm,0}}}\,,\ k_{F_\Lambda}\,,\ k_{F_{\Xi^{0,-}}}\,,\ k_{F_{\Delta^{++,+,0,-}}}\,, \tag{7.58}$$

determines the baryon chemical potentials via the relation $\mu^B = \omega^B(k_{F_B})$. This constitutes a maximum number of $b = 13$ unknowns (see table 5.1). Whether or not a given baryon state becomes actually populated depends, among other attributes, on the total baryon density, ρ, of the system. The expression for ρ is derived in equation (6.190).

2) Chemical equilibrium is imposed through the chemical potentials. Only two independent chemical potentials, μ^n and μ^e, corresponding to baryon and electric charge conservation [61], are involved. For a baryon of type B, the baryon chemical potential can be inferred from (4.5) to be given by

$$\mu^B \,=\, \mu^n \,-\, q^{\mathrm{el}}_B\, \mu^e\,. \tag{7.59}$$

Hence, only the knowledge of μ^n and μ^e is necessary for the determination of the baryon chemical potentials μ^B. The chemical potentials of the leptons (listed in table 6.1) obey

$$\mu^\mu = \mu^e \, . \tag{7.60}$$

The lepton energy–momentum relation (6.168) determines the lepton Fermi momenta,

$$k_{F_e} \, , \qquad k_{F_\mu} \, . \tag{7.61}$$

3) Equations (7.13), (7.25), (7.26), and (7.27) determine the baryon self-energies, $\mathbf{\Sigma}^B$, in case of the linear σ–ω field theory. The self-energies which arise from the exchange of π and ρ mesons among the baryons are listed in appendices C and D. The individual, non-vanishing self-energy contributions at the level of the HF approximation are

$$\mathbf{\Sigma}^{\mathrm{H},B}\Big|_{\sigma,\omega,\rho} \, , \qquad \mathbf{\Sigma}^{\mathrm{F},B}\Big|_{\sigma,\omega,\pi,\rho} \, , \tag{7.62}$$

which constitutes seven unknown functions.

4) The constraint of electric charge neutrality on neutron star matter, that is, $\rho^{\mathrm{el}}_{\mathrm{tot}} = \rho^{\mathrm{el}}_{\mathrm{Bary}} + \rho^{\mathrm{el}}_{\mathrm{Lep}} \equiv 0 + \rho^{\mathrm{el}}_{\mathrm{Mes}}$, leads to additional constraints on the Fermi momenta of the form

$$\sum_B q^{\mathrm{el}}_B (2J_B + 1) \frac{k^3_{F_B}}{6\pi^2} - \sum_{L=e,\mu} \frac{k^3_{F_L}}{3\pi^2} - \rho_M \Theta(\mu^M - m_M) = 0 \, , \tag{7.63}$$

where the last term accounts for the negative electric charges carried by condensed mesons of type M. As discussed in section 4.2, the only mesons that could plausibly condense in neutron star matter are the π^- [58, 61, 351, 368, 369, 370] or, alternatively, the currently more favored K^- [371, 372, 373]. Relation (7.63) follows readily from the total particle number densities of baryons and leptons, ρ and ρ^{Lep} respectively, given in equations (6.190) and (12.99).

In summary, the total number of unknowns encountered in either the relativistic Hartree or the relativistic HF treatment equals $(7 + b)$ and $(11 + b)$, respectively. Once these unknowns have been computed self-consistently from the matter equations compiled in items 1) through 4), the equation of state of the system can be computed via simple numerical integration techniques.

5) The total energy density, ϵ, at zero temperature follows from equation (12.44), or one of the relations derived from it, such as (12.53) and (12.54). The total pressure, P, follows from equation (12.63),

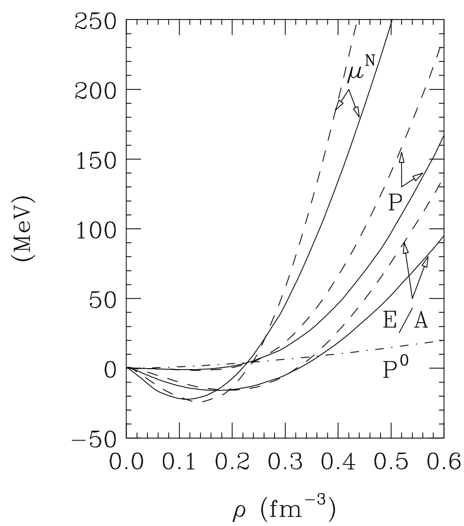

Figure 7.2. Energy per nucleon E/N, chemical nucleon potential μ^N, and pressure P of cold nuclear matter versus density, for Hartree parameter sets HI (dashed curves) and HII (solid curves) of table 7.2. The dot-dashed curve labeled P^0 shows the pressure of a free relativistic nucleon gas. (Reprinted courtesy of *Z. Phys.*)

or one of the relations derived from this expression, such as (12.65). Antiparticles make a contribution only at non-zero temperatures (section 12.2). Combining different ϵ values with their associated P values leads to the equation of state in the parametric form $P(\epsilon)$.

6) Equations (12.93) and (12.95) determine the total lepton energy density and lepton pressure, ϵ_{Lep} and P_{Lep}, respectively, which can be combined to the functional dependence $P_{\mathrm{Lep}}(\epsilon_{\mathrm{Lep}})$.

7.6 Properties of nuclear and neutron matter at zero and finite temperatures

In figure 7.2 we show the energy per nucleon, pressure and chemical potential computed for the relativistic Hartree approximation HI, Walecka's original parametrization of $\mathcal{L}$ in the scalar-vector approximation [92, 349]. Each quantity increases rather rapidly at higher density, that is, shows a rather stiff behavior, which is known to be a generic feature of the scalar-vector Lagrangian. Even the inclusion of π and ρ mesons does not change

Chapter 12

Models for the equation of state

We recall that the Lagrangian given in equation (5.1) depends on the spacetime coordinates x only through the fields and their gradients. Under the transformation $x'_\mu = x_\mu + \epsilon_\mu$ we have $\mathcal{L}' \equiv \mathcal{L}(x') \equiv \mathcal{L}[\chi(x'), \partial_\mu \chi(x')]$, and therefore

$$\delta\mathcal{L} = \mathcal{L}' - \mathcal{L} = \epsilon_\mu \, \partial^\mu \mathcal{L} \, . \tag{12.1}$$

Taylor expansion of $\delta\mathcal{L}$ gives

$$\delta\mathcal{L}(\chi, \partial^\mu \chi) = \frac{\partial \mathcal{L}}{\partial \chi} \, \delta\chi + \frac{\partial \mathcal{L}}{\partial(\partial^\mu \chi)} \, \delta(\partial^\mu \chi) \, , \tag{12.2}$$

with $\delta\chi = \chi(x+\epsilon) - \chi(x) = \epsilon_\mu \partial^\mu \chi$. Equations (12.1) and (12.2) can be combined to give

$$\epsilon_\mu \partial^\mu \mathcal{L} = \frac{\partial \mathcal{L}}{\partial \chi} \, \delta\chi + \frac{\partial \mathcal{L}}{\partial(\partial^\mu \chi)} \, \delta(\partial^\mu \chi) \, . \tag{12.3}$$

From (5.31) it is know that the variation of $\partial^\mu \chi$ obeys $\delta(\partial^\mu \chi) = \partial^\mu(\delta\chi)$. Hence, upon replacing $\partial\mathcal{L}/\partial\chi$ with the Euler–Lagrange equation $\partial\mathcal{L}/\partial\chi = \partial^\mu[\partial\mathcal{L}/\partial(\partial^\mu \chi)]$, we obtain from (12.3) the relation

$$\epsilon_\mu \partial^\mu \mathcal{L} = \partial^\mu \left(\frac{\partial \mathcal{L}}{\partial(\partial^\mu \chi)} \, \delta\chi \right) = \partial^\mu \left(\frac{\partial \mathcal{L}}{\partial(\partial^\mu \chi)} \, \epsilon_\nu \, \partial^\nu \chi \right) . \tag{12.4}$$

For arbitrary ϵ_μ is follows from (12.4) that

$$- \partial_\nu \mathcal{L} + \partial^\mu \Big(\frac{\partial \mathcal{L}}{\partial(\partial^\mu \chi)} \, \partial^\nu \chi \Big) = 0 \, , \tag{12.5}$$

which we write as

$$\partial^\mu \, T_{\mu\nu}(x) \; = \; 0 \, , \tag{12.6}$$

with the energy–momentum tensor defined as

$$T_{\mu\nu}(x) \equiv -\, g_{\mu\nu}\, \mathcal{L}(x) \;+\; \frac{\partial \mathcal{L}}{\partial(\partial^\mu \chi(x))}\, \partial_\nu \chi(x)\,. \tag{12.7}$$

In the case of neutron star matter the relevant matter fields are baryon, lepton and quark fields. For the baryon fields, for instance, equation (12.7) takes on the form

$$T_{\mu\nu}(x) \equiv -\, g_{\mu\nu}\, \mathcal{L}(x) + \sum_B \frac{\partial \mathcal{L}(x)}{\partial[\partial^\mu \psi_B(x)]}\, \partial_\nu \psi_B(x)\,. \tag{12.8}$$

Equation (12.6) constitutes a conservation law for $T_{\mu\nu}$, which follows from the invariance under spacetime transformations. The four quantities

$$P^\nu \equiv \int \mathrm{d}^3\boldsymbol{x}\, T^{0\nu}(\boldsymbol{x}, t)\,, \tag{12.9}$$

which correspond to total energy ($\nu = 0$) and three-momentum ($\nu = 1, 2, 3$), are time independent since

$$\dot{P}^\nu = \int \mathrm{d}^3\boldsymbol{x}\; \partial_0\, T^{0\nu}(\boldsymbol{x}, t) = -\int \mathrm{d}^3\boldsymbol{x} \sum_{i=1}^{3} \partial_i\, T^{i\nu}(\boldsymbol{x}, t) = 0\,, \tag{12.10}$$

provided that the fields vanish sufficiently rapidly for large arguments (that is, no energy or momentum escape at infinity). Finally we note that from (12.7),

$$T^{00} = -\mathcal{L} + \frac{\partial \mathcal{L}(x)}{\partial(\partial_0 \chi)}\, \partial^0 \chi\,. \tag{12.11}$$

Replacing $\partial\mathcal{L}/\partial(\partial_0\chi)$ with the associated conjugate field $\Pi(\boldsymbol{x}, t)$ gives

$$T^{00} = -\mathcal{L} + \Pi\, \dot{\chi} = \mathcal{H}(\boldsymbol{\pi}, \chi)\,, \tag{12.12}$$

where $\mathcal{H}$ denotes the Hamiltonian density. For the total energy density one thus obtains

$$\epsilon \equiv \, < \boldsymbol{\Phi}_0 | T^{00} | \boldsymbol{\Phi}_0 > \, = \, < \boldsymbol{\Phi}_0 | \mathcal{H} | \boldsymbol{\Phi}_0 > \,, \tag{12.13}$$

and for total pressure

$$\boldsymbol{P} = \int \mathrm{d}^3\boldsymbol{x}\; \psi_B^\dagger(x)\, (-\,\mathrm{i}\, \boldsymbol{\nabla})\, \psi_B(x)\,. \tag{12.14}$$

After these introductory remarks we turn to the main topic of this chapter, namely the calculation of the equation of state of neutron star matter described by the Lagrangian of (5.1). Because of $\partial\mathcal{L}/\partial(\partial^\mu\psi_B) = \mathrm{i}\bar{\psi}_B\gamma_\mu$ we obtain from (12.8)

$$\begin{aligned}T_{\mu\nu}(x) = &\sum_B \bar{\psi}_B(x)\,\big\{\mathrm{i}\,\gamma_\mu\partial_\nu - g_{\mu\nu}\big[\mathrm{i}\,\gamma^\lambda\partial_\lambda \,-\, m_B - g_{\sigma B}\,\sigma(x)\\ &- g_{\omega B}\,\gamma^\lambda\,\omega_\lambda(x)\big]\big\}\,\psi_B(x)\\ &- g_{\mu\nu}\Big\{-\frac{1}{2}\,\sigma(x)\,[\partial_\lambda\partial^\lambda \,+\, m_\sigma^2]\;\sigma(x) \,+\, \frac{1}{2}\,\partial_\lambda[\sigma(x)\partial^\lambda\sigma(x)] + \ldots\\ &- \frac{1}{2}\,\partial_\lambda[\omega_\kappa(x)\,F^{\lambda\kappa}(x)] \,+\, \frac{1}{2}\,\omega_\lambda(x)\,\big[\partial_\kappa F^{\kappa\lambda}(x) \,+\, m_\omega^2\,\omega^\lambda(x)\big]\Big\}\\ &+ g_{\mu\nu}\,\Big\{\frac{1}{3}\,b_N\,m_N\,[g_{\sigma N}\sigma(x)]^3 \,+\, \frac{1}{4}\,c_N\,[g_{\sigma N}\sigma(x)]^4\Big\}\,,\end{aligned} \tag{12.15}$$

where use of

$$\partial_\mu(\sigma\partial^\mu\sigma) = (\partial_\mu\sigma)\,(\partial^\mu\sigma) + \sigma\partial_\mu\partial^\mu\sigma \tag{12.16}$$

and

$$\partial_\mu(\omega_\nu\,F^{\mu\nu}) = \frac{1}{2}\,F_{\mu\nu}F^{\mu\nu} + \omega_\nu\partial_\mu F^{\mu\nu} \tag{12.17}$$

was made. For the sake of brevity, we have dropped in (12.15) the contributions that arise from π and ρ-meson exchange among the baryons. Below we shall see that it is rather straightforward to incorporate their contributions again. The divergences $\partial_\lambda[\sigma\partial^\lambda\sigma]$ and $\partial_\lambda[\omega_\kappa F^{\lambda\kappa}]$ in (12.15) can be discarded, since the diagonal matrix elements of a total divergence are zero. The remaining expressions are simplified by making use of the field equations for ψ_B, σ and ω_κ derived in (5.36), (5.43), and (5.52) respectively. One obtains

$$\begin{aligned}T_{\mu\nu}(x) = &\sum_B \Big\{\mathrm{i}\,\bar{\psi}_B(x)\gamma_\mu\partial_\nu\psi_B(x) - \frac{1}{2}\,g_{\mu\nu}\,g_{\sigma B}\,\bar{\psi}_B(x)\sigma(x)\psi_B(x)\\ &- \frac{1}{2}\,g_{\mu\nu}\,g_{\omega B}\,\bar{\psi}_B(x)\gamma^\kappa\omega_\kappa(x)\psi_B(x)\Big\} + \ldots\,.\end{aligned} \tag{12.18}$$

In the next step we shall replace the baryon field products with their associated two-point baryon Green functions, $\boldsymbol{g}_1^B$. Before however we need to make sure that the ordering of the field operators in (12.15) remains unchanged under the action of the time-ordering operator $\hat{T}$. This is readily accomplished by adding infinitesimal increments to the time arguments of the baryon field operators. We are then left with ($\partial_\nu = \partial/\partial x^\nu$)

$$\begin{aligned}T_{\mu\nu}(x) = &\sum_B \Big\{\mathrm{i}\lim_{x'\to x^+}\,\partial_\nu\,\hat{T}\big(\bar{\psi}_B(x')\gamma_\mu\psi_B(x)\big)\\ &- \frac{1}{2}\,g_{\mu\nu}\,g_{\sigma B}\,\hat{T}\big(\bar{\psi}_B(x^{++})\sigma(x)\psi_B(x^+)\big)\end{aligned}$$

$$- \frac{1}{2} g_{\mu\nu} \, g_{\omega B} \, \hat{T}\big(\bar{\psi}_B(x^{++}) \gamma^\mu \omega_\mu(x) \psi_B(x^+)\big) \Big\} \, . \quad (12.19)$$

The expectation value of $T_{\mu\nu}$ is then given by

$$\begin{aligned} < \mathbf{\Phi}_0 | T_{\mu\nu}(x) | \mathbf{\Phi}_0 > = \sum_B \Big\{ \mathrm{i} \lim_{x' \to x^+} \partial_\nu < \mathbf{\Phi}_0 | \hat{T}\big(\bar{\psi}_B(x') \gamma_\mu \psi_B(x)\big) | \mathbf{\Phi}_0 > \\ - \frac{1}{2} g_{\mu\nu} \, g_{\sigma B} < \mathbf{\Phi}_0 | \hat{T}\big(\bar{\psi}_B(x^{++}) \sigma(x) \psi_B(x^+)\big) | \mathbf{\Phi}_0 > \\ - \frac{1}{2} g_{\mu\nu} \, g_{\omega B} < \mathbf{\Phi}_0 | \hat{T}\big(\bar{\psi}_B(x^{++}) \gamma^\lambda \omega_\lambda(x) \psi_B(x^+)\big) | \mathbf{\Phi}_0 > \Big\} \, . \end{aligned} \quad (12.20)$$

Explicit expressions for the mesons fields $\sigma(x)$ and $\omega_\mu(x)$ were derived in equations (5.94) and (5.102). Substituting them into (12.20) gives

$$\begin{aligned} < \mathbf{\Phi}_0 | T_{\mu\nu}(x) | \mathbf{\Phi}_0 > = \sum_B \mathrm{i} \lim_{x' \to x^+} \partial_\nu < \mathbf{\Phi}_0 | \hat{T}\big(\bar{\psi}_B(x') \gamma_\mu \psi_B(x)\big) | \mathbf{\Phi}_0 > \\ + \frac{1}{2} g_{\mu\nu} \sum_{B,B'} g_{\sigma B} \, g_{\sigma B'} \int \mathrm{d}^4 x' \, \Delta^{0\sigma}(x, x') \\ \times < \mathbf{\Phi}_0 | \hat{T}\big(\bar{\psi}_B(x^{++}) \bar{\psi}_{B'}(x'^+) \psi_{B'}(x') \psi_B(x^+)\big) | \mathbf{\Phi}_0 > \\ - \frac{1}{2} g_{\mu\nu} \sum_{B,B'} g_{\omega B} \, g_{\omega B'} \int \mathrm{d}^4 x' \, \mathcal{D}^{0\omega}_{\lambda\kappa}(x, x') \\ \times < \mathbf{\Phi}_0 | \hat{T}\big(\bar{\psi}_B(x^{++}) \gamma^\lambda \bar{\psi}_{B'}(x'^+) \gamma^\kappa \psi_{B'}(x') \psi_B(x^+)\big) | \mathbf{\Phi}_0 > \, . \end{aligned} \quad (12.21)$$

12.1 Equation of state in relativistic Hartree and Hartree–Fock approximation

With the technique developed in section 5.3 (cf. discussion of figure 5.1) the latter two expectation values in (12.21) can be replaced with four-point baryon Green functions, $\boldsymbol{g}_2$. From (5.62) one reads off that

$$\begin{aligned} < \mathbf{\Phi}_0 | \hat{T}\big(\bar{\psi}_B(x^{++}) \bar{\psi}_{B'}(x'^+) \psi_{B'}(x') \psi_B(x^+)\big) | \mathbf{\Phi}_0 > \\ = - \boldsymbol{g}_2(x^+ B, x' B'; x'^+ B', x^{++} B) \, , \end{aligned} \quad (12.22)$$

while the first expectation value in (12.21) can be written in terms of the two-point baryon Green function,

$$\lim_{x' \to x^+} \boldsymbol{g}^B(x, x') = - \mathrm{i} < \mathbf{\Phi}_0 | \hat{T}\big(\bar{\psi}_B(x') \psi_B(x)\big) | \mathbf{\Phi}_0 > \, . \quad (12.23)$$

Upon substituting (12.22) and (12.23) into (12.21) and recalling the matrix structure $\bar{\psi}(x') \gamma_\mu \psi(x') \equiv \bar{\psi}_{\zeta'}(x') (\gamma_\mu)_{\zeta'\zeta} \psi_\zeta(x') = (\gamma_\mu)_{\zeta'\zeta} \bar{\psi}_{\zeta'}(x') \psi_\zeta(x')$, one gets

$$< \boldsymbol{\Phi}_0 | T_{\mu\nu}(x) | \boldsymbol{\Phi}_0 > = - \lim_{x' \to x^+} \sum_B \partial_\nu \left(\gamma_\mu\right)_{\zeta'\zeta} \boldsymbol{g}^B_{\zeta\zeta'}(x, x') - \frac{1}{2} g_{\mu\nu}$$

$$\sum_{BB'} \int \mathrm{d}^4 x' \left\{ g_{\sigma B}\, g_{\sigma B'}\, \Delta^{0\sigma}(x, x') - g_{\omega B}\, g_{\omega B'} \left(\gamma^\lambda\right)_{\zeta''\bar{\zeta}} \mathcal{D}^{0\omega}_{\lambda\kappa}(x, x') \left(\gamma^\kappa\right)_{\zeta'\bar{\zeta}'} \right\}$$

$$\times\, \boldsymbol{g}_2(x^+ B \bar{\zeta}, x' B' \bar{\zeta}'; x'^+ B' \zeta', x^{++} B \zeta'') \,. \tag{12.24}$$

In the next step we replace $\boldsymbol{g}_2$ with its HF approximated counterpart, which amounts to replace $\boldsymbol{g}_2$ with an antisymmetrized product of $\boldsymbol{g}_1$ functions, as given in equations (5.118) and (5.119). We then arrive for (12.24) at the expression

$$< \boldsymbol{\Phi}_0 | T_{\mu\nu}(x) | \boldsymbol{\Phi}_0 > = - \lim_{x' \to x^+} \sum_B \partial_\nu \left(\gamma_\mu\right)_{\zeta'\zeta} \boldsymbol{g}^B_{\zeta\zeta'}(x, x')) - \frac{1}{2} g_{\mu\nu}$$

$$\sum_{BB'} \int \mathrm{d}^4 x' \left\{ g_{\sigma B}\, g_{\sigma B'}\, \Delta^{0\sigma}(x, x') - g_{\omega B}\, g_{\omega B'} \left(\gamma^\lambda\right)_{\zeta''\bar{\zeta}} \mathcal{D}^{0\omega}_{\lambda\kappa}(x, x') \left(\gamma^\kappa\right)_{\zeta'\bar{\zeta}'} \right\}$$

$$\times \left\{ \boldsymbol{g}^B_{\bar{\zeta}\zeta''}(x^+, x^{++})\, \boldsymbol{g}^{B'}_{\bar{\zeta}'\zeta'}(x', x'^+) - \delta_{BB'}\, \boldsymbol{g}^B_{\bar{\zeta}\zeta'}(x^+, x'^+)\, \boldsymbol{g}^B_{\bar{\zeta}'\zeta''}(x', x^{++}) \right\} , \tag{12.25}$$

which reads in four-momentum space [cf. equations (B.23) and (B.24)]

$$< \boldsymbol{\Phi}_0 | T_{\mu\nu}(x) | \boldsymbol{\Phi}_0 > = - \lim_{x' \to x^+} \sum_B \partial_\nu \int \frac{\mathrm{d}^4 p}{(2\pi)^4}\, \mathrm{e}^{-\mathrm{i}p(x-x')} \left(\gamma_\mu\right)_{\zeta'\zeta} \boldsymbol{g}^B_{\zeta\zeta'}(p)$$

$$- \frac{1}{2} g_{\mu\nu} \sum_{BB'} \int \frac{\mathrm{d}^4 p}{(2\pi)^4} \int \frac{\mathrm{d}^4 q}{(2\pi)^4}\, \mathrm{e}^{\mathrm{i}\eta(p^0+q^0)} \Big\{ \big[g_{\sigma B}\, g_{\sigma B'}\, \Delta^{0\sigma}(0) - g_{\omega B}\, g_{\omega B'}$$

$$\left(\gamma^\lambda\right)_{\zeta''\bar{\zeta}} \mathcal{D}^{0\omega}_{\lambda\kappa}(0) \left(\gamma^\kappa\right)_{\zeta'\bar{\zeta}'} \big]\, \boldsymbol{g}^{B'}_{\bar{\zeta}'\zeta'}(q)\, \boldsymbol{g}^B_{\bar{\zeta}\zeta''}(p) - \delta_{BB'} \big[g^2_{\sigma B}\, \Delta^{0\sigma}(p-q) - g^2_{\omega B}$$

$$\left(\gamma^\lambda\right)_{\zeta''\bar{\zeta}} \mathcal{D}^{0\omega}_{\lambda\kappa}(0) \left(\gamma^\kappa\right)_{\zeta'\bar{\zeta}'} \big]\, \boldsymbol{g}^{B'}_{\bar{\zeta}\zeta'}(q)\, \boldsymbol{g}^B_{\bar{\zeta}'\zeta''}(p) \Big\} \,. \tag{12.26}$$

A comparison of (12.26) with the expression of the HF self-energy,

$$\begin{aligned} \boldsymbol{\Sigma}^B_{\zeta''\bar{\zeta}}(p) = & - \mathrm{i} \sum_{B'} \int \frac{\mathrm{d}^4 q}{(2\pi)^4}\, \mathrm{e}^{\mathrm{i}\eta q^0} \big\{ g_{\sigma B}\, g_{\sigma B'}\, \Delta^{0\sigma}(0) \\ & \qquad - g_{\omega B}\, g_{\omega B'} \left(\gamma^\lambda\right)_{\zeta''\bar{\zeta}} \mathcal{D}^{0\omega}_{\lambda\kappa}(0) \left(\gamma^\kappa\right)_{\zeta'\bar{\zeta}'} \big\}\, \boldsymbol{g}^{B'}_{\bar{\zeta}'\zeta'}(q) \\ & + \mathrm{i} \int \frac{\mathrm{d}^4 q}{(2\pi)^4}\, \mathrm{e}^{\mathrm{i}\eta q^0} \big\{ g^2_{\sigma B}\, \Delta^{0\sigma}(p-q) \\ & \qquad - g^2_{\omega B} \left(\gamma^\lambda\right)_{\zeta''\bar{\zeta}} \mathcal{D}^{0\omega}_{\lambda\kappa}(p-q) \left(\gamma^\kappa\right)_{\zeta'\bar{\zeta}'} \big\}\, \boldsymbol{g}^{B'}_{\bar{\zeta}\zeta'}(q) \\ & + \ \ldots \end{aligned} \tag{12.27}$$

derived in equation (5.124), reveals that (12.26) can be expressed in terms of the baryon self-energy in the following manner,

$$< \boldsymbol{\Phi}_0 | T_{\mu\nu}(x) | \boldsymbol{\Phi}_0 > = - \lim_{x' \to x^+} \sum_B \partial_\nu \int \frac{\mathrm{d}^4 p}{(2\pi)^4} \, \mathrm{e}^{-\mathrm{i}p(x-x')} \, \mathrm{Tr}\left(\gamma_\mu \, \boldsymbol{g}^B(p)\right) - \frac{\mathrm{i}}{2} \, g_{\mu\nu} \sum_B \int \frac{\mathrm{d}^4 p}{(2\pi)^4} \, \mathrm{e}^{\mathrm{i}\eta p^0} \, \mathrm{Tr}\left(\boldsymbol{\Sigma}^B(p) \, \boldsymbol{g}^B(p)\right) . \qquad (12.28)$$

The traces sum spin and isospin matrix indices, as illustrated in equation (5.129). Since the system's total energy density is given by $\epsilon = < \boldsymbol{\Phi}_0 | T_{00} | \boldsymbol{\Phi}_0 >$, according to equation (12.13), we read off from (12.28) that

$$\epsilon = - \sum_B \lim_{x' \to x^+} \partial_0 \int \frac{\mathrm{d}^4 p}{(2\pi)^4} \, \mathrm{e}^{-\mathrm{i}p(x-x')} \, (\gamma_0)_{\zeta\zeta'} \, \boldsymbol{g}^B_{\zeta'\zeta}(p) - \frac{\mathrm{i}}{2} \sum_B \int \frac{\mathrm{d}^4 p}{(2\pi)^4} \, \mathrm{e}^{\mathrm{i}\eta p^0} \, \boldsymbol{\Sigma}^B_{\zeta\zeta'}(p) \, \boldsymbol{g}^B_{\zeta'\zeta}(p) \, . \qquad (12.29)$$

Performing the differentiation with respect to the time coordinate x_0 in the first term simply gives a factor of $-\mathrm{i}p^0$. Moreover, the summations over the spin-isospin indices in both terms of (12.29) can be written as traces, as described in section 5.4, which leaves us with

$$\epsilon = \mathrm{i} \sum_B \int \frac{\mathrm{d}^4 p}{(2\pi)^4} \, \mathrm{Tr}\left\{ \mathrm{e}^{-\mathrm{i}p(x-x')} \, p^0 \, \gamma_0 \, \boldsymbol{g}^B(p) - \frac{1}{2} \, \mathrm{e}^{\mathrm{i}\eta p^0} \, \boldsymbol{\Sigma}^B(p) \, \boldsymbol{g}^B(p) \right\} . \qquad (12.30)$$

Lastly, we replace $\boldsymbol{g}^B(p)$ with its spectral representation given in (6.71) and perform the integration over the energy variable p^0 analytically. Details are outlined in appendix B. Restricting ourselves to the zero-temperature case for the moment (the extension to finite temperatures will be discussed in section 12.2), which implies closing the integration path in the upper half of the complex energy plane (cf. figure D.1), the result for the energy density then reads

$$\epsilon = \sum_B \int \frac{\mathrm{d}^3 \boldsymbol{p}}{(2\pi)^3} \, \mathrm{Tr}\left\{ \left(\gamma_0 \, \boldsymbol{\Xi}^B(p)\right) \omega^B(\boldsymbol{p}) - \frac{1}{2} \, \boldsymbol{\Sigma}^B(p) \, \boldsymbol{\Xi}^B(p) \right\} \Theta(p_{F_B} - |\boldsymbol{p}|) \, . \qquad (12.31)$$

Note from (12.31) that the two-point baryon Green function $\boldsymbol{g}^B_1$ needs not to be determined explicitly when ϵ is being calculated. The quantity that needs to be determined instead is the baryon spectral function $\boldsymbol{\Xi}^B$ associated with $\boldsymbol{g}_1^B$, which is considerably easier to accomplish than calculating $\boldsymbol{g}_1$ itself. We recall that this feature holds not only for ϵ but all the other properties of the many-body system too. After this parenthetical remark, let us turn to the traces in (12.31). These are to be evaluated with respect to the spin-isospin indices carried by the γ matrices and $\boldsymbol{\Xi}^B$. Proceeding as in section 7.1, one obtains

$$\begin{aligned}\mathrm{Tr}\,(\gamma^0\,\boldsymbol{\Xi}^B) =&\ \mathrm{Tr}\left\{\gamma^0\otimes\left(\mathbf{1}\,\Xi_S^B+\boldsymbol{\gamma}\cdot\hat{\boldsymbol{p}}\,\Xi_V^B+\gamma^0\,\Xi_0^B\right)\right\}\\ =&\ \mathrm{Tr}\,(\gamma^0\otimes\mathbf{1}^{\mathrm{iso}})\,\Xi_S^B+\mathrm{Tr}\,(\gamma^0\,\boldsymbol{\gamma}\cdot\hat{\boldsymbol{p}}\otimes\mathbf{1}^{\mathrm{iso}})\,\Xi_V^B\\ &+\mathrm{Tr}\,(\mathbf{1}^{\mathrm{Dirac}}\otimes\mathbf{1}^{\mathrm{iso}})\,\Xi_0^B=2\,\nu_B\,\Xi_0^B\,,\end{aligned}\tag{12.32}$$

since for the traces (cf. appendix A.3)

$$\mathrm{Tr}\,(\gamma^0\otimes\mathbf{1}^{\mathrm{iso}})=\mathrm{Tr}\,(\gamma^0)\ \ \mathrm{Tr}\,(\mathbf{1}^{\mathrm{iso}})=0\,,\tag{12.33}$$

$$\mathrm{Tr}\,(\gamma^0\,\boldsymbol{\gamma}\cdot\hat{\boldsymbol{p}}\otimes\mathbf{1}^{\mathrm{iso}})=\mathrm{Tr}\,(\gamma^0\,\boldsymbol{\gamma}\cdot\hat{\boldsymbol{p}})\ \ \mathrm{Tr}\,(\mathbf{1}^{\mathrm{iso}})=0\,,\tag{12.34}$$

and

$$\mathrm{Tr}\,(\mathbf{1}\otimes\mathbf{1}^{\mathrm{iso}})=\mathrm{Tr}\,(\mathbf{1})\ \ \mathrm{Tr}\,(\mathbf{1}^{\mathrm{iso}})=2\,(2J_B+1)(2I_B+1)\equiv 2\,\nu_B\,.\tag{12.35}$$

Similarly, one calculates for the trace of the second term in (12.31)

$$\begin{aligned}\mathrm{Tr}\,(\boldsymbol{\Xi}^B\ \boldsymbol{\Sigma}^B) =&\ \mathrm{Tr}\left\{\left(\mathbf{1}\,\Xi_S^B+\boldsymbol{\gamma}\cdot\hat{\boldsymbol{p}}\,\Xi_V^B+\gamma^0\,\Xi_0^B\right)\left(\mathbf{1}\,\Sigma_S^B+\boldsymbol{\gamma}\cdot\hat{\boldsymbol{p}}\,\Sigma_V^B+\gamma^0\,\Sigma_0^B\right)\right\}\\ =&\ 2\,\nu_B\left\{\Sigma_S^B\,\Xi_S^B-\Sigma_V^B\,\Xi_V^B+\Sigma_0^B\,\Xi_0^B\right\},\end{aligned}\tag{12.36}$$

where we have made use of

$$\begin{aligned}\mathrm{Tr}\left((\boldsymbol{\gamma}\cdot\hat{\boldsymbol{p}})\,(\boldsymbol{\gamma}\cdot\hat{\boldsymbol{p}})\right) =&\ \mathrm{Tr}\ \hat{p}^i\,\hat{p}^j\ \gamma^i\gamma^j\\ =&\ 2\ \mathrm{Tr}\ \hat{p}^i\,\hat{p}^j\ g^{ij}\,\mathbf{1}-\mathrm{Tr}\ \hat{p}^i\,\hat{p}^j\ \gamma^j\gamma^i\,,\end{aligned}\tag{12.37}$$

$$2\ \mathrm{Tr}\left((\boldsymbol{\gamma}\cdot\hat{\boldsymbol{p}})\,(\boldsymbol{\gamma}\cdot\hat{\boldsymbol{p}})\right)=-2\,\hat{\boldsymbol{p}}\,\hat{\boldsymbol{p}}\ \mathrm{Tr}\ \mathbf{1}\,,\tag{12.38}$$

$$\mathrm{Tr}\,(\boldsymbol{\gamma}\cdot\hat{\boldsymbol{p}})^2=-\,4\,\hat{\boldsymbol{p}}^2=-\,4\,,\tag{12.39}$$

and

$$\mathrm{Tr}\left((\boldsymbol{\gamma}\cdot\hat{\boldsymbol{p}})^2\otimes\mathbf{1}^{\mathrm{iso}}\right)=-2\,\nu_B\,.\tag{12.40}$$

Substituting (12.32) and (12.36) in (12.31) gives for the energy density

$$\begin{aligned}\epsilon =&\ 2\sum_B\nu_B\int\frac{\mathrm{d}^3\boldsymbol{p}}{(2\pi)^3}\,\omega^B(\boldsymbol{p})\,\Xi_0^B(\boldsymbol{p})\,\Theta(p_{F_B}-|\boldsymbol{p}|)\\ &-\sum_B\nu_B\int\frac{\mathrm{d}^3\boldsymbol{p}}{(2\pi)^3}\left\{\Sigma_S^B(\omega^B(\boldsymbol{p}),\boldsymbol{p})\,\Xi_S^B(\boldsymbol{p})-\Sigma_V^B(\omega^B(\boldsymbol{p}),\boldsymbol{p})\,\Xi_V^B(\boldsymbol{p})\right.\\ &\left.+\,\Sigma_0^B(\omega^B(\boldsymbol{p}),\boldsymbol{p})\,\Xi_0^B(\boldsymbol{p})\right\}\Theta(p_{F_B}-|\boldsymbol{p}|)\,.\end{aligned}\tag{12.41}$$

Alternatively, we may substitute the expression for the single-particle energy ω^B, derived in (6.149), into the first term of (12.41). Adopting $\Xi_0^B = \frac{1}{2}$ for the HF approximation [cf. (6.145)], one finds

$$\begin{aligned}\omega^B\,\Xi_0^B &= \Sigma_0^B\,\Xi_0^B + \frac{1}{2}\sqrt{(m_B^*)^2 + (p_B^*)^2} \\ &= \Sigma_0^B\,\Xi_0^B + \frac{(m_B^*)^2}{2\sqrt{(m_B^*)^2 + (p_B^*)^2}} + \frac{(p_B^*)^2}{2\sqrt{(m_B^*)^2 + (p_B^*)^2}}\,. \end{aligned} \tag{12.42}$$

A comparison of (12.42) with the spectral functions in HF approximation, given in equations (6.143) through (6.145), reveals that

$$\omega^B\,\Xi_0^B = m_B^*\,\Xi_S^B - p_B^*\,\Xi_V^B + \Sigma_0^B\,\Xi_0^B\,. \tag{12.43}$$

Substituting (12.43) into (12.41) and rearranging terms then gives

$$\begin{aligned}\epsilon = {} & 2\sum_B \nu_B \int \frac{\mathrm{d}^3\boldsymbol{p}}{(2\pi)^3}\,\left\{m_B\,\Xi_S^B(\boldsymbol{p}) - |\boldsymbol{p}|\,\Xi_V^B(\boldsymbol{p})\right\}\Theta(p_{F_B} - |\boldsymbol{p}|) \\ & + \sum_B \nu_B \int \frac{\mathrm{d}^3\boldsymbol{p}}{(2\pi)^3}\,\left\{\Sigma_S^B(\omega^B(\boldsymbol{p}),\boldsymbol{p})\,\Xi_S^B(\boldsymbol{p}) - \Sigma_V^B(\omega^B(\boldsymbol{p}),\boldsymbol{p})\,\Xi_V^B(\boldsymbol{p}) \right. \\ & \left. + \Sigma_0^B(\omega^B(\boldsymbol{p}),\boldsymbol{p})\,\Xi_0^B(\boldsymbol{p})\right\}\Theta(p_{F_B} - |\boldsymbol{p}|)\,. \end{aligned} \tag{12.44}$$

The contribution of the cubic and quartic terms of the σ-meson field in (12.15) to the total energy density follow as

$$\epsilon^{(\sigma^4)} = \frac{1}{2}\left\{\frac{1}{3}\,b_N\,m_N\,\left(\Sigma_S^{\mathrm{H},N}\right)^3 - \frac{1}{2}\,c_N\,\left(\Sigma_S^{\mathrm{H},N}\right)^4\right\}. \tag{12.45}$$

As we shall see in the second part of this book (see, for instance, chapter 13), knowledge of the total energy density is necessary when solving Einstein's field equations of general relativity, since it is the total energy density (besides other quantities like pressure) which enters in the source term of Einstein's field equations. The energy per baryon, measured relative to the particle masses, is obtained from the total energy density ϵ as

$$\frac{E}{A} = \frac{1}{\rho}\left\{\epsilon - \sum_B m_B\,\rho^B\right\}, \tag{12.46}$$

where ρ^B are the partial particle densities that were calculated in equations (6.187) and (6.186).

In the non-relativistic limit we have $\Sigma_S^B \to 0$ and $\Sigma_V^B \to 0$. Hence the single-particle energy takes on the familiar form

$$\sqrt{m_B^2 + \boldsymbol{p}^2} \approx m_B\left(1 + \frac{\boldsymbol{p}^2}{2\,m_B}\right). \tag{12.47}$$

Substituting (12.47) into (12.41) gives for the non-relativistic limit of the energy density (for more details, see section 12.5)

$$\epsilon = \sum_B \nu_B \int \frac{\mathrm{d}^3\boldsymbol{p}}{(2\pi)^3} \left\{ m_B + \frac{\boldsymbol{p}^2}{2\,m_B} + \frac{1}{2}\,\Sigma_0^B(\omega^B(\boldsymbol{p}) - \mu^B, \boldsymbol{p}) \right\} \Theta^B(\boldsymbol{p})\,, \tag{12.48}$$

where $\Theta(\boldsymbol{p}) \equiv \Theta(p_{F_B} - |\boldsymbol{p}|)$. The non-relativistic expression for the energy per baryon thus reads

$$\frac{E}{A} = \frac{1}{\rho} \sum_B \nu_B \int \frac{\mathrm{d}^3\boldsymbol{p}}{(2\pi)^3} \left\{ \frac{\boldsymbol{p}^2}{2\,m_B} + \frac{1}{2}\,\Sigma_0^B(\omega^B(\boldsymbol{p}) - \mu^B, \boldsymbol{p}) \right\} \Theta^B(\boldsymbol{p})\,. \tag{12.49}$$

The expression of the total energy density (12.41) can be brought into a more transparent form if the many-body system is studied in the relativistic Hartree approximation, as will be done next. For this purpose we replace both ω^B and the spectral functions Ξ_S^B, $\Xi_V^B = 0$ and Ξ_0^B by their Hartree approximated relations, given in (7.32) and (7.30) respectively. One readily finds (note that $\Sigma_V^B = 0$ for this approximation)

$$\begin{aligned} \epsilon^{\,\mathrm{H}} = 2 \sum_B \nu_B \int \frac{\mathrm{d}^3\boldsymbol{p}}{(2\pi)^3} & \left\{ \frac{1}{2}\Big(\Sigma_0^{\mathrm{H},B} + \sqrt{(m_B^*)^2 + \boldsymbol{p}^2} \Big) \right. \\ & \left. - \left[\frac{\Sigma_S^{\mathrm{H},B}\; m_B^*}{2\sqrt{(m_B^*)^2 + \boldsymbol{p}^2}} + \frac{1}{2}\Sigma_0^B \right] \right\} \Theta(p_{F_B} - |\boldsymbol{p}|)\,. \end{aligned} \tag{12.50}$$

Making use of the circumstance that the self-energies, and thus the effective baryon masses, are momentum independent for the relativistic Hartree approximation, we arrive for (12.50) at

$$\begin{aligned} \epsilon^{\,\mathrm{H}} = & \frac{1}{2} \sum_B \left(\Sigma_0^{\mathrm{H},B}\, \rho^B \right) - \frac{1}{2} \sum_B \left(\Sigma_S^{\mathrm{H},B}\, \bar{\rho}^B \right) \\ & + \sum_B \nu_B \int \frac{\mathrm{d}^3\boldsymbol{p}}{(2\pi)^3} \sqrt{(m_B^*)^2 + \boldsymbol{p}^2}\; \Theta(p_{F_B} - |\boldsymbol{p}|)\,. \end{aligned} \tag{12.51}$$

The quantities ρ and $\bar{\rho}$ denote baryon number density and scalar density, respectively, defined in equations (6.186) and (6.201). Finally after some straightforward algebraic manipulations (see appendix B.3), equation (12.51) can be brought into the alternative form

$$\begin{aligned} \epsilon^{\,\mathrm{H}} = \sum_B & \left\{ \frac{\nu_B}{12\,\pi^2}\, p_{F_B}^3\; \Sigma_0^{\mathrm{H},B} + \frac{\nu_B}{8\,\pi^2} \left((m_B^*)^2 + m_B\, m_B^* \right) \right. \\ & \times \left(p_{F_B}\, \epsilon_F^{\mathrm{H},B} - (m_B^*)^2\, \ln \left| \frac{p_{F_B} + \epsilon_F^{\mathrm{H},B}}{m_B^*} \right| \right) + \frac{\nu_B}{8\,\pi^2} \end{aligned} \tag{12.52}$$

$$\times \Big(p_{F_B}\, (\epsilon_F^{\mathrm{H},B})^3 - \frac{5}{2}\, (m_B^*)^2\, p_{F_B}\, \epsilon_F^{\mathrm{H},B} + \frac{3}{2}\, (m_B^*)^4\, \ln \Big| \frac{p_{F_B} + \epsilon_F^{\mathrm{H},B}}{m_B^*} \Big| \Big) \Big\}\,,$$

where $\epsilon_F^{\mathrm{H},B} \equiv \epsilon^{\mathrm{H},B}(p_{F_B})$, with $\epsilon^{\mathrm{H},B}$ defined in (7.31).

As a final point, we derive from (12.41) the energy density of asymmetric *neutron star matter* at zero temperature. It is illustrative to split up the result into the Hartree, ϵ^{H}, and Fock, ϵ^{F}, contribution [79]. One then finds for the Hartree density

$$\begin{aligned}
\epsilon^{\mathrm{H}} &= \frac{1}{2} \sum_B \big(\Sigma_0^{\mathrm{H},B} + I_{3B}\, \Sigma_{03}^{\mathrm{H},B} \big)\, \rho^{\mathrm{H},B} - \frac{1}{2} \sum_B \big(\Sigma_S^{\mathrm{H},B}\, \bar\rho^{\mathrm{H},B} \big) \\
&+ \frac{1}{2\pi^2} \sum_B (2J_B + 1) \int_0^{p_{F_B}} \mathrm{d}p\, \boldsymbol{p}^2 \sqrt{ \big(m_B + \Sigma_S^{\mathrm{H},B} \big)^2 + \boldsymbol{p}^2 } \\
&- \frac{1}{2} \Big\{ -\frac{1}{3}\, b_N\, m_N \big(\Sigma_S^{\mathrm{H},N} \big)^3 + \frac{1}{2}\, c_N\, \big(\Sigma_S^{\mathrm{H},N} \big)^4 \Big\} \\
&+ \frac{1}{2\pi^2} \sum_{L=e,\mu} (2J_L + 1) \int_0^{p_{F_B}} \mathrm{d}p\, \boldsymbol{p}^2\, \sqrt{ m_L^2 + \boldsymbol{p}^2 }\,. \qquad (12.53)
\end{aligned}$$

This result agrees, as it must be the case, with the energy density of Walecka's mean-field theory [61]. The Fock density is given by

$$\begin{aligned}
\epsilon^{\mathrm{F}} = \sum_B (2J_B + 1) \int \frac{\mathrm{d}^3\boldsymbol{p}}{(2\pi)^3} \big\{ &\boldsymbol{\Sigma}_S^{\mathrm{F},B}(\boldsymbol{p})\, \Xi_S^{\mathrm{H},B}(\boldsymbol{p}) - \boldsymbol{\Sigma}_V^{\mathrm{F},B}(\boldsymbol{p})\, \Xi_V^{\mathrm{H},B}(\boldsymbol{p}) \\
&+ \boldsymbol{\Sigma}_0^{\mathrm{F},B}(\boldsymbol{p})\, \Xi_0^{\mathrm{H},B}(\boldsymbol{p}) \big\}\, \Theta^B(\boldsymbol{p})\,. \qquad (12.54)
\end{aligned}$$

To calculate the system's pressure, we proceed in analogy to the calculation of the total energy density. The starting point is again the expression for the energy–momentum tensor derived in (12.28), whose diagonal elements T_{jj} specify the pressure P according to the relation [cf. (14.13)]

$$P = \frac{1}{3} \sum_{j=1}^{3}\ < \boldsymbol{\Phi}_0 | T_{jj} | \boldsymbol{\Phi}_0 >\ . \qquad (12.55)$$

Substituting T_{jj} of (12.28) into (12.55) leads to [$g_{ii} = -1$ according to (A.2)]

$$P = -\frac{1}{3} \sum_{j=1}^{3} \Big\{ \lim_{x' \to x^+}\ \partial_j \sum_B \int \frac{\mathrm{d}^4p}{(2\pi)^4}\, \mathrm{e}^{-\mathrm{i}p(x-x')}\, (\gamma_j)_{\zeta\zeta'}\, \boldsymbol{g}^B_{\zeta'\zeta}(p)$$

$$+\frac{\mathrm{i}}{2}\sum_B \int \frac{\mathrm{d}^4 p}{(2\pi)^4}\, \mathrm{e}^{\mathrm{i}\eta p^0}\, \boldsymbol{\Sigma}^B_{\zeta\zeta'}(p)\, \boldsymbol{g}^B_{\zeta'\zeta}(p) \Big\} . \qquad (12.56)$$

Since for the derivative operator $\partial_j = -\mathrm{i}p_j$, and $\lim_{x'\to x^+} \mathrm{e}^{-\mathrm{i}p(x-x')} = \mathrm{e}^{\mathrm{i}\eta p^0}$, equation (12.56) transforms into

$$P = \mathrm{i}\sum_B \int \frac{\mathrm{d}^4 p}{(2\pi)^4}\, \mathrm{e}^{\mathrm{i}\eta p^0} \left\{ \frac{1}{3}\,(\boldsymbol{\gamma}\cdot\boldsymbol{p})_{\zeta\zeta'} + \frac{1}{2}\,\boldsymbol{\Sigma}^B_{\zeta\zeta'}(p)\right\} \boldsymbol{g}^B_{\zeta'\zeta}(p) \,. \quad (12.57)$$

The integrals over p^0 can be evaluated via contour integration, as outlined in appendix B.1, which results essentially in Θ-functions. Making use of the expressions (B.9) and (B.19), equation (12.57) can be written as

$$P = \sum_B \int \frac{\mathrm{d}^3 \boldsymbol{p}}{(2\pi)^3}\ \mathrm{Tr}\left\{ \frac{1}{3}\,\boldsymbol{\gamma}\cdot\boldsymbol{p}\ \boldsymbol{\Xi}^B(\boldsymbol{p}) + \frac{1}{2}\,\boldsymbol{\Sigma}^B(\omega^B(\boldsymbol{p}),\boldsymbol{p})\ \boldsymbol{\Xi}^B(\boldsymbol{p})\right\} \Theta^B(\boldsymbol{p}) \,. \qquad (12.58)$$

The traces of the first term in (12.58) lead to

$$\begin{aligned} &\mathrm{Tr}\left\{\boldsymbol{\gamma}\cdot\boldsymbol{p}\ \big(\mathbf{1}\ \Xi_S + \boldsymbol{\gamma}\cdot\hat{\boldsymbol{p}}\ \Xi_V + \gamma^0\ \Xi_0\big)\otimes \mathbf{1}^{\mathrm{iso}}\right\} \\ &\qquad\qquad = \mathrm{Tr}\,(\boldsymbol{\gamma}\cdot\boldsymbol{p}\ \boldsymbol{\gamma}\cdot\hat{\boldsymbol{p}}\ \Xi_V)\ \ \mathrm{Tr}\,(\mathbf{1}^{\mathrm{iso}}) \,, \end{aligned} \qquad (12.59)$$

where

$$\begin{aligned} \mathrm{Tr}\,(\boldsymbol{\gamma}\cdot\boldsymbol{p}\ \boldsymbol{\gamma}\cdot\hat{\boldsymbol{p}}\ \Xi_V) &= -4\,p^j\hat{p}^j\ \Xi_V = -4\,|\boldsymbol{p}|\ \Xi_V \\ &= -2\,(2J_B+1)\,|\boldsymbol{p}| \,. \end{aligned} \qquad (12.60)$$

Hence one gets for (12.59) the relation

$$\mathrm{Tr}\left\{\boldsymbol{\gamma}\cdot\boldsymbol{p}\ (\mathbf{1}\ \Xi_S + \boldsymbol{\gamma}\cdot\hat{\boldsymbol{p}}\ \Xi_V + \gamma^0\ \Xi_0)\otimes \mathbf{1}^{\mathrm{iso}}\right\} = -2\,\nu_B\,|\boldsymbol{p}|\ \Xi_V \,. \quad (12.61)$$

The trace of the second term in (12.58) has already been calculated in (12.36). Substituting both results in (12.58) then leads to the expression

$$\begin{aligned} P = &-\frac{2}{3}\sum_B \nu_B \int \frac{\mathrm{d}^3 \boldsymbol{p}}{(2\pi)^3}\ |\boldsymbol{p}|\,\Xi^B_V(\boldsymbol{p})\,\Theta(p_{F_B} - |\boldsymbol{p}|) \\ &+ \sum_B \nu_B \int \frac{\mathrm{d}^3 \boldsymbol{p}}{(2\pi)^3}\ \big\{\Sigma^B_S(\omega^B(\boldsymbol{p}),\boldsymbol{p})\,\Xi^B_S(\boldsymbol{p}) - \Sigma^B_V(\omega^B(\boldsymbol{p}),\boldsymbol{p})\,\Xi^B_V(\boldsymbol{p}) \\ &\qquad + \Sigma^B_0(\omega^B(\boldsymbol{p}),\boldsymbol{p})\,\Xi^B_0(\boldsymbol{p})\big\}\,\Theta(p_{F_B} - |\boldsymbol{p}|) \,. \end{aligned} \qquad (12.62)$$

Alternatively, (12.62) may be written in the following manner,

$$\begin{aligned} P = \sum_B \nu_B \int \frac{\mathrm{d}^3 \boldsymbol{p}}{(2\pi)^3} &\Big\{\Sigma^B_S(\omega^B(\boldsymbol{p}),\boldsymbol{p})\ \Xi^B_S(\boldsymbol{p}) - \big[\Sigma^B_V(\omega^B(\boldsymbol{p}),\boldsymbol{p}) + \frac{2}{3}\,|\boldsymbol{p}|\big] \\ &\times\ \Xi^B_V(\boldsymbol{p}) + \Sigma^B_0(\omega^B(\boldsymbol{p}),\boldsymbol{p})\ \Xi^B_0(\boldsymbol{p})\Big\}\,\Theta(p_{F_B} - |\boldsymbol{p}|) \,. \end{aligned} \qquad (12.63)$$

The non-linear σ-meson interactions contribute to pressure as follows:

$$P^{(\sigma^4)} = \frac{1}{2}\Big\{ -\frac{1}{3}\, b_N\, m_N \left(\Sigma^{\mathrm{H},N}\right)^3 + \frac{1}{2}\, c_N \left(\Sigma^{\mathrm{H},N}\right)^4 \Big\}. \tag{12.64}$$

Above we have seen that for the relativistic Hartree approximation, the expression for the energy density could be brought into a more transparent form [cf. equations (12.50) and (12.51)]. Repeating these steps here again leads for the pressure given in (12.63) to

$$\begin{aligned} P^{\mathrm{H}} = {} & \frac{1}{2}\sum_B \left(\Sigma_0^{\mathrm{H},B} + I_{3B}\,\Sigma_{03}^{\mathrm{H},B}\right) \rho^{\mathrm{H},B} + \frac{1}{2}\sum_B \left(\Sigma_S^{\mathrm{H},B}\ \bar{\rho}^{\mathrm{H},B}\right) \\ & + \frac{1}{6\pi^2} \sum_B (2J_B+1) \int_0^{p_{F_B}} \mathrm{d}p\, \frac{\boldsymbol{p}^4}{\sqrt{(m_B + \Sigma_S^{\mathrm{H},B})^2 + \boldsymbol{p}^2}} \\ & + \frac{1}{2}\Big\{ -\frac{1}{3}\, b_N\, m_N \left(\Sigma_S^{\mathrm{H},N}\right)^3 + \frac{1}{2}\, c_N \left(\Sigma_S^{\mathrm{H},N}\right)^4 \Big\} \\ & + \frac{1}{6\pi^2} \sum_{L=e,\mu} (2J_L+1) \int_0^{p_{F_L}} \mathrm{d}p\, \frac{\boldsymbol{p}^4}{\sqrt{m_L^2 + \boldsymbol{p}^2}}\,, \end{aligned} \tag{12.65}$$

which, upon performing the momentum integrations (appendix B.3) and rearranging terms, takes on the final form

$$\begin{aligned} P^{\,\mathrm{H}} = \frac{1}{2\,\pi^2} \sum_B \nu_B \Big\{ & \frac{1}{12}\, p_{F_B}^3\, \epsilon_F^{\mathrm{H},B} - \frac{1}{8}\,(m_B^*)^2\, p_{F_B}\, \epsilon_F^{\mathrm{H},B} \\ & + \frac{1}{8}\,(m_B^*)^4\, \ln\, \frac{p_{F_B} + \epsilon_F^{\mathrm{H},B}}{m_B^*} \Big\}. \end{aligned} \tag{12.66}$$

The Fock contribution to pressure turns out to be given by $P^{\mathrm{F}} = \epsilon^{\mathrm{F}}$ [79].

12.2 Thermal bosons and antibaryons

In section 6.1 we have seen that at finite-temperatures not only particle and antiparticle states occur in the baryon propagator $\boldsymbol{g}^B(k)$, but because of the nuclear medium two new states, corresponding to holes in the particle Fermi sea and antiholes in the antiparticle Fermi sea, result, as illustrated in figures 6.2 and 6.3. The contribution of the antiholes, to which we refer as thermally excited antibaryons, are easily included in the self-energies and the equation of state by simply extending the path of contour integration in such a way that the antihole pole of figure 6.2 is enclosed too. The resulting paths are shown in figure D.1. This is ensured by simply adding $\lim_{x'\to x^-}$

to the expression $\lim_{x' \to x^+}$, the latter accounting for the medium-corrected baryon propagation only, everywhere in the text where it applies. As an example, the generalized expectation value of the energy momentum tensor (12.28) then reads

$$< \mathbf{\Phi}_0 | T_{\mu\nu}(x) | \mathbf{\Phi}_0 > = \Big(\lim_{x' \to x^+} + \lim_{x' \to x^-} \Big) \Big\{ -\partial_\nu \ \mathrm{Tr} \big(\gamma_\mu \, \boldsymbol{g}(x, x') \big) - \frac{g_{\mu\nu}}{2} \int \mathrm{d}^4 y \ \mathrm{Tr} \big(\mathbf{\Sigma}(x, y) \, \boldsymbol{g}(y, x') \big) \Big\} . \quad (12.67)$$

Aside from the thermally excited antibaryons, there will be thermal contributions of bosons too at finite temperature [324, 466]. Their contribution is derivable, for instance, from the energy-momentum tensor associated with these bosons,

$$\mathcal{T}_{\mu\nu} \equiv \sum_{M = \sigma, \omega, \ldots} T_{\mu\nu}^{(M)} , \quad (12.68)$$

with

$$T_{\mu\nu}^{(\sigma)}(x) = (\partial_\mu \sigma(x)) \, (\partial_\nu \sigma(x)) \, , \quad T_{\mu\nu}^{(\omega)}(x) = (\partial_\nu \omega^\lambda(x)) \, F_{\lambda\mu}(x) \, . \quad (12.69)$$

The expectation value of (12.68) can be written as [125]

$$< \mathbf{\Phi}_0 | \mathcal{T}_{\mu\nu}(x) | \mathbf{\Phi}_0 > \ = \mathrm{i} \lim_{x' \to x^+} \big\{ \nu_\sigma \partial_\mu \partial_\nu \Delta(x, x') + \nu_\omega \big(\partial_\nu \partial_\lambda \mathcal{D}^\lambda{}_\mu(x, x') - \partial_\nu \partial_\mu \mathcal{D}^\lambda{}_\lambda(x, x') \big) \big\} , \quad (12.70)$$

with ν_σ and ν_ω defined in equation (12.80). To transform (12.70) into a quantitatively tractable form let us introduce the expression for the boson two-point function, $\Delta(x, x')$. This is accomplished by deriving from the field equations (5.36) and (5.43), treated at the level of the HF approximation, the following relation for the propagator of scalar mesons [125],

$$\Delta(x, x') = \Delta^0(x, x') - \mathrm{i} \, g_{\sigma N}^2 \int \mathrm{d}^4 y \int \mathrm{d}^4 y' \ \Delta^0(x, y) \times \big\{ \boldsymbol{g}(y, y^+) \boldsymbol{g}(y', y'^+) - \boldsymbol{g}(y, y'^+) \boldsymbol{g}(y', y^+) \big\} \, \Delta^0(y', x') \, . \quad (12.71)$$

With the aid of this relation, one can replace the full meson propagator Δ (similarly for $\mathcal{D}$) in (12.70) with their free counterparts, Δ^0 and $\mathcal{D}^0$, since the contribution of the second term in equation (12.71) is zero in the Hartree approximation, and the exchange correction is known to be very small [467]. The momentum-space expression of $\Delta^0(x, x')$, which is recognized as the two-point Green function of free, scalar mesons at finite density and temperature, is found in close analogy to the derivation of the two-point Green function of baryons at finite temperature and density (cf. section 6.2.2). The only differences that arise originate from the different particle statistics. One arrives at [62]

$$\Delta^{0\sigma}(k) = \frac{-1}{2\,\omega^\sigma(\boldsymbol{k})}\Bigg\{\frac{1+f^\sigma(\boldsymbol{k})}{k^0-\omega^\sigma(\boldsymbol{k})+\mathrm{i}\,\eta} - \frac{f^\sigma(\boldsymbol{k})}{k^0-\omega^\sigma(\boldsymbol{k})-\mathrm{i}\,\eta} - \frac{1+f^\sigma(\boldsymbol{k})}{k^0+\omega^\sigma(\boldsymbol{k})-\mathrm{i}\,\eta} + \frac{f^\sigma(\boldsymbol{k})}{k^0+\omega^\sigma(\boldsymbol{k})+\mathrm{i}\,\eta}\Bigg\}. \tag{12.72}$$

The structure of the free vector propagator $\mathcal{D}^0_{\mu\nu}(k)$ is determined by (5.100). The Bose-Einstein distribution function, f^M, of thermal mesons of type M propagating with energy

$$\omega^M(\boldsymbol{k}) = \sqrt{\boldsymbol{k}^2+m_M^2}\,, \tag{12.73}$$

is given by

$$f^M(\boldsymbol{k}) = \frac{1}{\mathrm{e}^{\beta\,\omega^M(k)}-1}\,. \tag{12.74}$$

The total energy density of the system is given by

$$\epsilon = <\boldsymbol{\Phi}_0|T_{00}(x)+\mathcal{T}_{00}(x)|\boldsymbol{\Phi}_0>, \tag{12.75}$$

from which one derives [cf. equation (12.29)]

$$\begin{aligned}\epsilon = &-\sum_B\Big(\lim_{x'\to x^+}+\lim_{x'\to x^-}\Big)\,\partial_0\int\frac{\mathrm{d}^4q}{(2\pi)^4}\mathrm{e}^{-\mathrm{i}q(x-x')}\,\big(\gamma^0\big)_{\zeta\zeta'}\,\boldsymbol{g}^B_{\zeta'\zeta}(q)\\ &-\frac{\mathrm{i}}{2}\sum_B\int\frac{\mathrm{d}^4q}{(2\pi)^4}\,\big(\mathrm{e}^{\mathrm{i}\eta q^0}+\mathrm{e}^{-\mathrm{i}\eta q^0}\big)\,\boldsymbol{\Sigma}^B_{\zeta\zeta'}(q)\,\boldsymbol{g}^B_{\zeta'\zeta}(q)\\ &-\frac{1}{2}\Big(\frac{1}{3}\,b_N\,m_N\big(-\Sigma^{\mathrm{H},N}_S\big)^3+\frac{1}{2}\,c_N\,\big(\Sigma^{\mathrm{H},N}_S\big)^4\Big)\\ &-\mathrm{i}\sum_M\nu_M\int\frac{\mathrm{d}^4q}{(2\pi)^4}\,\mathrm{e}^{\mathrm{i}\eta k^0}\,q_0\,q_0\,\Delta^{0M}(q)\,,\end{aligned} \tag{12.76}$$

and for the system's pressure [cf. equation (12.55)],

$$\begin{aligned}P = &\frac{\mathrm{i}}{3}\sum_B\int\frac{\mathrm{d}^4q}{(2\pi)^4}\big(\mathrm{e}^{\mathrm{i}\eta q^0}+\mathrm{e}^{-\mathrm{i}\eta q^0}\big)\,(\boldsymbol{\gamma}\cdot\hat{\boldsymbol{p}})_{\zeta\zeta'}\,\boldsymbol{g}^B_{\zeta'\zeta}(q)\\ &+\frac{\mathrm{i}}{2}\sum_B\int\frac{\mathrm{d}^4q}{(2\pi)^4}\,\big(\mathrm{e}^{\mathrm{i}\eta q^0}+e^{-\mathrm{i}\eta q^0}\big)\,\boldsymbol{\Sigma}^B_{\zeta\zeta'}(q)\,\boldsymbol{g}^B_{\zeta'\zeta}(q)\end{aligned}$$

$$
+\frac{1}{2}\Big(\frac{1}{3}\,b_N\,m_N\big(-\Sigma_S^{\mathrm{H},N}\big)^3+\frac{1}{2}\,c_N\,\big(\Sigma_S^{\mathrm{H},N}\big)^4\Big)
-\frac{\mathrm{i}}{3}\,\sum_M\sum_{j=1}^{3}\nu_M\int\frac{\mathrm{d}^4q}{(2\pi)^4}\;\mathrm{e}^{\mathrm{i}\eta q^0}\,q_j\,q_j\,\Delta^{0M}(q)\,. \tag{12.77}
$$

Equations (12.76) and (12.77) ignore terms of the order $\mathcal{O}(\bar{\rho}-\bar{\rho}^{\mathrm{H}})$, where $\bar{\rho}^{\mathrm{H}}$ denotes the scalar density (6.200) calculated for the relativistic Hartree approximation. The last terms in (12.76) and (12.77) are the contributions to energy density and pressure that arise from thermal bosons. Performing the integrations over q^0 leads for the latter contributions to

$$
\mathcal{E}=\sum_M\nu_M\int\frac{\mathrm{d}^3\boldsymbol{q}}{(2\pi)^3}\,\sqrt{\boldsymbol{q}^2+m_M^2}\;f^M(\boldsymbol{q})\,, \tag{12.78}
$$

and

$$
\mathcal{P}=\frac{1}{3}\,\sum_M\nu_M\int\frac{\mathrm{d}^3\boldsymbol{q}}{(2\pi)^3}\,\frac{\boldsymbol{q}^2}{\sqrt{\boldsymbol{q}^2+m_M^2}}\;f^M(\boldsymbol{q})\,. \tag{12.79}
$$

The spin-isospin degeneracy factor of bosons is defined as

$$
\nu_M=(2I_M+1)\,(2J_M+1)\,, \tag{12.80}
$$

with spin and isospin quantum numbers, J_M and I_M, listed in table 5.2.

Finally, we insert the spectral decomposition derived for $\boldsymbol{g}^B$ in (6.71) into equations (12.76) and (12.77), leading for energy density and pressure to

$$
\begin{aligned}
\epsilon=\sum_B\nu_B\int\frac{\mathrm{d}^3\boldsymbol{q}}{(2\pi)^3}\big\{&\big[2\big(m_B\,\Xi_S^B(\boldsymbol{q})-|\boldsymbol{q}|\,\Xi_V^B(\boldsymbol{q})\big)+\big(\Sigma_S^B(\omega^B(\boldsymbol{q}),\boldsymbol{q})\,\Xi_S^B(\boldsymbol{q})\\
&-\Sigma_V^B(\omega^B(\boldsymbol{q}),\boldsymbol{q})\,\Xi_V^B(\boldsymbol{q})+\Sigma_0^B(\omega^B(\boldsymbol{q}),\boldsymbol{q})\,\Xi_0^B(\boldsymbol{q})\big)\big]\,f^B(\boldsymbol{q})\\
&-\big[2\big(m_B\,\bar{\Xi}_S^B(\boldsymbol{q})-|\boldsymbol{q}|\,\bar{\Xi}_V^B(\boldsymbol{q})\big)+\big(\Sigma_S^B(\bar{\omega}^B(\boldsymbol{q}),\boldsymbol{q})\,\bar{\Xi}_S^B(\boldsymbol{q})\\
&-\Sigma_V^B(\bar{\omega}^B(\boldsymbol{q}),\boldsymbol{q})\,\bar{\Xi}_V^B(\boldsymbol{q})+\Sigma_0^B(\bar{\omega}^B(\boldsymbol{q}),\boldsymbol{q})\,\bar{\Xi}_0^B(\boldsymbol{q})\big)\big]\,\bar{f}^B(\boldsymbol{q})\big\}\\
&-\frac{1}{2}\Big(-\frac{1}{3}\,b_N\,m_N\,\big(\Sigma_S^{\mathrm{H},N}\big)^3+\frac{1}{2}\,c_N\,\big(\Sigma_S^{\mathrm{H},N}\big)^4\Big)+\mathcal{E}\,,
\end{aligned} \tag{12.81}
$$

and

$$
\begin{aligned}
P=\sum_B\nu_B\int\frac{\mathrm{d}^3\boldsymbol{q}}{(2\pi)^3}\Big\{&-\frac{2}{3}|\boldsymbol{q}|\big(\Xi_V^B(\boldsymbol{q})\,f^B(\boldsymbol{q})\,-\bar{\boldsymbol{\Xi}}_V^B(\boldsymbol{q})\,\bar{f}^B(\boldsymbol{q})\big)\\
&+\big[\Sigma_S^B(\omega^B(\boldsymbol{q}),\boldsymbol{q})\,\Xi_S^B(\boldsymbol{q})-\Sigma_V^B(\omega^B(\boldsymbol{q}),\boldsymbol{q})\,\Xi_V^B(\boldsymbol{q})\\
&+\Sigma_0^B(\omega^B(\boldsymbol{q}),\boldsymbol{q})\,\Xi_0^B(\boldsymbol{q})\big]\,f^B(\boldsymbol{q})-\big[\Sigma_S^B(\bar{\omega}^B(\boldsymbol{q}),\boldsymbol{q})\,\bar{\boldsymbol{\Xi}}_S^B(\boldsymbol{q})
\end{aligned}
$$

$$- \Sigma_V^B(\bar\omega^B(\boldsymbol{q}),\boldsymbol{q})\,\bar{\boldsymbol{\Xi}}_V^B(\boldsymbol{q}) + \Sigma_0^B(\bar\omega^B(\boldsymbol{q}),\boldsymbol{q})\,\bar{\boldsymbol{\Xi}}_0^B(\boldsymbol{q})\big]\,\bar f^B(\boldsymbol{q})\Big\}$$
$$+ \frac{1}{2}\Big(-\frac{1}{3}\,b_N\,m_N\big(\Sigma_S^{\mathrm{H},N}\big)^3 + \frac{1}{2}\,c_N\big(\Sigma_S^{\mathrm{H},N}\big)^4\Big) + \mathcal{P}\,. \qquad (12.82)$$

With the aid of the individual expressions derived for Ξ_i^B and $\bar\Xi_i^B$ ($i = S, V, 0$) in (7.29), expressions (12.81) and (12.82) can be written in the relativistic *Hartree* approximation as

$$\epsilon^{\mathrm{H}} = \frac{1}{2}\sum_B \big(\Sigma_0^{\mathrm{H},B}\,\rho^B\big) - \frac{1}{2}\sum_B \big(\Sigma_S^{\mathrm{H},B}\,\bar\rho^B\big)$$
$$+ \frac{1}{2\,\pi^2}\sum_B \nu_B \int_0^\infty \mathrm{d}q\,q^2\,\sqrt{(m_B+\Sigma_S^{\mathrm{H},B})^2+\boldsymbol{q}^2}\,\big(f^B(\boldsymbol{q})+\bar f^B(\boldsymbol{q})\big)$$
$$- \frac{1}{2}\Big(-\frac{1}{3}\,b_N\,m_N\,\big(\Sigma_S^{\mathrm{H},N}\big)^3 + \frac{1}{2}\,c_N\,\big(\Sigma_S^{\mathrm{H},N}\big)^4\Big) + \mathcal{E}\,, \qquad (12.83)$$

and

$$P^{\mathrm{H}} = \frac{1}{2}\sum_B \big(\Sigma_0^{\mathrm{H},B}\,\rho^B\big) + \frac{1}{2}\sum_B \big(\Sigma_S^{\mathrm{H},B}\,\bar\rho^B\big)$$
$$+ \frac{1}{6\pi^2}\sum_B \nu_B \int_0^\infty \mathrm{d}q\,\frac{q^4}{\sqrt{(m_B+\Sigma_S^{\mathrm{H},B})^2+\boldsymbol{q}^2}}\,\big(f^B(\boldsymbol{q})+\bar f^B(\boldsymbol{q})\big)$$
$$+ \frac{1}{2}\Big(-\frac{1}{3}\,b_N\,m_N\,\big(\Sigma_S^{\mathrm{H},N}\big)^3 + \frac{1}{2}\,c_N\,\big(\Sigma_S^{\mathrm{H},N}\big)^4\Big) + \mathcal{P}\,. \qquad (12.84)$$

Another attractive simplification of expressions (12.81) and (12.82), which works very reasonable because of the rather weak energy and momentum dependence of the self-energies Σ_S and Σ_0 and the smallness of Σ_V [84, 125, 313, 468], consists in replacing the HF spectral functions (6.139) through (6.141) with their Hartree approximated counterparts derived in equations (6.143) through (6.148). Substituting the latter into (12.81) and (12.82), we find for ϵ and P in relativistic *Hartree–Fock*,

$$\epsilon^{\mathrm{H}} = 2\sum_B \nu_B \int \frac{\mathrm{d}^3\boldsymbol{q}}{(2\pi)^3}\,\big(m_B\,\Xi_S^{\mathrm{H},B}(\boldsymbol{q}) - |\boldsymbol{q}|\,\Xi_V^{\mathrm{H},B}(\boldsymbol{q})\big)\,\big(f^B(\boldsymbol{q})+\bar f^B(\boldsymbol{q})\big)$$
$$+ \sum_B \nu_B \int \frac{\mathrm{d}^3\boldsymbol{q}}{(2\pi)^3}\,\big\{\big(\Sigma_S^{\mathrm{H},B}(\boldsymbol{q})\,\Xi_S^{\mathrm{H},B}(\boldsymbol{q}) - \Sigma_V^{\mathrm{H},B}(\boldsymbol{q})\,\Xi_V^{\mathrm{H},B}(\boldsymbol{q})\big)$$
$$\times\,\big(f^B(\boldsymbol{q})+\bar f^B(\boldsymbol{q})\big) + \Sigma_0^{\mathrm{H},B}(\boldsymbol{q})\,\Xi_0^{\mathrm{H},B}(\boldsymbol{q})\,\big(f^B(\boldsymbol{q})-\bar f^B(\boldsymbol{q})\big)\big\}$$
$$- \frac{1}{2}\Big(-\frac{1}{3}\,b_N\,m_N\,\big(\Sigma_S^{\mathrm{H},N}\big)^3 + \frac{1}{2}\,c_N\,\big(\boldsymbol{\Sigma}_S^{\mathrm{H},N}\big)^4\Big) + \mathcal{E}\,, \qquad (12.85)$$

$$\epsilon^{\mathrm{F}} = \sum_B \nu_B \int \frac{\mathrm{d}^3\boldsymbol{q}}{(2\pi)^3} \left\{ \left(\Sigma_S^{\mathrm{F},B}(\boldsymbol{q})\, \Xi_S^{\mathrm{H},B}(\boldsymbol{q}) - \Sigma_V^{\mathrm{F},B}\, \Xi_V^{\mathrm{H},B}(\boldsymbol{q}) \right) \right.$$
$$\left. \times \left(f^B(\boldsymbol{q}) + \bar{f}^B(\boldsymbol{q}) \right) + \Sigma_0^{\mathrm{F},B}(\boldsymbol{q})\, \Xi_0^{\mathrm{H},B}(\boldsymbol{q}) \left(f^B(\boldsymbol{q}) - \bar{f}^B(\boldsymbol{q}) \right) \right\}, \quad (12.86)$$

and

$$P^{\mathrm{H}} = -\frac{2}{3} \sum_B \nu_B \int \frac{\mathrm{d}^3\boldsymbol{q}}{(2\pi)^3} \, |\boldsymbol{q}| \, \Xi_V^{\mathrm{H},B}(\boldsymbol{q}) \left(f^B(\boldsymbol{q}) + \bar{f}^B(\boldsymbol{q}) \right)$$
$$+ \sum_B \nu_B \int \frac{\mathrm{d}^3\boldsymbol{q}}{(2\pi)^3} \left\{ \left(\Sigma_S^{\mathrm{H},B}(\boldsymbol{q})\, \Xi_S^{\mathrm{H},B}(\boldsymbol{q}) - \Sigma_V^{\mathrm{H},B}(\boldsymbol{q})\, \Xi_V^{\mathrm{H},B}(\boldsymbol{q}) \right) \right.$$
$$\left. \times \left(f^B(\boldsymbol{q}) + \bar{f}^B(\boldsymbol{q}) \right) + \Sigma_0^{\mathrm{H},B}(\boldsymbol{q})\, \Xi_0^{\mathrm{H},B}(\boldsymbol{q}) \left(f^B(\boldsymbol{q}) - \bar{f}^B(\boldsymbol{q}) \right) \right\}$$
$$+ \frac{1}{2} \Big(-\frac{1}{3}\, b_N\, m_N \left(\Sigma_S^{\mathrm{H},N} \right)^3 + \frac{1}{2}\, c_N \left(\Sigma_S^{\mathrm{H},N} \right)^4 \Big) + \mathcal{P}, \quad (12.87)$$
$$P^{\mathrm{F}} = \epsilon^{\mathrm{H}}. \quad (12.88)$$

The total contributions to energy density and pressure in relativistic Hartree–Fock then follow from (12.85) to (12.88) as

$$\epsilon = \epsilon^{\mathrm{H}} + \epsilon^{\mathrm{F}}, \quad \text{and} \quad P = P^{\mathrm{H}} + \epsilon^{\mathrm{F}}. \quad (12.89)$$

The simpler mathematical structure of these expressions originates to a great deal from the symmetry relations between the particle and antiparticle baryon spectral functions (6.143) to (6.148). As it must be, these relations bear a strong resemblance with the corresponding ones derived in a somewhat different mathematical framework by Serot and Walecka [92].

12.3 Equation of state of a relativistic lepton gas

The calculation of energy density and pressure of a free, relativistic lepton gas may serve as a further simple case to demonstrate the principle ideas behind the Green function technique. We start from the energy–momentum tensor of such a system, which follows from equation (12.7) for $\mathcal{L} = \mathcal{L}_L$ [cf. (5.15)] and by replacing the summation over B with the summation over $L = e^-, \mu^-$. One then obtains for the momentum tensor's expectation value [79]

$$< \boldsymbol{\Phi}_0 | T_{\mu\nu}^{\mathrm{Lep}}(x) | \boldsymbol{\Phi}_0 > = - \lim_{x' \to x^+} \sum_{L=e,\mu} \partial_\nu \; \mathrm{Tr} \left(\gamma_\mu \, \boldsymbol{g}^L(x, x') \right), \quad (12.90)$$

whose Fourier transform is given by

$$< \boldsymbol{\Phi}_0 | T_{\mu\nu}^{\mathrm{Lep}}(x) | \boldsymbol{\Phi}_0 > = - \lim_{x' \to x^+} \partial_\nu \sum_{L=e,\mu} \int \frac{\mathrm{d}^4 q}{(2\pi)^4} \mathrm{e}^{-\mathrm{i}q(x-x')} \; \mathrm{Tr} \left(\gamma_\mu \, \boldsymbol{g}^L(q) \right). \quad (12.91)$$

Substituting $\boldsymbol{g}^L$ by its spectral representation, derived in (6.156), performing the contour integration and lastly inserting the lepton spectral functions (6.165) into the resulting expression gives for the energy density $\epsilon_{\rm Lep} \equiv < \boldsymbol{\Phi}_0 | T_{00}^{\rm Lep} | \boldsymbol{\Phi}_0 >$ of the lepton gas

$$\epsilon_{\rm Lep} = \frac{1}{2\pi^2} \sum_{L=e,\mu} (2J_L + 1) \int_0^{k_{F_L}} {\rm d}q \, \boldsymbol{q}^2 \sqrt{m_L^2 + \boldsymbol{q}^2} \, . \tag{12.92}$$

The factor $2J_L+1$ accounts for the spin degeneracy of leptons (see table 6.1), and k_{F_L} denote their Fermi momenta. It is a simple exercise to calculate the momentum integral in (12.92) analytically. The result is given in equation (B.30). Substituting this expression into (12.92) leads to the final result for $\epsilon_{\rm Lep}$,

$$\begin{aligned}\epsilon_{\rm Lep} = \frac{1}{16\,\pi^2} \sum_{L=e,\mu} (2J_L + 1) \Big\{ & k_{F_L} \left(2\, k_{F_L}^2 + m_L^2\right) \sqrt{m_L^2 + k_{F_L}^2} \\ & - m_L^4 \, \ln\left(\frac{k_{F_L} + \sqrt{m_L^2 + k_{F_L}^2}}{m_L} \right) \Big\} \, .\end{aligned} \tag{12.93}$$

The pressure, obtained as $P_{\rm Lep} \equiv \frac{1}{3} \sum_{i=1}^{3} < \boldsymbol{\Phi}_0 | T_{ii}^{\rm Lep} | \boldsymbol{\Phi}_0 >$, is given by

$$P_{\rm Lep} = \frac{1}{6\pi^2} \sum_{L=e,\mu} (2J_L + 1) \int_0^{k_{F_L}} {\rm d}q \, \frac{\boldsymbol{q}^4}{\sqrt{m_L^2 + \boldsymbol{q}^2}} \, . \tag{12.94}$$

Making use of the analytical result for the momentum integral, given in (B.29), leads to

$$\begin{aligned}P_{\rm Lep} = \frac{1}{6\,\pi^2} \sum_{L=e,\mu} (2J_L + 1) \Big\{ & \frac{k_{F_L}}{4} \left\{ k_{F_L}^2 - \frac{3}{2}\, m_L^2 \right\} \sqrt{m_L^2 + k_{F_L}^2} \\ & + \frac{3}{8}\, m_L^4 \, \ln\left(\frac{k_{F_L} + \sqrt{m_L^2 + k_{F_L}^2}}{m_L} \right) \Big\} \, .\end{aligned} \tag{12.95}$$

The calculation of the lepton density, denoted by ρ^L, can be performed in close analogy to the calculation of the baryon number density in section 12.4. One gets

$$\rho^L = {\rm i} \lim_{x' \to x^+} \gamma^0_{\zeta\zeta'} \, \boldsymbol{g}^L_{\zeta'\zeta}(x, x') \tag{12.96}$$

$$= \mathrm{i} \int \frac{\mathrm{d}^4 q}{(2\pi)^4} \, \mathrm{e}^{\mathrm{i}\eta q^0} \, \gamma^0_{\zeta\zeta'} \, \boldsymbol{g}^L_{\zeta'\zeta}(q) \tag{12.97}$$

$$= 2\,(2J_L + 1) \int \frac{\mathrm{d}^3 \boldsymbol{q}}{(2\pi)^3} \, \Xi^L_0(\boldsymbol{q}) \, \Theta^L(\boldsymbol{q}) = \frac{2J_L + 1}{2} \, \frac{k^3_{F_L}}{3\,\pi^2} \, . \tag{12.98}$$

The lepton distribution function has been abbreviated to $\Theta^L(\boldsymbol{q}) \equiv \Theta(k_{F_L} - |\boldsymbol{q}|)$. Finally the total number density of leptons, ρ^{Lep}, is obtained as

$$\rho^{\mathrm{Lep}} \equiv \sum_L \rho^L \, . \tag{12.99}$$

12.4 Equation of state in relativistic ladder approximation

To derive the equation of state for this many-body approximation, we choose, for the sake of illustration, a mathematical route different from the one adopted for the HF case. We begin with going back to equation (12.21). Since no approximations have been introduced in deriving this relation, it serves as the starting point for deriving the equation of state for both the relativistic HF and relativistic ladder approximation. Here, however, we shall put the derivation of the equation of state on more intuitive grounds by starting from the system's Hamiltonian density, complementary to sketching the derivation of the equation of state from the energy–momentum tensor too.

The energy density of the system described by the Lagrangian (5.1) can be split up into the following three contributions [117, 118, 122]:

$$\epsilon \equiv \frac{1}{\Omega} \int_\Omega \mathrm{d}^3 \boldsymbol{x} \, < \boldsymbol{\Phi}_0 | \mathcal{H}^0_{\mathrm{B}}(x) + \mathcal{H}^0_{\mathrm{M}}(x) + \mathcal{H}^{\mathrm{I}}(x) | \boldsymbol{\Phi}_0 > , \tag{12.100}$$

where Ω denotes the volume. The individual terms in (12.100) originate from free baryons, free mesons, and from the interactions between the baryons mediated by mesons. For what follows, it is convenient to write (12.100) in the form $\epsilon \equiv \epsilon^0_{\mathrm{B}} + \epsilon^0_{\mathrm{M}} + \epsilon_{\mathrm{I}}$. The first term of this decomposition, ϵ^0_{B}, constitutes the ground-state expectation value, that is $< \boldsymbol{\Phi}_0 | \mathcal{H}^0_{\mathrm{B}} | \boldsymbol{\Phi}_0 >$, of the Hamilton density of free baryons, which follows from (12.12) in the form

$$\mathcal{H}^0_{\mathrm{B}}(x) = \sum_B \bar{\psi}_B(x) \left(\gamma^\mu p_\mu + m_B \right) \psi_B(x) \, . \tag{12.101}$$

When calculating $< \boldsymbol{\Phi}_0 | \mathcal{H}^0_{\mathrm{B}} | \boldsymbol{\Phi}_0 >$ one encounters the ground-state expectation value $< \boldsymbol{\Phi}_0 | \bar{\psi}_B \psi_B | \boldsymbol{\Phi}_0 >$ which can be replaced with its associated two-point Green function, derived in (5.63). Subsequent Fourier transformation then leads to the analog of (12.23) given by [125, 313]

$$\epsilon^0_{\rm B} = - \lim_{x' \to x^+} \sum_B \partial_0 \int \frac{{\rm d}^4 q}{(2\pi)^4} \, {\rm e}^{-{\rm i}q(x-x')} \, \gamma^0_{\zeta\zeta'} \, \boldsymbol{g}^B_{\zeta'\zeta}(q) \, . \tag{12.102}$$

A comparison of this expression with equation (12.29) reveals that the first term there is the energy density that originates from free baryons. Since this term transforms, after contour integration and calculation of the trace, into the first term in (12.44), we can write for (12.102) the relation

$$\epsilon^0_{\rm B} = 2 \sum_B \nu_B \int \frac{{\rm d}^3 \boldsymbol{q}}{(2\pi)^3} \, \big\{ m_B \, \Xi^B_S(\boldsymbol{q}) - |\boldsymbol{q}| \, \Xi^B_V(\boldsymbol{q}) \big\} \Theta^B(\boldsymbol{q}) \, . \tag{12.103}$$

What remains to be calculated are the energy densities $\epsilon^0_{\rm M}$ and $\epsilon^{\rm I}$ that originate from the other two terms in (12.100). These contributions are found most readily by noticing that all the terms in (12.21) that arise from baryon–meson interactions (that is, all terms except the first expression, which, as seen just above, corresponds to free baryon propagation) can be written in accordance with equations (5.153) through (5.155) in the form $\Gamma^{MB}\Gamma^{MB'}\Delta^M \boldsymbol{g}_2^{B'B} = \mathbf{V}^{BB'} \boldsymbol{g}_2^{B'B}$. Hence we arrive for $\epsilon^0_{\rm M} + \epsilon^{\rm I}$ at

$$\begin{aligned} \epsilon^0_{\rm M} + \epsilon^{\rm I} = - \frac{1}{2\,\Omega} \sum_{BB'} \int_\Omega {\rm d}^3 \boldsymbol{x} \; &< x_1\zeta_1, x_2\zeta_2 | \mathbf{V}^{BB'} | x_3\zeta_3, x_4\zeta_4 > \\ &\times \; \boldsymbol{g}_2^{B'B}(x_3\zeta_3, x_4\zeta_4; x_1^+\zeta_1, x_2^+\zeta_2) \, . \end{aligned} \tag{12.104}$$

Because equations (5.175) and (5.186) can be combined to the operator equation $\mathbf{V}\boldsymbol{g}_2 = {\rm i}\,\boldsymbol{\Sigma}\,\boldsymbol{g}_1$, we may bring (12.104) into the form

$$\begin{aligned} \epsilon^0_{\rm M} + \epsilon^{\rm I} = \sum_B \nu_B \int \frac{{\rm d}^3 \boldsymbol{q}}{(2\pi)^3} \big\{ &\Sigma^B_S(\omega^B(\boldsymbol{q}), \boldsymbol{q}) \, \Xi^B_S(\boldsymbol{q}) - \Sigma^B_V(\omega^B(\boldsymbol{q}), \boldsymbol{q}) \, \Xi^B_V(\boldsymbol{q}) \\ &+ \Sigma^B_0(\omega^B(\boldsymbol{q}), \boldsymbol{q}) \, \Xi^B_0(\boldsymbol{q}) \big\} \, \Theta^B(\boldsymbol{q}) \, . \end{aligned} \tag{12.105}$$

The integrals in equations (12.103) and (12.105) can be calculated via straightforward numerical methods once the baryon spectral functions and self-energies have been computed self-consistently from the equations summarized in section 11.1. Parenthetically we note that the result obtained above for the total energy density, $\epsilon = \epsilon^0_{\rm B} + \epsilon^0_{\rm M} + \epsilon_{\rm I}$, coincides of course with (12.44) derived, however, from the energy-momentum tensor.

The energy per baryon, E/A, internal energy density, $\mathcal{E}^{\rm int}$, and pressure, P, are obtainable from the total energy density, ϵ. For the former two, one has

$$\frac{E(\rho)}{A} = \frac{\mathcal{E}^{\rm int}(\rho)}{\rho}\,, \quad \text{with} \quad \frac{\mathcal{E}^{\rm int}(\rho)}{\rho} = \frac{\epsilon(\rho)}{\rho} - m_N\,, \qquad (12.106)$$

and m_N the nucleon mass. One sees from (12.106) that the internal energy is defined as the volume density of the energy per baryon. Generally $\mathcal{E}^{\rm int}$ includes all forms of energy except the rest mass of the baryons. We shall encounter this quantity again when calculating the total baryon mass of stars [cf. equations (15.90) and (15.91)]. Finally, at zero temperature the pressure of the system follows from the thermodynamic relation

$$P = \rho^2 \frac{\partial}{\partial\rho}\frac{E(\rho)}{A} = \rho^2 \frac{\partial}{\partial\rho}\frac{\epsilon(\rho)}{\rho}\,. \qquad (12.107)$$

Having derived the expression for the equation of state, we turn now to the numerical outcome for the energy per baryon as a function of total baryon density ρ and asymmetry δ, computed for the modern boson-exchange interactions A, B and C of Brockmann and Machleidt (BM), and the Groningen B interaction. The BM potentials differ mainly with respect to the strength of the tensor force, which increases from A to C. Since this force is the main agent that determines the location of the saturation point of nuclear matter, it is interesting to see whether the saturation energies predicted by these potentials, plotted as a function of baryon density (or Fermi momentum), fall in a narrow band – known as the Coester band, as it is the case for non-relativitsic theories of matter (cf. chapter 12). The answer is given in figure 12.1. The correct binding energy of nuclear matter at the empirical saturation density, $E/A(\rho) \simeq 15$ MeV, is only obtained for BM B, while the other interactions overbind or underbind nuclear matter.

As described in chapter 10, we perform the calculation of the T-matrix in the full Dirac space spanned by the components of the nucleon spinors, which is therefore a matrix in the 16×16 direct product space of the two particles. The T-matrix is calculated from the partial wave expanded integral equation (5.203). McNeil, Shephard and Wallace [469] have suggested a decomposition of T into scalar, vector, tensor, pseudovector and axial Fermi invariants, ${}^S\mathsf{T}$, ${}^V\mathsf{T}$, ${}^T\mathsf{T}$, ${}^P\mathsf{T}$ and ${}^A\mathsf{T}$ respectively, according to the scheme

$$\begin{aligned}\mathsf{T} = \sum_{S,V,T,P,A} & {}^S\mathsf{T}\,\mathbf{1}^{(1)}\mathbf{1}^{(2)} + {}^V\mathsf{T}\,\gamma_\mu^{(1)}\gamma^{(2)\mu} + {}^T\mathsf{T}\,\sigma_{\mu\nu}^{(1)}\sigma^{(2)\mu\nu} \\ & + {}^P\mathsf{T}\,\gamma_5^{(1)}\gamma_5^{(2)} + {}^A\mathsf{T}\,\gamma_5^{(1)}\gamma_\mu^{(1)}\gamma_5^{(2)}\gamma^{(2)\mu}\,. \end{aligned} \qquad (12.108)$$

This however constitutes a non-unique ansatz for T that may lead, depending on the decomposition, to different results for the baryon self-energy [103, 119]. The equation of state, on the other hand, appears

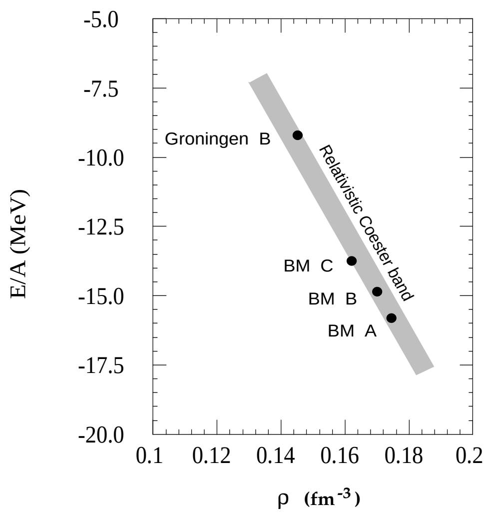

Figure 12.1. Relativistic Coester band associated with RBHF$^{(1)}$ calculations performed for potentials BM A through BM C, and Groningen B. The data are given in tables 12.1 and 12.2.

to be rather insensitive against the chosen decomposition [468]. The superscripts in (12.108) denote the particle (1 or 2) acted on by the matrix, and all spacetime variables are contracted to create Lorentz scalars. Our determination of the **T**-matrix also avoids another popular approximation, namely the fitting procedure of Machleidt, Holinde and Elster [119] which ignores the momentum dependence of the baryon self-energies Σ_S and Σ_0 completely, together with the well-justified approximation $\Sigma_V = 0$ [468]. The – then constant – self-energies Σ_S and Σ_0 are extracted from the positive energy spinor matrix elements $\Sigma_{\Phi\Phi}$ of (9.65) via a fitting procedure.

These different approximation techniques imposed onto one and the same many-body approximation, RBHF, renders a comparison of the corresponding numerical outcome non-trivial, even when the underlying nucleon–nucleon interaction is the same. A close similarity between our treatment and Brockmann's is accomplished by replacing in each iteration step the momentum dependent self-energies by their momentum averaged counterparts. This version is denoted by RBHF$^{(2)}$. It is numerically far less time consuming than RBHF$^{(1)}$, the iteration procedure which keeps the full momentum dependence. Calculations performed for positive-energy spinors only and momentum independent self-energies are donoted by RBHF$^{(3)}$.

The impact of the different approximation techniques RBHF$^{(1)}$ to

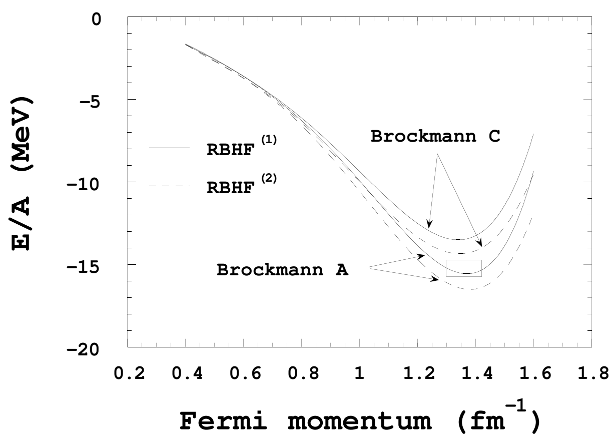

Figure 12.2. Energy per nucleon versus Fermi momentum of symmetric nuclear matter in RBHF for BM potentials A and C [449]. The solid (dashed) curves correspond to the treatment with (averaged) momentum dependency of the self-energies. The square indicates empirical saturation values. (Reprinted courtesy of *Phys. Rev.*)

RBHF$^{(3)}$ on the saturation properties of symmetric nuclear matter is shown in tables 12.1 and 12.2, and figure 12.2 [101, 458]. One sees that agreement between the full treatment, RBHF$^{(1)}$, and the results of Brockmann and Machleidt, RBHF$^{(2)}$, is relatively good. The full treatment leads to somewhat less binding, and the saturation density appears to vary only little too. The less physical $\mathbf{\Lambda}^{00}$ approximation, which is the simplest of the ladder approximations, is known to give more binding than the RHBF approximation [117, 118]. This feature is confirmed by our calculations too, as can be seen from tables 12.1 and 12.2. The other two $\mathbf{\Lambda}$ approximations, $\mathbf{\Lambda}^{10}$ and $\mathbf{\Lambda}^{11}$, are numerically so demanding that they have not been applied to asymmetric nuclear matter calculations yet. But from non-relativistic calculations one would expect them to give too little ($\mathbf{\Lambda}^{10}$) or about the correct ($\mathbf{\Lambda}^{10}$) binding energy [324]. The nuclear matter properties computed for the Groningen potential B are compiled in table 12.2, and graphically illustrated in figure 12.3. There, we also perform a comparison with the results of ter Haar and Malfliet [93], which are based on the decomposition of the scattering $\mathbf{T}$-matrix into the five Fermi invariants

Table 12.1. Saturation properties of symmetric nuclear matter computed for different many-body approximations. The nucleon–nucleon interactions are the BM potentials A, B, C [104]. The notation is as follows, RBHF$^{(1)}$: RBHF calculation in full basis and for momentum dependent self-energies; RBHF$^{(2)}$: RBHF calculation in full basis but for momentum-averaged self-energies; RBHF$^{(3)}$: RBHF calculation for positive-energy spinors only and momentum independent self-energies; $\mathbf{\Lambda}^{00(2)}$: same as RBHF$^{(2)}$ but for $\mathbf{\Lambda}^{00}$ propagator instead of $\mathbf{\Lambda}^{\mathrm{RBHF}}$.

Method	Potential	E/A (MeV)	ρ_0 (fm^{-3})	k_{F_0} (fm^{-1})	K (MeV)
RBHF$^{(1)}$	A	−15.72	0.174	1.37	336
RBHF$^{(2)}$	A	−16.49	0.174	1.37	280
RBHF$^{(3)}$	A	−15.59	0.185	1.40	290
$\mathbf{\Lambda}^{00(2)}$	A	−23.51	0.215	1.47	297
RBHF$^{(1)}$	B	−14.81	0.170	1.36	264
RBHF$^{(2)}$	B	−15.73	0.172	1.37	249
RBHF$^{(3)}$	B	−13.60	0.174	1.37	249
$\mathbf{\Lambda}^{00(2)}$	B	−21.90	0.210	1.46	260
RBHF$^{(1)}$	C	−13.73	0.162	1.34	268
RBHF$^{(2)}$	C	−14.38	0.170	1.36	258
RBHF$^{(3)}$	C	−12.26	0.155	1.32	185
$\mathbf{\Lambda}^{00(2)}$	C	−20.57	0.206	1.45	293

Table 12.2. Saturation properties of symmetric nuclear matter obtained for the Groningen-B potential [470]. The different methods are explained in the text.

Method	E/A (MeV)	ρ_0 (fm^{-3})	k_{F_0} (fm^{-1})	K (MeV)
RBHF$^{(1)}$	−9.21	0.145	1.29	191
RBHF$^{(2)}$	−9.68	0.152	1.31	183
$\mathbf{\Lambda}^{00(1)}$	−13.92	0.181	1.39	264
$\mathbf{\Lambda}^{00(2)}$	−14.53	0.189	1.41	178

of (12.108). This leads to deviations from the non-composed treatment, RBHF$^{(1)}$, of about 5 MeV at saturation density.

Next, let us turn to the interesting case of asymmetric nuclear matter. The energy per nucleon of such matter as a function of baryon density

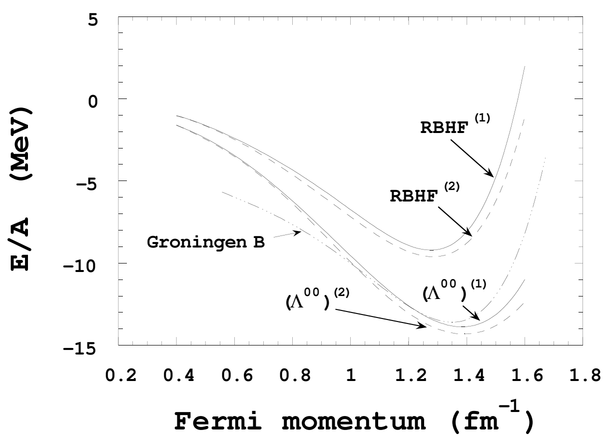

Figure 12.3. Energy per nucleon of nuclear matter computed for different many-body approximations [449]. The underlying potential in each case is Groningen B. The individual approximations are, RBHF$^{(1)}$ and $\mathbf{\Lambda}^{00(1)}$: relativistic T-matrix calculation in RBHF and $\mathbf{\Lambda}^{00}$ approximation where full momentum dependence of self-energy is kept; RBHF$^{(2)}$ and $\mathbf{\Lambda}^{00(2)}$: same as RBHF$^{(1)}$ and $\mathbf{\Lambda}^{00(1)}$ but for momentum averaged self-energy; Groningen B: RBHF calculation based on the decomposition of the T-matrix into the Fermi invariants listed in equation (12.108). (Reprinted courtesy of *Phys. Rev.*)

is displayed in figures 12.4 and 12.5. The asymmetrie parameter $\delta = (\rho^n - \rho^p)/\rho$ varies from 0 to 1, where the limiting vlaues corresponds to symmetric nuclear matter and pure neutron matter, respectively [101, 458]. One recognizes that the results are almost identical for pure neutron matter, since the different tensor forces of the potentials are not relevant for such matter. Figure 12.6 shows the energy per baryon computed for the $\mathbf{\Lambda}^{00}$ approximation. Engvik *et al* have calculated the properties of asymmetric matter for the BM potential A, adopting the Brockmann–Machleidt approximation but a different Pauli exclusion operator [454]. This makes an immediate comparison difficult. Subject to this caveat, a comparison with the E/A curves shows an agreement of similar quality as for the Brockmann-Machleidt calculations of symmetric matter (figure 12.2). To give an example, the deviation at nuclear matter saturation is approximately 2 MeV for pure neutron matter.

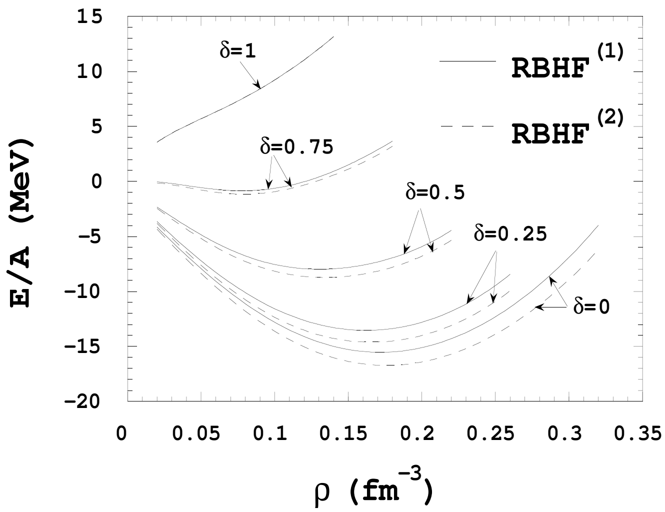

Figure 12.4. Binding energy per nucleon versus density for different asymmetries in the RBHF approximation (BM potential A) [449]. (Reprinted courtesy of *Phys. Rev.*)

Of great interest for neutron star calculations is the behavior of the energy per particle at equilibrium density as a function of asymmetry, displayed in figure 12.7. Of even greater interest may be the density dependence of the symmetry energy, e^{sym}, because of its importance for astrophysics (see below). The latter is shown in figure 12.8. The monotonic growth of these curves with density, which is also obtained for relativistic Hartree and HF calculations, seems to be a generic feature of relativistic theories of dense matter [471]. Relativistic HF and BHF calculations, for instance, predict an almost linear increase of the symmetry energy with density up to typically $5\,\rho_0$ followed by a slight flattening at still higher densities [473]. This appears to be quite different for several non-relativistic many-body calculations, like the ones based on Skyrme forces (e.g. force S III) or the modern Argonne–Urbana nucleon–nucleon interaction AV_{14}+UVII, where the symmetry energy bends over at higher nuclear densities ($\rho_0 = 0.15$ fm^{-3} [460] and about $6\,\rho_0$ [463], respectively). What is really causing this behavior appears to be not completely clear

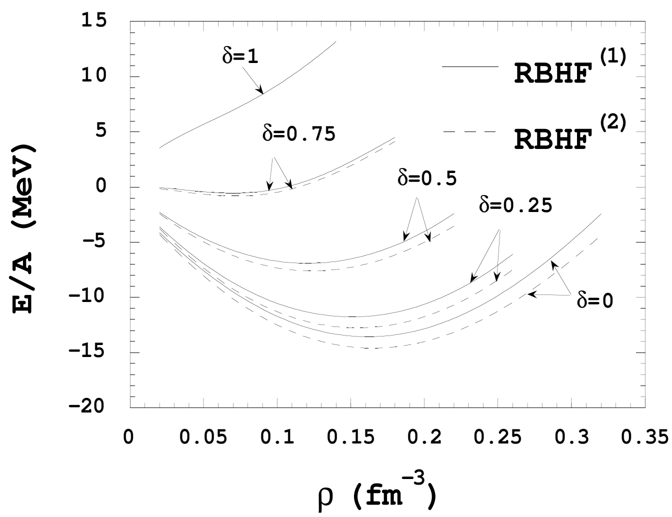

Figure 12.5. Binding energy per nucleon versus density for different asymmetries in the RBHF approximation (BM potential C) [449]. (Reprinted courtesy of *Phys. Rev.*)

yet. It could be caused by the employed nucleon–nucleon interaction rather than the many-body method itself [472]. The accurate knowledge of the behavior of $e^{\rm sym}(\rho)$ is of great astrophysical importance for two reasons. The first being that it is this quantity which effectively determines the proton fraction Y_p of neutron star matter. Theories predicting a monotonic increase of $e^{\rm sym}(\rho)$, for instance, lead preferably to critical proton fractions $Y_p \gtrsim 11$ %, beyond which the protons have large enough Fermi momenta so that the reactions $n \to p + e^- + \bar{\nu}_e$ and $p + e^- \to n + \nu_e$, known as direct Urca processes (section 19.5.2), can occur without a bystander particle. By means of these reactions neutron stars can cool very efficiently, as we shall see in chapter 19. The second reason concerns the radii and the crustal extent of neutron stars, which is determined by the density dependence of $e^{\rm sym}(\rho)$ too (section 14.4).

The properties of symmetric as well as asymmetric nuclear matter computed for RBHF are compared with those computed for of a broad variety of competing dense matter calculations in table 12.3. These range

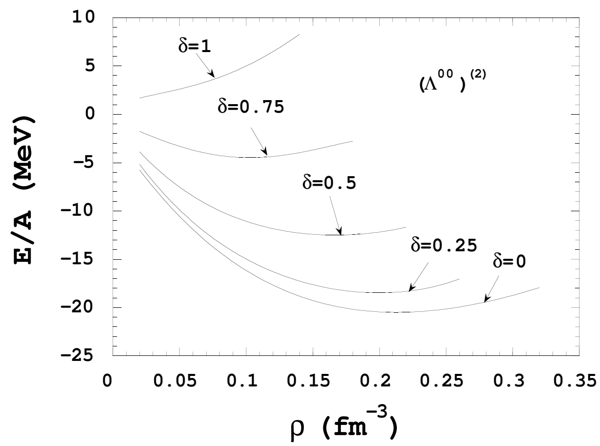

Figure 12.6. Binding energy per nucleon versus density for different asymmetries in the $\mathbf{\Lambda}^{00}$ approximation (BM potential C) [449]. (Reprinted courtesy of *Phys. Rev.*)

from relativistic Hartree and HF calculations to several non-relativistic calculations [460, 474]. The Hartree calculations are based on two frequently used parameter sets, LN1 and NL-SH. The HF results are taken from [460]. SkM* and S III denote two well-known Skyrme forces, FRDM is the latest and most sophisticated version of the droplet-model mass formulae, while ETFSI-1 denotes the first mass formula based entirely on microscopic forces [474]. As mentioned before the agreement of the bulk properties with the accepted values of the mass formula is quite satisfactory. Also the value of the symmetry parameter a_{sym} is located within the accepted boundaries. The values of L and K^*, which are much more uncertain than the value of a_{sym}, lie between the values computed for the relativistic Hartree parametrization NL-SH and the Skyrme parametrization SkM*, and comply nicely with the systematics already established by non-relativistic fits to the nuclear data. For instance, increasing values of a_{sym} are accompanied by increasing values of L [475]. Although these parametrizations have been used very often in the past, they nevertheless have some deficiencies [453, 474, 476].

We close this section with testing the validity of the quadratic approximation for the symmetry energy, which is of the form [cf. equation

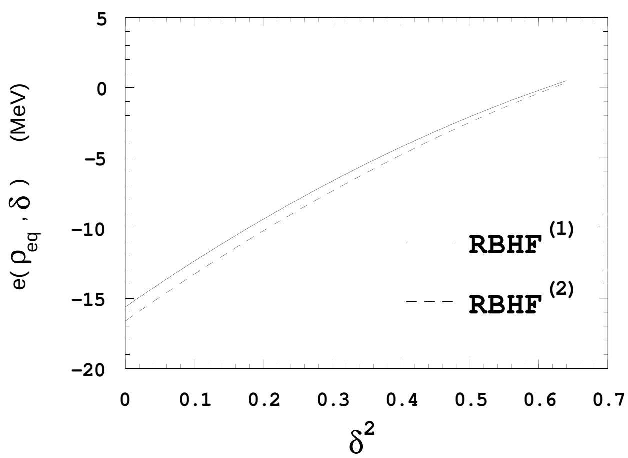

Figure 12.7. Energy per particle (11.4) at equilibrium as a function of asymmetry δ, computed for BM potential A [449]. (Reprinted courtesy of *Phys. Rev.*)

(11.2)]

$$e(\rho, \delta) = e(\rho, 0) + e^{\mathrm{sym}}(\rho)\, \delta^2 \,. \tag{12.109}$$

This approximation is known to hold for the non-relativistic Brueckner approximation [464]. It is evident from figure 12.9 that this approximation is also obeyed to a very high degree by the RBHF approximation.

12.5 Non-relativistic limit

In the non-relativistic treatment the self-energies of equation (6.83) satisfy

$$\Sigma_S^B(k) \;\to\; 0\,, \qquad \Sigma_V^B(k) \;\to\; 0\,, \qquad \Sigma_0^B(k) \;\to\; \Sigma^B(k)\,, \tag{12.110}$$

which leads to the replacements

$$m_B^* \to m_B\,, \quad k_B^* \to k\,, \quad W^B \to \sqrt{m_B^2 + \boldsymbol{k}^2} \approx m_B + \frac{\boldsymbol{k}^2}{2\, m_B}\,. \tag{12.111}$$

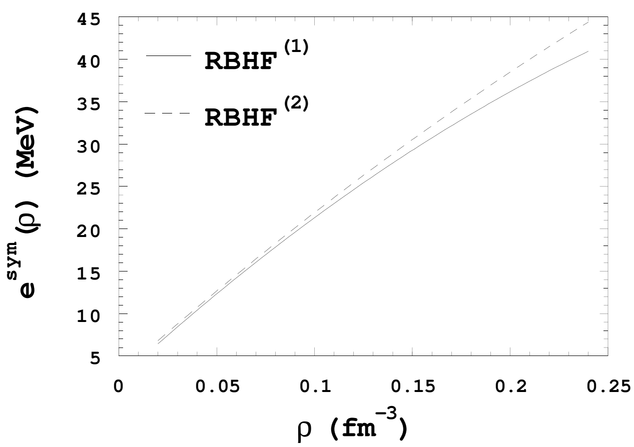

Figure 12.8. Symmetry energy (11.5) as a function of density computed for BM potential A [449]. (Reprinted courtesy of *Phys. Rev.*)

The relativistic energy–momentum relation of equation (6.149) is to be replaced according to

$$\omega^B(\boldsymbol{k}) \to \omega^B(\boldsymbol{k}) - m_B \equiv \epsilon^B(\boldsymbol{k}) = \frac{\boldsymbol{k}^2}{2\, m_B} + \Sigma^B(\epsilon^B(\boldsymbol{k}) - \mu^B, \boldsymbol{k})\,. \quad (12.112)$$

The spectral function $\boldsymbol{\Xi}^B(\boldsymbol{k})$ of equation (6.163) plays the role of a momentum-density function, that is,

$$\Xi^B(k^0, \boldsymbol{k}) = n^B(|\boldsymbol{k}|)\; \delta(k^0 - \epsilon^B(\boldsymbol{k}) + \mu^B)\,, \quad (12.113)$$

with [cf. equation (9.46)]

$$n^B(|\boldsymbol{k}|) \equiv \left| 1 - \frac{\partial \Sigma^B}{\partial \omega} \right|^{-1}_{\omega^B = \epsilon^B(k)}\,. \quad (12.114)$$

Equations (12.113) and (12.114) are well-know results of the non-relativistic Green function theory [316, 339]. The expressions of energy density and baryon number density follow from equations (12.103) and (12.105), and

Table 12.3. Properties of symmetric and asymmetric nuclear matter computed for different approximation techniques. Bro A, Bro B and Bro C refer to RBHF calculations (RBHF$^{(2)}$) performed for BM potentials A, B and C. All other entries are explained in the text.

	E/A (MeV)	ρ_0 (fm^{-3})	K (MeV)	$a_{\rm sym}$ (MeV)	L (MeV)	K^* (MeV)
Bro A	−16.49	0.174	280	34.4	81.9	−66.4
Bro B	−15.73	0.172	249	32.8	90.2	9.97
Bro C	−14.38	0.170	258	31.5	76.1	−35.1
RHF$^{(1)}$	−15.75	0.148	610	28.9	132	466
RHF$^{(2)}$	−15.75	0.148	360	43.3	135	105
RHF$^{(3)}$	−15.75	0.148	460	38.6	138	276
NL 1	−16.42	0.152	212	43.5	140	143.0
NL-SH	−16.35	0.146	356	36.1	114	79.82
SkM*	−15.78	0.160	217	30.0	45.8	−155.9
SIII	−15.86	0.145	355	28.2	9.9	−393.7
FRDM	−16.25	0.152	240	32.7	0	–
ETFSI-1	−15.87	0.161	235	27.0	−9.29	−336.8

(6.186) respectively, as

$$\epsilon = 2 \sum_B \nu_B \int \frac{\mathrm{d}^3\boldsymbol{k}}{(2\pi)^3} \left\{ \frac{\boldsymbol{k}^2}{2\, m_B} + \frac{1}{2}\, \Sigma^B(\epsilon^B(\boldsymbol{k}) - \mu^B, \boldsymbol{k}) \right\} n^B(|\boldsymbol{k}|)\, \Theta^B(\boldsymbol{k}) \,, \tag{12.115}$$

and

$$\rho = 2 \sum_B \nu_B \int \frac{\mathrm{d}^3\boldsymbol{k}}{(2\pi)^3}\, n^B(|\boldsymbol{k}|)\, \Theta(k_{F_B} - |\boldsymbol{k}|) \,. \tag{12.116}$$

We recall that in the non-relativistic $\boldsymbol{\Lambda}$ theory the single-particle basis are *a priori* given plane-wave functions. In the relativistic approach the basis consists of self-consistent, effective Dirac spinors. Their density dependence has an important influence on the saturation mechanism of nuclear matter [117] and hence on the nuclear equation of state itself. Introducing the definitions

$$\boldsymbol{k}_+ \;=\; \frac{1}{2}\,\boldsymbol{K} \,+\, \boldsymbol{q} \qquad \boldsymbol{k}_- \;=\; \frac{1}{2}\,\boldsymbol{K} \,-\, \boldsymbol{q} \,, \tag{12.117}$$

the integral equation of the T-matrix in the plane-wave basis reads [316]

$$< \boldsymbol{k} | \mathsf{T}_{\boldsymbol{K}}(E) | \boldsymbol{k}' > = < \boldsymbol{k} | 2\, \mathsf{V}^{\rm a} | \boldsymbol{k}' >$$

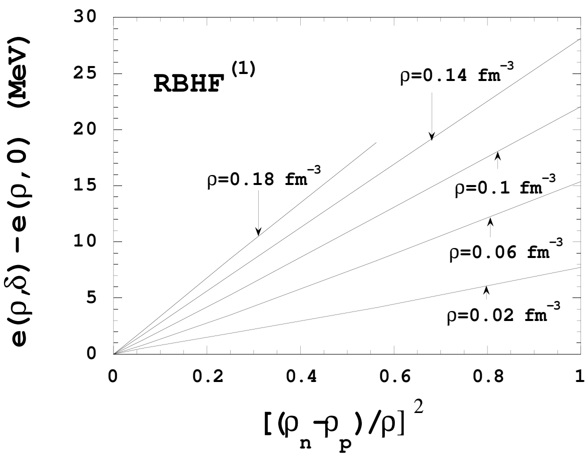

Figure 12.9. Test of the quadratic approximation of the symmetry energy, for five selected densities ρ [449]. The calculations are performed for the RBHF$^{(1)}$ approximation (BM potential A). In accordance with (12.109), the slope of each curve is to a good approximation equal to $e^{\rm sym}(\rho)$. (Reprinted courtesy of *Phys. Rev.*)

$$+ \int \frac{\mathrm{d}^3\boldsymbol{q}}{(2\pi)^3} < \boldsymbol{k}|\mathbf{V}^{\rm a}|\boldsymbol{q} > \boldsymbol{\Lambda}(\boldsymbol{k}_+, \boldsymbol{k}_-; E) < \boldsymbol{q}|\mathbf{T}_{\boldsymbol{K}}(E)|\boldsymbol{k}' > , \qquad (12.118)$$

where $2\,\mathbf{V}^{\rm a} = \mathbf{V} - \mathbf{V}^{\rm ex}$ denotes the antisymmetrized nucleon–nucleon interaction in free space [316]. The non-relativistic $\boldsymbol{\Lambda}^{00}$ nuclear matter propagator has the form [compare with equation (9.54)]

$$\boldsymbol{\Lambda}^{00}(\boldsymbol{k}_+, \boldsymbol{k}_-; E) = \left[E - \frac{\boldsymbol{k}_+^2}{2\,m_B} - \frac{\boldsymbol{k}_-^2}{2\,m_B} + 2\,\mu^B \right]^{-1} , \qquad (12.119)$$

and the non-relativistic Brueckner propagator reads

$$\boldsymbol{\Lambda}^{\rm BHF}(\boldsymbol{k}_+, \boldsymbol{k}_-; E) = 2\,\pi\,\frac{\Theta(|\boldsymbol{k}_+| - k_{F_B})\;\Theta(|\boldsymbol{k}_-| - k_{F_B})}{E - \epsilon^B(|\boldsymbol{k}_+|) - \epsilon^B(|\boldsymbol{k}_-|) + i\,\eta} , \qquad (12.120)$$

whose relativistic counterpart was given in (9.60). The on-shell mass operator in the $\boldsymbol{\Lambda}^{00}$ approximation is given by

$$\Sigma^B(\hat\epsilon_1, \boldsymbol{k}_1) = \frac{1}{2} \sum_{B'} \int \frac{\mathrm{d}^3\boldsymbol{k}_2}{(2\pi)^3} \left\{ \left\langle \frac{\boldsymbol{k}_1 - \boldsymbol{k}_2}{2} \right| \mathbf{T}^{00}_{\boldsymbol{k}_1+\boldsymbol{k}_2}(\hat\epsilon_1^B + \hat\epsilon_2^{B'}) \left| \frac{\boldsymbol{k}_1 - \boldsymbol{k}_2}{2} \right\rangle \right.$$

$$- \left\langle \frac{\boldsymbol{k}_1 - \boldsymbol{k}_2}{2} \middle| \mathsf{T}^{00}_{\boldsymbol{k}_1+\boldsymbol{k}_2}(\hat{\epsilon}^B_1 + \hat{\epsilon}^{B'}_2) \middle| \frac{\boldsymbol{k}_2 - \boldsymbol{k}_1}{2} \right\rangle \Bigg\} , \quad (12.121)$$

where $\hat{\epsilon}^B_i \equiv \epsilon^B(\boldsymbol{k}_i) - \mu^B$ and $i = 1, 2$.

12.6 Collection of selected neutron star matter equations of state

In this section we introduce a broad collection of different, competing models for equation of state of superdense neutron (star) matter. Some of these models describe conventional neutron star matter in phase equilibrium with quarks. Others account for meson condensates or variations in the hyperon population depending on the underlying many-body method. This broad sample of equations of state will be applied in the second part of the book, starting with chapter 13, to the analysis of the structure and stability of models of rapidly spinning neutron and quark matter stars. Non-rotating stellar models will be treated as a byproduct. In doing so, we shall be particularly concerned with testing the compatibility of these equations of state, which predict quite different neutron star properties, with the body of observed data of pulsars – like rotational periods, masses, radii, redshifts, or cooling data. Not all equations of state may accommodate the observed data, specifically the just mentioned rotational periods and masses. This attains its particular interest in view of the rapid discovery pace of millisecond pulsars [477], which imposes the double constraint of fast rotation and a large enough neutron star mass. Moreover, the determination of the smallest possible rotational pulsar period sheds light on the true ground state of strongly interacting matter.

The features of the total collection of equations of state are summarized in table 12.4, and their properties are compiled in tables 12.5 to 12.7. The graphical illustrations are given in figures 12.10 to 12.14. This collection is divided into two categories, that is, non-relativistic potential model equations of state, and relativistic equations of state determined in the framework of the relativistic nuclear field theories discussed in the previous chapters of this book. For the non-relativistic models 12 to 17 of table 12.4, the starting point is a phenomenological nucleon–nucleon interaction, $\boldsymbol{V}_{ij}$. In the case of the equations of state reported here, different two-nucleon potentials, denoted by $\boldsymbol{V}_{ij}$, which fit the nucleon–nucleon scattering data and deuteron properties, have been employed. Most of these two-nucleon potentials are supplemented with three-nucleon interactions, $\boldsymbol{V}_{ijk}$. The Hamiltonian $\mathcal{H}$ is therefore of the form

$$\mathcal{H} = \sum_i \frac{-\hbar^2}{2\,m} \boldsymbol{\nabla}^2_i + \sum_{i<j} \boldsymbol{V}_{ij} + \sum_{i<j<k} \boldsymbol{V}_{ijk} \, . \quad (12.122)$$

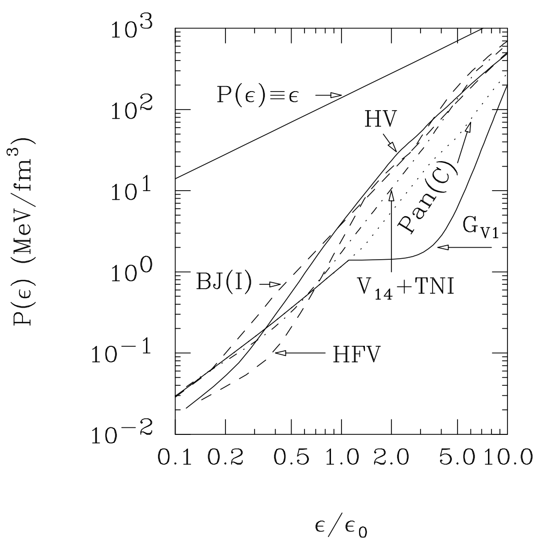

Figure 12.10. Graphical illustration of EOSs BJ(I), Pan(C), V_{14}+TNI, HV, and HFV [446]. Details about these EOSs are listed in table 12.4.

The many-body method adopted to solve the Schroedinger equation is based on the variational approach [478, 479, 480] where a variational trial function $|\Psi_v>$ is constructed from a symmetrized product of two-body correlation operators (F_{ij}) acting on an unperturbed ground state, that is,

$$|\Psi_v> = \Big[\hat{S} \prod_{i<j} F_{ij}\Big] |\Phi> \,, \tag{12.123}$$

where $|\Phi>$ denotes the antisymmetrized Fermi-gas wave function,

$$|\Phi> = \hat{A} \prod_{j} \exp\big(\mathrm{i}\, \boldsymbol{p}_j \cdot \boldsymbol{x}_j\big) \,. \tag{12.124}$$

The correlation operator contains variational parameters which are varied to minimize the energy per baryon for a given density ρ [463, 478, 479, 480],

$$E_{\rm var}(\rho) = \min \left\{ \frac{<\Psi_v \,|\, \mathcal{H} \,|\, \Psi_v>}{<\Psi_v \,|\, \Psi_v>} \right\} \geq E_0 \,. \tag{12.125}$$

As indicated in (12.125), $E_{\rm var}$ constitutes an upper bound to the ground-state energy E_0. The energy density $\epsilon(\rho)$ and pressure $P(\rho)$ are obtained from equations (12.106) and (12.107).

The TF96 equation of state of table 12.4, recently calculated by Strobel *et al* [471], is based on the new Thomas–Fermi approach of Myers and Swiatecki [408, 481, 482, 483, 484]. The effective interaction v_{12} of this new approach consists of the Seyler-Blanchard potential of [485], generalized by the addition of one momentum dependent and one density dependent term [408],

$$v_{12} = -\frac{2\,T_0}{\rho_0}\,Y\big(r_{12}\big) \times \left\{\frac{1}{2}(1\mp\xi)\,\alpha - \frac{1}{2}(1\mp\zeta)\Big(\beta\Big(\frac{p_{12}}{k_{F_0}}\Big)^2 - \gamma\,\frac{k_{F_0}}{p_{12}} + \sigma\Big(\frac{2\bar{\rho}}{\rho_0}\Big)^{\frac{2}{3}}\Big)\right\}. \quad (12.126)$$

The upper (lower) sign in (12.126) corresponds to nucleons with equal (unequal) isospin. The quantities k_{F_0}, T_0 $(= k_{F_0}^2/2m)$, and ρ_0 are the Fermi momentum, the Fermi energy and the particle density of symmetric nuclear matter. The potential's radial dependence is describe by the normalized Yukawa interaction

$$Y\big(r_{12}\big) = \frac{1}{4\,\pi\,a^3}\,\frac{\mathrm{e}^{-\,r_{12}/a}}{r_{12}/a}\,. \quad (12.127)$$

Its strength depends both on the magnitude of the particles' relative momentum, p_{12}, and on an average of the densities at the locations of the particles. The parameters ξ and ζ, generally taken to be different from one another, were introduced in order to achieve better agreement with asymmetric nuclear systems, and the behavior of the optical potential is improved by the term $\sigma(2\bar{\rho}/\rho_0)^{2/3}$. Here the average density is defined by $\overline{\rho}^{2/3} = (\rho_1^{2/3} + \rho_2^{2/3})/2$, where ρ_1 and ρ_2 are the relevant densities of the interacting particle (neutron or protons) at points 1 and 2. For the seven free parameters – adjusted to the properties of finite nuclei, the parameters of the mass formula, and the behavior of the optical potential – the following values were deduced [408]:

$$\alpha = 1.94684\,,\quad \beta = 0.15311\,,\quad \gamma = 1.13672\,,\quad \sigma = 1.05$$
$$\xi = 0.27976 \quad \zeta = 0.55665\,,\quad a = 0.59294 \text{ fm}\,. \quad (12.128)$$

This set of parameters leads to the nuclear matter properties at saturation listed in the last line of table 12.7.

The new force has the advantage over the standard Seyler–Blanchard interaction [485, 486] to not only reproduce the ground-state properties of finite nuclei and infinite symmetric nuclear matter, but also the optical potential and, as revealed by a comparison with the theoretical investigations of Friedman and Pandharipande [383], the properties of pure neutron matter (model V_{14}+TNI in figure 12.10) too. These features make the new Thomas–Fermi model a very attractive method for the investigation of the properties of dense nuclear matter treated in the non-relativistic framework.[1] Aside from V_{14}+TNI, we shown in figure 12.10 also the older, and by now outdated, Pan(C) model for the equation of state of neutron star matter proposed by Pandharipande already back in 1971 [406]. Nevertheless this model attains its particular interest because of its extreme softness – i.e. relatively little pressure for a given density – for it constitutes a lower bound on the pressure that must be provided by a given model for the nuclear equation of state that successfully accommodates both pulsars with rotational periods down to the smallest rotational periods yet known, 1.6 ms, and masses larger than typically $1.5\,M_\odot$. While the former constraint is easily fulfilled by Pan(C) [106, 107], the mass constraint is not. One sees that Pan(C) is considerably softer than the other two non-relativistic equations of state shown in this figure, BJ(I) and V_{14}+TNI. The BJ(I) and Pan(C) models account for baryon population in neutron star matter which leads to a weak flattening of the pressure curves at densities greater than two and four times normal nuclear matter density, respectively. The pressure associated with the relativistic equations of state HV and HFV is shown too for the purpose of comparison. The Hartree–Fock equation of state HFV becomes stiffer than Hartree HV at $\epsilon \gtrsim 3\epsilon_0$ which has its origin in the exchange (Fock) contribution $\Sigma^{\mathrm{F},B}$ to the baryon self-energy. By definition, the exchange term is absent in the Hartree treatment. The structures in the HFV and HV equations of state in the form of a slight softening at densities of around $1.6\,\epsilon_0$ and $2\,\epsilon_0$, respectively, corresponds to the onset of hyperon populations, which set in somewhat earlier than for the two non-relativistic models described just above. As known from figures 7.23 and 7.24, those hyperons that become populated first are the Σ^- and Λ, respectively. A further constraining model on the pressure as a function of density is the equation of state denoted G_{V1} in figure 12.10. It is based on an investigation of the limiting rotational Kepler period of neutron stars that is performed *without* taking recourse to any particular models of dense matter but derives the limit only on the general principles that (a) Einstein's equations describe stellar structure, (b) matter is microscopically stable, and (c) causality is not violated [490]. On this basis, a lower bound for the smallest possible Kepler period for a $M = 1.442\,M_\odot$ neutron star of $P_{\mathrm{K}} = 0.33$ ms was established. Hence, the G_{V1} curve sets an *absolute* limit on rapid rotation on any star bound by gravity. Of course the equation of state that nature has chosen need not be the one that allows stars to rotate

[1] For an early application of the Thomas–Fermi method to the stellar matter problem, see Hartmann *et al* [487]. More recent Thomas–Fermi calculations of the properties of infinite nuclear matter as well as finite nuclei based on the Seyler-Blanchard force can be found in [488, 489].

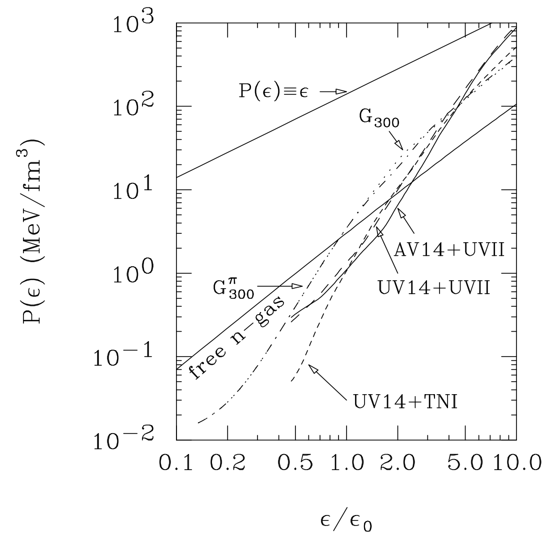

Figure 12.11. Graphical illustration of EOSs AV_{14} + UVII, UV_{14} + UVII, UV_{14}+TNI, G_{300}, and G^{π}_{300} [446]. Details about these EOSs are listed in table 12.4.

most rapidly, so the above is a strict model independent limit.

Figure 12.11 compares the non-relativistic equations of state of Wiringa, Fiks, and Fabrocini (WFF) with two relativistic ones. We recall that only the latter two describe neutron star matter in terms of baryons in generalized β-equilibrium with leptons. The eventual condensation of pions in dense neutron star matter is taken into account in equation of state G^{π}_{300}, additionally to baryon population. According to this equation of state, condensation is predicted to set in at about $1.5\,\epsilon_0$. This can be seen by comparing the dash-dotted and dotted curves in figure 12.11 with one another. At densities $\epsilon \gtrsim 4\,\epsilon_0$ the non-relativistic WFF models behave stiffer than the relativistic ones, violating causality – an issue that will be discussed immediately below – at densities around $8\,\epsilon_0$. The AV_{14}+UVII and UV_{14} + UVII equations of state are rather similar to each other at subnuclear densities which is not the case for the third WFF potential model, UV_{14}+TNI, which accounts for three-nucleon interactions in matter.

A very comforting feature of the relativistic equations of state is that they do not violate causality, that is, the velocity of a signal, given by

$$v_{\mathrm{s}} = c\,\sqrt{\mathrm{d}P/\mathrm{d}\epsilon}\ , \tag{12.129}$$

is smaller than the velocity of light, c, at all densities. This becomes very

Figure 12.12. Velocity of sound, $v_{\rm s}$, in units of the speed of light, c, as a function of energy density calculated for several selected equations of state of table 12.4.

obvious by looking at figure 12.12 which shows the behavior of $v_{\rm s}$ in dense neutron star matter for a few selected equations of state, both relativistic as well as non-relativistic ones. It is however not entirely clear how serious a constraint on the equation of state this constitutes. The reasons being that (12.129) holds exactly only if neutron star matter is neither dispersive nor absorptive [246]. Both is not the case rigorously. Hence, more accurately stated, what is being expressed in (12.129) holds only if the hydrodynamic phase velocity of sound waves, given by $v_\varphi \equiv c\sqrt{{\rm d}P/{\rm d}\epsilon}$, is equal to the velocity of light, which, as just stated, is only the case if effects arising from dispersion and absorption are either absent or insignificantly small. Otherwise one has for the signal velocities $v_{\rm signal} = v_\varphi < c$. If one does accept the relation (12.129) as a criteria for causality violation, then it follows that all the non-relativistic models of our collection of equations of state violate causality, some at smaller densities than others as shown in the last column of table 12.7). However, two of those models, $\rm UV_{14}$+TNI and TF96, do not violate causality up to the highest densities relevant for the construction of models of neutron stars from them. The equations of state BJ(I) and Pan(C) violate causality at about 23 times the density of normal nuclear matter, not much above the central densities of the maximum-mass neutron stars constructed for these equations of state .

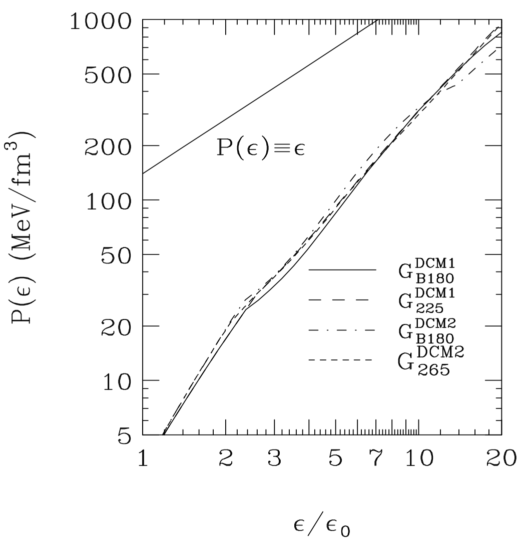

Figure 12.13. Graphical illustration of EOSs G_{B180}^{DCM1}, G_{225}^{DCM1}, G_{B180}^{DCM2}, and G_{265}^{DCM2} [446]. Models G_{B180}^{DCM1} and G_{B180}^{DCM2} account for quark deconfinement. Details about these EOSs are listed in table 12.4.

The equations of state V_{14}+TNI, AV_{14}+UVII and UV_{14}+UVII become superluminal at considerably smaller densities, between six to seven times normal nuclear matter density, which is less than the central densities encountered in the maximum neutron star mass models constructed from these equations of state. Again, the extent to which these conclusions apply rests entirely on (12.129) whose validity as yet seems no to be too compelling.

Asymptotically, the relativistic equations of state approach $P \to \epsilon$ because the repulsion arises from the exchange of vector mesons. Such a behavior of vector meson interactions has been remarked on by Zel'dovich [491, 492]. It can be seen explicitly by examining equations (12.53) and (12.65) for ϵ and P in the limit of large density. As $k_{F_B} \to \infty$, the mass terms in the integrals can be ignored. The σ field is bounded by the order of the baryon mass. Then it follows that [61]

$$\epsilon \longrightarrow \frac{1}{2} \sum_B \Big(\frac{g_{\omega B}}{m_\omega} \, \rho^B \Big)^2 + \frac{1}{2} \sum_B \Big(\frac{g_{\rho B}}{m_\rho} \, I_{3B} \, \rho^B \Big)^2 + \sum_B \frac{2 J_B + 1}{8 \, \pi^2} \, k_{F_B}^4 \,, \tag{12.130}$$

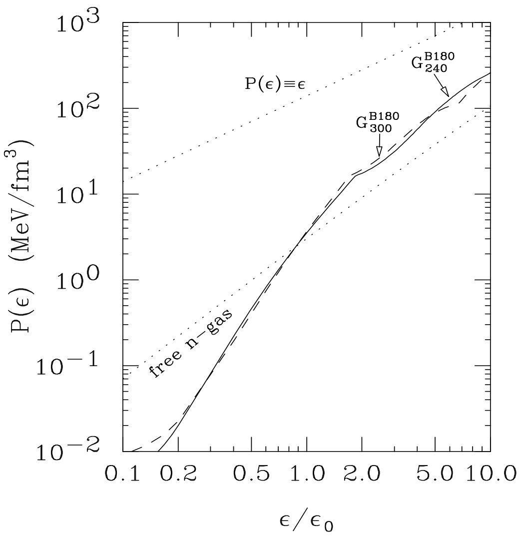

Figure 12.14. Graphical illustration of EOSs G_{B180}^{K240} and G_{B180}^{K300} accounting for quark deconfinement [66]. Details about these EOSs are listed in table 12.4.

and

$$P \longrightarrow \frac{1}{2}\sum_B \Big(\frac{g_{\omega B}}{m_\omega}\,\rho^B\Big)^2 + \frac{1}{2}\sum_B \Big(\frac{g_{\rho B}}{m_\rho}\,I_{3B}\,\rho^B\Big)^2 + \frac{1}{3}\sum_B \frac{2J_B+1}{8\,\pi^2}\,k_{F_B}^4\,. \tag{12.131}$$

Since $\rho^B \propto k_{F_B}^3$, we find from these two relations that P approaches ϵ from *below*, and the speed of sound, $\sqrt{\mathrm{d}P/\mathrm{d}\epsilon}$, approaches but will stay below the speed of light.

The relativistic derivative coupling Lagrangian of Zimanyi and Moszkowski [350] was adopted in the determination of the equations of state denoted by DCM1 in figure 12.13, while those labeled DCM2 correspond to the *hybrid coupling* model. Both types of couplings were described in detail in section 7.3. We recall that in the framework of the latter coupling, the scalar field (σ meson) is coupled to both the Yukawa point *and* derivative coupling to baryons and the ω and ρ-meson vector fields. This improves the agreement with the incompressibility of nuclear matter and effective nucleon mass at saturation density. Zimanyi and Moszkowski originally have introduced a purely derivative coupling of the scalar field to the baryons and mesons. The possibility of a phase

Table 12.4. Overview of the broad collection of neutron star matter EOSs. For their tabulated representations, see appendix J. Further details about these EOSs are compiled in tables 12.5, 12.6 and 12.7.

Label	EOS	Many-body approximation †	References
	Relativistic field-theoretical equations of state		
1	G_{300}	RH	[354]
	$G_{300}^{K^-}$	RH	[354]
	G_{B180}^{K300}	RH + MIT	[66]
2	HV	RH	[61, 79]
3	G_{B180}^{DCM2}	RH + MIT	[88]
	G_{B180}^{K240}	RH + MIT	[66]
4	G_{265}^{DCM2}	RH	[86]
	G_{M78}^{K240}	RH	[66]
5	G_{300}^{π}	RH	[354]
6	G_{200}^{π}	RH	[91]
7	Λ_{Bonn}^{00}+HV	RBHF + RH	[109]
8	G_{225}^{DCM1}	RH	[86]
9	G_{B180}^{DCM1}	RH + MIT	[88]
10	HFV	RHF	[79]
11	Λ_{HEA}^{00}+HFV	RBHF + RHF	[109]
	Λ_{BroB}^{RBHF}+HFV	RBHF + RHF	[459, 449]
	Non-relativistic potential-model equations of state		
12	BJ(I)	Var	[407]
13	UV_{14}+TNI	Var	[463]
14	V_{14}+TNI	Var	[383]
15	UV_{14}+UVII	Var	[463]
16	AV_{14}+UVII	Var	[463]
17	Pan(C)	Var	[406]
18	TF96	TF	[471]

† The following abbreviations are used: RH=Relativistic Hartree, RHF=Relativistic Hartree Fock, RBHF=Relativistic Brueckner Hartree Fock, Var=Variational method, TF=Thomas Fermi method, MIT=MIT bag model.

transition of the dense neutron star core to 3-flavor quark matter, outlined in chapter 8, is taken into account in models G_{B180}^{DCM1} and G_{B180}^{DCM2} of figure 12.13, and G_{B180}^{K240} and G_{B180}^{K300} of figure 12.14. The transition sets in typically somewhat about $2\,\epsilon_0$ and, because it introduces additional degrees of freedom, lowers the pressure for a given density relative to those equations of state which stay in the confined hadronic matter phase. The

Table 12.5. Properties of the relativistic, field-theoretical EOSs listed in table 12.4.

Label	EOS	Composition	Interaction (meson exchange)
1	G_{300}	$p, n, \Lambda, \Sigma^{\pm,0}, \Xi^{0,-}, e^-, \mu^-$	σ, ω, ρ
	$G_{300}^{K^-}$	$p, n, \Lambda, \Sigma^{\pm,0}, \Xi^{0,-}, e^-, \mu^-$	σ, ω, ρ
		$+ K^-$ condensate	
	G_{B180}^{K300}	$p, n, \Lambda, \Sigma^{\pm,0}, \Xi^{0,-}, e^-, \mu^-$	σ, ω, ρ
		$+ u, d, s$ quark matter	
2	HV	$p, n, \Lambda, \Sigma^{\pm,0}, \Xi^{0,-}, e^-, \mu^-$	σ, ω, ρ
3	G_{B180}^{DCM2}	$p, n, \Lambda, \Sigma^{\pm,0}, \Xi^{0,-}, e^-, \mu^-$	σ, ω, ρ
		$+ u, d, s$ quark matter	
	G_{B180}^{K240}	$p, n, \Lambda, \Sigma^{\pm,0}, \Xi^{0,-}, e^-, \mu^-$	σ, ω, ρ
		$+ u, d, s$ quark matter	
4	G_{265}^{DCM2}	$p, n, \Lambda, \Sigma^{\pm,0}, \Xi^{0,-}, e^-, \mu^-$	σ, ω, ρ
	G_{M78}^{K240}	$p, n, \Lambda, \Sigma^{\pm,0}, \Xi^{0,-}, e^-, \mu^-$	σ, ω, ρ
5	G_{300}^{π}	$p, n, \Lambda, \Sigma^{\pm,0}, \Xi^{0,-}, e^-, \mu^-$	σ, ω, ρ
		$+ \pi^-$ condensate	
6	G_{200}^{π}	$p, n, \Lambda, \Sigma^{\pm,0}, \Xi^{0,-}, e^-, \mu^-$	σ, ω, ρ
		$+ \pi^-$ condensate	
7	Λ_{Bonn}^{00}+HV	$p, n, \Lambda, \Sigma^{\pm,0}, \Xi^{0,-}, e^-, \mu^-$	$\sigma, \omega, \pi, \rho, \eta, \delta$
8	G_{225}^{DCM1}	$p, n, \Lambda, \Sigma^{\pm,0}, \Xi^{0,-}, e^-, \mu^-$	σ, ω, ρ
9	G_{B180}^{DCM1}	$p, n, \Lambda, \Sigma^{\pm,0}, \Xi^{0,-}, e^-, \mu^-$	σ, ω, ρ
		$+ u, d, s$ quark matter	
10	HFV	$p, n, \Lambda, \Sigma^{0,-}, \Delta^-, e^-, \mu^-$	$\sigma, \omega, \pi, \rho$
11	Λ_{HEA}^{00}+HFV	$p, n, \Lambda, \Sigma^{0,-}, \Delta^-, e^-, \mu^-$	$\sigma, \omega, \pi, \rho, \eta, \delta, \phi$
	Λ_{BroB}^{RBHF}+HFV	$p, n, \Lambda, \Sigma^{0,-}, \Delta^-, e^-, \mu^-$	$\sigma, \omega, \pi, \rho, \eta, \delta$

mixed quark–hadron phase ends, that is, the pure quark phase begins, between ~ 7 and $15\,\epsilon_0$, depending on the input parameters (cf. table 7.1). We stress again that these density values are rather different from those determined by others in earlier investigations on the quark–hadron phase transition in neutron star matter for reasons that have been outlined in chapter 8. As we shall see in section 17.3.3, neutron star models constructed for these equations of state contain – besides nucleons and hyperons – a large percentage of u, d and s quarks in their interiors. For that reason such objects are called *hybrid stars* [88]. We recall that the notion *hybrid* is used for both the chosen type of nuclear coupling, i.e. hybrid derivative coupling or standard Yukawa coupling as discussed in section 7.3, as well as the quark–hadron composition of neutron star matter. If not stated

Table 12.6. Properties of the non-relativistic EOSs listed in table 12.4.

Label	EOS	Composition	Interaction
12	BJ(I)	$p, n, \Lambda, \Sigma^{\pm,0}, \Xi^{0,-}, \Delta, e^-, \mu^-$	2-nucleon potential
13	UV_{14}+TNI	p, n, e^-, μ^-	2-nucleon potential V_{14} +3-nucleon interaction
14	V_{14}+TNI	n	2-nucleon potential V_{14} +3-nucleon interaction
15	UV_{14}+UVII	p, n, e^-, μ^-	2-nucleon potential V_{14} +3-nucleon potential VII
16	AV_{14}+UVII	p, n, e^-, μ^-	2-nucleon potential AV_{14} +3-nucleon potential VII
17	Pan(C)	$p, n, \Lambda, \Sigma^{\pm,0}, \Xi^{0,-}, \Delta, e^-, \mu^-$	2-nucleon potential
18	TF96	p, n, e^-, μ^-	Seyler-Blanchard

otherwise, henceforth the notion hybrid will take reference to the star's composition. A bag constant of $B^{1/4} = 180$ MeV has been used in each case for the determination of the above hybrid-star matter equations of state. This choice places the energy per baryon of u, d, s quark matter at about 1100 MeV, way above the energy per baryon in infinite nuclear matter. Hence, u, d, s quark matter here is far from being absolutely stable. The latter option, absolute stability, was discussed in section 2.3.1, where we found that strange quark matter, made up entirely of chemically equilibrated u, d, s quarks, can be absolutely stable in the framework of the bag model for some range of parameters, like bag constants that lie in the range $145 \leq B^{1/4} \leq 160$ MeV for a free, relativistic massless quark gas. Of course, the bag model computations are no doubt unreliable. So whether or not strange matter is indeed absolutely stable is probably outside the predictive ability of the bag model. Nevertheless one may argue that some of the qualitative features extracted from the perturbative analysis may surely have some correspondence in the full non-perturbative theory. In any event, we can conclude for sure that *if* strange quark matter should indeed be absolutely stable, then a mixed quark–hadron phase can not exist inside neutron stars (cf. section 2.3).

A further difference between the two categories of equations of state of our collection originates not only from the quark degrees of freedom taken into account in a few of these models, but from the different baryonic degrees of freedom too. So do not all the non-relativistic equations of state describe neutron star matter in full β-equilibrium between nucleons and hyperons, as can be seen from entries 13 through 16 and 18 in

Table 12.7. Nuclear matter properties at saturation density of the EOSs compiled in table 12.4. The listed quantities are: energy per baryon E/A, incompressibility K, effective nucleon mass M^*, ($\equiv m_N^*/m_N$), symmetry energy $a_{\rm sym}$.

Label	EOS	E/A (MeV)	ρ_0 (fm^{-3})	K (MeV)	M^* (MeV)	$a_{\rm sym}$ (MeV)	ϵ/ϵ_0 †
		Relativistic field-theoretical EOSs					
1	G_{300}	-16.3	0.153	300	0.78	32.5	–
	$\mathrm{G}_{\mathrm{B180}}^{\mathrm{K300}}$	-16.3	0.153	300	0.70	32.5	–
2	HV	-15.98	0.145	285	0.77	36.8	–
3	$\mathrm{G}_{\mathrm{B180}}^{\mathrm{DCM2}}$	-16.0	0.16	265	0.796	32.5	–
	$\mathrm{G}_{\mathrm{B180}}^{\mathrm{K240}}$	-16.3	0.153	240	0.78	32.5	–
4	$\mathrm{G}_{265}^{\mathrm{DCM2}}$	-16.0	0.16	265	0.796	32.5	–
	$\mathrm{G}_{\mathrm{M78}}^{\mathrm{K240}}$	-16.3	0.153	240	0.78	32.5	–
5	G_{300}^{π}	-16.3	0.153	300	0.78	32.5	–
6	G_{200}^{π}	-15.95	0.145	200	0.8	36.8	–
7	$\Lambda_{\mathrm{Bonn}}^{00}$+HV	-11.9	0.134	186	0.79	21.3	–
8	$\mathrm{G}_{225}^{\mathrm{DCM1}}$	-16.0	0.16	225	0.796	32.5	–
9	$\mathrm{G}_{\mathrm{B180}}^{\mathrm{DCM1}}$	-16.0	0.16	225	0.796	32.5	–
10	HFV	-15.54	0.159	376	0.62	30	–
11	$\Lambda_{\mathrm{HEA}}^{00}$+HFV	$-\ 8.7$	0.132	115	0.82	29	–
	$\Lambda_{\mathrm{BroB}}^{\mathrm{RBHF}}$+HFV	-15.73	0.172	249	0.73	34.3	–
		Non-relativistic potential-model EOSs					
12	BJ(I)	~ -10	~ 0.18	–	–	–	23.1
13	UV_{14}+TNI	-16.6	0.157	261	0.65	30.8	14
14	V_{14}+TNI	-16.00	0.159	240	0.64	–	5.6
15	UV_{14}+UVII	-11.5	0.175	202	0.79	29.3	6.5
16	AV_{14}+UVII	-12.4	0.194	209	0.66	27.6	7.2
17	Pan(C)	~ -10	~ 0.18	60	–	35	23.6
18	TF96	-16.24	0.161	234	–	32.7	13

† Energy density in units of normal nuclear matter density beyond which the velocity of sound in neutron matter becomes superluminal, that is, $v_{\rm s}/c > 1$. No entry means that causality is not violated.

table 12.4). What these models describe is neutron star matter composed of only neutrons, or made up of neutrons and protons in β-equilibrium with electrons and muons, neither of which however is the true ground state of neutron star matter predicted by theory [61, 62, 406, 407]. Indeed already the very early discussion of Ambartsumyan and Saakyan [493] based on a Fermi gases made a very plausible case for the existence of a hyperon charge on neutron stars. This was confirmed by later

Chapter 13

General relativity in a nutshell

With central mass densities of up to several 10^{15} g/cm^3, neutron stars and their hypothetical strange counterparts constitute objects of highly compressed matter. As already remarked at the beginning of this book (see, for instance, figure 3.2), such objects possess masses of $M \sim 1.5\,M_\odot$ and radii of $R \sim 10$ km making the ratio $2M/R$, which may be considered as a critical measure for the 'strength' of gravity, as large as bout 40% or more.[1] For such large values of $2M/R$ the geometry of spacetime is changed considerably from flat space. It is therefore imperative to construct models of neutron and strange quark matter stars framework of Einstein's general theory of relativity, in which the gravitational force is replace by the concept of curved spacetime, as caused by a compact star. Besides the crucial classical tests of Einstein's theory, which allow one to discriminate between the predictions of the general theory of relativity and that of Newtonian theory, each one deciding unequivocally in favor of the general theory of relativity, recently Hulse and Taylor were able to test the validity of Einstein's theory from studying the motion of the binary pulsars system PSR 1913+16 [133]. Their study confirmed the theory with unprecedented accuracy.

In general relativity the curvature in the geometry of four-dimensional spacetime, which manifests itself as gravitation (and vice versa), is the result of mass. In the case of a compact stellar configuration, it is the star's mass that acts as the source which curves the geometry of spacetime inside and outside of the star. If the star is rotating, then the so-called Lense–Thirring [505] or frame dragging effect comes into play, which describes the onset of rotation of the local inertial frames, induced by the mass of the rotating star, in the direction of the star's rotation (see, for example,

[1] For the purpose of comparison, this ratio amounts about 10^{-6} for the sun, 10^{-9} for the Earth, and 10^{-25} for a human body.

references [506, 507, 508, 509]). This effect has no analogy in classical Newtonian mechanics and therefore may be hard to be imagined intuitively. At the bottom of the heart of this effect lies the question of whether or not non-uniform motion is, like uniform motion, relative too. It was studied by Newton in 1686 using a vessel filled with water. He argued that a bucket's rotation was absolute because water in it will be forced up the sides of the vessel due to the centrifugal force. If the bucket is considered fixed and the cosmos rotating about it, then what causes the water to rise up the sides of the vessel? In 1883, E. Mach reexamined Newton's discussion of inertial forces on a fluid contained in a rotating vessel, in an attempt to understand better how inertial forces arise. He suggested that the shape of a water surface may depend on the rotation of the vessel if the sides of the vessel increase in thickness and mass till they were ultimately several leagues thick. The calculation of such effects became possible when Einstein formulated his general theory of relativity in 1916, and was carried out in 1918 by Thirring[505]. Using the weak-field approximation to Einstein's equations, he found that a slowly rotating mass shell drags along the inertial frames within it. More recently, Brill and Cohen clarified the connection of the frame dragging effect with Mach's principle [508]. Thirring's result is valid only when the induced rotation rate is small compared to the rotation rate of the shell. For decades the frame dragging problem remained dormant, for it appeared to have only little physical significance for actual stellar phenomena. The observation of rapidly spinning neutron stars whose enormous mass concentrations in their centers cause the local inertial frames there to corotate at about half the star's rotational frequency, as we shall see in chapters 15 and 17, has renewed considerable interest in this phenomenon.

Before we proceed to the construction of models of neutron and strange matter stars, the general theory of relativity, which culminate in Einstein's field equations, will be reviewed next. We begin with putting together some basic elements of tensor analysis.

13.1 Some formulae of tensor analysis

As in flat spacetime, generalized coordinates in curved four-dimensional space are denoted as $x^\mu = x^0, x^1, x^2, x^3$, $x'^\mu = x'^0, x'^1, x'^2, x'^3$, etc, where $\mu, \nu, \ldots$ assume values 0,1,2,3. In our case, the zero-components of x^μ generally refers to time, t, while x^1, x^2, x^3 stand for r, θ, ϕ. The new set of coordinates x'^μ are functions of the old coordinates by the functions $x'^\mu = x'^\mu(x^0, x^1, x^2, x^3)$. Generally, superscripts refer to *contravariant* quantities, while subscripts indicate *covariant* quantities. Multiplication of a contravariant vector a^μ with a covariant vector b_μ gives [510]

$$a^\mu\, b_\mu \equiv \sum_{\mu=0}^{4} a^\mu\, b_\mu = a^0\, b_0 + a^1\, b_1 + a^2\, b_2 + a^3\, b_3\,. \tag{13.1}$$

As indicated in (13.1) the double occurrence of dummy suffixes in a given term of a tensor expression will always be taken to denote summation over the four values 1,2,3,4. Multiplication of contravariant and covariant tensors of rank two gives

$$a^{\mu\nu}\, b_{\mu\nu} \equiv \sum_{\mu=0}^{4}\sum_{\nu=0}^{4} a^{\mu\nu}\, b_{\mu\nu} = a^{00}\, b_{00} + a^{01}\, b_{01} + \ldots + a^{33}\, b_{33}\,, \tag{13.2}$$

where generally the rank r of a tensor is equal to the total number of indices $\mu, \nu, \ldots$ carried by a quantity. The values of a contravariant tensor of rank two, $T^{\alpha\beta}$, are transformed in accordance with

$$T'^{\mu\nu} = \frac{\partial x'^\mu}{\partial x^\alpha}\, \frac{\partial x'^\nu}{\partial x^\beta}\, T^{\alpha\beta}\,, \tag{13.3}$$

while for a covariant tensor of the same rank

$$T'_{\mu\nu} = \frac{\partial x^\alpha}{\partial x'^\mu}\, \frac{\partial x^\beta}{\partial x'^\nu}\, T_{\alpha\beta}\,. \tag{13.4}$$

Tensors of mixed contravariant and covariant nature or of higher rank can be similarly defined in accordance with the general expression

$$T'^{\mu\nu\ldots}_{\ \rho\sigma\ldots} = \frac{\partial x'^\mu}{\partial x^\alpha}\, \frac{\partial x'^\nu}{\partial x^\beta}\, \frac{\partial x^\gamma}{\partial x'^\rho}\, \frac{\partial x^\delta}{\partial x'^\sigma}\, \ldots\, T^{\ \alpha\beta\ldots}_{\ \gamma\delta\ldots}\,. \tag{13.5}$$

We recall that the requirement that any relativistic equation must remain invariant under coordinate transformation (covariance), that is, its mathematical structure must be the same in all coordinate systems is one of the key elements of general relativity. This is not to be confused, however, with the fact that the content of the equations of physics may change when we change to new coordinate systems as due to a change in gravitational field rather than to a change in the absolute motion of the spatial framework, as the principle of equivalence permits us. The requirement of covariance is automatically fulfilled by tensor equations. Examples of tensors of different rank are listed in the following. Let us begin with the simplest case, namely a tensor of rank zero (scalar invariant). It transforms under (13.5) as:

$$s' = s\,. \tag{13.6}$$

Contravariant tensor of rank one (vector):

$$a'^{\mu} = \frac{\partial x'^{\mu}}{\partial x^{\alpha}}\, a^{\alpha}\,. \tag{13.7}$$

Covariant tensor of rank one:

$$a'_{\mu} = \frac{\partial x^{\alpha}}{\partial x'^{\mu}}\, a_{\alpha}\,. \tag{13.8}$$

Mixed tensor of rank two:

$$T'^{\nu}_{\mu} = \frac{\partial x'^{\nu}}{\partial x^{\alpha}}\, \frac{\partial x^{\beta}}{\partial x'^{\mu}}\, T^{\ \alpha}_{\beta}\,. \tag{13.9}$$

Symmetric tensor:

$$T^{\,\mu\nu} = T^{\,\nu\mu}\,. \tag{13.10}$$

Metric tensor:

$$g^{\mu\nu} = g^{\nu\mu}\,. \tag{13.11}$$

An infinitesimal difference in coordinate position is given by $\mathrm{d}x^{\mu} \equiv \mathrm{d}x^0, \mathrm{d}x^1, \mathrm{d}x^2, \mathrm{d}x^3$ from which one obtains for the scalar interval (line element) $\mathrm{d}s$ associated with $\mathrm{d}x^{\mu}$ the expression

$$\mathrm{d}s^2 = g_{\mu\nu}\, \mathrm{d}x^{\mu}\, \mathrm{d}x^{\nu}\,. \tag{13.12}$$

The determinant formed from the components of $g_{\mu\nu}$ is abbreviated to

$$g \equiv \det(g_{\mu\nu}) \equiv |g_{\mu\nu}|\,. \tag{13.13}$$

Finally we note that the components of the mixed tensor g^{ν}_{μ} are given by

$$g^{\nu}_{\mu} = \delta^{\nu}_{\mu} = \begin{cases} 1 & \text{if } \ \mu = \nu\ , \\ 0 & \text{if } \ \mu \neq \nu\ . \end{cases} \tag{13.14}$$

The Galilean values of $g_{\mu\nu}$ in flat space are $\delta_{\mu\nu} = \pm 1, 0$, where only the diagonal components are different from zero.

13.2 Tensor manipulations

Raising, lowering, and change of indices is accomplished via the metric tensor $g^{\mu\nu}$ as follows:

$$a^{\nu} = g^{\nu\mu}\, a_{\mu}\,, \quad a_{\mu} = g^{\mu\nu}\, a^{\nu}\,, \quad a^{\nu} = g^{\nu}_{\mu}\, a^{\mu}\,. \tag{13.15}$$

Other frequently encountered manipulations are:

Contraction,

$$T_{\nu}^{\ \nu} = g_{\nu\mu} T^{\nu\mu} = T_{0}^{\ 0} + T_{1}^{\ 1} + T_{2}^{\ 2} + T_{3}^{\ 3} \,. \tag{13.16}$$

Addition,

$$a_\mu = b_\mu + c_\mu = (b_0 + c_0), (b_1 + c_1), (b_2 + c_2), (b_3 + c_3) \,. \tag{13.17}$$

Outer product,

$$\begin{aligned} a_\mu^\nu = b_\mu\, c^\nu = {} & b_0\, c^0 \quad b_0\, c^1 \quad b_0\, c^2 \quad b_0\, c^3 \\ & b_1\, c^0 \quad b_1\, c^1 \quad b_1\, c^2 \quad b_1\, c^3 \\ & b_2\, c^0 \quad b_2\, c^1 \quad b_2\, c^2 \quad b_2\, c^3 \\ & b_3\, c^0 \quad b_3\, c^1 \quad b_3\, c^2 \quad b_3\, c^3 \,. \end{aligned} \tag{13.18}$$

Inner product,

$$a = a_\nu^\nu = b_\nu\, c^\nu = b_0\, c^0 + b_1\, c^1 + b_2\, c^2 + b_3\, c^3 \,. \tag{13.19}$$

13.3 Einstein's field equations

Equipped with the mathematical formalism summarized in sections 13.1 and 13.2, we now proceed to the formulation of Einstein's general theory of relativity, which, as mentioned before, culminates in his field equations. The basis elements of this theory can be formulated as follows [511]:

(i) The geometry of spacetime is described by the line element, $\mathrm{d}s$, given by $\mathrm{d}s^2 = g_{\mu\nu}\, \mathrm{d}x^\mu\, \mathrm{d}x^\nu$. The metric tensor is itself a function of spacetime coordinates.

(ii) The amount of mass energy in a unit volume is determined by the stress–energy (energy–momentum) tensor $T^{\mu\nu}$. For a gas or perfect fluid,

$$T^{\mu\nu} = (\epsilon + P)\, u^\mu\, u^\nu + P\, g^{\mu\nu} \,, \tag{13.20}$$

where ϵ is the energy density of the matter as measured in its restframe, P is the pressure, and u^μ is the four-velocity of the gas. A perfect fluid is a fluid or gas that moves trough spacetime with a four-velocity which may vary from event to event, and exhibits a density of mass energy ϵ and an isotropic pressure P in the restframe of each fluid element. Shear stresses, anisotropic pressure, and viscosity must be absent, or the fluid is not perfect.

(iii) Conservation of energy–momentum,

$$\frac{1}{\sqrt{-g}}\frac{\partial}{\partial x^\nu}\left(\sqrt{-g}\,T^{\ \nu}_{\mu}\right)-\frac{1}{2}\,T^{\,\nu\lambda}\,\frac{\partial}{\partial x^\mu}\,g_{\nu\lambda}=0\,, \tag{13.21}$$

where $g=\det(g_{\mu\nu})$. For a perfect fluid in flat space one immediately derives from (13.20)

$$\frac{\partial}{\partial x^\nu}T^{\,\mu\nu}\,,=\frac{\partial P}{\partial x_\mu}+\frac{\partial}{\partial x^\nu}\left[(\epsilon+P)\,u^\mu\,u^\nu\right]=0\,, \tag{13.22}$$

and by substituting $u^i=v^i\,u^0$ it becomes Euler's equation,

$$\frac{\partial \boldsymbol{v}}{\partial t}+(\boldsymbol{v}\cdot\boldsymbol{\nabla})\,\boldsymbol{v}=-\,\frac{1-\boldsymbol{v}^2}{\epsilon+P}\left(\boldsymbol{\nabla}\,P+\boldsymbol{v}\,\frac{\partial P}{\partial t}\right). \tag{13.23}$$

(iv) Riemann–Christoffel curvature tensor, $R^{\,\tau}{}_{\mu\nu\sigma}$, is the agent by which curves in spacetime produce the relative acceleration of geodesics,

$$R^{\,\tau}{}_{\mu\nu\sigma}=\frac{\partial}{\partial x^\nu}\,\Gamma^\tau_{\mu\sigma}-\frac{\partial}{\partial x^\sigma}\,\Gamma^\tau_{\mu\nu}+\Gamma^\kappa_{\mu\sigma}\,\Gamma^\tau_{\kappa\nu}-\Gamma^\kappa_{\mu\nu}\,\Gamma^\tau_{\kappa\sigma}\,. \tag{13.24}$$

(v) Christoffel symbols (of the second kind), which are not third-rank tensors, are defined by the relations

$$\Gamma^\sigma_{\mu\nu}\equiv\frac{1}{2}\,g^{\sigma\lambda}\left(\frac{\partial}{\partial x^\nu}\,g_{\mu\lambda}+\frac{\partial}{\partial x^\mu}\,g_{\nu\lambda}-\frac{\partial}{\partial x^\lambda}\,g_{\mu\nu}\right), \tag{13.25}$$

where

$$\Gamma^\sigma_{\lambda\sigma}=\frac{\partial}{\partial x^\lambda}\log_{\mathrm{e}}\sqrt{-g}=\frac{1}{\sqrt{-g}}\,\frac{\partial}{\partial x^\lambda}\,\sqrt{-g}\,, \tag{13.26}$$

which alternatively can be written as

$$\Gamma^\sigma_{\lambda\sigma}=\Gamma^\sigma_{\sigma\lambda}=\frac{1}{2}\,g^{\mu\nu}\,\frac{\partial}{\partial x^\lambda}\,g_{\mu\nu}\,. \tag{13.27}$$

Notice that the Christoffel symbols obey $\Gamma^\sigma_{\mu\nu}=\Gamma^\sigma_{\nu\mu}$. The Christoffel symbol of the first kind are defined as

$$\begin{aligned}[\lambda\nu,\mu]&\equiv g_{\mu\sigma}\,\Gamma^\sigma_{\lambda\nu}\\ &=\frac{1}{2}\,g_{\mu\sigma}\,g^{\sigma\tau}\Big(\frac{\partial}{\partial x^\nu}\,g_{\lambda\tau}+\frac{\partial}{\partial x^\lambda}\,g_{\nu\tau}-\frac{\partial}{\partial x^\tau}\,g_{\lambda\nu}\Big)\\ &=\frac{1}{2}\Big(\frac{\partial}{\partial x^\nu}\,g_{\lambda\mu}+\frac{\partial}{\partial x^\lambda}\,g_{\nu\mu}-\frac{\partial}{\partial x^\mu}\,g_{\lambda\nu}\Big)=[\lambda\nu,\mu]\,.\end{aligned} \tag{13.28}$$

(vi) Using the Christoffel symbols, the equation expressing the conservation of energy–momentum becomes

$$T^{\mu\nu}{}_{;\sigma} = \frac{\partial}{\partial x^\sigma} T^{\mu\nu} + \Gamma^\mu_{\lambda\sigma} T^{\lambda\nu} + \Gamma^\nu_{\lambda\sigma} T^{\mu\lambda} , \tag{13.29}$$

or

$$T^{\mu\nu}{}_{;\mu} = \frac{\partial}{\partial x^\mu} T^{\mu\nu} + \Gamma^\mu_{\lambda\mu} T^{\lambda\nu} + \Gamma^\nu_{\lambda\mu} T^{\mu\lambda} , \tag{13.30}$$

$$= \frac{1}{\sqrt{-g}} \frac{\partial}{\partial x^\mu} \left(\sqrt{-g}\, T^{\mu\nu}\right) + \Gamma^\nu_{\lambda\mu} T^{\mu\lambda} . \tag{13.31}$$

(vii) Above, the semicolon denotes the covariant divergence. For a contravariant vector, a^μ, and a covariant vector, a_μ, the covariant derivatives are

$$a^\mu{}_{;\nu} = \frac{\partial}{\partial x^\nu} a^\mu + \Gamma^\mu_{\lambda\nu} a^\lambda \tag{13.32}$$

and

$$a_{\mu;\nu} = \frac{\partial}{\partial x^\nu} a_\mu - \Gamma^\lambda_{\mu\nu} a_\lambda . \tag{13.33}$$

For any vector

$$a^\mu{}_{;\mu} = \frac{\partial}{\partial x^\mu} a^\mu + \Gamma^\mu_{\lambda\mu} a^\lambda = \frac{1}{\sqrt{-g}} \frac{\partial}{\partial x^\lambda} \left(\sqrt{-g}\, a^\lambda\right) . \tag{13.34}$$

The following properties hold:

$$(A\, a^\mu{}_\nu + B\, b^\mu{}_\nu)_{;\lambda} = A\, a^\mu{}_{\nu;\lambda} + B\, b^\mu{}_{\nu;\lambda} , \tag{13.35}$$

$$(a^\mu{}_\nu\, b^\lambda)_{;\kappa} = a^\mu{}_{\nu;\kappa}\, b^\lambda + a^\mu{}_\nu\, b^\lambda{}_{;\kappa} . \tag{13.36}$$

For tensors we note that

$$\left(T^{\ldots\nu\ldots}_{\ldots\mu\ldots}\right)_{;\sigma} = \frac{\partial T^{\ldots\nu\ldots}_{\ldots\mu\ldots}}{\partial x^\sigma} + \Gamma^\nu_{\sigma\lambda} T^{\ldots\lambda\ldots}_{\ldots\mu\ldots} + \ldots - \Gamma^\lambda_{\mu\sigma} T^{\ldots\nu\ldots}_{\ldots\lambda\ldots} - \ldots , \tag{13.37}$$

where '$+\ldots$' ('$-\ldots$') indicates that a similar term is to be added (subtracted) for each additional contravariant (covariant) index. Examples of (13.37) are

$$T^{\mu\lambda}{}_{\lambda;\sigma} = \frac{\partial}{\partial x^\sigma} T^{\mu\lambda}{}_\lambda + \Gamma^\mu_{\sigma\kappa} T^{\kappa\lambda}{}_\lambda , \tag{13.38}$$

$$g_{\mu\nu;\,\lambda} = \frac{\partial}{\partial x^\lambda}\, g_{\mu\nu} - \Gamma^\kappa_{\mu\lambda}\, g_{\kappa\nu} - \Gamma^\kappa_{\nu\lambda}\, g_{\mu\kappa} = 0\,. \tag{13.39}$$

Moreover we note for tensors

$$g_{\mu\nu,\lambda} \equiv \frac{\partial}{\partial x^\lambda}\, g_{\mu\nu} = \Gamma^\kappa_{\lambda\mu}\, g_{\kappa\nu} + \Gamma^\kappa_{\lambda\nu}\, g_{\kappa\mu}\,, \tag{13.40}$$

$$g^{\mu\nu}{}_{,\lambda} \equiv \frac{\partial}{\partial x^\lambda}\, g^{\mu\nu} = -\,\Gamma^\mu_{\kappa\lambda}\, g^{\kappa\nu} - \Gamma^\nu_{\kappa\lambda}\, g^{\kappa\mu}\,, \tag{13.41}$$

$$g^{\nu\mu}{}_{;\lambda} = g^{\mu\nu}{}_{;\lambda} = 0\,. \tag{13.42}$$

(viii) The production of curvature by mass energy is specified by Einstein's field equations,

$$G_{\mu\nu} = 8\,\pi\, T_{\mu\nu}\,, \quad \text{where} \quad G_{\mu\nu} \equiv R_{\mu\nu} - \frac{1}{2}\, g_{\mu\nu}\, R \tag{13.43}$$

is the Einstein tensor, which for empty space reduce to

$$R_{\mu\nu} = 0\,. \tag{13.44}$$

The Ricci tensor is obtained from the Riemann tensor by contraction, that is, $R_{\mu\nu} = R^\tau{}_{\mu\sigma\nu}\, g^\sigma{}_\tau = R^\tau{}_{\mu\tau\nu}$, which leads to

$$R_{\mu\nu} = \frac{\partial}{\partial x^\nu}\, \Gamma^\sigma_{\mu\sigma} - \frac{\partial}{\partial x^\sigma}\, \Gamma^\sigma_{\mu\nu} + \Gamma^\kappa_{\mu\sigma}\, \Gamma^\sigma_{\kappa\nu} - \Gamma^\kappa_{\mu\nu}\, \Gamma^\sigma_{\kappa\sigma} \tag{13.45}$$

$$= \frac{\partial}{\partial x^\sigma}\, \Gamma^\sigma_{\mu\nu} + \Gamma^\sigma_{\mu\lambda}\, \Gamma^\lambda_{\sigma\nu} + \frac{\partial^2}{\partial x^\mu \partial x^\nu} \log_{\mathrm{e}}\sqrt{-g} - \Gamma^\lambda_{\mu\nu} \frac{\partial}{\partial x^\lambda} \log_{\mathrm{e}}\sqrt{-g}\,. \tag{13.46}$$

The scalar curvature of spacetime, R, also known as the Ricci scalar follows from Ricci's tensor as

$$R = R_{\mu\nu}\, g^{\mu\nu} = R^\mu{}_\mu. \tag{13.47}$$

Einstein's field equations follow from the assumptions that the ratio of gravitational and inertial mass is a universal constant, that the laws of nature are expressed in the simplest possible set of equations that are covariant for all systems of spacetime coordinates, and that the laws of special relativity hold locally in a coordinate system with a vanishing gravitational field.

(ix) In a gravitational field, a particle moves along a geodesic line which is specified by the geodesic differential equation

$$\frac{\mathrm{d}^2 x^\mu}{\mathrm{d}s^2} + \Gamma^\mu_{\kappa\sigma} \frac{\mathrm{d}x^\kappa}{\mathrm{d}s} \frac{\mathrm{d}x^\sigma}{\mathrm{d}s} = 0\,. \tag{13.48}$$

Light rays are represented by null geodesics for which $\mathrm{d}s = 0$

(x) An observer's proper reference frame is formed by an orthonormal tetrad which keeps its time-leg tangent to the observer's world line. Expressed in less mathematical terms, the measurements performed by an observer, who moves along a worldline trough spacetime, in his own neighborhood (with distances small compared to the radii of curvature of spacetime) are called the values of the measured quantities relative to the observer's proper reference frame. The laws of physics expressed in the proper reference frame are those of flat spacetime (i.e. special relativity) as augmented by an inertial (or, according to the equivalence principle, gravitational) acceleration.

(xi) An observer's proper time, τ, is governed by the metric along his world line,

$$\mathrm{d}\tau = \sqrt{-\,\mathrm{d}s^2} = \sqrt{-\,g_{\mu\nu}\,\mathrm{d}x^\mu\,\mathrm{d}x^\nu}\,, \tag{13.49}$$

where the world line is described by any time parameter, t, $x^\nu = x^\nu(t)$.

(xii) In any infinitesimal neighborhood of any point in spacetime, the proper time intervals must satisfy the laws of special relativity. That is, locally the line element, $\mathrm{d}s$, becomes the Minkowski metric given in rectangular coordinates by

$$\mathrm{d}s^2 = -\mathrm{d}t^2 + \mathrm{d}x^2 + \mathrm{d}y^2 + \mathrm{d}z^2\,, \tag{13.50}$$

and by

$$\mathrm{d}s^2 = -\mathrm{d}t^2 + \mathrm{d}r^2 + r^2\,\mathrm{d}\theta^2 + r^2\,\sin^2\theta\,\mathrm{d}\phi^2 \tag{13.51}$$

in the case of spherical coordinates. In each case the coordinates are measured in an inertial frame of reference. In Minkowski spacetime, $\mathrm{d}s$ is invariant under the Lorentz transformation, geometry is Euclidean, space is flat, and the interval of proper time, $\mathrm{d}\tau$, is given by

$$d\tau = \sqrt{1 - \boldsymbol{V}^2}\,\mathrm{d}t\,, \tag{13.52}$$

which is the interval read by a clock moving at the velocity $\boldsymbol{V}$,

$$|\boldsymbol{V}| = \sqrt{\left(\frac{\mathrm{d}x}{\mathrm{d}t}\right)^2 + \left(\frac{\mathrm{d}y}{\mathrm{d}t}\right)^2 + \left(\frac{\mathrm{d}z}{\mathrm{d}t}\right)^2}\,. \tag{13.53}$$

(xiii) For a spherically symmetric gravitational field outside a massive non-rotating body in vacuum (where $R_{\mu\nu} = 0$), the line element, $\mathrm{d}s$, becomes the Schwarzschild metric given by

$$\mathrm{d}s^2 = -\left(1 - \frac{2\,M}{r}\right)\,\mathrm{d}t^2 + \left(1 - \frac{2\,M}{r}\right)^{-1}\,\mathrm{d}r^2 + r^2\,\mathrm{d}\theta^2 + r^2\,\sin^2\theta\,\mathrm{d}\phi^2\,. \tag{13.54}$$

Here, r, θ, and ϕ are spherical coordinates where origin is at the center of the massive object, and M is the mass which determines the Newtonian gravitational field M/r.

The exact solution of Einstein's field equations (13.43) in empty space, $R_{\mu\nu} = 0$, obtained by Schwarzschild in 1916 [512], describes the geometry of spacetime outside of a spherically symmetric, non-pulsating distribution of matter. In this case the metric functions, which enter in the underlying line element, are particularly simple. Proceeding one step further and solving the field equations (13.43) for a a spherically symmetric stellar object made up of a perfect fluid, whose energy-stress tensor has a relatively simple form, one arrives at the so-called Tolman–Oppenheimer–Volkoff (TOV) equations . These can be solved, by means of applying straightforward numerical techniques (such as Runge-Kutta integration), for a given model for the equation of state of the stellar matter, as will be discussed in great detail in chapter 14. Rotation complicates the construction of stellar models considerably, as we shall see in chapter 15. The reason for this is threefold. For one, rotating stars are rotationally deformed, that is, they are flattened at the pole but grow in size in the equatorial direction, which leads to a dependence of the metric on the polar angle, in addition to the radial dependence. Secondly, rotation stabilizes a star against gravitational collapse. It can therefore carry more mass than it would be the case if the star would be non-rotating. Being more massive, however, means that the geometry of spacetime will changed too. This makes the line element of a rotating star depend on the star's rotational frequency. Thirdly, there is the above mentioned frame dragging effect which imposes an additional self-consistency condition on the stellar structure, since the strength of the dragging of the local inertial frames depends on the star's properties, like mass (profile) and rotational frequency. So in order to construct models of rotating compact stars, one has to put the Einstein equations on a two-dimensional numerical grid, spanned by θ and r, and solve them self-consistently until convergency is achieved for a given model for the equation of state. These points render stellar structure calculations of rotationally deformed bodies considerably more complicated than those of non-rotating, spherically symmetric bodies. In the latter case, as shall be seen immediately below, one can carry out the analytical analysis all the way to the condition of hydrostatic equilibrium in general relativity theory, known as the TOV equations.

Chapter 14

Structure equations of non-rotating stars

In this chapter we shall derive the stellar structure equations of non-rotating, spherically symmetric objects in the framework of Einstein's general theory of relativity. As already mentioned in chapter 13, at the bottom of the heart of Einstein's theory lies, besides the equivalence principle, the requirement that any relativistic equation must remain covariant under coordinate transformation, that is, its mathematical structure must be the same in all coordinate systems. This requirement is automatically fulfilled by tensor equations. The chief objective of the next section will be to demonstrate this explicitly for the energy–momentum tensor of a perfect fluid.

14.1 Energy–momentum tensor in covariant form

The energy–momentum tensor is a tensor of rank two. To derive its covariant representation, we perform a coordinate transformation of the energy–momentum tensor $\overset{0}{T}{}^{\alpha\beta}$ given in a proper reference frame $\overset{0}{x}{}^{\mu} = (\overset{0}{x}{}^{0}, \overset{0}{x}{}^{1}, \overset{0}{x}{}^{2}, \overset{0}{x}{}^{3})$ to the coordinate system $x^{\mu} = (x^0, x^1, x^2, x^3)$ of actual interest, which moves relative to $\overset{0}{x}{}^{\mu}$. Approximating the stellar matter by an *ideal* (or perfect) fluid, which is an excellent approximation as long as one is interested in the global structural properties of compact stars, as is the case here, then the components of $\overset{0}{T}{}^{\alpha\beta}$ in a momentarily comoving reference frame are given by (for the sake of brevity, henceforth we shall drop the notion momentarily),

$$\overset{0}{T}{}^{\alpha\beta} = \begin{pmatrix} \overset{0}{\epsilon} & 0 & 0 & 0 \\ 0 & \overset{\circ}{P}_{xx} & \overset{\circ}{P}_{xy} & \overset{\circ}{P}_{xz} \\ 0 & \overset{\circ}{P}_{yx} & \overset{\circ}{P}_{yy} & \overset{\circ}{P}_{yz} \\ 0 & \overset{\circ}{P}_{zx} & \overset{\circ}{P}_{zy} & \overset{\circ}{P}_{zz} \end{pmatrix} = \begin{pmatrix} \overset{0}{\epsilon} & 0 & 0 & 0 \\ 0 & \overset{\circ}{P} & 0 & 0 \\ 0 & 0 & \overset{\circ}{P} & 0 \\ 0 & 0 & 0 & \overset{\circ}{P} \end{pmatrix} . \tag{14.1}$$

Equation (14.1) is a direct manifestation of the definition of a perfect fluid in relativity, defined as a fluid that has *no viscosity* and *no heat conduction* in the comoving reference frame. The quantities $\overset{0}{\epsilon}$ and $\overset{\circ}{P}$ in (14.1) denote energy density and pressure measured by a local observer comoving with $\overset{0}{x}{}^{\mu}$. No heat conduction implies that $\overset{0}{T}{}^{0i} = \overset{0}{T}{}^{i0} = 0$ in (14.1). Energy can flow only if particles flow. Viscosity is a force parallel to the interface between particles. Its absence means that the forces should always be perpendicular to the interface, i.e. $\overset{0}{T}{}^{ij}$ should be zero unless $i = j$. This means that $\overset{0}{T}{}^{ij}$ should be a diagonal matrix. Moreover, it must be diagonal in *all* comoving reference frames, since no viscosity is a statement independent of the spatial axes. The only matrix diagonal in all frames is a multiple of the identity: all its diagonal terms are equal. Thus, an x surface will have across it only a force in x direction, and similarly for y and z. These forces-per-unit-area are all equal, and are called the pressure, P. So one has $\overset{0}{T}{}^{ij} = \overset{\circ}{P}\,\delta^{ij}$. From six possible quantities (the number of independent elements in the 3×3 symmetric matrix $\overset{0}{T}{}^{ij}$) the zero-viscosity assumption therefore reduces the number of functions to just one in (14.1), the pressure [513].

The two restrictions – no heat conduction and no viscosity – made in the definition of (14.1) enormously simplify the energy–momentum tensor, as we now see. Let us consider the fluid to be at rest in the coordinate system $\overset{0}{x}{}^{\mu}$, that is,

$$\frac{\mathrm{d}\overset{0}{x}{}^{1}}{\mathrm{d}\tau} = \frac{\mathrm{d}\overset{0}{x}{}^{2}}{\mathrm{d}\tau} = \frac{\mathrm{d}\overset{0}{x}{}^{3}}{\mathrm{d}\tau} = 0\,. \tag{14.2}$$

The transformation of $\overset{0}{T}{}^{\alpha\beta}$ to another comoving reference frame is accomplished by the following manipulations,

$$T^{\mu\nu} = \frac{\partial x^{\mu}}{\partial \overset{0}{x}{}^{\alpha}} \frac{\partial x^{\nu}}{\partial \overset{0}{x}{}^{\beta}} \overset{0}{T}{}^{\alpha\beta} \tag{14.3}$$

$$= \frac{\partial x^{\mu}}{\partial \overset{0}{x}{}^{\alpha}} \frac{\partial x^{\nu}}{\partial \overset{0}{x}{}^{\alpha}} \overset{0}{T}{}^{\alpha\alpha} \tag{14.4}$$

$$= \frac{\partial x^{\mu}}{\partial \overset{0}{x}{}^{0}} \frac{\partial x^{\nu}}{\partial \overset{0}{x}{}^{0}} \overset{0}{\epsilon} + \frac{\partial x^{\mu}}{\partial \overset{0}{x}{}^{i}} \frac{\partial x^{\nu}}{\partial \overset{0}{x}{}^{i}} \overset{\circ}{P}\,, \tag{14.5}$$

where (14.3) is nothing but the transformation law for a rank-two tensor. Equation (14.4) reflects the diagonal structure of the energy–momentum tensor, which, via (14.1), leads immediately to (14.5). To simplify (14.5) we write in the first place for the contravariant components of the metric tensor in the new coordinates in terms of their values in the old coordinates

$$g^{\mu\nu} = \frac{\partial x^\mu}{\partial \overset{0}{x}{}^\alpha} \frac{\partial x^\nu}{\partial \overset{0}{x}{}^\beta} \overset{0}{g}{}^{\alpha\beta} \,, \tag{14.6}$$

which on substituting the simple values of $\overset{0}{g}{}^{\alpha\beta}$ gives

$$g^{\mu\nu} = -\frac{\partial x^\mu}{\partial \overset{0}{x}{}^0} \frac{\partial x^\nu}{\partial \overset{0}{x}{}^0} + \frac{\partial x^\mu}{\partial \overset{0}{x}{}^i} \frac{\partial x^\nu}{\partial \overset{0}{x}{}^i} \,. \tag{14.7}$$

In the second place, we write for the macroscopic velocity of the fluid with respect to the new coordinate system

$$\frac{\mathrm{d}x^\mu}{\mathrm{d}\tau} = \frac{\partial x^\mu}{\partial \overset{0}{x}{}^\nu} \frac{\mathrm{d}\overset{0}{x}{}^\nu}{\mathrm{d}\tau} \,, \tag{14.8}$$

which reduces to

$$\frac{\mathrm{d}x^\mu}{\mathrm{d}\tau} = \frac{\partial x^\mu}{\partial \overset{0}{x}{}^\nu} \delta^{\nu 0} = \frac{\partial x^\mu}{\partial \overset{0}{x}{}^0} \,, \tag{14.9}$$

owing to the value zero for the spatial components of velocity ($\mathrm{d}\overset{0}{x}{}^i/\mathrm{d}\tau = 0$) and the value unity ($\mathrm{d}\overset{0}{x}{}^0/\mathrm{d}\tau = 1$) for its temporal component in the old coordinates. Substituting (14.7) and (14.9) into equation (14.5) leads to

$$\begin{aligned} T^{\mu\nu} &= \frac{\mathrm{d}x^\mu}{\mathrm{d}\tau} \frac{\mathrm{d}x^\nu}{\mathrm{d}\tau} \overset{0}{\epsilon} + \frac{\partial x^\mu}{\partial \overset{0}{x}{}^i} \frac{\partial x^\nu}{\partial \overset{0}{x}{}^i} \overset{\circ}{P} \\ &= \frac{\mathrm{d}x^\mu}{\mathrm{d}\tau} \frac{\mathrm{d}x^\nu}{\mathrm{d}\tau} \overset{0}{\epsilon} + \left\{ \frac{\partial x^\mu}{\partial \overset{0}{x}{}^0} \frac{\partial x^\nu}{\partial \overset{0}{x}{}^0} + g^{\mu\nu} \right\} \overset{\circ}{P} \\ &= \frac{\mathrm{d}x^\mu}{\mathrm{d}\tau} \frac{\mathrm{d}x^\nu}{\mathrm{d}\tau} \overset{0}{\epsilon} + \left\{ \frac{\mathrm{d}x^\mu}{\mathrm{d}\tau} \frac{\mathrm{d}x^\nu}{\mathrm{d}\tau} + g^{\mu\nu} \right\} \overset{\circ}{P} \,, \end{aligned} \tag{14.10}$$

which allows us to express the energy–momentum tensor for a perfect fluid in the very useful and general form

$$T^{\mu\nu} = u^\mu \, u^\nu \left(\overset{0}{\epsilon} + \overset{\circ}{P} \right) + g^{\mu\nu} \, \overset{\circ}{P} \,. \tag{14.11}$$

The quantities u^μ and u^ν are four-velocities, defined as

$$u^\mu \equiv \frac{\mathrm{d}x^\mu}{\mathrm{d}\tau} \,, \qquad u^\nu \equiv \frac{\mathrm{d}x^\nu}{\mathrm{d}\tau} \,. \tag{14.12}$$

They are the components of the macroscopic velocity of the fluid with respect to the actual coordinate system that is being used. For the coordinate system in which the fluid is at rest one has $\mathrm{d}x^\mu/\mathrm{d}\tau = (\mathrm{d}x^0/\mathrm{d}\tau, \mathrm{d}\boldsymbol{x}/\mathrm{d}\tau) = (1,0,0,0) = \delta^{\mu 0}$, and thus from equation (14.11)

$$\overset{0}{\epsilon} = T^{00}\,, \quad \text{and} \quad \overset{\circ}{P} = \frac{1}{3}\sum_{i=1}^{3} T^{ii}\,. \tag{14.13}$$

Note that equation (14.11) is a tensor equation and thus is valid in any comoving (locally inertial) coordinate system. The equivalence principle guarantees that equation (14.11) holds in flat spacetime as well as in curved spacetime. Having a manifestly covariant expression at hand for the source term of Einstein's field equations (13.43), we now proceed to solve them for spherically symmetric stellar objects.

14.2 Tolman–Oppenheimer–Volkoff equation

After these considerations we proceed to derive the stellar structure equations of a non-rotating, static (that is, non-pulsating), spherically symmetric compact star. The metric of such an object has the form [509, 511, 512]

$$\mathrm{d}s^2 = -\mathrm{e}^{2\,\Phi(r)}\,\mathrm{d}t^2 + \mathrm{e}^{2\,\Lambda(r)}\,\mathrm{d}r^2 + r^2\,\mathrm{d}\theta^2 + r^2\sin^2\!\theta\,\mathrm{d}\phi^2\,, \tag{14.14}$$

where $\Phi(r)$ and $\Lambda(r)$ are the radially varying metric functions. Hereafter we shall drop the arguments of these functions quite often. Introducing the covariant components of the metric tensor as

$$g_{tt} = -\,\mathrm{e}^{2\,\Phi}\,,\; g_{rr} = \mathrm{e}^{2\,\Lambda}\,,\; g_{\theta\theta} = r^2\,,\; g_{\phi\phi} = r^2\sin^2\!\theta\,, \tag{14.15}$$

the line element (14.14) can be written in the generally covariant expression for interval:

$$\mathrm{d}s^2 = g_{\mu\nu}\,\mathrm{d}x^\mu\,\mathrm{d}x^\nu\,. \tag{14.16}$$

The contravariant components of the metric tensor are obtained via the relation

$$g^{\mu\nu}\,g_{\nu\lambda} = \delta^\mu{}_\nu\,, \tag{14.17}$$

where $\delta^\mu{}_\nu$ is the four-dimensional Kronecker delta [cf. equation (13.14)]. One then finds

$$g^{tt} = -\,\mathrm{e}^{-\,2\,\Phi}\,,\; g^{rr} = \mathrm{e}^{-\,2\,\Lambda}\,,\; g^{\theta\theta} = r^{-2}\,,\; g^{\phi\phi} = \frac{1}{r^2\,\sin^2\!\theta}\,. \tag{14.18}$$

Note that because of the underlying symmetries, the only functional dependence that enters in the metric is the dependence on radial distance

r, measured from the star's origin. The components of the metric tensor can be grouped together to a 4×4 matrix as

$$(g^{\mu\nu}) = \begin{pmatrix} -\,\mathrm{e}^{-2\,\Phi} & 0 & 0 & 0 \\ 0 & \mathrm{e}^{-2\,\Lambda} & 0 & 0 \\ 0 & 0 & r^{-2} & 0 \\ 0 & 0 & 0 & (r\sin\theta)^{-2} \end{pmatrix}, \qquad (14.19)$$

with column and row labels μ and ν running from $0, 1, 2, 3$, or alternatively from t, r, θ, ϕ. Finally, noticing that $g^{\mu}{}_{\lambda} = g^{\mu\nu} g_{\nu\lambda}$, according to the transformation law (13.15), we find from (14.17) that the mixed components of the metric tensor obey $g^{\mu}{}_{\lambda} = \delta^{\mu}{}_{\nu}$, and therefore

$$g^{t}{}_{t} = g^{r}{}_{r} = g^{\theta}{}_{\theta} = g^{\phi}{}_{\phi} = 1\,. \qquad (14.20)$$

The determinant of $g_{\mu\nu}$ is readily found from (14.15),

$$g \equiv \det(g_{\mu\nu}) = -\,\mathrm{e}^{2\,\Phi}\,\mathrm{e}^{2\,\Lambda}\,r^4\,\sin^2\theta\,. \qquad (14.21)$$

Having specified the metric, we can now proceed to calculate the Einstein tensor associated with our problem. Note that all quantities whose knowledge is necessary to calculate the Einstein tensor – from the Riemann tensor $R^{\tau}{}_{\mu\sigma\nu}$ to the curvature scalar R – are given in terms of the components of the metric tensor and derivatives thereof. Our chief task therefore will be to perform step by step the numerous (in general partial) differentiations of the metric tensor with respect to the coordinate variables t, r, θ, ϕ, which ultimately will lead us to the expression for the Einstein tensor associated with the metric (14.15).

Those quantities to be determined first in this step-by-step analysis are the Christoffel symbols $\Gamma^{\sigma}_{\mu\nu}$ introduced in (13.25). The non-vanishing symbols to the form of line element (14.15) of a spherically symmetric body are

$$\Gamma^{r}_{tt} = \mathrm{e}^{2\,\Phi-2\,\Lambda}\,\Phi'\,, \quad \Gamma^{t}_{tr} = \Phi'\,, \quad \Gamma^{r}_{rr} = \Lambda'\,,$$

$$\Gamma^{\theta}_{r\theta} = r^{-1}\,, \quad \Gamma^{\phi}_{r\phi} = r^{-1}\,, \quad \Gamma^{r}_{\theta\theta} = -\,r\,\mathrm{e}^{-2\,\Lambda}\,,$$

$$\Gamma^{\phi}_{\theta\phi} = \frac{\cos\theta}{\sin\theta}\,, \quad \Gamma^{r}_{\phi\phi} = -\,r\,\sin^2\theta\,\mathrm{e}^{-2\,\Lambda}\,, \quad \Gamma^{\theta}_{\phi\phi} = -\sin\theta\,\cos\theta\,. \qquad (14.22)$$

Here and in the following accents denote differentiation with respect to the radial coordinate r, as, for instance, $\Phi' \equiv \mathrm{d}\Phi/\mathrm{d}r$ and $\Phi'' \equiv \mathrm{d}^2\Phi/\mathrm{d}r^2$. Because of the relatively simple mathematical form of the metric (14.14), the number on non-vanishing Christoffel symbols turns out to be of manageable size. As already mentioned at the beginning of this chapter, this is no longer the case for a rotationally deformed star, whose metric functions, because of rotational deformation, depends also on the polar angle θ. Moreover the dragging of local inertial frames manifests itself in the occurrence of an additional non-diagonal metric term, $g^{t\phi}$.

With the Christoffel symbols at our disposal, we now proceed with the calculation of the Riemann–Christoffel tensor $R^{\tau}{}_{\mu\nu\sigma}$, the Ricci tensor $R_{\mu\nu}$ and the Ricci scalar R, given in equations (13.24), (13.45), and (13.47) respectively, of which the Einstein tensor is composed of. The following combinations of Christoffel symbols enter in the calculation of $R^{\tau}{}_{\mu\nu\sigma}$:

$$\Gamma^{\lambda}_{t\kappa}\,\Gamma^{\kappa}_{\lambda t} = (\Gamma^{t}_{tt})^2 + 2\,\Gamma^{t}_{ti}\,\Gamma^{i}_{tt} + \Gamma^{i}_{tj}\,\Gamma^{j}_{it} = 2\,(\Phi')^2\,\mathrm{e}^{2\,\nu-2\,\Lambda}\,,$$

$$\Gamma^{\lambda}_{r\kappa}\,\Gamma^{\kappa}_{\lambda r} = (\Gamma^{t}_{rt})^2 + 2\,\Gamma^{t}_{ri}\,\Gamma^{i}_{tr} + \Gamma^{i}_{rj}\,\Gamma^{j}_{ir} = (\Phi')^2 + (\Lambda')^2 + \frac{2}{r^2}\,,$$

$$\Gamma^{\lambda}_{\theta\kappa}\,\Gamma^{\kappa}_{\lambda\theta} = (\Gamma^{t}_{\theta t})^2 + 2\,\Gamma^{t}_{\theta i}\,\Gamma^{i}_{t\theta} + \Gamma^{i}_{\theta j}\,\Gamma^{j}_{i\theta} = -\,2\,\mathrm{e}^{-2\,\Lambda} + \cot^2\theta\,,$$

and

$$\Gamma^{\lambda}_{\phi\kappa}\,\Gamma^{\kappa}_{\lambda\phi} = (\Gamma^{t}_{\phi t})^2 + 2\,\Gamma^{t}_{\phi i}\,\Gamma^{i}_{t\phi} + \Gamma^{i}_{\phi j}\,\Gamma^{j}_{i\phi} = -\,2\left(\sin^2\theta\,\mathrm{e}^{-2\,\Lambda} + \cos^2\theta\right).$$

Substituting these results into (13.24) gives for the non-vanishing components of the Riemann–Christoffel tensor:

$$R^{t}{}_{rtr} = -\,\Phi'' - \left(\Phi'\right)^2 + \Phi'\,\Lambda'\,,$$

$$R^{t}{}_{\theta t\theta} = -\,r\,\Phi'\,\mathrm{e}^{-2\,\Lambda}\,,\quad R^{t}{}_{\phi t\phi} = -\,r\,\Phi'\sin^2\theta\;\mathrm{e}^{-2\,\Lambda}\,,$$

$$R^{r}{}_{ttr} = \left\{-\,\Phi'' - \left(\Phi'\right)^2 + \Phi'\,\Lambda'\right\}\mathrm{e}^{2\,\Phi-2\,\Lambda}\,,$$

$$R^{r}{}_{\theta r\theta} = r\,\Lambda'\,\mathrm{e}^{-2\,\Lambda}\,,\quad R^{r}{}_{\phi r\phi} = \Lambda'\,r\;\sin^2\theta\;\mathrm{e}^{-2\,\Lambda}\,,$$

$$R^{\theta}{}_{tt\theta} = -\,\Phi'\,r\,\mathrm{e}^{2\,\Phi-2\,\Lambda}\,,\quad R^{\theta}{}_{rr\theta} = -\frac{1}{r}\,\Lambda'\,,$$

$$R^{\theta}{}_{\phi\theta\phi} = \sin^2\theta\left(1-\mathrm{e}^{-2\,\Lambda}\right),\quad R^{\phi}{}_{tt\phi} = -\,\Phi'\,r\,\mathrm{e}^{2\,\Phi-2\,\Lambda}\,,$$

$$R^{\phi}{}_{rr\phi} = -\frac{1}{r}\,\Lambda'\,, \quad R^{\phi}{}_{\theta\theta\phi} = -1 + \mathrm{e}^{-2\,\Lambda}\,. \tag{14.23}$$

For the sake of completeness, we also give the components of the pure covariant Riemann–Christoffel tensor. These are given by

$$R_{trtr} = \Phi''\,\mathrm{e}^{2\,\Phi} + \big(\Phi'\big)^2\,\mathrm{e}^{2\,\Phi} - \Phi'\,\mathrm{e}^{2\,\Phi}\,\Lambda'\,,$$

$$R_{t\theta t\theta} = \Phi'\,r\,\mathrm{e}^{2\,\Phi-2\,\Lambda}\,, \quad R_{t\phi t\phi} = \Phi'\,r\,\sin^2\theta\;\mathrm{e}^{2\,\Phi-2\,\Lambda}\,,$$

$$R_{r\theta r\theta} = r\,\Lambda'\,, \quad R_{r\phi r\phi} = \Lambda'\,r\,\sin^2\theta\,,$$

$$R_{\theta\phi\theta\phi} = r^2\sin^2\theta\,\big(1 - \mathrm{e}^{-2\,\Lambda}\big)\,. \tag{14.24}$$

Using the values of the Christoffel symbols listed in (14.22), the components of the Ricci tensor read

$$\begin{aligned}
R_{tt} &= \big\{-\Phi'\,\Lambda' + \Phi'' + \big(\Phi'\big)^2 + 2\,r^{-1}\,\Phi'\big\}\,\mathrm{e}^{2\,\Phi-2\,\Lambda}\,,\\
R_{rr} &= -\,\Phi'' - \big(\Phi'\big)^2 + \Phi'\,\Lambda' + \frac{2}{r}\,\Lambda'\,,\\
R_{\theta\theta} &= \big\{-\,r\,\Phi' + r\,\Lambda' + \mathrm{e}^{2\,\Lambda} - 1\big\}\,\mathrm{e}^{-2\,\Lambda}\,,\\
R_{\phi\phi} &= -\sin^2\theta\,\big\{r\Phi' - r\,\Lambda' - \mathrm{e}^{2\,\Lambda} + 1\big\}\,\mathrm{e}^{-2\,\Lambda}\,.
\end{aligned} \tag{14.25}$$

The components of the mixed Ricci tensor are obtained from

$$R^{\sigma}{}_{\lambda} = g^{\sigma\tau}\,R_{\tau\lambda}\,, \tag{14.26}$$

with $R_{\tau\lambda}$ given by equation (13.45). One arrives for the individual components at,

$$\begin{aligned}
R^{t}{}_{t} &= \Big\{-\frac{1}{4}\,\big(\Phi'\big)^2 + \frac{1}{4}\,\Phi'\,\Lambda' - \frac{1}{2}\,\Phi'' - \frac{1}{r}\,\Phi'\Big\}\,\mathrm{e}^{-\Lambda}\,,\\
R^{r}{}_{r} &= -\,\Big\{\frac{1}{4}\,\big(\Phi'\big)^2 - \frac{1}{4}\,\Phi'\,\Lambda' + \frac{1}{2}\,\Phi'' - \frac{1}{r}\,\Lambda'\Big\}\,\mathrm{e}^{-\Lambda}\,,\\
R^{\theta}{}_{\theta} &= -\,\frac{1}{r^2}\,\mathrm{e}^{-\Lambda}\Big\{1 - \frac{1}{2}\,r\,\Lambda' + \frac{1}{2}\,r\,\Phi'\Big\} + \frac{1}{r^2}\\
R^{\phi}{}_{\phi} &= R^{\theta}{}_{\theta}\,.
\end{aligned} \tag{14.27}$$

Finally, the Ricci scalar, which follows from (13.47), has the form

$$\begin{aligned}
R = \big\{ &+ 2\,\Phi'\,\Lambda'\,r^2 - 2\,\Phi''\,r^2 - 2\,\big(\Phi'\big)^2\,r^2 - 4\,r\,\Phi'\\
&+ 4\,r\,\Lambda' + 2\,\mathrm{e}^{2\,\Lambda} - 2\big\}\;r^{-2}\,\mathrm{e}^{-2\,\Lambda}\,.
\end{aligned} \tag{14.28}$$

The Einstein tensor, $G_{\mu\nu}$, could now be calculated from equations (14.25) and (14.28). However, it is more convenient to transform $G_{\mu\nu}$ to its mixed representation $G^{\mu}{}_{\nu}$, which is readily accomplished, according to the rules outlined in section 13.1, by multiplying the Einstein tensor $G_{\kappa\nu}$ with the metric tensor $g^{\mu\kappa}$ and summing over κ. This leads for the metric tensor in (13.43) to $g^{\mu\kappa} g_{\mu\nu} = \delta^{\kappa}{}_{\nu}$, where, as known from equation (13.14), the elements of $\delta^{\kappa}{}_{\nu}$ possess a particularly simple form. The Einstein tensor (13.43) in the mixed representation thus reads

$$G^{\mu}{}_{\nu} \equiv R^{\mu}{}_{\nu} - \frac{1}{2}\,\delta^{\mu}{}_{\nu}\,R = 8\,\pi\,T^{\mu}{}_{\nu}\,, \tag{14.29}$$

with

$$T^{\mu}{}_{\nu} = (\epsilon + P)\,\frac{\mathrm{d}x^{\mu}}{\mathrm{d}\tau}\,\frac{\mathrm{d}x_{\nu}}{\mathrm{d}\tau} + \delta^{\mu}{}_{\nu}\,P\,. \tag{14.30}$$

As already noted, the connection between the distribution of matter and energy, contained in the energy–momentum tensor, with the geometry of spacetime is the physical content of Einstein's field equations (14.29). The left-hand side of this equation gives a quantity whose tensor divergence is known to be identically equal to zero. In accordance with the rules of covariant differentiation introduced in (13.37), we may write as an immediate consequence of (14.29),

$$T^{\mu}{}_{\nu;\,\mu} \equiv \frac{\partial}{\partial x^{\mu}} T^{\mu}{}_{\nu} + \Gamma^{\mu}_{\kappa\mu}\,T^{\kappa}{}_{\nu} - \Gamma^{\kappa}_{\nu\mu}\,T^{\mu}{}_{\kappa} = 0\,. \tag{14.31}$$

This expression reduces in *flat* spacetime, that is, in a local inertial frame, to its special relativistic form given by

$$T^{\mu}{}_{\nu;\,\mu} = \frac{\partial}{\partial x^{\mu}} T^{\mu}{}_{\nu} = 0\,. \tag{14.32}$$

For the metric of (14.14) the covariant derivative of $T^{\mu}{}_{\nu}$ is given by

$$T^{\mu}{}_{\nu;\,\mu} = (\epsilon + P)\,\Phi' + P'\,. \tag{14.33}$$

Below we shall demonstrate that already from (14.31) alone one can draw many important conclusions as to the behavior of matter and energy.

Before however, we give the components of the Einstein tensor in the mixed representation. These are obtained by substituting the expressions listed in (14.27) into (14.29), leading to

$$G^{t}{}_{t} = R^{t}{}_{t} - \frac{1}{2}\,R = \mathrm{e}^{-2\,\Lambda}\Big(\frac{1}{r^2} - 2\,\frac{\Lambda'}{r}\Big) - \frac{1}{r^2}\,, \tag{14.34}$$

$$G^{r}{}_{r} = R^{r}{}_{r} - \frac{1}{2}\,R = \mathrm{e}^{-2\,\Lambda}\Big(2\,\frac{\Phi'}{r} + \frac{1}{r^2}\Big) - \frac{1}{r^2}\,, \tag{14.35}$$

$$G^{\theta}{}_{\theta} = R^{\theta}{}_{\theta} - \frac{1}{2}\,R = \mathrm{e}^{-2\,\Lambda}\Big(\Phi'' - \Phi'\,\Lambda' + (\Phi')^2 + \frac{\Phi' - \Lambda'}{r}\Big)\,, \tag{14.36}$$

and

$$G^{\phi}{}_{\phi} = G^{\theta}{}_{\theta}\,. \tag{14.37}$$

For the sake of completeness, we also list the purely covariant components of the Einstein tensor, which are given by

$$\begin{aligned}
G_{tt} &= \big(2\,r\,\Lambda' + \mathrm{e}^{2\,\Lambda} - 1\big)\,r^{-2}\,\mathrm{e}^{2\,\Phi - 2\,\Lambda}\,,\\
G_{rr} &= \big(2\,r\,\Phi' - \mathrm{e}^{2\,\Lambda} + 1\big)\,r^{-2}\,,\\
G_{\theta\theta} &= \big\{r\big(\Phi' - \Lambda' - \Phi'\,\Lambda'\,r + r\,\Phi'' + \big(\Phi'\big)^2\,r\big)\big\}\,\mathrm{e}^{-2\,\Lambda}\,,\\
G_{\phi\phi} &= \big\{r\,\sin^2\!\theta\big(\Phi' - \Lambda' - \Phi'\,\Lambda'\,r + r\,\Phi'' + \big(\Phi'\big)^2\,r\big)\big\}\,\mathrm{e}^{-2\,\Lambda}\,.
\end{aligned} \tag{14.38}$$

The purely contravariant components are given by

$$\begin{aligned}
G^{\,tt} &= \frac{2\,\Lambda'}{\mathrm{e}^{2\,\Phi}\,r\,\mathrm{e}^{2\,\Lambda}} + \frac{1}{\mathrm{e}^{2\,\Phi}\,r^2} - \frac{1}{\mathrm{e}^{2\,\Phi}\,r^2\,\mathrm{e}^{2\,\Lambda}}\,,\\
G^{\,rr} &= \frac{2\,\Phi'}{\mathrm{e}^{4\,\Lambda}\,r} - \frac{1}{r^2\,\mathrm{e}^{2\,\Lambda}} + \frac{1}{\mathrm{e}^{4\,\Lambda}\,r^2}\,,\\
G^{\,\theta\theta} &= \frac{\Phi'}{r^3\,\mathrm{e}^{2\,\Lambda}} - \frac{\Lambda'}{r^3\,\mathrm{e}^{2\,\Lambda}} - \frac{\Phi'\,\Lambda'}{r^2\,\mathrm{e}^{2\,\Lambda}} + \frac{\Phi''}{r^2\,\mathrm{e}^{2\,\Lambda}} + \frac{\big(\Phi'\big)^2}{r^2\,\mathrm{e}^{2\,\Lambda}}\,,\\
G^{\,\phi\phi} &= \frac{\Phi'}{r^3\,\sin^2\!\theta\,\mathrm{e}^{2\,\Lambda}} - \frac{\Lambda'}{r^3\,\sin^2\!\theta\,\mathrm{e}^{2\,\Lambda}} - \frac{\Phi'\,\Lambda'}{r^2\,\sin^2\!\theta\,\mathrm{e}^{2\,\Lambda}}\\
&\quad + \frac{\Phi''}{r^2\,\sin^2\!\theta\,\mathrm{e}^{2\,\Lambda}} + \frac{\big(\Phi'\big)^2}{r^2\,\sin^2\!\theta\,\mathrm{e}^{2\,\Lambda}}\,.
\end{aligned} \tag{14.39}$$

Those components of the Einstein tensor that are not listed above are understood to be equal to zero. Combining the expressions derived in equations (14.34) to (14.37) with (14.29) and (14.30) leads to the following field equations,

$\mu = \nu = t$:

$$\mathrm{e}^{-2\,\Lambda}\Big(2\,\frac{\Lambda'}{r} - \frac{1}{r^2}\Big) + \frac{1}{r^2} = 8\,\pi\,\epsilon\,, \tag{14.40}$$

$\mu = \nu = r$:

$$\mathrm{e}^{-2\,\Lambda}\Big(2\,\frac{\Phi'}{r} + \frac{1}{r^2}\Big) - \frac{1}{r^2} = 8\,\pi\,P\,, \tag{14.41}$$

$\mu = \nu = \theta$:

$$\mathrm{e}^{-2\,\Lambda}\Big(\Phi'' - \Phi'\,\Lambda' + (\Phi')^2 + \frac{\Phi' - \Lambda'}{r}\Big) = 8\,\pi\,P\,, \tag{14.42}$$

$\mu = \nu = \phi$:

$$G^{\phi}{}_{\phi} = G^{\theta}{}_{\theta}, \quad \text{and} \quad T^{\phi}{}_{\phi} = T^{\theta}{}_{\theta} \,. \tag{14.43}$$

In deriving equations (14.40) through (14.43), we made us of the fact that we are dealing with a *static* stellar configuration, in which case one derives from the line element (14.16)

$$\frac{\mathrm{d}r}{\mathrm{d}\tau} = \frac{\mathrm{d}\theta}{\mathrm{d}\tau} = \frac{\mathrm{d}\phi}{\mathrm{d}\tau} = 0 \quad \Rightarrow \quad \frac{\mathrm{d}t}{\mathrm{d}\tau} = \mathrm{e}^{-\Phi} \,. \tag{14.44}$$

This implies for the mixed components of the energy–momentum tensor of (14.30) that

$$T^{t}{}_{t} = -\,\epsilon \,, \qquad T^{i}{}_{i} = P \,. \tag{14.45}$$

The first relation in (14.45) follows because

$$\frac{\mathrm{d}x^t}{\mathrm{d}\tau} \equiv \frac{\mathrm{d}t}{\mathrm{d}\tau} = \mathrm{e}^{-\Phi} \,, \tag{14.46}$$

and therefore

$$\frac{\mathrm{d}x_t}{\mathrm{d}\tau} = g_{t\sigma} \frac{\mathrm{d}x^\sigma}{\mathrm{d}\tau} = \mathrm{e}^{-2\,\Phi} \frac{\mathrm{d}t}{\mathrm{d}\tau} = -\,\mathrm{e}^{\Phi} \,. \tag{14.47}$$

The second relation follows trivially from (14.30) since $\mathrm{d}x^i/\mathrm{d}\tau = 0$ ($i = 1, 2, 3$) for the static stellar configuration.

In the next step let us turn our interest for a moment toward the general properties of the energy–momentum tensor, for some of its properties will be very useful to bring the stellar structure equations (14.40) through (14.43) into a more illuminating form. We begin with abbreviating the fluid's four-velocity as $u^\mu = \mathrm{d}x^\mu/\mathrm{d}\tau$ and $u_\nu = \mathrm{d}x_\nu/\mathrm{d}\tau$. Covariant differentiation of (14.30) then leads to

$$0 = T^{\mu}{}_{\nu\,;\,\mu} = (\epsilon + P)_\mu \, u^\mu \, u_\nu + (\epsilon + P)(u_{\nu\,;\,\mu} \, u^\mu + u_\nu \, u^\mu{}_{;\,\mu}) + \delta^\mu{}_\nu \, P_{;\,\mu} \,, \tag{14.48}$$

where we have used that $\delta^\mu{}_{\nu\,;\,\mu} = 0$, which follows from $\delta^\mu{}_{\nu\,;\,\mu} = (g^{\mu\kappa} g^{\kappa\nu})_{;\,\mu} = 0$. Noticing that the four-velocity is given by

$$u^\mu = (u^0, u^1, u^2, u^3) = \frac{\mathrm{d}x^\mu}{\mathrm{d}\tau} = \Big(\frac{\mathrm{d}x^0}{\mathrm{d}\tau}, \frac{\mathrm{d}x^1}{\mathrm{d}\tau}, \frac{\mathrm{d}x^2}{\mathrm{d}\tau}, \frac{\mathrm{d}x^3}{\mathrm{d}\tau}\Big) \,, \tag{14.49}$$

and upon calculating the square of it, one arrives at

$$u^\mu \, u_\mu = u^\mu \, g_{\mu\nu} \, u^\nu = g_{00} \, (u^0)^2 + g_{ii} \, (u^i)^2 = -\,1 \,. \tag{14.50}$$

In flat space, equation (14.50) reduces to the familiar relation

$$u^\mu\, u_\mu = -\,(u^0)^2 + \boldsymbol{u}^2 = -1\,. \tag{14.51}$$

To extract the Euler equation of relativistic hydrodynamics from $T^{\,\mu}{}_{\nu;\,\mu} = 0$, we project equation (14.48) perpendicular to $\boldsymbol{u}$ by applying the projection tensor [509]

$$\mathsf{P}^{\lambda\nu} \equiv u^\lambda\, u^\nu + g^{\lambda\nu}\,, \tag{14.52}$$

to $T^{\,\mu}{}_{\nu;\,\mu}$, that is $\mathsf{P}^{\lambda\nu} T^{\,\mu}{}_{\nu;\,\mu} = 0$. This leaves us with the expression

$$\mathsf{P}^{\lambda\nu}\big\{(\epsilon+P)_\mu\, u_\nu\, u^\mu + (\epsilon+P)(u_{\nu;\,\mu}\, u^\mu + u_\nu\, u^\mu{}_{;\,\mu}) + \delta_\nu{}^\mu P_{,\,\mu}\big\} = 0\,. \tag{14.53}$$

The first term on the right-hand side of (14.53) vanishes, which follows from the normalization condition of the four-velocity, $u^\nu\, u_\nu = -1$, and the relation $g^{\lambda\nu}\, u_\nu = u^\lambda$ applied to

$$(u^\lambda\, u^\nu + g^{\lambda\nu})\, u_\nu\, u^\mu = 0\,. \tag{14.54}$$

We are thus left with

$$(\epsilon+P)(u^\lambda\, u^\nu\, u_{\nu;\,\mu}\, u^\mu + g^{\lambda\nu} u_{\nu;\,\mu}\, u^\mu) + (u^\lambda\, u^\mu P_{,\,\mu} + g^{\lambda\mu} P_{,\,\mu}) = 0\,, \tag{14.55}$$

where $P_{,\,\mu}$ denotes the usual subscripted notation to indicate the differentiation of P with respect to x^μ, i.e. $\partial P/\partial x^\mu \equiv P_{,\,\mu}$.

To carry the evaluation of (14.55) further, we note that

$$g^{\lambda\nu}\, u_{\nu;\,\mu} = (g^{\lambda\nu}\, u_\nu)_{;\mu} = u^\lambda{}_{;\,\mu}\,, \tag{14.56}$$

and from the normalization condition (14.50) of u^μ,

$$0 = (u^\nu\, u_\nu)_{;\,\mu} = u^\nu{}_{;\,\mu}\, u_\nu + u^\nu\, u_{\nu;\,\mu} = 2\, u^\nu{}_{;\,\mu}\, u_\nu\,, \tag{14.57}$$

from which it follows that

$$u^\nu{}_{;\,\mu}\; u_\nu = u^\nu\; u_{\nu;\,\nu} = 0\,. \tag{14.58}$$

To arrive at the last equality in (14.57) use of

$$u^\nu\, u_{\nu;\,\mu} = g^{\nu\tau}\, u_\tau\; (g_{\nu\sigma}\, u^\sigma)_{;\,\mu} = g^{\nu\tau}\, g_{\nu\sigma}\, u_\tau\, u^\sigma{}_{;\,\mu} = \delta^\tau{}_\sigma\, u_\tau\, u^\sigma{}_{\;\mu} = u_\nu\, u^\nu{}_{;\,\mu} \tag{14.59}$$

was made. With the aid of (14.56) and (14.58), equation (14.55) can be written as

$$(\epsilon+P)\, u^\lambda{}_{;\mu}\, u^\mu + (u^\lambda\, u^\mu\, P_{,\,\mu} + g^{\lambda\mu}\, P_{,\,\mu}) = 0\,, \tag{14.60}$$

which, upon multiplication with $g_{\lambda\sigma}$, transforms after some algebraic manipulations to

$$(\epsilon + P)\, u_{\sigma;\,\mu}\, u^{\mu} + P_{,\sigma} + P_{,\mu}\, u^{\mu}\, u_{\sigma} = 0\,. \tag{14.61}$$

This relation is known as Euler's equation, which determines the flow lines to which u is tangent. It has precisely the same form as the corresponding flat-spacetime Euler equation. Note that the pressure gradient, not gravity, is responsible for all deviations of flow lines from geodesics. Let us now choose the fluid's rest frame and compute the zero-component of the equation of motion from $T^{\mu}{}_{\nu}$. In this case $u^0 = 1$, $\boldsymbol{u} = 0$, and $u^0{}_{;\,\mu} = 0$. Hence the relation $0 = u^{\nu}\, T^{\mu}{}_{\nu;\,\mu}$ reduces to

$$0 = u^{\nu}\, T^{\,\mu}{}_{\nu;\,\mu} = T^{\,\mu}{}_{0;\,\mu}\,, \tag{14.62}$$

which, on substituting the energy–momentum tensor (14.30), can be written in the manner

$$\begin{aligned} 0 =&\ \big((\epsilon + P)\, u^{\mu}\, u_0 + \delta^{\mu}{}_0\, P\big)_{;\mu} \\ =&\ -(\epsilon + P)_{,\,\mu}\, u^{\mu} - (\epsilon + P)\, u^{\mu}{}_{;\,\mu} + \delta^{\mu}{}_0\, P_{,\,\mu}\,. \end{aligned} \tag{14.63}$$

Performing the summation over μ leaves us with

$$0 = \frac{\mathrm{d}\epsilon}{\mathrm{d}t} + (\epsilon + P)\, u^{\mu}{}_{;\mu}\,. \tag{14.64}$$

With the baryon number density ρ in the fluid's rest frame, defined as $\rho = A/V$, the number flux vector of baryons, $\rho\, u^{\mu}$, is conserved. Hence, in the rest frame we have

$$0 = (\rho\, u^{\mu})_{;\,\mu} = \rho_{,\,\mu}\, u^{\mu} + \rho\, u^{\mu}{}_{;\,\mu} = \frac{\mathrm{d}\rho}{\mathrm{d}t} + \rho\, u^{\mu}{}_{;\,\mu}\,. \tag{14.65}$$

Equation (14.65) enables us to eliminate the term $u^{\mu}{}_{;\,\mu}$ in (14.64), leading to

$$\frac{\mathrm{d}\epsilon}{\mathrm{d}t} = \frac{\epsilon + P}{\rho}\, \frac{\mathrm{d}\rho}{\mathrm{d}t}\,. \tag{14.66}$$

Equation (14.66) is recognized as the first law of thermodynamics for a relativistic fluid,

$$\mathrm{d}\epsilon = \frac{\epsilon + P}{\rho}\, \mathrm{d}\rho + T\, \rho\, \mathrm{d}s\,, \tag{14.67}$$

for which the entropy per baryon, s, is conserved along a flow line, $\mathrm{d}s/\mathrm{d}\tau = 0$. The values of ρ, ϵ, P, T and s in (14.67) measure, as usual, the physical quantities in the rest frame of a fluid element. That is, the baryon number density ρ is understood to give the number of baryons per unit three-dimensional volume of rest frame, with antibaryons (if any) counted negatively (cf. section 6.3). In accordance with the field-theoretical part of this book, ϵ denotes the total mass energy – including rest mass, thermal energy, compressional energy, etc – contained in a unit three-dimensional volume of the rest frame. The quantity s is the entropy per baryon, $s = S/A$, in the rest frame. Thus, the entropy per unit volume is given by $\rho\, s$. Finally, P and T are the isotropic pressure and temperature in the rest frame. With these conventions the law of energy conservation in flat spacetime dictates that

$$\mathrm{d}(\epsilon\, A/\rho) = -\, P\, \mathrm{d}(A/\rho) + T\, \mathrm{d}(A\, s)\,, \tag{14.68}$$

which, for a fixed number, A, of baryons leads immediately to (14.67). There is no reason for surprise at this circumstance, for, by virtue of the principle of equivalence, the first law of thermodynamics, expressed in the proper reference frame of a fluid element, is identical to the first law in flat spacetime. We shall encounter equation (14.67) in chapter 19 again when discussing the cooling behavior of compact stars.

Let us turn back to the Euler equation (14.61) for a moment. For the fluid of a static star we have $\mathrm{d}\epsilon/\mathrm{d}t = \mathrm{d}\rho/\mathrm{d}t = 0$, and a fluid four-velocity of $u^\nu = (u^t, 0, 0, 0)$. The expression of u^t is readily obtained from the normalization condition (14.50),

$$-\,1 = u^\nu\, u_\nu = u^\nu\, g_{\nu\mu}\, u^\mu = (u^t)^2\, g_{tt} = -\,(u^t)^2\, \mathrm{e}^{2\,\Phi}\,, \tag{14.69}$$

with g_{tt} known from equation (14.15), as

$$u^t = \mathrm{e}^{-\Phi}\,. \tag{14.70}$$

Because only $P_{,\,r}$ is non-zero, the only non-trivial component of the Euler equation (14.61) is

$$(\epsilon + P)\, u_{r;\,\mu}\, u^\mu + P_{,\,r} = 0\,. \tag{14.71}$$

Writing the covariant derivative $u_{r;\,\mu}$ in the form

$$u_{r;\,\mu} = \frac{\partial u_r}{\partial x^\mu} - \Gamma^\lambda_{r\mu}\, u_\lambda = -\,\Gamma^\lambda_{r\mu}\, u_\lambda \tag{14.72}$$

enables us to express (14.71) as

$$\frac{\mathrm{d}P}{\mathrm{d}r} = (\epsilon + P)\, \Gamma^\lambda_{r\mu}\, u_\lambda\, u^\mu = -\,(\epsilon + P)\, \frac{\mathrm{d}\Phi}{\mathrm{d}r}\,. \tag{14.73}$$

To arrive at the latter equality, we have made us of (only u^t is non-zero)

$$\Gamma^{\lambda}_{r\mu}\, u_\lambda\, u^\mu = \Gamma^t_{rt}\, u_t\, u^t = \Phi'\, u_t\, u^t = -\,\Phi' \,, \tag{14.74}$$

with Γ^t_{rt} given in equation (14.22).

The stellar structure equations in their final form are now readily found as follows. Let us introduce the quantity $m(r)$ as

$$m(r) \equiv 4\,\pi \int_0^r \mathrm{d}r\, r^2\, \epsilon(r) \quad \Rightarrow \quad \frac{\mathrm{d}m}{\mathrm{d}r} = 4\,\pi\, r^2\, \epsilon(r) \,, \tag{14.75}$$

which can be interpreted as the amount of mass energy contained in a sphere of radius r. At the star's origin we impose the condition $m(0) = 0$. With this definition Einstein's field equation (14.40) can then be integrated. This is accomplished by multiplying both sides of (14.40) with r^2 and noticing that

$$\mathrm{e}^{-2\,\Lambda}\, 2\,\Lambda'\, r - \mathrm{e}^{-2\,\Lambda} + 1 = -\,\frac{\mathrm{d}}{\mathrm{d}r}\left(\mathrm{e}^{-2\,\Lambda}\, r - r\right) \,.$$

The integration then yields

$$\mathrm{e}^{-2\,\Lambda} = 1 - \frac{2\,m}{r} \,. \tag{14.76}$$

In the next step we add the field equations (14.40) and (14.41) which gives

$$8\,\pi\,(\epsilon + P) = \frac{2}{r}\,\mathrm{e}^{-2\,\Lambda}\,(\Lambda' + \Phi') \,. \tag{14.77}$$

The metric function Λ in (14.77) can be eliminated with the help of (14.76). For this purpose we differentiate (14.76) with respect to r, which gives

$$-2\,\Lambda'\,\mathrm{e}^{-2\,\Lambda} = \frac{2}{r}\left(\frac{m}{r} - m'\right) \,, \tag{14.78}$$

and substitute this result into (14.77). After some straightforward algebraic manipulations one arrives at

$$8\,\pi\, P = -\,\frac{2\,m}{r^3} + 2\left(1 - \frac{2\,m}{r}\right)\frac{\Phi'}{r} \,. \tag{14.79}$$

Solving this expression for Φ gives

$$\Phi' = \frac{4\,\pi\, r^3\, P + m}{r^2\,(1 - 2\,m/r)} \,, \tag{14.80}$$

with the boundary condition at the star's surface

$$\Phi(r = R) = \frac{1}{2} \ln\Big(1 - \frac{2\,M}{R}\Big)\,, \tag{14.81}$$

where M and R denote the star's mass and radius, respectively (details will be discussed immediately below). Finally substituting from (14.73) for Φ', we arrive for the pressure gradient inside a spherically symmetric configuration at the final result

$$\frac{\mathrm{d}P(r)}{\mathrm{d}r} = -\frac{\{\epsilon(r) + P(r)\}\,\{4\pi r^3 P(r) + m(r)\}}{r^2\left(1 - \frac{2\,m(r)}{r}\right)}\,, \tag{14.82}$$

with the central pressure $P(r = 0) \equiv P(\epsilon_c)$ and ϵ_c as the star's central mass energy density. Equation (14.82) is know as the Tolman–Oppenheimer–Volkoff (TOV) equation [514]. This equation is fundamental to the description of the structure of a hydrostatically stable stellar configuration treated in the framework of Einstein's general theory of relativity. As in classical Newtonian mechanics, so also in Einstein's theory, the forces that act on a mass shell inside the star is the pressure force of the stellar matter enclosed in that shell, which act in the radial outward direction. Gravity pulls on that mass shell in the radial inward direction such that both forces, because of hydrostatic equilibrium, counterbalance each other. In the classical limit one has $P \ll \epsilon$, $P \ll m$ and $m \ll r$ in (14.82), which leads to a pressure gradient given by $\mathrm{d}P/\mathrm{d}r = \epsilon\, m/r^2$. This relation reveals that Einstein's theory increases (the magnitude of) the pressure gradient over what one obtains from the Newtonian treatment, which is quite crucial for stellar bodies, for there are *no* mass or radius limits in Newtonian theory. Neutron stars could therefore be made as massive as one pleases, in sharp contrast to Einstein's theory where neutron stars with too high a central density are subject to gravitational collapse. Let us see how this comes out when integrating (14.82). First one has to specify a model for the equation of statein the form $P(\epsilon)$ and a value of the central density, ϵ_c. This determines P_c while P' and m vanish at $r = 0$. Equation (14.75) then determines m for an infinitesimal increase in r. Plugging in these values for m, ϵ_c and P_c into (14.82) determines the value of P', allowing the determination of P at the next step. For the P thus found the equation of state determines ϵ, and we go over the whole process once again to determine the values of the variables at the next step. In this way, the computation of P, ϵ, and m for successively increasing values of r goes on until we arrive at $P = 0$,[1] which is identified as the radius,

[1] The Tolman–Oppenheimer–Volkoff equation (14.82) guarantees that the pressure will decrease monotonically so long as the chosen model for the equation of state obeys the reasonable restriction $\epsilon \geq 0$ for all $P \geq 0$ (cf. section 3.1).

R, of the star, and the value of m there is the star's total mass energy, M. If desired, the metric function Φ can be obtained by simultaneously integrating (14.80) too, for an arbitrarily specified value of Φ at the star's center, $\Phi_0 \equiv \Phi(r = 0)$. After having reached the surface, Φ is to be renormalized by adding a constant to it everywhere, so that it obeys the boundary condition (14.81). The iteration procedure of equations (14.75) and (14.82) is repeated for different values of ϵ_c, leading each time to a particular relativistic stellar model, whose structure functions Φ, m, ϵ, P, ρ satisfy the equations of stellar structure. Notice that for any fixed choice of the equation of state of the form $P(\epsilon)$, or $P = P(\rho)$, $\epsilon = \epsilon(\rho)$, the stellar models form a *one-parameter* sequence (parameter ϵ_c). Once the central density has been specified, the model is determined uniquely.

We finish this section with pointing out that the mass $M \equiv m(r = R)$, contained inside a sphere of Schwarzschild radius $r = R$ is to be identified with the star's *gravitational mass*. From (14.75) one sees that M is given by

$$M = 4\,\pi \int_0^R \mathrm{d}r\, r^2\, \epsilon(r)\,. \tag{14.83}$$

It is this quantity which has to be identified with the total mass energy of the system because it governs the geometry exterior to the matter and therefore fixes such observables as the period of a planetary orbit, precession of perihelion, and gravitational bending of a light ray [69].

For later use we also define the *proper* star mass given by

$$M_{\mathrm{P}} = 4\pi \int_0^R \mathrm{d}r\; r^2\; \frac{\epsilon(r)}{\sqrt{1 - \frac{2\,m(r)}{r}}}\,. \tag{14.84}$$

In contrast to (14.75), the volume element in the integral of (14.84) is the *proper* volume. Hence the name proper mass for the mass defined in (14.84). The gravitational mass differs from the proper mass on two accounts [69]. Firstly, the quantity $\epsilon(r)$ in (14.83) is not simply the baryon number density, $\rho(r)$, multiplied by the mass per baryon in cold, catalyzed matter at zero pressure ($\frac{1}{56}$ of the mass of one ^{56}Fe atom),

$$\epsilon \neq \rho \times \frac{1}{56} M(^{56}\mathrm{Fe})\,, \tag{14.85}$$

but the mass energy density *exceeds* that product by an amount equivalent to the mass energy of compression. Secondly, what is being integrated in

(14.75) to get M is not the energy density $\epsilon(r)$ itself, but energy density multiplied by a factor which is less than 1. This can be seen by writing (14.75) formally as

$$M = \int \mathrm{d}^3\boldsymbol{r} \, \frac{1}{\sqrt{1 - \frac{2\,m(r)}{r}}} \, \epsilon(r) \, \sqrt{1 - \frac{2\,m(r)}{r}} \, \Theta(R - r) \qquad (14.86)$$

and introducing the proper volume element,

$$dV_{\rm prop} = 4\,\pi\,r^2 \, \frac{1}{\sqrt{1 - \frac{2\,m(r)}{r}}} \, \mathrm{d}r \, . \qquad (14.87)$$

Equation (14.86) then takes on the form

$$M = \int \mathrm{d}V_{\rm prop} \, \epsilon(r) \, \sqrt{1 - \frac{2\,m(r)}{r}} \, \Theta(R - r) \, . \qquad (14.88)$$

The square root in (14.88) in effect corrects for the negative gravitational potential energy of the interaction of the mass with itself. Hence, the factor which multiplies the proper volume – and which in this sense constitutes the integrand – is $\epsilon(r)\sqrt{1 - 2m(r)/r}$, a quantity evidently *smaller* than $\epsilon(r)$. Equation (14.75), superficially identical with the non-relativistic integral for the mass, is evidently quite subtle. It allows both for the work of compression (positive) and the potential energy of gravitation (negative), as pointed out by Harrison and Wheeler [69].

We next introduce the total baryon number, A, of a neutron star. The expression for A as an integral over the number density of baryons, ρ, follows directly from the differential form of the baryon conservation law $[(-g)^{1/2}\rho u^\mu]_{,\mu} = 0$ [515]. The expression is given by

$$A = \int \mathrm{d}^3\boldsymbol{x} \, \sqrt{-\,g} \, \rho \, u^t \, . \qquad (14.89)$$

Substituting the expressions for $\sqrt{-g}$ and the four-velocity u^t, given in (14.21) and (14.70) respectively, into equation (14.89) and performing straightforward algebraic manipulations, with $\mathrm{e}^{-2\,\Lambda}$ taken from (14.76), then gives

$$A = 4\pi \int_0^R \mathrm{d}r \, r^2 \, \frac{\rho(r)}{\sqrt{1 - \frac{2\,m(r)}{r}}} \, . \qquad (14.90)$$

Multiplication of A with the rest mass-energy associated with a single neutron, m_n, leads to the so-called star's *baryon mass*,

$$M_{\rm A} = m_n \, A \, . \qquad (14.91)$$

The binding energy, E_B, of a relativistic star is defined to be the difference between its gravitational mass and the mass of all its matter when cold and dispersed, $m_n A$. Thus, with the aid of (14.91), one has

$$E_B = M - M_{\rm A}\,. \tag{14.92}$$

A calculation of the binding energy is, therefore, equivalent to a calculation of the total baryon number. Finally, we note that combining (14.80) with the Tolman–Oppenheimer–Volkoff equation (14.82) leads for the following, alternative differential equation for the metric function Φ,

$$\frac{\mathrm{d}\Phi(r)}{\mathrm{d}r} = -\frac{1}{\epsilon(r) + P(r)}\,\frac{\mathrm{d}P(r)}{\mathrm{d}r}\,. \tag{14.93}$$

Since $m(r) = M$ and $P(r) = 0$ for $r \geq R$, one obtains from (14.93) for $\Phi(r)$ outside of the star

$$\mathrm{e}^{2\,\Phi(r)} = 1 - \frac{2\,M}{r}\,, \qquad r \geq R\,. \tag{14.94}$$

The other metric function, $\Lambda(r)$, in the line element (14.14) is known from (14.76) to read

$$\mathrm{e}^{-2\,\Lambda(r)} = 1 - \frac{2\,m(r)}{r}\,, \qquad r \geq 0\,, \tag{14.95}$$

inside and outside of the star.

14.3 Stability against radial oscillations

Stellar bodies that are in hydrostatic equilibrium are not automatically stable against oscillations about their equilibrium configurations or other – more complex – types of vibrations, such as torsional or octupole eigenmodes. The so-called *radial* vibrations [516, 517, 518] have been studied most in the literature, while, in contrast to this, the quantitative stability analysis of stars against *non-radial* pulsations still appears to be in its infancy [519, 520]. The reason being that radial oscillations are associated with vibrations about a given stellar equilibrium configuration that preserve the star's spherical symmetry, while non-radial oscillations deform a star away from spherical symmetry (cf. figures 14.1 and 14.2) which is accompanied by the emission of gravitational waves.

Very recently, a simple but efficient method to adequately analyze the vibrational and seismological properties of compact stars performing non-radial oscillations was developed by Bastrukov *et al* [521, 522, 523, 524]. It

References

[1] Greiner W and Stöcker H (ed) 1990 *Proc. NATO Advanced Study Institute on The Nuclear Equation of State, Peniscola* NATO ASI Series B vol 216A&B (New York: Plenum Press)

[2] Greiner W Stöcker H and Gallmann A (ed) 1994 *Proc. NATO Advanced Study Institute on Hot and Dense Nuclear Matter, Bodrum* NATO ASI Series B vol 335 (New York: Plenum Press)

[3] Stöcker H Gallmann A and Hamilton J H (ed) 1997 *Proc. Int. Conf. on Nuclear Physics at the Turn of the Millennium: Structure of Vacuum & Elementary Matter, Wilderness* (Singapore: World Scientific)

[4] Gutbrod H and Stöcker H 1991 *Scientific American, November issue* p 32

[5] Timmes F X Woosley S E and Weaver T A 1996 *ApJ* **457** 834

[6] Bethe H A and Brown G E 1985 *Scientific American, May issue* p 32

[7] Bethe H A 1990 *Rev. Mod. Phys.* **62** 801

[8] Müller E 1990 *J. Phys. G: Nucl. Part. Phys.* **16** 1571

[9] Woosley S E and Weaver T A 1992 *Theory of Neutron Star Formation, in: The Structure and Evolution of Neutron Stars* ed D Pines R Tamagaki and S Tsuruta (New York: Addison-Wesley) p 235

[10] *The Physics of Pulsars* ed A M Lenchek (New York: Gordon and Breach, 1972)

[11] Smith F G 1977 *Pulsars* (Cambridge: Cambridge University Press)

[12] Manchester R N and Taylor J H 1977 *Pulsars* (San Francisco: Freeman and Company)

[13] Lyne A G and Graham–Smith F 1990 *Pulsar Astronomy* (Cambridge: Cambridge University Press)

[14] Blandford R D Hewish A Lyne A G and Mestel L 1992 *Pulsars as Physics Laboratories Phil. Trans. R. Soc.* A **341** pp 1–192

[15] Nagase F 1989 *Publ. Astron. Soc. Japan* **41** 1

[16] Wheeler J A 1966 *Ann. Rev. Astron. Astrophys.* **4** 393

[17] Blandford R D and Narayan R 1992 *Ann. Rev. Astron. Astrophys.* **30** 311

[18] Pines D and Alpar M A 1992 *Inside Neutron Stars: A 1990 Perspective, in: The Structure and Evolution of Neutron Stars* ed D Pines R Tamagaki and S Tsuruta (New York: Addison-Wesley) p 7

[19] Taylor J H and Stinebring D R 1986 *Ann. Rev. Astron. Astrophys.* **24** 285

[20] Glendenning N K 1990 *Mod. Phys. Lett.* **A5** 2197

[21] Lyne A G 1995 *IAU Symposium No 165: Compact Stars in Binaries, The Hague* ed E P J van den Heuvel

[22] Lyne A G 1997 *Millisecond Pulsar Searches, in: Proc. 7th M Grossmann Meeting on General Relativity, Stanford* ed R T Jantzen and G MacKeiser (Singapore: World Scientific)

[23] Camilo F 1995 *Millisecond Pulsar Searches, in: The Lives of Neutron Stars* ed M A Alpar Kiziloglu Ü and van Paradijs J (Dordrecht: Kluwer) p 243
Camilo F 1996 *Present and Future Pulsar Searches, in: Proc. High Sensitivity Radio Astronomy* (Cambridge: Cambridge University Press)

[24] Bhattacharya D and van den Heuvel E P J 1991 *Phys. Rep.* **203** 1

[25] Backer D C and Kulkarni S R 1990 *Physics Today* **43** 26

[26] Glendenning N K 1991 *Nuclear and Particle Astrophysics, in: Proc. Int. Summer School on the Structure of Hadrons and Hadronic Matter, Dronten* ed O Scholten and J H Koch (Singapore: World Scientific) p 275

[27] Witten E 1984 *Phys. Rev.* D **30** 272

[28] Alcock C Farhi E and Olinto A V 1986 *ApJ* **310** 261

[29] Haensel P Zdunik J L and Schaeffer R 1986 *Astron. & Astrophys.* **160** 121

[30] Kettner Ch Weber F Weigel M K and Glendenning N K 1995 *Phys. Rev.* D **51** 1440

[31] Thorsett S E Arzoumanian Z McKinnon M M and Taylor J H 1993 *ApJ* **405** L29

[32] Nagase F 1992 *Properties of Neutron Stars from X-ray Pulsar Observation, in: The Structure and Evolution of Neutron Stars* ed D Pines R Tamagaki and S Tsuruta (New York: Addison-Wesley) p 77

[33] Manchester R N 1992 *Radio Pulsar Timing, in: The Structure and Evolution of Neutron Stars* ed D Pines R Tamagaki and S Tsuruta (New York: Addison-Wesley) p 32

[34] Trümper J 1992 *Royal Astron. Soc.* **33** 165

[35] Trümper J 1993 *Science* **260** 1769

[36] Iwasawa K Koyama K and Halpern J P 1992 *Cyclotron Lines and the Pulse Period Change of X-ray Pulsar 1E2259+586, in: The Structure and Evolution of Neutron Stars* ed D Pines R Tamagaki and S Tsuruta (New York: Addison-Wesley) p 203

[37] Ögelman H 1995 *X-Ray Observations of Cooling Neutron Stars, in: The Lives of Neutron Stars* ed M A Alpar Kiziloglu Ü and van Paradijs J (Dordrecht: Kluwer) p 101

[38] Trümper J Pietsch W Reppin C Voges W Staubert R and Kendziorra E 1978 *ApJ* **219** L105

[39] Voges W Pietsch W Reppin C Trümper J Kendziorra E and Staubert R 1982 *ApJ* **263** 803

[40] Wheaton W 1979 *Nature* **282** 240

[41] Makishima K 1992 *Magnetic Fields of Binary X-ray Pulsars, in: The Structure and Evolution of Neutron Stars* ed D Pines R Tamagaki and S Tsuruta (New York: Addison-Wesley) p 86

[42] Walter F M Wolk S J and Neuhäuser R 1996 *Nature* **379** 233

[43] Prakash M 1997 *AIP Conf. Proceedings, Big Sky* vol 412 ed T W Donnelly (New York: American Institute of Physics) p 1007

[44] Prakash M and Lattimer J M 1997 *The Radius of the Neutron Star RXJ185635–3754 and Implications for the Equation of State* (SUNY Preprint)

[45] Hoshi R 1992 *Mass–Radius Relations in X-ray Pulsars, in: The Structure and Evolution of Neutron Stars* ed D Pines R Tamagaki and S Tsuruta (New York: Addison-Wesley) p 98

[46] Liang E P 1986 *ApJ* **304** 682

[47] Hillebrandt W Müller E and Mönchmeyer R 1990 *Constraints on the Nuclear Equation of State from Type II Supernovae and Newly Born Neutron Stars, in: The Nuclear Equation of State* NATO ASI Series B vol 216A ed W Greiner and H Stöcker (New York: Plenum Press) p 689

[48] Backer D C Kulkarni S R Heiles C Davis M M and Goss W M 1982 *Nature* **300** 615

[49] Woosley S E 1986 *Nucleosynthesis and Chemical Evolution, in: 16th Advanced Course, Swiss Society of Astrophysics and Astronomy* ed B Hauck *et al* (Geneva: Geneva Observatory) p 1

[50] Woosley S E and Weaver T A 1986 Ann. Rev. Astron. Astrophys. **24** 205

[51] Hillebrandt W 1987, *NATO ASI on High Energy Phenomena Around Collapsed Stars* ed F Pacini (Dodrecht: Reidel Publishing Company) p 73

[52] Kahana S H 1989 *Ann. Rev. Nucl. Part. Sci.* **39** 231

[53] Cooperstein J and Baron E 1990 *Supernovae* ed A Petschek (Berlin: Springer-Verlag)

[54] Bethe H A 1971 *Ann. Rev. Nucl. Sci.* **21** 93

[55] Ruderman M 1972 *Ann. Rev. Astron. Astrophys.* **10** 427

[56] Börner G 1972 *On the Properties of Matter in Neutron Stars, Habilitation Thesis* (University of Munich, Germany)

[57] Arnett W D and Bowers R L 1977 *ApJ Suppl.* **33** 415

[58] Baym G 1978 *Neutron Stars and the Physics of Matter at High Density, in: Nuclear Physics with Heavy Ions and Mesons, Les Houches* session XXX vol 2 ed R Balian M Rho and G Ripka (Amsterdam: North-Holland) p 745

[59] Baym G and Pethick Ch 1979 *Ann. Rev. Astron. Astrophys.* **17** 415

[60] Canuto V 1978 *Proc. Int. School Phys. Enrico Fermi, course LXV* (New York: North-Holland) 448

[61] Glendenning N K 1985 *ApJ* **293** 470

[62] Weber F and Glendenning N K 1993 *Hadronic Matter and Rotating Relativistic Neutron Stars, in: Proc. of Nankai Summer School Astrophysics and Neutrino Physics, Tianjin* ed D H Feng G Z He and X Q Li (Singapore: World Scientific) p 64–183

[63] Lamb F K 1991 *Neutron Stars and Black Holes, in: Frontiers of Stellar Evolution* vol 20 ed D L Lambert (ASP Conference Series) p 299

[64] Pines D Tamagaki R and Tsuruta S (ed) 1992 *Conf. Proc. of The Structure and Evolution of Neutron Stars* (New York: Addison-Wesley)
[65] Muto T Takatsuka T Tamagaki R and Tatsumi T 1993 *Prog. Theor. Phys. Suppl.* **112** 221.
[66] Glendenning N K 1997 *Compact Stars, Nuclear Physics, Particle Physics, and General Relativity* (New York: Springer-Verlag)
[67] Prakash M Bombaci I Prakash M Ellis P J Lattimer J M and Knorren R 1997 *Phys. Rep.* **280** 1
[68] Feynman R P Metropolis N and Teller E 1949 *Phys. Rev.* **75** 1561
[69] Harrison B K and Wheeler J A 1965 *Gravitation Theory and Gravitational Collapse* ed B K Harrison K S Thorne M Wakano and J A Wheeler (Chicago: University of Chicago Press) pp 1–177
[70] Baym G Pethick C and Sutherland P 1971 *ApJ* **170** 299
[71] Baym G Bethe H A and Pethick C J 1971 *ApJ* **175** 225
[72] Negele J W and Vautherin D 1973 *Nucl. Phys.* **A178** 123
[73] Fritzsch H Gell–Mann M and Leutwyler H 1973 *Phys. Lett.* **47B** 365
[74] Baym G and Chin S 1976 *Phys. Lett.* **62B** 241
[75] Keister B D and Kisslinger L S 1976 *Phys. Lett.* **64B** 117
[76] Chapline G and Nauenberg M 1976 *Nature* **264** 235; 1977 *Phys. Rev.* D **16** 450
[77] Fechner W B and Joss P C 1978 *Nature* **274** 347
[78] Glendenning N K 1982 *Phys. Lett.* **114B** 392; 1985 *ApJ* **293** 470; 1987 *Z. Phys.* A **326** 57; 1987 *Z. Phys.* A **327** 295
[79] Weber F and Weigel M K 1989 *Nucl. Phys.* **A505** 779
[80] Thorne K S 1966 *Proc. Int. School of Phys. Enrico Fermi, course 35, High Energy Astrophysics* ed L Gratton (New York: Academic Press) p 166
[81] Bowers R L Campbell J A and Zimmermann R L 1973 *Phys. Rev.* D **7** 2278; 2289
[82] Moszkowski S A 1974 *Phys. Rev.* D **9** 1613
[83] Leung Y C 1989 *Physics of Dense Matter* (Singapore: World Scientific)
[84] Weber F and Weigel M K 1989 *Nucl. Phys.* **A493** 549
[85] Weber F and Weigel M K 1989 *Nucl. Phys.* **A495** 363c
[86] Glendenning N K Weber F and Moszkowski S A 1992 *Phys. Rev.* C **45** 844
[87] Glendenning N K 1991 *Nucl. Phys.* B *Proc. Suppl.* **24B** 110
[88] Glendenning N K 1992 *Phys. Rev.* D **46** 1274
[89] Glendenning N K and Pei S 1995 *APH NS, Heavy Ion Physics* **1** 323
[90] Glendenning N K 1995 *Phys. Rep.* **264** 143
[91] Glendenning N K 1986 *Phys. Rev. Lett.* **57** 1120
[92] Serot B D and Walecka J D 1986 *Adv. Nucl. Phys.* **16** 1
[93] Ter Haar B and Malfliet R 1987 *Phys. Rep.* **149** 208
[94] Gambhir Y K Ring P and Thimet A 1990 *Ann. Phys., NY* **198** 132
[95] Reinhard P G 1989 *Rep. Prog. Phys.* **55** 439
[96] Lalazissis G A and Sharma M M 1995 *Nucl. Phys.* **A586** 201
[97] Lalazissis G A Sharma M M and Ring P 1996 *Nucl. Phys.* **A597** 35

[98] Bouyssy A Marcos S Mathiot J F and Van Giai N 1985 *Phys. Rev. Lett.* **55** 1731

[99] Bouyssy A Mathiot J F and Van Giai N 1987 *Phys. Rev.* C **30** 380

[100] Jetter M Weber F and Weigel M K 1991 *Europhys. Lett.* **14** 633

[101] Huber H Weber F and Weigel M K 1993 *Phys. Lett.* **317B** 485

[102] Huber H Weber F and Weigel M K 1996 *Nucl. Phys.* **A596** 684

[103] Nuppenau C Lee Y J and Mac Kellar A D 1989 *Nucl. Phys.* **A504** 839

[104] Brockmann R and Machleidt R 1990 *Phys. Rev.* C **42** 1965

[105] Friedman J L Ipser J R and Parker L 1984 *Nature* **312** 255

[106] Friedman J L Ipser J R and Parker L 1986 *ApJ* **304** 115

[107] Friedman J L Ipser J R and Parker L 1989 *Phys. Rev. Lett.* **62** 3015

[108] Lattimer J M Prakash M Masak D and Yahil A 1990 *ApJ* **355** 241

[109] Weber F Glendenning N K and Weigel M K 1991 *ApJ* **373** 579

[110] Weber F and Glendenning N K 1991 *Z. Phys.* A **339** 211

[111] Weber F and Glendenning N K 1991 *Phys. Lett.* **265B** 1

[112] Weber F and Glendenning N K 1992 *ApJ* **390** 541

[113] Weber F Glendenning N K and Weigel M K 1991 *Rotating Neutron Stars and the Equation of State of Dense Matter, in: Prog. in High Energy Physics* ed W-Y Pauchy Hwang S-C Lee C-E Lee and D J Ernst (New York: North-Holland) p 309

[114] Weber F and Glendenning N K 1992 *Impact of the Nuclear Equation of State on Models of Rotating Neutron Stars, Proc. Int. Workshop on Unstable Nuclei in Astrophysics, Tokyo* ed S Kubono and T Kajino (Singapore: World Scientific) p 307

[115] Hartle J B 1967 *ApJ* **150** 1005

[116] Hartle J B and Thorne K S 1968 *ApJ* **153** 807

[117] Poschenrieder P and Weigel M K 1988 *Phys. Lett.* **200B** 231

[118] Poschenrieder P and Weigel M K 1988 *Phys. Rev.* C **38** 471

[119] Machleidt R Holinde K and Elster Ch 1987 *Phys. Rep.* **149** 1

[120] Holinde K Erkelenz K and Alzetta R 1972 *Nucl. Phys.* **A194** 161; **A198** 598

[121] Celenza L S and Shakin C M 1986 *Relativistic Nuclear Structure Physics* World Scientific Lecture Notes in Physics vol 2 (Singapore: World Scientific)

[122] Horowitz C J and Serot B D 1987 *Nucl. Phys.* **A464** 613

[123] Götz J Ramschütz J Weber F and Weigel M K 1989 *Phys. Lett.* **226B** 213

[124] Ramschütz J Weber F and Weigel M K 1990 *J. Phys. G: Nucl. Part. Phys.* **16** 987

[125] Weber F and Weigel M K 1988 *Z. Phys.* A **330** 249

[126] Hewish A Bell S J Pilkington J D H Scott P F and Collins R A 1968 *Nature* **217** 709

[127] Pacini F 1967 *Nature* **216** 567

[128] Pacini F 1968 *Nature* **219** 146

[129] Gold T 1968 *Nature* **218** 731; 1969 **221** 25

[130] Gunn J E and Ostriker J P 1969 *Nature* **221** 455

[131] Ostriker J P and Gunn J E 1969 *ApJ* **157** 1395
[132] Gunn J E and Ostriker J P 1970 *ApJ* **160** 979
[133] Hulse R A and Taylor J H 1975 *ApJ* **195** L51
[134] Brown G E and Bethe H A 1994 *ApJ* **423** 659
[135] Ellis P J Lattimer J M and Prakash M 1996 *Comments Nucl. Part. Phys.* **22** (no 2) 63
[136] Ter Haar D 1972 *Phys. Rep.* **3** 57
[137] Michel F C 1982 *Rev. Mod. Phys.* **54** 1
[138] Trimble V 1968 *Astron. J.* **73** 535
[139] Brown G E 1996 *Supernova Explosions, Black Holes and Nucleon Stars, in: Proc. Nucl. Phys. Conf. – INPC '95, Beijing* ed S Zuxun and X Jincheng (Singapore: World Scientific) p 623
[140] Glendenning N K 1982 *Phys. Lett.* **114B** 392; 1985 *ApJ* **293** 470; 1987 *Z. Phys.* A **326** 57; **327** 295; 1989 *Nucl. Phys.* **A493** 521
[141] Madsen J 1988 *Phys. Rev. Lett.* **61** 2909
[142] Madsen J 1994 *Physics and Astrophysics of Strange Quark Matter, in: Proc. of 2nd Int. Conf. on Phys. and Astrophys. of Quark-Gluon Plasma, Calcutta* ed B Sinha Y P Viyogi and S Raha (Singapore: World Scientific) p 186
[143] Friedman J L 1990 *How Fast can Pulsars Spin?, in: General Relativity and Gravitation* ed N Ashby D F Bartlett and W Wyss (Cambridge: Cambridge University Press)
[144] Caldwell R R and Friedman J L 1991 *Phys. Lett.* **264B** 143
[145] Madsen J 1997 *AIP Conf. Proc. 412, Big Sky* ed T W Donnelly (New York: American Institute of Physics) p 999
[146] Alcock C and Olinto A V 1988 *Ann. Rev. Nucl. Part. Sci.* **38** 161
[147] Glendenning N K 1990 *Mod. Phys. Lett.* **5** 713
[148] Glendenning N K and Weber F 1992 *ApJ* **400** 647
[149] Glendenning N K 1990 *Strange Quark Matter Stars, in: Proc. Int. Workshop on Relativ. Aspects of Nucl. Phys., Rio de Janeiro* ed T Kodama K C Chung S J B Duarte and M C Nemes (Singapore: World Scientific)
[150] Bodmer A R 1971 *Phys. Rev.* D **4** 1601
[151] Terazawa H 1979 *INS Report 338* (Univ. of Tokyo); 1989 *J. Phys. Soc. Japan* **58** 3555; 4388; 1990 **59** 1199
[152] Madsen J and Haensel P (ed) 1991 *Proc. Int. Workshop on Strange Quark Matter in Physics and Astrophysics, Aarhus Nucl. Phys.* B *Proc. Suppl.* **24B** p 1
[153] Liu H C and Shaw G L 1984 *Phys. Rev.* D **30** 1137
[154] Greiner C Koch P and Stöcker H 1987 *Phys. Rev. Lett.* **58** 1825
[155] Greiner C Rischke D H Stöcker H and Koch P 1988 *Phys. Rev.* D **38** 2797
[156] Shaw G L Shin M Dalitz R H and Desai M 1989 *Nature* **337** 436
[157] Greiner C and Stöcker H 1991 *Phys. Rev.* D **44** 3517

[158] Barz H W Friman B L Knoll J and Schulz H 1991 *Proc. of Int. Workshop on Strange Quark Matter in Physics and Astrophysics, Aarhus* ed J Madsen and P Haensel *Nucl. Phys.* B *Proc. Suppl.* **24B**

[159] Crawford H J Desai M S and Shaw G L 1992 *Phys. Rev.* D **45** 857

[160] Usov V V 1998 *Phys. Rev. Lett.* **80** 230

[161] McLerran L 1989 *Strange Matter: A Short Review, in: The Nuclear Equation of State (Part B)* NATO ASI Series vol 216B ed W Greiner and H Stöcker (New York: Plenum Press) p 155

[162] Madsen J 1993 *Phys. Rev. Lett.* **70** 391

[163] Heiselberg H Pethick C J and Staubo E F 1993 *Phys. Rev. Lett.* **70** 1355

[164] Alcock C and Farhi E 1985 *Phys. Rev.* D **32** 1273

[165] Applegate J and Hogan C 1985 *Phys. Rev.* D **31** 3037

[166] Madsen J Heiselberg H and Riisager K 1986 *Phys. Rev.* D **34** 2947

[167] Madsen J and Olesen M L 1991 *Phys. Rev.* D **43** 1069; **44** 566 (erratum)

[168] Ruderman M A 1969 *Nature* **223** 597

[169] Baym G and Pines D 1971 *Ann. Phys., NY* **66** 816

[170] Olinto A V 1987 *Phys. Lett.* **192B** 71

[171] Frieman J A and Olinto A V 1989 *Nature* **341** 633

[172] Horvath J E and Benvenuto O G 1988 *Phys. Lett.* **213B** 516

[173] Alpar M A 1987 *Phys. Rev. Lett.* **58** 2152

[174] Glendenning N K Kettner Ch and Weber F 1995 *Phys. Rev. Lett.* **74** 3519

[175] De Rújula A and Glashow S L 1984 *Nature* **312** 734

[176] Price P B 1988 *Phys. Rev.* D **38** 3813

[177] Bjorken J D and McLerran L 1979 *Phys. Rev.* D **20** 2353

[178] Chin S A and Kerman A K 1979 *Phys. Rev. Lett.* **43** 1292

[179] Chinellato J A *et al* (Brazil–Japan Collaboration) 1990 *Proc. 21st Int. Cosmic Ray Conf., Adelaide* vol 8 ed R J Protheroe (Northfield, South Australia: Graphic Services) p 259

[180] Jaffe R L 1977 *Phys. Lett.* **38** 195

[181] Baym G Kolb E W McLerran L Walker T P and Jaffe R L 1985 *Phys. Lett.* **160B** 181

[182] Terazawa H 1991 *J. Phys. Soc. Japan* **60** 1848

[183] Terazawa H 1993 *J. Phys. Soc. Japan* **62** 1415

[184] Michel F C 1988 *Phys. Rev. Lett.* **60** 677

[185] Benvenuto O G Horvath J E and Vucetich H 1989 *Int. J. Mod. Phys.* A **4** 257

Benvenuto O G and Horvath J E 1989 *Phys. Rev. Lett.* **63** 716

[186] Horvath J E Benvenuto O G and Vucetich H 1992 *Phys. Rev.* D **45** 3865

[187] Weber F and Glendenning N K 1993 *Neutron Stars, Strange Stars, and the Nuclear Equation of State, in: Proc. 1st Symp. on Nucl. Phys. in the Universe, Oak Ridge* ed M W Guidry and M R Strayer (Bristol: IOP Publishing) p 127

[188] Glendenning N K Kettner Ch and Weber F 1995 *ApJ* **450** 253

[189] Haensel P and Zdunik J L 1989 *Nature* **340** 617

[190] Glendenning N K 1989 *Phys. Rev. Lett.* **63** 2629

[191] Glendenning N K 1990 *Supernovae, Compact Stars and Nuclear Physics, in: Proc. of 1989 Int. Nucl. Phys. Conf., Sao Paulo* vol 2 ed M S Hussein *et al* (Singapore: World Scientific)

[192] Sawyer R F 1989 *Phys. Lett.* **233B** 412

[193] Weber F Kettner Ch Weigel M K and Glendenning N K 1995 *Strange Matter Stars, in: Proc. Int. Symp. on Strangeness and Quark Matter* ed G Vassiliadis A D Panagiotou B S Kumar and J Madsen (Singapore: World Scientific) p 308

[194] Kettner Ch Weber F Weigel M K and Glendenning N K 1995 *Stability of Strange Quark Stars with Nuclear Crust against Radial Oscillations, in: Proc. Int. Symp. on Strangeness and Quark Matter* ed G Vassiliadis A D Panagiotou B S Kumar and J Madsen (Singapore: World Scientific) p 333

[195] Glendenning N K Kettner Ch and Weber F 1995 *Possible New Class of Dense White Dwarfs, in: Proc. Int. Conf. on Strangeness in Hadronic Matter* AIP 340 ed J Rafelski (New York: American Institute of Physics) p 46

[196] Romanelli P F C 1986 *Strange Star Crusts, BS Thesis* (MIT, USA)

[197] Benvenuto O G and Althaus L G 1996 *ApJ* **462** 364; *Phys. Rev.* D **53** 635

[198] Weber F Schaab Ch Weigel M K and Glendenning N K 1997 *From Quark Matter to Strange Machos, in: Frontier Objects in Astrophysics and Particle Physics, Vulcano* ed F Giovannelli and G Mannocchi (Bologna: Editrice Compositori) p 87

[199] Ghosh S K Phatak S C Sahu P K 1996 *Nucl. Phys.* **A596** 670
Dai Z Lu T and Peng Q 1993 *Phys. Lett.* **319B** 199

[200] Horvath J E Vucetich H and Benvenuto O G 1993 *Mon. Not. R. Astron. Soc.* **262** 506

[201] Cho S J Lee K S and Heinz U 1994 *Phys. Rev.* D **50** 4771

[202] Kumar B S 1995 *Strange Quark Matter: Past, Present, and Future, in: Proc. Int. Symp. on Strangeness and Quark Matter* ed G Vassiliadis A D Panagiotou B S Kumar and J Madsen (Singapore: World Scientific) p 318

[203] Pretzl K (NA52 collaboration) 1997 (Private communication)

[204] Wilk G and Wlodarczyk Z 1996 *J. Phys. G: Nucl. Part. Phys.* **22** (no 10) L105

[205] Saito T Hatano Y Fukuda Y and Oda H 1990 *Phys. Rev. Lett.* **65** 2094

[206] Saito T 1995 *Test of the CRASH Experiment Counters with Heavy Ions, in: Proc. Int. Symp. on Strangeness and Quark Matter* ed G Vassiliadis A D Panagiotou B S Kumar and J Madsen (Singapore: World Scientific) p 259

[207] Ichimura M *et al* 1993 *Nuovo Cimento* A **36** 843

[208] Shaulov S B 1996 *APH NS, Heavy Ion Physics* **4** 403

[209] MACRO collaboration 1992 *Phys. Rev. Lett.* **69** 1860

[210] De Rújula A Glashow S L Wilson R R and Charpak G 1983 *Phys. Rep.* **99** 341

[211] Price P B 1984 *Phys. Rev. Lett.* **52** 1265

[212] Brügger M Lützenkirchen K Polikanov S Herrmann G Overbeck M Trautmann N Breskin A Chechik R Fraenkel Z and Smilansky U 1989 *Nature* **337** 434

[213] Thomas J and Jacobs P 1995 *A Guide to the High Energy Heavy Ion Experiments* (Lawrence Livermore National Laboratory, UCRL-ID-119181)

[214] Rusek A *et al* (E886 collaboration) 1996 *Phys. Rev.* C **54** R15

[215] Belz J *et al* (E888 collaboration) 1996 *Phys. Rev.* D **53** R3487

[216] Belz J *et al* (E888 collaboration) 1996 *Phys. Rev. Lett.* **76** 3277

[217] Pretzl K *et al* (NA52 collaboration) 1995 *Search for Strange Quark Matter in Relativistic Heavy Ion Collisions at CERN, in: Proc. Int. Symp. on Strangeness and Quark Matter* ed G Vassiliadis A D Panagiotou B S Kumar and J Madsen (Singapore: World Scientific) p 230

[218] Dittus F *et al* (NA52 collaboration) 1995 *First Look at NA52 Data on Pb–Pb Interactions at 158 A GeV/c, in: Proc. Int. Conf. on Strangeness in Hadronic Matter* AIP 340 ed J Rafelski (New York: American Institute of Physics) p 24

[219] Pretzl K *et al* (NA52 collaboration) 1997 *Search for Strangelets and Production of Antinuclei in Pb–Pb Collisions at CERN, in: Proc. Int. Conf. on Nucl. Phys. at the Turn of the Millennium: Structure of Vacuum & Elementary Matter* ed H Stöcker A Gallmann and J H Hamilton (Singapore: World Scientific) p 379

[220] Price P B 1978 *Phys. Rev.* D **18** 1382

[221] Saito T 1995 *Proc. 24th Int. Cosmic Ray Conf., Rome* **1** p 898

[222] Miyamura O 1995 *Proc. 24th Int. Cosmic Ray Conf., Rome* **1** p 890

[223] Capdevielle J N 1995 *Proc. 24th Int. Cosmic Ray Conf., Rome* **1** p 910

[224] Shapiro S L and Teukolsky S A 1983 *Black Holes, White Dwarfs, and Neutron Stars* (New York: Wiley & Sons)

[225] Meszaros P 1992 *High Energy Radiation from Magnetized Neutron Stars* (Chicago: University of Chicago Press)

[226] Hartmann D 1994 *High Energy Astrophysics* ed J M Matthews (Singapore: World Scientific)

[227] Fishman G J and Meegan Ch A 1995 *Ann. Rev. Astron. Astrophys.* **33** 415

[228] Piran T 1997 *Unsolved Problems in Astrophysics* ed J N Bahcall and J P Ostriker (Princeton: Princeton University Press)

[229] Haensel P Paczynski B and Amsterdamski P 1991 *ApJ* **375** 209

[230] Gladysz–Dziaduś E and Panagiotou A D 1995 *Strangelet Formation in Centauro Cosmic Ray Events, in: Proc. Int. Symp. on Strangeness and Quark Matter* ed G Vassiliadis A D Panagiotou B S Kumar and J Madsen (Singapore: World Scientific) p 265

[231] Bahcall J N 1978 *Ann. Rev. Astron. Astrophys.* **16** 241

[232] Taylor J H and Weisberg J M 1989 *ApJ* **345** 434

[233] Thielemann F K Nomoto K and Hashimoto M 1992 *Neutron Star Masses from Supernova Explosions, in: The Structure and Evolution of Neutron Stars* ed D Pines R Tamagaki and S Tsuruta (New York: Addison-Wesley) p 298

[234] Thielemann F K Hashimoto M Nomoto K 1996 *ApJ* **460** 408

[235] Rappaport S A and Joss P C 1983 *Accretion Driven Stellar X-Ray Sources* ed W H G Lewin and E P J van den Heuvel (Cambridge: Cambridge University Press)

[236] Joss P C and Rappaport S A 1984 *Ann. Rev. Astron. Astrophys.* **22** 537

[237] Bildsten L and Cutler C 1995 *ApJ* **449** 800

[238] Kaaret P Ford E and Chen K 1997 *ApJ* **480** L27

[239] Alpar M A and Shaham J 1985 *Nature* **316** 239

[240] Lamb F K Shibazaki N Alpar M A and Shaham J 1985 *Nature* **317** 681

[241] Epstein R I Lamb F K and Piedhorsky W C 1986 *X-Ray Variability in Astrophysics, in: Los Alamos Science* **13** ed N G Cooper (Los Alamos: LANL) p 34

[242] Shapiro I I 1964 *Phys. Rev. Lett.* **13** 789

[243] Weinberg S 1972 *Gravitation and Cosmology* (New York: Wiley & Sons)

[244] Rhoades C E and Ruffini R 1974 *Phys. Rev. Lett.* **32** 324

[245] Sabbadini A G and Hartle J B 1977 *Ann. Phys., NY* **104** 95

[246] Hartle J B 1978 *Phys. Rep.* **46** 201

[247] Glendenning N K 1998 *Pulsar Signal of Deconfinement, in: Proc. Quark Matter 1997, Tsukuba Nucl. Phys.* **A638** (1998) 239c

[248] Shibazaki N Murakami T Shaham J and Nomoto K 1989 *Nature* **342** 656

[249] Bell J F Kulkarni S R Bailes M Leitch E M and Lyne A G 1995 *ApJ* **452** L121

[250] Van Paradijs J 1978 *ApJ* **234** 609

[251] Fujimoto M Y and Taam R E 1986 *ApJ* **305** 246

[252] Yancopoulos S D Hamilton T T Helfand D J 1994 *ApJ* **429** 832

[253] Walter F M Lattimer J M Prakash M Matthews L An P and Neuhäuser R 1997 *HST cycle 7 General Observer Proposal*

[254] Brown G E 1997 Phys. Blätter **53** 671

[255] Li G Q Lee C H and Brown G E 1997 *Nucl. Phys.* **A625** 372

[256] Li G Q Lee C H and Brown G E 1997 *Phys. Rev. Lett.* **79** 5214

[257] Wasserman I and Shapiro S L 1983 *ApJ* **265** 1036

[258] Ruderman M A 1987 *High Energy Phenomena around Collapsed Stars* ed F Pacini (Dodrecht: Reidel Publishing Company)

[259] Lyne A G Pritchard R S Graham–Smith F and Camilo F 1996 *Nature* **381** 497

[260] Lyne A G Pritchard R S and Graham–Smith F 1993 *Mon. Not. R. Astron. Soc.* **265** 1003

[261] Kaspi V M Manchester R N Siegman B Johnston S and Lyne A G 1994 *ApJ* **422** L83

[262] Boyd P T *et al* 1995 *ApJ* **448** 365

[263] Shemar S L and Lyne A G 1996 *Mon. Not. R. Astron. Soc.* **282** 667

[264] Lyne A G Kaspi V M Bailes M Manchester R N Taylor H and Arzoumanian Z 1996 *Mon. Not. R. Astron. Soc.* **281** L14
[265] Anderson P W and Itoh N 1975 *Nature* **256** 25
[266] Pines D and Alpar M A 1985 *Nature* **316** 27
[267] Alpar M A 1992 *Some Topics in Neutron Star Superfluid Dynamics, in: The Structure and Evolution of Neutron Stars* ed D Pines R Tamagaki and S Tsuruta (New York: Addison-Wesley) p 148
[268] Clark J W Davé R D and Chen J M C 1992 *Microscopic Calculations of Superfluid Gaps, in: The Structure and Evolution of Neutron Stars* ed D Pines R Tamagaki and S Tsuruta (New York: Addison-Wesley) p 134
[269] Epstein R I Link B and Baym G 1992 *Superfluid Dynamics in the Inner Crust of Neutron Stars, in: The Structure and Evolution of Neutron Stars* ed D Pines R Tamagaki and S Tsuruta (New York: Addison-Wesley) p 156
[270] Alpar M A Cheng K S and Pines D 1989 *ApJ* **346** 823
[271] Sedrakian A 1995 *Mon. Not. R. Astron. Soc.* **277** 225
[272] Sedrakian A and Sedrakian D M 1995 *ApJ* **447** 305
[273] Sedrakian A Sedrakian D M Cordes J and Terzian Y 1995 *ApJ* **447** 324
[274] Baym G and Pethick C 1975 *Ann. Rev. Nucl. Sci.* **25** 27
[275] Trimble V and Rees M 1970 *Astrophys. Lett.* **5** 93
[276] Börner G and Cohen J M 1973 *ApJ* **185** 959
[277] Brecher K and Burrows A 1980 *ApJ* **240** 642
[278] Ramaty R and Meszaros P 1981 *ApJ* **250** 384
[279] Ruderman M 1992 *Neutron Star Crust Braking and Magnetic Field Evolution, in: The Structure and Evolution of Neutron Stars* ed D Pines R Tamagaki and S Tsuruta (New York: Addison-Wesley) p 353
[280] Sedrakyan D M 1970 *Nature, London* **228** 1074; *Astrophysics* **6** 339
[281] Chakrabarty S Bandyopadhyay D and Pal S 1997 *Phys. Rev. Lett.* **78** 2898
[282] Becker W Predehl P Trümper J and Ögelman H 1992 *IAU Circular* **5554** p 1
[283] Finley J and Ögelman H 1993 *IAU Circular* **5787**
[284] Becker W 1993 *IAU Circular* **5805**
[285] Becker W and Aschenbach B 1995 *The Lives of Neutron Stars* ed M A Alpar Ü Kiziloglu and J van Paradijs (Dordrecht: Kluwer) p 47
[286] Seward F Harnden F Murdin P and Clark D 1983 *ApJ* **267** 698
[287] Trussoni E Brinkmann W Ögelman H Hasinger G and Aschenbach B 1990 *Astron. & Astrophys.* **234** 403
[288] Finley J P Ögelman H Hasinger G and Trümper J 1993 *ApJ* **410** 323
[289] Safi–Harb S and Ögelman H 1995 *The Lives of Neutron Stars* ed M A Alpar Ü Kiziloglu and J van Paradijs (Dordrecht: Kluwer) p 53
[290] Yancopoulos S D Hamilton T D and Helfland D J 1993 *Bull. American Astron. Soc.* **25** 912
[291] Seward F and Wang Z R 1988 *ApJ* **332** 199
[292] Becker W and Trümper J 1993 *Nature* **365** 528
[293] Ögelman H Finley J and Zimmermann H 1993 *Nature* **361** 136

[294] Finley J P Ögelman H and Kiziloglu Ü 1992 *ApJ* **394** L21
[295] Halpern J and Ruderman M 1993 *ApJ* **415** 286
[296] Ögelman H and Finley J 1993 *ApJ* **413** L31
[297] Negele J W and Vautherin D 1973 *Nucl. Phys.* **A207** 298
[298] Abrahams A M and Shapiro S L 1991 *ApJ* **374** 652
[299] Friedman E Gal A and Batty C J 1994 *Nucl. Phys.* **A579** 518
[300] Barth R *et al* 1997 *Phys. Rev. Lett.* **78** 4027
[301] Cassing W Bratkovskaya E L Mosel U Teis S and Sibirtsev A 1997 *Nucl. Phys.* **A614** 415
Bratkovskaya E L Cassing W and Mosel U 1997 *Nucl. Phys.* **A622** 593
[302] Weise W 1998 *Quarks, Hadrons and Dense Nuclear Matter, in: Trends in Nuclear Physics – 100 years later, Les Houches* (Technical University of Munich Preprint TUM/T39–97–1, to be published by Elsevier Science Publishers).
[303] Dashen R F and Rajaraman R 1974 *Phys. Rev.* D **10** 696; 708
[304] Rajaraman R 1979 *Elementarity of Baryon Resonances in Nuclear Matter, in: Mesons in Nuclei* vol III ed M Rho and D Wilkinson (Amsterdam: North-Holland) p 197
[305] Particle Data Group 1984 *Rev. Mod. Phys.* **56** S1
[306] Holzenkamp B Holinde K and Speth J 1989 *Nucl. Phys.* **A500** 485
[307] Holinde K 1981 *Phys. Rep.* **68** 121
[308] Boguta J and Bodmer A R 1977 *Nucl. Phys.* **A292** 413
[309] Boguta J and Rafelski J 1977 *Phys. Lett.* **71B** 22
[310] Brown G E and Rho M 1991 *Phys. Rev. Lett.* **66** 2720
[311] Guichon P A M Saito K Rodionov E and Thomas A W 1996 *Nucl. Phys.* **A601** 349
[312] Saito K Tsushima K and Thomas A W 1997 *Phys. Rev.* C **55** 2637
[313] Weber F and Weigel M K 1989 *J. Phys. G: Nucl. Part. Phys.* **15** 765
[314] Wilets L 1979 *Green's Functions Method for the Relativistic Field Theory Many-Body Problem, in: Mesons in Nuclei* vol III ed M Rho and D Wilkinson (Amsterdam: North-Holland) p 791
[315] Weber F and Weigel M K 1990 *Nucl. Phys.* **A519** 303c
[316] Weigel M K and Wegmann G 1971 *Fortschr. Phys.* **19** 451
[317] Müther H Prakash M and Ainsworth T L 1987 *Phys. Lett.* **199B** 469
[318] Martin P C and Schwinger J 1959 *Phys. Rev.* **115** 1342
[319] Erkelenz K 1974 *Phys. Rev.* C **13** 191
[320] Machleidt R 1989 *Adv. Nucl. Phys.* **19** 188
[321] Iachello F Jackson A D and Landé A 1973 *Phys. Lett.* **43B** 191
[322] Höhler G and Pietarinen E 1975 *Nucl. Phys.* **B95** 210
[323] Grein W 1977 *Nucl. Phys.* **B131** 255
[324] Weber F and Weigel M K 1985 *Phys. Rev.* C **32** 2141
[325] Jackson A D 1983 *Ann. Rev. Nucl. Part. Sci.* **33** 105
[326] Haug P K 1969 *Dissertation* (University of Frankfurt, Germany)
[327] Joachain Ch J 1975 *Quantum Collision Theory* (Amsterdam: North-Holland)

[328] Salpeter E and Bethe H A 1951 *Phys. Rev.* **84** 1232
[329] Nakanishi N 1969 *Prog. Theor. Phys. Suppl.* **43** 131
[330] Woloshyn R M and Jackson A D 1973 *Nucl. Phys.* **B64** 269
[331] Zuilhof M J and Tjon J A 1982 *Phys. Rev.* C **26** 1277
[332] Blankenbecler R and Sugar R 1966 *Phys. Rev.* **142** 1051
[333] Reiner A S 1964 *Phys. Rev.* **133** 1105
[334] Barton G 1965 *Introduction to Dispersion Techniques in Field Theory* (New York: Benjamin)
[335] Arfken G 1985 *Mathematical Methods for Physicists* (Orlando: Academic Press)
[336] Weber F and Weigel M K 1990 *Europhys. Lett.* **12** 603
[337] Dolan L and Jackiw R 1974 *Phys. Rev.* D **9** 3320
[338] Kadanoff L P and Baym G 1962 *Quantum Statistical Mechanics* (New York: Benjamin)
[339] Fetter A L and Walecka J D 1971 *Quantum Theory of Many-Particle Systems* (New York: McGraw Hill)
[340] Bernard C W 1974 *Phys. Rev.* D **9** 3312
[341] Shuryak E V 1980 *Phys. Rep.* **61** 71
[342] Gross D J Pisarski R D and Yaffe L G 1981 *Rev. Mod. Phys.* **53** 43
[343] Puff R D 1961 *Ann. Phys., NY* **13** 317
[344] Bowers R L and Zimmerman R L 1973 *Phys. Rev.* D **7** 296
[345] Bowers R L Gleeson A M and Pedigo R D 1975 *Phys. Rev.* D **12** 3043; 3056
[346] Bjorken J D and Drell S D 1965 *Relativistic Quantum Fields* (New York: Mc Graw-Hill)
[347] Johnson M H and Teller E 1955 *Phys. Rev.* **98** 783
[348] Duerr H P 1956 *Phys. Rev.* **103** 469
[349] Walecka J D 1974 *Ann. Phys., NY* **83** 491
[350] Zimanyi J and Moszkowski S A 1990 *Phys. Rev.* C **42** 1416
[351] Glendenning N K Banerjee B and Gyulassy M 1983 *Ann. Phys., NY* **149** 1
[352] Particle Data Group 1976 *Rev. Mod. Phys.* **48** 30
[353] Sakurai J J 1966 *Phys. Rev. Lett.* **17** 1021
[354] Glendenning N K 1989 *Nucl. Phys.* **A493** 521
[355] Horowitz C J and Serot B D 1983 *Nucl. Phys.* **A399** 529
[356] Boguta J 1982 *Phys. Lett.* **109B** 251
[357] Waldhauser B M Maruhn J A Stöcker H and Greiner W 1987 *Z. Phys.* A **328** 19
[358] Waldhauser B M Theis J Maruhn J A Stöcker H and Greiner W 1987 *Phys. Rev.* C **36** 1019
[359] Pannert W Ring P and Boguta J 1987 *Phys. Rev. Lett.* **59** 2420
[360] Glendenning N K 1987 *Phys. Lett.* **185B** 275; *Nucl. Phys.* **A469** 600
[361] Glendenning N K and Moszkowski S A 1991 *Phys. Rev. Lett.* **67** 2414
[362] Boguta J and Bohrmann S 1981 *Phys. Lett.* **102B** 93
[363] Walker G E 1986 *Nucl. Phys.* **A450** 287c.

[364] Rufa M Schaffner J Marhun J Stöcker H Greiner W and Reinhard P G 1990 *Phys. Rev.* C **42** 2469
[365] Millener D J Dover C B and Gal A 1988 *Phys. Rev.* C **38** 2700
[366] Weisskopf V F 1957 *Rev. Mod. Phys.* **29** 174
[367] Hugenholtz N M and Van Hove L 1958 *Physica* **24** 363
[368] Banerjee B Glendenning N K and Gyulassy M 1981 *Nucl. Phys.* **A361** 326
[369] Glendenning N K Hecking P and Ruck V 1983 *Ann. Phys., NY* **149** 22
[370] Campbell D K 1977 *Field Theory, Chiral Symmetry, and Pion-Nucleus Interaction, in: Nuclear Physics with Heavy Ions and Mesons, Les Houches* vol 2 (Amsterdam: North-Holland) p 549
[371] Kaplan D and Nelson A 1986 *Phys. Lett.* **175B** 57
[372] Brown G E Kubodera K and Rho M 1987 *Phys. Lett.* **192B** 273
[373] Lee C H and Rho M 1995 *Kaon Condensation in Dense Stellar Matter, in: Proc. Int. Symp. on Strangeness and Quark Matter* ed G Vassiliadis A Panagiotou B S Kumar and J Madsen (Singapore: World Scientific) p 283
[374] Ainsworth T L Baron E Brown G E Cooperstein J and Prakash M 1987 *Nucl. Phys.* **A464** 740
[375] Kruse H Jacak B and Stöcker H 1985 *Phys. Rev. Lett.* **54** 289
[376] Molitoris J J and Stöcker H 1985 *Phys. Rev.* C **32** 346
[377] Kruse H *et al* 1985 *Phys. Rev.* C **31** 1770
[378] Stock R *et al* 1982 *Phys. Rev. Lett.* **49** 1236
[379] Harris J W *et al* 1987 *Phys. Rev. Lett.* **58** 463
[380] Renfordt R E 1984 *Phys. Rev. Lett.* **53** 763
[381] Glendenning N K 1988 *Phys. Rev.* C **37** 2733
[382] Waldhauser B M Maruhn J A Stöcker H and Greiner W 1988 *Phys. Rev.* C **38** 1003
[383] Friedman B and Pandharipande V R 1981 *Nucl. Phys.* **A361** 502
[384] Harris J W *et al* 1985 *Phys. Lett.* **153B** 377
1984 *Phys. Rev. Lett.* **52** 289
[385] Ter Haar B and Malfliet R 1986 *Phys. Rev. Lett.* **56** 1237
[386] Sauer G Chandra H and Mosel U 1976 *Nucl. Phys.* **A264** 221
[387] Freedman R A 1977 *Phys. Lett.* **71B** 369
[388] Schmidt K E and Pandharipande V R 1979 *Phys. Lett.* **87B** 11
[389] Lattimer J M 1981 *Ann. Rev. Nucl. Part. Sci.* **31** 337; 1992 *The Equation of State in Neutron Star Matter, in: The Structure and Evolution of Neutron Stars* ed D Pines R Tamagaki and S Tsuruta (New York: Addison-Wesley) p 50
[390] Huber H Weber F Weigel M K and Schaab Ch 1998 *Int. J. Mod. Phys.* E **7** (no 3) 301
[391] Garpman S I A Glendenning N K and Karant Y J 1979 *Nucl. Phys.* **A322** 382
[392] Itoh N Mitake S Iyetomi H and Ichimaru S 1983 *ApJ* **273** 774
[393] Itoh N Hayashi H and Kohyama Y 1993 *ApJ* **418** 405
Itoh N and Kohyama Y 1993 *ApJ* **404** 268

[394] Østgaard E 1992 *Electrical Conductivity in Neutron Stars, in: Proc. 1st Symp. on Nucl. Phys. in the Universe, Oak Ridge* ed M W Guidry and M R Strayer (Bristol: IOP Publishing) p 471

[395] Itoh N and Hiraki K 1994 *ApJ* **435** 784
Itoh N Kotouda T and Hiraki K 1995 *ApJ* **455** 244

[396] Keil W and Janka H T 1995 *Astron. & Astrophys.* **296** 145

[397] Schröter A *et al* 1994 *Z. Phys.* A **350** 101

[398] Senger P 1996 *Heavy Ion Physics* **4** 317

[399] Waas T Rho M and Weise W 1997 *Nucl. Phys.* **A617** 449

[400] Schaffner J and Mishustin I N 1996 *Phys. Rev.* C **53** 1416

[401] Tamagaki R 1991 *Prog. Theor. Phys.* **85** 321

[402] Sakai T Mori J Buchmann A J Shimizu K and Yazaki K 1997 *Nucl. Phys.* **A625** 192

[403] Faessler A Buchmann A J Krivoruchenko M I and Martemyanov B V 1997 *Phys. Lett.* **391B** 255

[404] Faessler A Buchmann A J and Krivoruchenko M I 1997 *Phys. Rev.* C **56** 1576

[405] Glendenning N K and Schaffner–Bielich J 1998 *Phys. Rev.* C **58** 1298

[406] Pandharipande V R 1971 *Nucl. Phys.* **A178** 123

[407] Bethe H A and Johnson M 1974 *Nucl. Phys.* **A230** 1

[408] Myers W D and Swiatecki W J 1996 *Nucl. Phys.* **A601** 141

[409] Glendenning N K 1990 *Neutron Stars, Fast Pulsars, Supernovae and the Equation of State of Dense Matter, in: Proc. NATO Advanced Study Institute on The Nuclear Equation of State, Peniscola* NATO ASI Series B vol 216A ed W Greiner and H Stöcker (New York: Plenum Press) p 751

[410] Kapusta J I and Olive K A 1990 *Phys. Rev. Lett.* **64** 13

[411] Baym G 1992 *Ultrarelativistic Heavy-Ion Collisions and Neutron Stars, in: The Structure and Evolution of Neutron Stars* ed D Pines R Tamagaki and S Tsuruta (New York: Addison-Wesley) p 188

[412] Brown G E and Weise W 1976 *Phys. Rep.* **27** 1

[413] Migdal A B 1978 *Rev. Mod. Phys.* **50** 107

[414] Baym G and Campbell D K 1979 *Chiral Symmetry and Pion Condensation, in: Mesons in Nuclei* vol III ed M Rho and D Wilkinson (Amsterdam: North-Holland) p 1031

[415] Muto T and Tatsumi T 1987 *Prog. Theor. Phys.* **78** 1405

[416] Takatsuka T Tamiya K Tatsumi T and Tamagaki R 1978 *Prog. Theor. Phys.* **59** 1933

[417] Bäckman S O and Weise W 1979 *Pion Condensation and the Pion-Nuclear Interaction, in: Mesons in Nuclei* vol III ed M Rho and D Wilkinson (Amsterdam: North-Holland) p 1095

[418] Barshay S and Brown G E 1973 *Phys. Lett.* **47B** 107

[419] Brown G E Kubodera K Page D and Pizzochero P 1988 *Phys. Rev.* D **37** 2042

[420] Tatsumi T and Muto T 1991 *Nuclei in the Cosmos* ed H Oberhummer and C Rolfs (Berlin: Springer-Verlag)

[421] Umeda H Nomoto K Tsuruta S Muto T and Tatsumi T 1992 *Neutron Star Cooling and Pion Condensation, in: The Structure and Evolution of Neutron Stars* ed D Pines R Tamagaki and S Tsuruta (New York: Addison-Wesley) p 406

[422] Tatsumi T 1988 *Prog. Theor. Phys.* **80** 22

[423] Page D and Baron E 1990 *ApJ* **354** (1990) L17

[424] Thorsson V Prakash M and Lattimer J M 1994 *Nucl. Phys.* **A572** 693

[425] Glendenning N K Pei S and Weber F 1997 *Phys. Rev. Lett.* **79** 1603

[426] Chapline G and Nauenberg M 1977 *Ann. New York Academy of Sci.* **302** 191

[427] Gentile N A Aufderheide M B Mathews G J Swesty F D and Fuller G M 1993 *ApJ* **414** 701

[428] Prakash M Cooke J R and Lattimer J M 1995 *Phys. Rev.* D **52** 661

[429] Hasenfratz A and Hasenfratz P 1985 *Ann. Rev. Nucl. Part. Sci.* **35** 559

[430] Ellis J Kapusta J I and Olive K A 1991 *Nucl. Phys.* **B348** 345

[431] Bethe H A Brown G E and Cooperstein J 1987 *Nucl. Phys.* **A462** 791

[432] Serot B D and Uechi H 1987 *Ann. Phys., NY* **179** 272

[433] Ravenhall D G Pethick C J and Wilson J R 1983 *Phys. Rev. Lett.* **50** 2066

[434] Ravenhall D G Pethick C J and Lattimer J M 1983 *Nucl. Phys.* **A407** 571

[435] Williams R D and Koonin S E 1985 *Nucl. Phys.* **A435** 844

[436] Hermann B 1996 *Master Thesis* (University of Munich, Germany)

[437] Glendenning N K and Pei S 1995 *Phys. Rev.* C **52** 2250

[438] Heiselberg H 1995 *Quark Matter Structure in Neutron Stars, in: Proc. Int. Symp. on Strangeness and Quark Matter* ed G Vassiliadis A D Panagiotou B S Kumar and J Madsen (Singapore: World Scientific) p 298

[439] Poschenrieder P 1987 *Dissertation* (University of Munich, Germany)

[440] Rose M E 1957 *Elementary Theory of Angular Momentum* (New York: Wiley)

[441] Erkelenz K Alzetta R and Holinde K 1971 *Nucl. Phys.* **A176** 413

[442] Ho–Kim Q and Khanna F C 1974 *Ann. Phys., NY* **86** 233

[443] Wegmann G 1968 *Z. Phys.* **211** 235

[444] Wegmann G and Weigel M K 1968 *Phys. Lett.* **26B** 245

[445] Jacob M and Wick G C 1959 *Ann. Phys., NY* **7** 404

[446] Weber F 1992 *Hadron Physics and Neutron Star Properties* Habilitation Thesis (University of Munich, Germany)

[447] Huber H 1993 *Master Thesis* (University of Munich, Germany)

[448] De Jonga F and Malfliet R 1991 *Phys. Rev.* C **44** 998

[449] Huber H Weber F and Weigel M K 1995 *Phys. Rev.* C **51** 1790

[450] Brockmann R and Toki H 1992 *Phys. Rev. Lett.* **68** 3408

[451] Haddad S and Weigel M K 1993 *Phys. Rev.* C **48** 2740

[452] Haddad S and Weigel M K 1994 *Nucl. Phys.* **A578** 471

[453] Von-Eiff D Stocker W and Weigel M K 1994 *Phys. Rev.* C **50** 1436

[454] Engvik L Hjorth–Jensen M Osnes E Bao G and Østgaard E 1994 *Phys. Rev. Lett.* **73** 2650

[455] Bao G Engvik L Hjorth–Jensen M Osnes E and Østgaard E 1994 *Nucl. Phys.* **A575** 707

[456] Bao G Østgaard E and Dybvik B 1994 *Int. J. Mod. Phys.* D **3** 813

[457] Engvik L Osnes E Hjorth–Jensen M Bao G and Østgaard E 1996 *ApJ* **469** 794

[458] Huber H Weigel M K and Weber F 1994 *The Relativistic Treatment of Symmetric and Asymmetric Nuclear Matter, in: Proc of NATO Advanced Study Institute on Hot and Dense Nuclear Matter* Series B vol 335 ed W Greiner H Stöcker and A Gallmann (New York: Plenum Press) p 799

[459] Huber H Weber F and Weigel M K 1994 *Phys. Rev.* C **50** R1287

[460] Lopez–Quelle M Marcos S Niembro R Bouyssy A and Van Giai N 1988 *Nucl. Phys.* **A483** 479

[461] Bernardos P Fomenko V N Van Giai N Quelle M L Marcos S Niembro R and Savushkin L N 1983 *Phys. Rev.* C **48** 2665

[462] Zhang J K Jin Y and Onley D S 1993 *Phys. Rev.* C **48** 2697

[463] Wiringa R B Fiks V and Fabrocini A 1988 *Phys. Rev.* C **38** 1010

[464] Bombaci I and Lombardo U 1991 *Phys. Rev.* C **44** 1892

[465] Rapp R Durso J W and Wambach J 1997 *Nucl. Phys.* **A651** 501

[466] Glendenning N K 1987 *Nucl. Phys.* **A469** 600

[467] Anastasio M R Celenza L S and Shakin C M 1981 *Phys. Rev.* C **23** 2258

[468] Sehn L Fuchs C and Faessler A 1997 *Phys. Rev.* C **56** 216

[469] McNeil J A Ray L and Wallace S J 1983 *Phys. Rev.* C **27** 2123

[470] Ter Haar B and Malfliet R 1987 *Phys. Rev. Lett.* **59** 1652

[471] Strobel K Weber F Weigel M K and Schaab Ch 1997 *Int. J. Mod. Phys.* E **6** (no 4) 669

[472] Baldo M Bombaci I and Burgio G F 1998 (to appear in *Astron. & Astrophys.*, astro-ph/9707277)

[473] Lee C H Kuo T T S Li G Q and Brown G E 1997 *Phys. Lett.* **412B** 235

[474] Von-Eiff D Pearson J M Stocker W and Weigel M K 1994 *Phys. Lett.* **324B** 279

[475] Farine M Coté J and Pearson J M 1981 *Phys. Rev.* C **24** 303

[476] Von-Eiff D Pearson J M Stocker W and Weigel M K 1994,*Phys. Rev.* C **50** 831

[477] Backer D C 1990 (Private communication)

[478] Sprung D W L 1972 *Adv. Nucl. Phys.* **5** 225

[479] Day B D *Rev. Mod. Phys.* **51** 821

[480] Pandharipande V R and Wiringa R B 1979 *Rev. Mod. Phys.* **51** 821

[481] Myers W D and Swiatecki W J 1990 *Ann. Phys., NY* **204** 401

[482] Myers W D and Swiatecki W J 1991 *Ann. Phys., NY* **211** 292

[483] Myers W D and Swiatecki W J 1995 *The Nuclear Thomas–Fermi Model, in: Proc. XXIX Zakopane School of Physics, Zakopane* ed R Broda and W Meczynski *Acta Physica Polonica* **B26** 111; (*see also* 1996 **B27** 99; 1997 **B28** 9; 1998 **B29** 313)

Myers W D and Swiatecki W J 1998 *Phys. Rev.* C **57** 3020

[484] Myers W D and Swiatecki W J 1994 *Thomas–Fermi Treatment of Nuclear Masses, Deformations and Density Distributions, in: Proc. 4th KINR Int. School on Nuclear Physics, Kiev* ed F A Ivanyuk p 40

[485] Seyler R G and Blanchard C H 1961 *Phys. Rev.* **124** 227; 1963 **131** 355

[486] Myers W D 1977 *Droplet Model of Atomic Nuclei* (New York: McGraw Hill)

Myers W D and Swiatecki W 1969 *Ann. Phys., NY* **55** 395

Myers W D and Schmidt K H 1983 *Nucl. Phys.* **A410** 61

[487] Hartmann D El Eid M F and Barranco M 1984 *Astron. & Astrophys.* **131** 249

[488] Randrup J and Medeiros E L 1991 *Nucl. Phys.* **A529** 115

[489] Randrup J and Medeiros E L 1992 *Phys. Rev.* C **45** 372

[490] Glendenning N K 1992 *Phys. Rev.* D **46** 4161

[491] Zel'dovich Ya B 1962 *Sov. Phys.–JETP* **14** 1143

[492] Zel'dovich Ya B and Novikov I D 1971 *Relativistic Astrophysics* vol I II (Chicago, University of Chicago Press); 1983 vol II

[493] Ambartsumyan V A and Saakyan G S 1960 *Soviet Astr.–AJ* **4** 187; 1963 *Astron. Zh.* **37** 193

[494] Langer W D and Rosen L C 1970 *Astrophys. and Space Sci.* **6** 217

[495] Libby L M and Thomas F J 1969 *Phys. Lett.* **30B** 88

[496] Pandharipande V R and Garde V K 1972 *Phys. Lett.* **39B** 608

[497] Banerjee P K and Sprung D W L 1971 *Can. J. Phys.* **49** 1871

[498] Mahaux C 1981 *Brueckner Theory of Infinite Fermi Systems* Lecture Notes in Physics vol 138 (Berlin: Springer-Verlag)

[499] Fiset E O and Foster T C 1972 *Nucl. Phys.* **A184** 588

[500] Ho–Kim Q and Khanna F C 1974 *Ann. Phys., NY* **86** 233

[501] Coester F Cohen S Day B and Vincent C M 1970 *Phys. Rev.* C **1** 769

[502] Wong C W 1972 *Ann. Phys., NY* **72** 107

[503] Celenza L S and Shakin C M 1981 *Phys. Rev.* C **24** 2704

[504] Green A M 1976 *Rep. Prog. Phys.* **39** 1109

[505] Thirring H 1918 *Phys. Zeitschr.* **19** 33

[506] Hönl H and Soergel–Fabricius Ch 1961 *Z. Phys.* **163** 571

[507] Hönl H and Dehnen H 1962 *Z. Phys.* **166** 544

[508] Brill D R and Cohen J M 1966 *Phys. Rev.* **143** 1011

[509] Misner Ch W Thorne K S and Wheeler J A 1973 *Gravitation* (San Francisco: Freeman and Company)

[510] Lightman A P Press W H Price R H Teukolsky S A 1975 *Problem Book in Relativity and Gravitation* (Princeton: Princeton University Press)

[511] Tolman R C 1987 *Relativity, Thermodynamics and Cosmology* (New York: Dover Publications)

[512] Schwarzschild K 1916 *Sitzber. Deut. Akad. Wiss. Berlin, Kl. Math.-Phys. Tech.* pp 424–434

[513] Schutz B F 1990 *A First Course in General Relativity* (Cambridge: Cambridge University Press)

[514] Oppenheimer J R and Volkoff G M 1939 *Phys. Rev.* **55** 374

[515] Misner C W and Sharp D H 1964 *Phys. Rev.* **136** 571

[516] Ledoux P and Warlaven Th 1958 *Handbuch der Physik* vol 51 ed S Flügge (Berlin: Springer-Verlag) p 353
Ledoux P *Handbuch der Physik* vol 51 ed S Flügge (Berlin: Springer-Verlag) p 635

[517] Unno W Osaki Y Ando H and Shibahashi H 1979 *Nonradial Oscillations of Stars* (Tokyo: University Press)

[518] Cox J P 1980 *Theory of Stellar Pulsations* (Princeton: Princeton University Press)

[519] Thorne K S and Campolattaro A 1967 *ApJ* **149** 591
Price R and Thorne K S 1969 *ApJ* **155** 163
Thorne K S 1969 *ApJ* **158** 1; 997
Campolattaro A and Thorne K S 1970 *ApJ* **159** 847

[520] Ferrari V 1992 *Non-radial Oscillations of Stars in General Relativity: a Scattering Problem*, *Phil. Trans. R. Soc. Lond.* A **340** pp 423–445

[521] Bastrukov S Molodtsova I Papoyan V and Weber F 1996 *J. Phys. G: Nucl. Part. Phys.* **22** L33

[522] Bastrukov S Molodtsova I Papoyan V and Weber F 1996 Proc. VII Int. Conf. on Symmetry Methods in Physics, Dubna vol 1, ed A N Sissakian and G S Pogosyan (JINR Dubna: ISBN 5–85165–452–X) p 42

[523] Bastrukov S and Podgainy D 1997 *Astron. J.* **74** 39
Bastrukov S Molodtsova I Papoyan V and Podgainy D 1997 *Astrophys.* **40** 77

[524] Bastrukov S Weber F and Podgainy D 1999 *J. Phys. G: Nucl. Part. Phys.* **25** 1

[525] Bertsch G F 1974 *Ann. Phys., NY* **86** 138
Bertsch G F 1978 *Nuclear Physics with Heavy Ions and Mesons* vol 1 ed R Balian M Rho and G Ripka (Amsterdam: North-Holland) p 175

[526] Nix J R and Sierk A J 1980 *Phys. Rev.* C **21** 396
Bastrukov S I and Molodtsova I V 1995 *Phys. Part. Nucl.* **26** 180
Bastrukov S I Libert J and Molodtsova I V 1978 *Int. J. Mod. Phys.* E **6** (no 1) 89

[527] Nörenberg W 1986 *New Vistas in Nuclear Dynamics* ed P J Brussard and J H Koch (New York: Plenum press)

[528] Bastrukov S I Podgainy D V Molodtsova I V and Kosenko G 1998 *J. Phys. G: Nucl. Part. Phys.* **24** L1
Bastrukov S I Podgainy D V 1998 *Physica* **A250** (no 3–4) 435

[529] Koester D and Chanmugam G 1990 *Rep. Prog. Phys.* **53** 837

[530] Hansen C J and Van Horn H M 1979 *ApJ* **233** 253

[531] Hansen C J 1980 *Nonradial and Nonlinear Stellar Pulsations* Lecture Notes in Physics ed H A Hill and W A Dziembowski (Berlin: Springer-Verlag) p 445

[532] McDermott P N Van Horn H M and Hansen C J 1988 *ApJ* **325** 725

[533] Saakian G S 1995 *Physics of Neutron Stars* (JINR, Dubna)

[534] Chandrasekhar S 1964 *Phys. Rev. Lett.* **12** 114
[535] Bardeen J M Thorne K S and Meltzer D W 1966 *ApJ* **145** 505
[536] Friedman J L and Ipser J R 1992 *Rapidly Rotating Relativistic Stars Phil. Trans. R. Soc. Lond.* A **340** pp 391–422
[537] Bardeen J M 1972 *Rapidly Rotating Stars, Disks and Black Holes, in: Black Holes* ed C DeWitt and B S DeWitt (New York: Gordon and Breach)
[538] Datta B Sahu P K Anand J D and Goyal A 1992 *Phys. Lett.* **283B** 313
[539] Vät H M and Chanmugam G 1992 *Astron. & Astrophys.* **260** 250
[540] Hillebrandt W and Steinmetz K O 1976 *Astron. & Astrophys.* **53** 283
[541] Lattimer J 1998 (Private communication)
[542] Schaab Ch Weber F Weigel M K and Glendenning N K 1996 *Nucl. Phys.* **A605** 531
[543] Ruffini R 1978 *Physics and Astrophysics of Neutron Stars and Black Holes* (Amsterdam: North-Holland) p 287
[544] Lattimer J M and Yahil A 1989 *ApJ* **340** 426
[545] Ruderman M A and Fowler W A 1971 *Elementary Particles, in: Science, Technology and Society* ed L C L Yuan (New York: Academic Press) p 72
[546] Alonso J D and Ibanez–Cabanell J H 1985 *ApJ* **291** 308
[547] Wilson J R 1972 *ApJ* **176** 195
[548] Abramowicz M A and Wagoner R V 1976 *ApJ* **204** 896
[549] Lightman A P and Shapiro S L 1976 *ApJ* **207** 263
[550] Butterworth E M and Ipser J R 1975 *ApJ* **200** L103; **204** 200
[551] Butterworth E M and Ipser J R 1976 *ApJ* **204** 200
[552] Butterworth E M 1979 *ApJ* **231** 219
[553] Butterworth E M 1976 *ApJ* **204** 561
[554] Datta B 1988 *Fundamentals of Cosmic Physics* **12** 151
[555] Eriguchi Y 1993 *Rotating Objects and Relativistic Physics* ed F J Chinea and L M González–Romero (Berlin: Springer-Verlag)
[556] Eriguchi Y Hachisu I and Nomoto K 1994 *Mon. Not. R. Astron. Soc.* **266** 179
[557] Neugebauer G and Herold H 1992 *Gravitational Fields of Rapidly Rotating Neutron Stars, in: Relativistic Gravity Research* Lecture Notes in Physics vol 410 , ed J Ehlers and G Schäfer (Berlin: Springer-Verlag) p 305; p 319
[558] Salgado M Bonazzola S Gourgoulhon E and Haensel P 1994 *Astron. & Astrophys.* **291** 155
[559] Cook G B Shapiro S L Teukolsky S A 1994 *ApJ* **422** 227
[560] Cook G B Shapiro S L Teukolsky S A 1994 *ApJ* **424** 823
[561] Hartle J B and Sharp D H 1967 *ApJ* **147** 317
[562] Hegyi D J 1977 *ApJ* **217** 244
[563] Cutler C Lindblom L and Splinter R J 1990 *ApJ* **363** 603
[564] Nomoto K and Tsuruta S 1987 *ApJ* **312** 711
[565] Eisenhart L 1926 *Differential Geometry* (Princeton: Princeton University Press)
[566] Irvine J M 1978 *Neutron Stars* (Oxford: Clarendon Press)
[567] Kapoor R C and Datta B 1984 *Mon. Not. R. Astron. Soc.* **209** 895

[568] Buchdahl H A 1959 *Phys. Rev.* **116** 1027
[569] Bondi H 1964 *Proc. Roy. Soc.* **A284** 303
[570] Hartle J B 1973 *Astrophys. and Space Sci.* **24** 385
[571] Ray A and Datta B 1984 *ApJ* **282** 542
[572] Abramowitz M and Stegun I A 1964 *Handbook of Mathematical Functions* (Washington DC: Government Printing Office)
[573] Sedrakian D M Papoian V V and Chubarian E V 1970 *Mon. Not. R. Astron. Soc.* **149** 25
[574] Arutyunyan G G Sedrakian D M and Chubaryan É V 1971 *Astrofizika* **7** (no 3) 467
[575] Friedman J L and Schutz B F 1978 *ApJ* **222** 281
[576] Friedman J L 1983 *Phys. Rev. Lett.* **51** 11
[577] Chandrasekhar S 1969 *Ellipsoidal Figures of Equilibrium* (New Haven: Yale University Press)
[578] Detweiler S L and Lindblom L 1977 *ApJ* **213** 193
[579] Wu X Müther H Soffel M Herold H and Ruder H 1991 *Astron. & Astrophys.* **246** 411
[580] Datta B and Ray A 1983 *Mon. Not. R. Astron. Soc.* **204** 75
[581] Shapiro S L Teukolsky S A and Wasserman I 1983 *ApJ* **272** 702
[582] Bardeen J M and Wagoner R V 1971 *ApJ* **167** 359
[583] Abramowicz M A and Prasanna A R 1990 *Mon. Not. R. Astron. Soc.* **245** 720
[584] Abramowicz M A 1990 *Mon. Not. R. Astron. Soc.* **245** 733
[585] Lindblom L 1986 *ApJ* **303** 146
[586] Chandrasekhar S 1970 *Phys. Rev. Lett.* **24** 611
[587] Friedman J L 1978 *Comm. Math. Phys.* **62** 247
[588] Lindblom L 1992 *Instabilities in Rotating Neutron Stars, in: The Structure and Evolution of Neutron Stars* ed D Pines R Tamagaki and S Tsuruta (New York: Addison-Wesley) p 122
[589] Lindblom L and Detweiler S L 1977 *ApJ* **211** 565
[590] Lindblom L and Hiscock W A 1983 *ApJ* **267** 384
[591] Ipser J R and Managan R A 1985 *ApJ* **292** 517
[592] Managan R A 1985 *ApJ* **294** 463
[593] Ipser J R and Lindbolm L 1989 *Phys. Rev. Lett.* **62** 2777
[594] Ipser J R and Lindblom L 1990 *ApJ* **355** 226
[595] Ipser J R and Lindblom L 1991 *ApJ* **373** 213
[596] Ipser J R and Lindblom L 1991 *ApJ* **379** 285
[597] Cutler C and Lindblom L 1991 *Ann. N. Y. Acad. Sci.* **631** 97
[598] Sawyer R F 1989 *Phys. Rev.* D **39** 3804
[599] Flowers E and Itoh N 1976 *ApJ* **206** 218
[600] Flowers E and Itoh N 1979 *ApJ* **230** 847
[601] Mendell G 1991 *ApJ* **380** 515

[602] Lindblom L and Mendell G 1992 *Superfluid Effects on the Stability of Rotating Neutron Stars, in: The Structure and Evolution of Neutron Stars* ed D Pines R Tamagaki and S Tsuruta (New York: Addison-Wesley) p 188
[603] Baumgart D and Friedman J L 1986 *Proc. Roy. Soc. London* **A405** 65
[604] Cutler C and Lindblom L 1987 *ApJ* **314** 234
[605] Managan R A 1986 *ApJ* **309** 598
[606] Detweiler S L 1975 *ApJ* **197** 203
[607] Lamb H 1881 *Proc. London Math. Soc.* **13** 51
[608] Tsuruta S 1979 *Phys. Rep.* **56** 237
[609] Takatsuka T 1996 *Prog. Theor. Phys. Suppl.* **95** 901
[610] Lindblom L 1987 *ApJ* **317** 325
[611] Hartle J B and Munn M W 1975 *ApJ* **198** 467
[612] Friedman J L Ipser J R and Sorkin R D 1988 *ApJ* **325** 722
[613] Straumann N 1992 *Fermion and Boson Stars, in: Relativistic Gravity Research* Lecture Notes in Physics vol 410 ed J Ehlers and G Schäfer (Berlin: Springer-Verlag) p 267
[614] Imamura J Durisen R Friedman J L 1985 *ApJ* **294** 474
[615] Weber F Glendenning N K and Pei S 1997 Signal for the Quark-Hadron Phase Transition in Rotating Hybrid Stars, in: *Proc. 3rd Int. Conf. on Phys. and Astrophys. of Quark-Gluon Plasma* ed D C Sinha D K Srivastava and Y P Viyogi (New Delhi: Narosa Publishing House) p 237
[616] Weber F and Glendenning N K 1997 (unpublished calculations)
[617] Mottelson B R and Valatin J G 1960 *Phys. Rev. Lett.* **5** 511
[618] Stephens F S and Simon R S 1972 *Nucl. Phys.* **A183** 257
[619] Johnson A Ryde H and Hjorth S A 1972 *Nucl. Phys.* **A179** 753
[620] Sato K and Suzuki H 1989 *Prog. Theor. Phys.* **81** 997
[621] Madsen J 1998 *Phys. Rev. Lett.* **81** 3311
[622] Chodos A Jaffe R L Johnson K Thorne C B and Weisskopf V F 1974 *Phys. Rev.* D **9** 3471
[623] Shuryak E V 1988 *The QCD Vacuum, Hadrons, and The Superdense Matter* (Singapore: World Scientific)
[624] Chmaj T and Slominiski W 1988 *Phys. Rev.* D **40** 165
[625] Freedman B A and McLerran L D 1977 *Phys. Rev.* D **16** 1130; 1147; 1169
[626] Freedman B A and McLerran L D 1978 *Phys. Rev.* D **17** 1109
[627] Farhi E and Jaffe R L 1984 *Phys. Rev.* D **30** 2379
[628] Burrows A 1988 *ApJ* **335** 891
[629] Kettner Ch 1994 *Master Thesis* (University of Munich, Germany)
[630] Misner C W and Zapolsky H S 1964 *Phys. Rev. Lett.* **12** 635
[631] Madsen J 1992 *Phys. Rev.* D **46** 3290
[632] Haensel P and Zdunik J L 1991 *Nucl. Phys.* B *Proc. Suppl.* **24B** 139
[633] Pizzochero P 1991 *Phys. Rev. Lett.* **66** 2425
[634] Schertler K Greiner C and Thoma M 1997 *Nucl. Phys.* **A616** 659
[635] Wang Ch and Wang W 1991 *Commun. Theor. Phys.* **15** 347
[636] Schaab Ch 1998 *Dissertation* (University of Munich, Germany)

[637] McKenna J and Lyne A G 1990 *Nature* **343** 349
[638] Canuto V and Chitre S M 1974 *Phys. Rev.* D **9** 1587
[639] Alcock C *et al* 1991 *Robotic Telescopes in the 1990's* ed A V Filipenko (San Francisco: ASP)
[640] Paczynski B 1986 *ApJ* **304** 1
[641] Griest K 1991 *ApJ* **366** 412
[642] Griest K 1993 *The Search for the Dark Matter: WIMPs and MACHOs, in: Texas/Pascos '92, Berkeley* vol 688 ed C W Akerlof and M A Srednicki (New York: Annals New York Academy of Sciences).
[643] Hewitt J N 1993 *Gravitational Lenses, in: Texas/Pascos '92, Berkeley* vol 688 ed C W Akerlof and M A Srednicki (New York: Annals New York Academy of Sciences)
[644] Gould A 1992 *ApJ* **392** 234
[645] Bennett D P *et al* 1993 *The First Data from the MACHO Experiment, in: Texas/Pascos '92, Berkeley* vol 688 ed C W Akerlof and M A Srednicki (New York: Annals New York Academy of Sciences)
[646] Magneville C 1993 *Status Report on the French Search for MACHOs in the Galactic Halo, in: Texas/Pascos '92, Berkeley* vol 688 ed C W Akerlof and M A Srednicki (New York: Annals New York Academy of Sciences)
[647] Sutherland W *et al* 1995 *Nucl. Phys. Proc. Suppl.* **38** 379
[648] Weber F and Glendenning N K 1993 *Interpretation of Rapidly Rotating Pulsars, in: Proc of Nuclei in the Cosmos, Karlsruhe* ed F Käppeler and K Wisshak (Bristol: IOP Publishing) p 399
[649] Lang K R 1992 *Astrophysical Data, Planets and Stars* (New York: Springer)
[650] Cottingham W N Kalafatis D and Vinh Mau R 1994 *Phys. Rev. Lett.* **73** 1328
[651] Weber F and Glendenning N K 1994 *Fast Pulsars, Compact Stars, and the Strange Matter Hypothesis, in: Proc of 2nd Int. Conf. on Phys. and Astrophys. of Quark-Gluon Plasma, Calcutta* ed B Sinha Y P Viyog and S Raha (Singapore: World Scientific) p 343
[652] Weber F and Glendenning N K 1995 *Fast Pulsars, Strange Stars, and Strange Dwarfs, in: Proc of the 17th Texas Symposium on Relativ. Astrophys., Munich* vol 759 ed H Böhringer G E Morfill, and J Trümper (New York: Annals New York Academy of Sciences) p 303
[653] Burrows A and Lattimer J M 1986 *ApJ* **307** 178
[654] Thorne K 1977 *ApJ* **212** 825
[655] Misner C W and Sharp D H 1965 *Phys. Rev. Lett.* **15** 279
[656] Linquist R W 1966 *Ann. Phys., NY* **37** 487
[657] Gudmundson E Pethick C and Epstein R 1983 *ApJ* **272** 286
[658] Van Riper K A 1988 *ApJ* **329** 339
[659] Van Riper K A 1991 *ApJ Suppl.* **75** 449
[660] Itoh N Kohyama Y Matsumoto N and Seki M 1984 *ApJ* **285** 758
[661] Mitake S Ichimaru S and Itoh N 1984 *ApJ* **277** 375
[662] Gnedin O Y and Yakovlelv D 1995 *Nucl. Phys.* **A582** 697

[663] Haensel P 1991 *Transport Properties of Strange Matter, in: Proc. Int. Workshop on Strange Quark Matter in Physics and Astrophysics, Aarhus* ed J Madsen and P Haensel *Nucl. Phys.* B *Proc. Suppl.* **24B** p 23 CAMK Preprint **228**

[664] Itoh N Tomoo A Nakagawa M and Kohyama Y 1989 *ApJ* **339** 354

[665] Itoh N and Kohyama Y 1983 *ApJ* **275** 859

[666] Pethick C and Thorsson V 1994 *Phys. Rev. Lett.* **72** 1964

[667] Takatsuka T and Tamagaki R 1993 *Prog. Theor. Phys. Suppl.* **112** 27

[668] Ainsworth T Wambach J and Pines D 1989 *Phys. Lett.* **222B** 173
Wambach J Ainsworth T L and Pines D 1993 *Nucl. Phys.* **A555** 128

[669] Amundsen L and Østgaard E 1985 *Nucl. Phys.* **A442** 163

[670] Wambach J Ainsworth T and Pines D 1991 *Neutron Stars: Theory and Observation* ed J Ventura and D Pines (Dordrecht: Kluwer Academic Publishers) pp 37–48

[671] Schaab Ch Weber F and Weigel M K 1998 *Astron. & Astrophys.* **335** 596

[672] Alm Th Röpke G Sedrakian A and Weber F 1996 *Nucl. Phys.* **A604** 491

[673] Bailin D and Love A 1984 *Phys. Rep.* **107** 325

[674] Page D 1995 *Rev. Mex. Fis.* **41** *Suppl. 1* 178

[675] Chen J Clark J Davé R and Khodel V 1993 *Nucl. Phys.* **A555** 59

[676] Maxwell O 1979 *ApJ* **231** 201

[677] Friman B and Maxwell O 1979 *ApJ* **232** 541

[678] Lattimer J M Pethick C J Prakash M and Haensel P 1991 *Phys. Rev. Lett.* **66** 2701

[679] Maxwell O Brown G Campbell D Dashen R and Manassah J 1977 *ApJ* **216** 77

[680] Thorsson V Prakash M Tatsumi T and Pethick C 1995 *Phys. Rev.* D **52** 3739

[681] Price C 1980 *Phys. Rev.* D **22** 1910

[682] Duncan R C Shapiro S L and Wasserman I 1983 *ApJ* **267** 358

[683] Iwamoto N 1980 *Phys. Rev. Lett.* **44** 1637; 1982 *Ann. Phys., NY* **141** 1

[684] Pethick C Ravenhall P and Lorenz C 1995 *Nucl. Phys.* **A584** 675

[685] Itoh N Kohyama Y Matsumoto N and Seki M 1984 *ApJ* **280** 787

[686] Itoh N Kohyama Y Matsumoto N and Seki M 1984 *ApJ* **285** 304

[687] Tsuruta S and Cameron A G W 1966 *Can. J. Phys.* **44** 1863

[688] Glen G and Sutherland P 1980 *ApJ* **239** 671

[689] Richardson M Van Horn K R and Malone R 1982 *ApJ* **255** 624

[690] Voskresenskiĭ D and Senatorov A 1896 *Zh. Eksp. Teor. Fiz.* **90** 1505

[691] Voskresenskiĭ D and Senatorov A 1987 *Sov. J. Nucl. Phys.* **45** 411

[692] Schaab C Voskresenskiĭ D Sedrakian A Weber F and Weigel M K 1997 *Astron. & Astrophys.* **321** 591

[693] Boguta J 1981 *Phys. Lett.* **106B** 255

[694] Prakash M Prakash M Lattimer J M and Pethick C J 1992 *ApJ* **390** L77

[695] Haensel P and Gnedin O Y 1994 *Astron. & Astrophys.* **290** 458

[696] Schaab Ch 1995 *Master Thesis* (University of Munich, Germany)

[697] Muto T and Tatsumi T 1992 *Phys. Lett.* **283B** 165

[698] Bailin D and Love A 1979 *J. Phys.* **A12** L283

[699] Elgarøy Ø Engvik L Hjorth–Jensen M and Osnes E 1996 *Phys. Rev. Lett.* **77** 1429

[700] Hailey C J and Craig W W 1995 *ApJ* **455** L151

[701] Page D Shibanov Y A and Zavlin V E *Röntgenstrahlung from the Universe, Prof. Int. Conf. on X-Ray Astron. and Astrophys.* MPE Report **263** (Garching, Germany) p 103

[702] Greiveldinger C *et al* 1996 *ApJ* **465** L35

[703] Anderson S Cordova F Pavlov G Robinson C and Thompson R 1993 *ApJ* **414** 867

[704] Halpern J P and Wang F Y H 1997 *ApJ* **477** 905

[705] Meyer R Parlov G and Mészáros P 1994 *ApJ* **433** 265

[706] Pavlov G Zavlin V Trümper J and Neuhäuser R 1996 *ApJ* **472** L33

[707] Page D and Applegate J H 1992 *ApJ* **394** L17

[708] Gnedin O Y and Yakovlev D G 1993 *Astron. Lett.* **19** 104

[709] Umeda H Nomoto K Tsuruta S Muto T and Tatsumi T 1994 *ApJ* **431** 309 Umeda H Tsuruta S and Nomoto K 1994 *ApJ* **433** 256

[710] Lattimer J M Van Riper K A Prakash M and Prakash M 1994 *ApJ* **425** 802

[711] Page D 1993 *The Geminga Neutron Star: Evidence for Nucleon Superfluidity at very high Density, in: Proc. 1st Symp. on Nucl. Phys. in the Universe, Oak Ridge* ed M R Strayer and M W Guidry (Bristol: IOP Publishing) p 151

[712] Page D 1994 *ApJ* **428** 250

[713] Page D 1992 *High Energy Phenomenology* ed R Huerta and M A Perez (Singapore: World Scientific) p 347

[714] Schaab Ch Hermann B Weber F and Weigel M K 1997 *ApJ* **480** L111

[715] Schaab Ch Hermann B Weber F and Weigel M K 1997 *J. Phys. G: Nucl. Part. Phys.* **23** 1

[716] Pethick C 1992 *Rev. Mod. Phys.* **64** 1133

[717] Alpar M A and Ögelman H 1990 *ApJ* **349** L55

[718] Shibazaki N and Lamb F 1989 *ApJ* **346** 808

[719] Umeda H Shibazaki N Tsuruta S and Nomoto K 1993 *ApJ* **408** 186

[720] Sedrakian A and Sedrakian D 1993 *ApJ* **413** 658

[721] Reisenegger A 1995 *ApJ* **442** 749

[722] Van Riper K A Link B and Epstein R I 1995 *ApJ* **448** 294